Universidade do Minho
Escola de Medicina

Bárbara Filipa Mendes Pinheiro

Studying the neuroprotective role of bone marrow-derived mesenchymal stem cell secretome using *in vitro* and *in vivo* models of Parkinson's disease

março de 2022

Studying the neuroprotective role of bone marrow-derived mesenchymal stem cell secretome using *in vitro* and *in vivo* models of Parkinson's disease
Bárbara Filipa Mendes Pinheiro
UMinho | 2022

Universidade do Minho
Escola de Medicina

Bárbara Filipa Mendes Pinheiro

Studying the neuroprotective role of bone marrow-derived mesenchymal stem cell secretome using *in vitro* and *in vivo* models of Parkinson's disease

Tese de Doutoramento
Doutoramento em Ciências da Saúde

Trabalho efetuado sob a orientação do
Doutor António José Braga Osório Gomes Salgado
e da
Doutora Luísa Alexandra Meireles Pinto

março de 2022

DIREITOS DE AUTOR E CONDIÇÕES DE UTILIZAÇÃO DO TRABALHO POR TERCEIROS

Este é um trabalho académico que pode ser utilizado por terceiros desde que respeitadas as regras e boas práticas internacionalmente aceites, no que concerne aos direitos de autor e direitos conexos.

Assim, o presente trabalho pode ser utilizado nos termos previstos na licença abaixo indicada.

Caso o utilizador necessite de permissão para poder fazer um uso do trabalho em condições não previstas no licenciamento indicado, deverá contactar o autor, através do RepositóriUM da Universidade do Minho.



Atribuição-SemDerivações

CC BY-ND

https://creativecommons.org/licenses/by-nd/4.0/

ACKNOWLEDGMENTS/AGRADECIMENTOS

Chegar ao fim desta jornada não seria possível sem o importante contributo de várias pessoas e instituições, e a quem gostaria de expressar a minha profunda gratidão. Agradeço ao meu supervisor António Salgado pelo apoio a todos os níveis, dando-me sempre liberdade para pensar e colocar em prática as minhas ideias. Foram 7 anos a trabalhar juntos, e só guardo boas memórias. À minha co-supervisora Luísa Pinto por toda a disponibilidade, compreensão e por ter aceitado este desafio. A special thanks to Jens Schamwborn and all the DVB team for accepting me in the lab, where I learned a lot and progressed as a scientist. Cláudia, Sònia and Gonzie, thank you for making me feel at home during this time in Luxembourg. A toda a ReNEU Team, em especial à Sofia Serra por todos estes anos de partilha de secretária e longas conversas, ao Diogo e ao Jonas pelas risadas, e à Sandra pela sua generosidade. À minha querida Ana, amiga e maravilhosa colega, que sempre me tranquilizou nas horas de dúvida. À Carina e à Sara, que embora não fazendo parte da minha equipa, foram incansáveis sempre que precisei de ajuda. À Cláudia, à Joana Correia, à Dani e à Verónica, por toda a amizade e leveza que sempre me transmitiram. À Rita e ao Pedro pelas videochamadas, jantares, e por toda a força e motivação que deram nesta reta final. À minha amiga de sempre e para sempre Joana: quando olho para trás, já é difícil imaginar uma conquista minha na qual não estiveste presente. A toda a minha família, em especial aos meus queridos Pais e Irmão Daniel, pois sem eles nada disto faria sentido. À minha Ritinha que mais que uma prima é uma irmã. À Camila, a minha pessoa de quatro patas que todos os dias me traz mais alegria. Ao meu grande amor, Eduardo. Começamos juntos e terminámos juntos. O teu apoio incondicional e ternura tornou este desafio mais fácil; por isso, obrigada por tudo...que foi tanto!

The work presented in this thesis was developed in the Life and Health Sciences Research Institute (ICVS), School of Medicine, University of Minho, Braga, Portugal. Financial support was provided by grants from the Foundation for Science and Technology (FCT/SFRH/BD/120124/2016 and COVID/BD/151719/2021 to Bárbara Pinheiro). ICVS Scientific Microscopy Platform, member of the national infrastructure PPBI-Portuguese Platform of Bioimaging PPBI-POCI-01-0145-FEDER-022122; National funds, through the FCT-project UIDB/50026/2020 and UIDP/50026/2020; the projects NORTE-01-0145-FEDER-000013, NORTE-01-0145-FEDER-000023, and NORTE-01-0145-FEDER-000039, supported by Norte Portugal Regional Operational Programme (NORTE 2020), under the PORTUGAL 2020 Partnership Agreement, through the European Regional Development Fund (ERDF); Competitiveness Internationalization Operational Programme (POCI), and by National funds, through the FCT, under the scope of the project POCI-01-0145-FEDER-032619. This work was also partially funded by Iniciativa Ibérica de Investigación y Innovación Biomedica and Fundación "a Caixa", under the scope of the "la Caixa" Foundation Health Research 2020 Call (HR20-00249). Part of the work was also developed at Luxembourg Centre for Systems and Biomedicine (LCSB) at Luxembourg University and financially supported by the Fonds National de la Recherche (FNR) Luxembourg (INTER/MERA/17/11760144, FNR/PoC16/11559169). Furthermore, the project is part of the The National Centre of Excellence in Research on Parkinson's Disease (NCER-PD) which is funded by the Luxembourg National Research Fund (FNR/NCER13/BM/11264123). This project has received funding from the European Union's Horizon 2020 research and innovation programme H2020-FETPROACT-2018-01 under grant agreement No 824070.



STATEMENT OF INTEGRITY

I hereby declare having conducted this academic work with integrity. I confirm that I have not used plagiarism or any form of undue use of information or falsification of results along the process leading to its elaboration.

I further declare that I have fully acknowledged the Code of Ethical Conduct of the University of Minho.

Estudo do papel neuroprotetor do secretoma de células estaminais mesenquimatosas derivadas da medula óssea usando modelos *in vitro* e *in vivo* da doença de Parkinson

RESUMO

A doença de Parkinson (DP) é a doença motora mais comum, afetando cerca de 6.1 milhões de pessoas mundialmente. Sintomas motores como bradicinesia, tremor em repouso e rigidez muscular são as principais características clínicas da DP. No entanto, sintomas não motores são também determinantes na qualidade de vida e da incapacidade geral do doente. Perda neuronal na substância nigra *pars compacta* (SNpc) que causa uma deficiência de dopamina (DA) ao nível do estriado, bem como inclusões intracelulares que contêm agregados de α-sinucleína, são as principais características neuropatológicas da doença. As abordagens terapêuticas atualmente disponíveis estão focadas na substituição dos níveis de DA, mas não são capazes de retardar, interromper ou reverter a neurodegeneração subjacente à DP. As células estaminais mesenquimatosas (MSCs) são uma das fontes celulares mais amplamente estudadas para aplicações em medicina regenerativa, particularmente devido à libertação de fatores solúveis e vesículas, coletivamente conhecido como secretoma. O principal objetivo desta tese foi estudar o potencial terapêutico do secretoma de MSCs derivadas da medula óssea (BM-MSCs) usando diferentes modelos da doença. Numa primeira fase, usamos um sistema de organóides humanos específicos do mesencéfalo para modelar a DP *in vitro* com recurso a dois modelos diferentes, nomeadamente, um modelo induzido pela neurotoxina 6-hidroxidopamina (6-OHDA), e um modelo genético da DP ligado a uma mutação na proteína DJ-1. O secretoma das BM-MSCs foi capaz de proteger a perda neuronal dopaminérgica, bem como a fragmentação das neurites dopaminérgicas, sendo estes efeitos mais evidentes no modelo genético. Em seguida, otimizamos os parâmetros de cultura das BM-MSCs através da introdução do lisado plaquetário humano (hPL) como suplemento para a sua expansão em cultura. *In vivo,* o nosso objetivo passou por realizar uma extensa caracterização do modelo 6-OHDA unilateral e intra-estriatal de ratinho, para mais tarde avaliar os efeitos do secretoma das BM-MSCs, comparando duas vias diferentes de administração de secretoma: injeções intracerebrais (administração única) com administração sistémica repetida. O secretoma das BM-MSCs levou à recuperação da função motora e proteção dos neurónios dopaminérgicos, no entanto, as múltiplas administrações sistémicas mostraram um efeito terapêutico de maior magnitude, sendo este resultado da extrema relevância do ponto de vista da aplicação clínica. Além disso, a análise proteómica revelou a identificação de várias proteínas neuroreguladoras no secretoma das BM-MSCs expandidas em hPL, reforçando o uso deste suplemento como uma alternativa viável face às abordagens mais convencionais. Concluindo, o nosso estudo produziu contribuições importantes para projetar novas abordagens clínicas livres de células para a DP com base na administração de secretoma.

Palavras-chave: células estaminais mesenquimatosas, doença de Parkinson, neuroproteção, secretoma

Studying the neuroprotective role of bone marrow-derived mesenchymal stem cell secretome using *in vitro* and *in vivo* models of Parkinson's disease

ABSTRACT

Parkinson's disease (PD) is the most common movement disorder that affects 6.1 million individuals worldwide. Motor symptoms such as bradykinesia, rest tremor, and rigidity, are the core PD clinical features. Nonetheless, non-motor symptoms have been recognized as determinants of the patient's quality of life and overall disability. Neuronal loss in the substantia nigra *pars compacta* (SNpc), which causes striatal dopamine (DA) deficiency, and intracellular inclusions containing aggregates of α-synuclein are the neuropathological hallmarks of PD. Currently available therapeutical approaches are focused on replacing DA levels, which are not able to slow, halt or reverse PD underlying neurodegeneration. Mesenchymal stem cells (MSCs) are one of the most extensively studied cell sources for regenerative medicine applications, particularly due to the release of soluble factors and vesicles, known as secretome. The main goal of this thesis was to address the therapeutic potential of the secretome collected from bone marrow-derived MSCs (BM-MSCs) using different models of the disease. Firstly, we took advantage of an optimized human midbrain-specific organoid system to model PD *in vitro* using two different models namely, a neurotoxin-induced model through 6-hydroxydopamine (6-OHDA) exposure, and a genetic PD model linked to a mutation in the DJ-1 protein. The secretome of BM-MSCs was able to protect from the dopaminergic neuronal loss, as well as from induced fragmentation of dopaminergic neurites, being these effects more evident in the genetic model. Following on this we further optimize the culturing parameters of BM-MSCs, through the introduction of human platelet lysate (hPL) as a supplement for their expansion in culture. *In vivo*, we aimed to perform an extensive characterization of a unilateral intrastriatal 6-OHDA PD mouse model, to further evaluate the effects of BM-MSC secretome comparing two different routes of secretome administration: intracerebral injections (single administration) with multiple systemic administration. The BM-MSC secretome led to motor function recovery and dopaminergic loss protection, however, multiple systemic administrations showed a higher magnitude therapeutical effect being this result of the extreme relevance from the clinical application point of view. Moreover, proteomic analysis revealed the identification of several important neuroregulatory proteins in the secretome of hPL expanded BM-MSCs, reinforcing the use of this supplement as a feasible alternative over more conventional approaches. Overall, our study made important contributions to designing new cell-free clinical approaches for PD based on secretome administration.

Keywords: Mesenchymal stem cells, neuroprotection, Parkinson's disease, secretome

TABLE OF CONTENTS

ACKNOWLEDGMENTS/AGRADECIMENTOS iii

RESUMO v

ABSTRACT vi

TABLE OF CONTENTS vii

LIST OF ABBREVIATIONS ix

LIST OF FIGURES xi

LIST OF TABLES xiii

Chapter 1. Introduction 1

1. Parkinson's disease 3

1.1. Epidemiology and magnitude 3

1.1.1. Prevalence, incidence, and demographics 3

1.1.2. Risk factors 4

1.2. Clinical presentation of Parkinson's disease 9

1.2.1. Prodomal phase 10

1.2.2. Clinical phase 13

1.3. Motor circuit pathophysiology 15

1.4. Neuropathology 18

1.5. Mechanisms of neurodegeneration 21

1.5.1. α-synuclein misfolding and aggregation 21

1.5.2. Dysfunctional protein clearance systems 22

1.5.3. Altered mitochondrial function 25

1.5.4. Neuroinflammation 26

1.5.5. Iron accumulation 27

1.5.6. Oxidative stress 28

2. Experimental models of Parkinson's disease 29

2.1. In vitro 29

2.1.1. Cell lines, primary cultures and organotypic cultures 30

2.1.2. Stem cell-derived neurons for Parkinson's modeling 30

2.1.3. Brain organoids 32
2.2. In vivo 40
2.2.1. Neurotoxic models 41
2.2.2. Genetic-based models 44
3. Current treatments and therapies in development for Parkinson's disease 46
3.1. Dopamine biosynthesis and metabolism 46
3.1.1. Dopaminergic pharmacological targets 47
3.2. Non-dopaminergic pharmacological targets 49
3.3. Deep brain stimulation 50
3.4. Gene therapy 50
3.5. Cell-based therapy 51
4. Mesenchymal stem cells: focus on secretome as a cell-free therapy for Parkinson's disease 52
4.1. Mesenchymal stem cells 52
4.2. The concept of secretome 54
4.3. Mesenchymal stem cell therapeutical effects in Parkinson's disease 55
5. Conclusions 59
Chapter 2. Research aims 89
Chapter 3. Modeling Parkinson's disease in human midbrain-specific organoids to study the neuroprotective potential of mesenchymal stem cell secretome 91
Chapter 4. Unilateral intrastriatal 6-hydroxydopamine lesion in mice: a closer look into non-motor phenotype and glial response 128
Chapter 5. Multiple systemic administration of mesenchymal stem cell secretome showed a higher therapeutical magnitude effect *versus* intracerebral injections in a mouse model of Parkinson's disease 160
Chapter 6. General discussion and future perspectives 197

LIST OF ABBREVIATIONS

#

6-OHDA – 6-hydroxydopamine

A

AADC – Aromatic amino acid decarboxylase

ADH – Alcohol dehydrogenase

ALDH – Aldehyde dehydrogenase

ASCs – Adipose tissue MSCs

B

BBB – Blood-brain barrier

BDNF – Brain-derived neurotrophic factor

bFGF – Basic fibroblast growth factor

BM-MSCs – Bone marrow-derived MSCs

BMP – Bone morphogenetic protein

C

CM – Conditioned medium

CMA – Chaperone-mediated autophagy

CNS – Central nervous system

COMT – Catechol-O-methyl transferase

D

DA – Dopamine

DALYs – Disability-adjusted life years

DAT – Dopamine transporter

DOPAC – 3,4-dihydroxyphenylacetic acid

DOPAL – 3,4-dihydroxyphenylacetaldehyde

DOPET – 3,4-dihydroxyphenylethanol

E

EBs – Embryoid bodies

ECM – Extracellular matrix

EGF – Epidermal growth factor

F

FAD – Flavin adenine dinucleotide

FGF – Fibroblast growth factor

FOXA2 – Forkhead box A2

G

GABA – Gamma-aminobutyric acid

GBA – Glucocerebrosidase

GDNF - Glial cell line-derived neurotrophic factor

GIRK2 – G-protein-regulated inward-rectifier potassium channel 2

GPe – External globus pallidus

GPi – Internal globus pallidus

GWAS – Genome wide association studies

H

hMOs – Human midbrain-specific organoids

HPL – Human platelet lysate

HVA – Homovanillic acid

I

IGF-1 – Insulin-like growth factor-1

i.p. – Intraperitoneal

iPSCs – Induced pluripotent stem cells

ISCT – International Society for Cellular Therapy

L

LAS – Lysosomal autophagy system

LBs – Lewy bodies

L-DOPA – L-dihydroxyphenylalanine

LMX1A – LIM homeobox transcription factor 1 alpha

LRRK2 – Leucine-rich repeat kinase 2

M

MAO – Monoamine oxidase

MDS – Movement Disorder Society

MFB – Medial forebrain bundle

MMP-2 – Metalloproteinase 2 protein

MPTP – 1-methyl-4-phenyl-1,2,3,6-tetrahydropyridine

MRI – Magnetic resonance imaging

MSCs – Mesenchymal stem cells

MSNs – Medium spiny neurons

N

NGF – Nerve growth factor

NESCs – Neuroepithelial stem cells

NSCs – Neural stem cells

NT3 – Neurotrophic factor 3

O

OTX2 – Orthodenticle homeobox 2

P

PAX6 – Paired box protein 6

PBS – Phosphate-buffered saline

PD – Parkinson's disease

PEDF – Pigment epithelium-derived factor

Pen-Strep – Penicillin-streptomycin

PET – Positron emission tomography

PINK1 – PTEN-induced putative kinase

PNS – Peripheral nervous system

PRKN – Parkin

R

RBD – REM-sleep behavior disorder

ROS – reactive oxygen species

S

SDF-1 – Stromal cell-derived factor 1

SDI – Socio-demographic Index

SHH – Sonic hedgehog

SPECT – Single photon emission computed tomography

SNpc – Substantia nigra *pars compacta*

SNpr – Substantia nigra *pars reticulata*

STN – Subthalamic nucleus

T

TGF-β – Transforming growth factor beta

TH – Tyrosine hydroxylase

U

UPDRS – Unified Parkinson's Disease Rating Scale

UPS – Ubiquitin-proteasome system

V

VEGF – Vascular endothelial growth factor

W

WJ-MSCs – Wharton's Jelly-derived MSCs

LIST OF FIGURES

CHAPTER 1. Introduction

Figure 1. Clinical symptoms associated with Parkinson's disease progression.

Figure 2. Motor circuitry affected in Parkinson's disease.

Figure 3. Molecular mechanisms involved in Parkinson's disease.

Figure 4. Organoid differentiation protocols and application of human midbrain-specific organoids (hMOs).

Figure 5. Mesenchymal stem cells and their therapeutical potential in Parkinson's disease.

CHAPTER 3. Modeling Parkinson's disease in human midbrain-specific organoids to study the neuroprotective potential of mesenchymal stem cell secretome

Figure 1. Derivation of hMOs from hvNESCs.

Figure 2. Characterization of hMOs at day 30 of the differentiation protocol.

Figure 3. Effects of BM-MSC secretome in the 6-OHDA-induced PD model.

Figure 4. Representative images of the 6-OHDA-induced degeneration and BM-MSC secretome treatment effects.

Figure 5. Derivation of isogenic hMOs derived from the control C4 (wild-type line) and C4Mut (mutant line) hNESCs.

Figure 6. Effects of BM-MSC secretome in the DJ-1 genetic PD model.

Figure 7. Representative images of the DJ-1-related phenotypes in hMOs and BM-MSC secretome treatment effects.

Supplementary Figure S1. Human ventralized neuroepithelial stem cells used in Model 1.

Supplementary Figure S2. Human neuroepithelial stem cells used in Model 2.

Supplementary Figure S1. High-content image analysis workflow.

Supplementary Figure S2. Characterization of glial differentiation at day 30 of the differentiation protocol.

Supplementary Figure S3. Example of a fragmented neurite after 6-OHDA treatment.

CHAPTER 4. Unilateral intrastriatal 6-hydroxydopamine lesion in mice: a closer look into non-motor phenotype and glial response

Figure 1. 6-OHDA intrastriatal lesion effects on motor behavioral tasks.

Figure 2. Impact of 6-OHDA intrastriatal lesion on anxiety- and depressive-like behavior.

Figure 3. Histological and neurochemical characterization of intrastriatal 6-OHDA lesions.

Figure 4. Astroglial reaction after 6-OHDA intrastriatal lesion.

Figure 5. Microglial response after 6-OHDA intrastriatal lesion.

Figure 6. Experimental design.

Supplementary Figure S1. Raw data relative to main Figure 3.

Supplementary Figure S2. Microglia morphology quantification workflow.

Supplementary Figure S3. Raw data relative to main Figure 4 and Figure 5.

Supplementary Figure S4. Correlation between dopaminergic loss and microglial cells.

Supplementary Figure S5. Impact of sex in behavioral and histological outcomes after 6-OHDA intrastriatal lesion.

CHAPTER 5. Multiple systemic administration of mesenchymal stem cell secretome showed a higher therapeutical magnitude effect *versus* intracerebral injections in a mouse model of Parkinson's disease

Figure 4. Experimental design.

Figure 5. Motor behavioral analysis of 6-OHDA-lesioned animals after administration of BM-MSC secretome.

Figure 6. Histological analysis of the striatum and SNpc.

Figure 4. Proteomic analysis of BM-MSC secretome.

Figure 7. Profile of neuroregulatory proteins present in the secretome of BM-MSCs.

Supplementary Figure S1. Weight gain.

Supplementary Figure S2. Phenotypic parameters of the SHIRPA protocol.

LIST OF TABLES

CHAPTER 1. Introduction

Table 1. Genetic and phenotypic features of the monogenic Parkinson's disease syndromes.

BOX 1. Diagnostic criteria for Parkinson's disease.

Table 2. Characteristics, uses, and limitations of Parkinson's disease genetic-based models.

Table 3. Current and planned trials of human stem cell-derived neuronal products.

CHAPTER 3. Modeling Parkinson's disease in human midbrain-specific organoids to study the neuroprotective potential of mesenchymal stem cell secretome

Supplementary Table S1. List of primary antibodies.

Supplementary Table S2. Features from image analysis.

CHAPTER 4. Unilateral intrastriatal 6-hydroxydopamine lesion in mice: a closer look into non-motor phenotype and glial response

Supplementary Table S1. Statistical reports of all performed analysis in main Figures.

Supplementary Table S2. Statistical reports of all performed analysis in supplementary Figures.

Supplementary Table S3. Perioperative health assessment and procedures after 6-OHDA injection in mice.

Supplementary Table S4. Confocal microscopy for glial reaction: acquisition parameters.

CHAPTER 5. Multiple systemic administration of mesenchymal stem cell secretome showed a higher therapeutical magnitude effect *versus* intracerebral injections in a mouse model of Parkinson's disease

Supplementary Table S1. Statistical summary.

Supplementary Table S2. List of proteins identified in BM-MSC secretome using Untargeted mass spectrometry proteomic analysis.

CHAPTER 1

Introduction

Part of this chapter is based on the following publication:

Bárbara Mendes-Pinheiro[1,2], Ana Marote[1,2], Cláudia R. Marques[1,2], Fábio G. Teixeira[1,2], Jorge C. Ribeiro[1,2], António J. Salgado[1,2]. (2020). Applications of the stem cell secretome in regenerative medicine. *Mesenchymal Stem Cells in Human Health and Diseases*, Chapter 5. pp. 79-114. doi.org/10.1016/B978-0-12-819713-4.00005-0

[1]Life and Health Sciences Research Institute (ICVS), School of Medicine, University of Minho, Campus de Gualtar, 4710-057 Braga, Portugal;
[2]ICVS/3B's - PT Government Associate Laboratory, 4805-017 Guimarães, Portugal.

1. Parkinson's disease

Parkinson's disease (PD) was firstly described by the physician James Parkinson in 1817 in 'An essay on the Shaking Palsy'. Despite his study being only based on six cases, it was sufficient to describe accurately the cardinal motor symptoms of PD (Parkinson, 2002). Since that, important discoveries have improved our understanding of PD and its determinants. On one hand, genetic studies showed that PD is a heterogeneous disease, giving insights into its etiology and pathogenesis, and on the other hand, epidemiological studies have contributed with important evidence about the role of behavioral and environmental factors in disease progression. Unfortunately, although a lot has been learned about PD, a cure still does not exist, and the development of disease-modifying therapies that delay or stop PD progression is still needed. In this section, we will provide a broad characterization of PD at the epidemiological and clinical level, as well as describe the pathophysiology and the cellular and molecular mechanisms underlying PD. Moreover, we will characterize the different models used to study the disease and discuss new therapeutical approaches.

1.1. Epidemiology and magnitude

1.1.1. Prevalence, incidence, and demographics

According to the Global Burden of Disease Study, neurological conditions are the main cause of disability worldwide, with PD being the fastest growing among them (Dorsey et al., 2018b). PD is the most frequent type of parkinsonism, with a crude incidence rate in high-income countries of 14 per 100 000 people in the total population, and 160 per 100 000 people aged 65 years or older (Ascherio and Schwarzschild, 2016). Prevalence is substantially higher than incidence because this is a chronic condition with a protracted course. In 2016, an estimated 6.1 million people worldwide were diagnosed with PD, up 2.4 times from 1990. By 2030, these numbers are predicted to double (Dorsey et al., 2018a). This rise in prevalence can be attributed to better methods for diagnosing PD, higher knowledge and earlier recognition of the condition, aging populations, longer life expectancy, and possibly increasing environmental exposures linked with industrialization (Armstrong and Okun, 2020). In Portugal, PD affects 18 496 individuals, holding the third highest increase in age-standardized prevalence (31.9%), death counts (34.3%), and disability-adjusted life years (DALYs) from 1990 to 2016 within western Europe (Dorsey et al., 2018a). PD is uncommon in those under the age of 50, and its prevalence rises with age, peaking between the ages of 85 and 89 (Armstrong and Okun, 2020). Nonetheless, it has long been known that a tiny percentage of patients develop PD at a young age,

which is usually connected to genetic mutations that generate monogenic forms of the disease (Tysnes and Storstein, 2017). Even though PD has long been thought to affect people of both sexes equally, current data suggest that males are impacted by the disease at a higher rate than females, with a male to female ratio of 1.4 (Dorsey et al., 2018a).

PD affects individuals globally, thus demographics and ethnicity differences also have an impact on both incidence and prevalence differences (Abbas et al., 2018). Data from 2016 demonstrated that 34.4% of the people with PD lived in high Socio-demographic Index (SDI) countries and 50.8% in the high middle or middle SDI, against 14.8% living in low-middle or low SDI. The higher environmental exposure to pesticides, metals, and solvents duo to industrialization in countries with greater SDI might contribute to this variation (Dorsey et al., 2018a). Additionally, studies have shown variations in PD numbers attributed to ethnic differences across regions. Higher rates were reported for Hispanics and Caucasians, followed by Asians and Africans within the United States of America. These differences could represent a genetic susceptibility but could also result from sampling bias due to socioeconomic and cultural factors. Interestingly, the prevalence rates for African Americans and Japanese Americans were higher in comparison with similar populations in their native countries, suggesting a role of environmental factors in disease development (Abbas et al., 2018).

1.1.2. Risk factors

PD is recognized as a multifactorial disease and the result of a complex interplay between endogenous and exogenous factors. Besides age, which is the utmost risk factor for developing PD, gender and genetics are examples of other internal and non-modifying factors (Ascherio and Schwarzschild, 2016). Genome-wide association studies (GWAS) discovered that more than 20 single nucleotide polymorphisms are significantly linked to PD, thereby emphasizing a genetic contribution (Belvisi et al., 2020b). Likewise, several epidemiological studies explored the role of environmental or behavioral factors in the etiology of PD. Exposure to pesticides, consumption of dairy products, history of melanoma, and traumatic brain injury, as well as nonuse of caffeine and nicotine, are among the factors considered by these studies (Ascherio and Schwarzschild, 2016).

Gender

The function of biological sex, along with aging, genetics, environment, and immunological condition, is a crucial element in the development and phenotypic expression of PD In 2016, women made up

47.5% (2.9 million) of the overall number of people with PD, while men made up 52.5% (3.2 million) (Dorsey et al., 2018a). This disproportion has been suggested to be related to a protective effect of female-specific hormones and genetic mechanisms (Poewe et al., 2017). Increased occupational stress and contact with environmental risk factors with neurotoxic potential, to which men are more frequently exposed, might also contribute to this pattern (Cerri et al., 2019; Dorsey et al., 2018a). Different studies also showed that PD male patients have worse cognitive declines and male sex is the principal predictive factor for mild cognitive impairment and its more rapid progression in the severe stage of the disease (Cerri et al., 2019). Although PD affects more men than women, it is known that women have a higher mortality rate and faster progression of the disease. They have a greater risk of developing dyskinesia, and motor and non-motor fluctuations, as well as are more tending to report urinary complaints and depression. Moreover, women have delayed access to medical specialist care, which might result in under-treatment, including decreased use of neurosurgical interventions. Importantly, women are under-represented in PD trials (Bloem et al., 2021; Cerri et al., 2019).

Genetics

The discovery of the first monogenic form of PD has revolutionized what was previously thought. that this disease has a considerable non-genetic etiology (Polymeropoulos et al., 1997). Although monogenic forms account only for about 10% of PD cases, they are important to improve our understanding of PD pathophysiology (Bloem et al., 2021). To date, most PD genetic studies are focused on mutations in the following genes: SNCA, leucine-rich repeat kinase 2 (LRRK2), PTEN-induced putative kinase (PINK1), parkin (PRKN), DJ-1 and glucocerebrosidase (GBA) (Domingo and Klein, 2018). The identification of these proteins and the complex pathogenesis caused by their mutations allowed the discovery of neurodegeneration pathways that can be common between inherited and idiopathic PD. The genes involved in familial PD and its phenotypic features are summarized in Table 1.

Table 1. Genetic and phenotypic features of the monogenic Parkinson's disease syndromes

Genetic features			Phenotypic features		
Gene	**Locus**	**Mutation(s)**	**Motor**	**Non-motor**	**Others**
Autosomal-dominant /Sporadic					
SNCA	PARK1 4q21 PARK 4 4q21	Missense mutations (A53T, A30P, E46K, G50D) Duplication Triplication	Ranging from typical PD to early-onset; aggressive course especially in triplication carriers	Prominent especially in triplication carriers	Family members may have other Lewy body-related diseases like dementia
LRRK2	PARK8 12q12	G2019S, R1441C/G/H, Y1699C, I2020T	Typical PD, tremor-dominant at onset	Less common	Very common among North Africa Arabs
GBA	no PARK locus 1q21	Missense mutations (N370S, L444P)	Typical PD	Probably similar to typical PD	Lewy body pathology
VPS35	PARK17 16q12	Missense mutations (D620N)	Typical PD	Probably similar to PD	Good levodopa response
Autossomal-recessive					
PINK1	PARK6 1p36	Homozygous or compound heterozygous One heterozygous mutation	Early-onset PD	Higher rate of psychiatric symptoms vs PRKN	May mimic sporadic typical PD
PRKN	PARK2 6q25.2-q27	Homozygous or compound heterozygous One heterozygous mutation	Early-onset PD, dystonia is a common early sigh	Dementia almost always absent	Absence of Lewy body pathology
DJ-1	PARK7 1p36.23	Homozygous or compound heterozygous	Early onset PD	Similar to PINK1/PRKN	Significantly less common than PINK1 and PRKN

α-synuclein, encoded by SNCA gene, is a synaptic vesicle protein highly expressed in the central nervous system (CNS) and peripheral nervous system. It has been associated with several functions including mitochondrial function, lipid binding, regulation of glucose levels and dopamine (DA) biosynthesis, modulation of vesicle trafficking, among others (Domingo and Klein, 2018). Paradoxically, is the major component of Lewy bodies (LBs) in PD patients, and missense mutations (A53E, A53T, A53V, A30P, E46K, H50Q, and G51D) as well as copy number variations (duplication or triplication) of SNCA led to autosomal dominant familial PD forms (Emamzadeh, 2016). Earlier age of disease onset,

faster progression of motor signs, and presence of prominent non-motor features including rapid cognitive decline are shared features of all SNCA mutations (Trinh et al., 2018). Although mutations in this gene are known to cause familial forms of PD, GWAS have also identified SNCA as one of the greatest risk loci linked with idiopathic PD, which indicates its important role in PD pathogenesis (Soldner et al., 2016).

While SNCA-associated mutations are maybe the most relevant to idiopathic PD, LRRK2 mutations are the most common familial form of the disease. LRRK2 is a highly conserved large multidomain protein that belongs to the ROCO protein family, with a role in neurite outgrowth, phosphorylation of different proteins, and modulation of synaptic vesicle endocytosis and endocytic membrane trafficking via rab-GTPases interactions (Esteves and Cardoso, 2017; Rui et al., 2018). Seven different LRRK2 mutations have been clearly linked to PD, being the G2019S mutation the most common and found in 4% of patients with hereditary PD and in 1% of patients with the idiopathic form of the disease (Domingo and Klein, 2018). Clinically, LRRK2 mutations lead to a phenotype that is often indistinguishable from idiopathic PD (Domingo and Klein, 2018).

GBA mutations are the greatest risk factor for PD and are associated with an enhanced risk of developing synucleinopathies. The gene encoding glucocerebrosidase, *GBA*, is a lysosomal enzyme that catalyzes the hydrolysis of glucosylceramide (GlcCer) to glucose and ceramide. The inherited deficiency of this enzyme is the most common lysosomal storage disorder, known to cause Gaucher's disease (GD) (Sidransky and Lopez, 2012). The link between GBA gene and PD emerged after the first study reporting that patients with this disease exhibited symptoms of parkinsonism (Sidransky, 2004). Thereafter, other studies confirmed the link between PD and GBA mutation including insertion, deletion, frameshift, and point mutations in GBA (O'Regan et al., 2017). Approximately 5-10% of PD patients carry GBA mutations, and its most common mutations (N370S and L444P), account for 3% of GBA-liked PD (Domingo and Klein, 2018). Clinically, these mutation carriers tend to have an earlier onset and more cognitive symptoms, in addition to severe motor symptoms (Bloem et al., 2021).

Mutations in PINK1 and PRKN are the major causes of autosomal recessive and early-onset PD, with the frequent PRKN mutations accounting for more than 77% cases of juvenile PD (people younger than 20 years) and 10-20% of young-onset PD (Bloem et al., 2021). PINK1 is a mitochondria-targeted serine/threonine-protein kinase, that in normal conditions is cleaved and released into the cytosol for degradation, and it has been shown to protect cells against oxidative stress-induced apoptosis (Deas et al., 2009; Pickrell and Youle, 2015). On the other hand, PRKN is an E3 ubiquitin-protein ligase, residing

in the cytosol, that is recruited to depolarize mitochondria to mediate the selective autophagic removal of the damaged organelle (mitophagy) (Marotta et al., 2020; Pickrell and Youle, 2015). Although PINK1 localizes to mitochondria and PRKN in the cytosol, genetic studies in Drosophila demonstrated that these proteins work together in the same pathway, regulating mitochondria dynamics (Pickrell and Youle, 2015). PINK1 and PRKN disease are commonly slowly progressive and respond well to antiparkinsonian treatment (Bloem et al., 2021).

DJ-1 is the third recessive PD gene, and a significantly less common cause of early-onset PD compared with the two genes described above, accounting for only 1-2% of cases (Domingo and Klein, 2018). DJ-1 is expressed in almost all cells and tissues, including the brain. The DJ-1 protein is a multifunctional protein that participates in transcriptional regulation, antioxidative stress reaction, and chaperone, protease, and mitochondrial regulation (Ariga et al., 2013). Since this protein acts as a sensor for oxidative stress is thought to have cellular protective properties (Domingo and Klein, 2018). The clinical manifestations for this gene mutation are similar to the other recessive PD syndromes.

Non-genetic factors

The discovery that intravenous use of 1-methyl-4-phenyl-1,2,3,6-tetrahydropyridine (MPTP), traded in the '80s as synthetic heroin in California, led to the development of severe parkinsonism in a number of addicted individuals (Langston et al., 1983). Since then, several environmental and lifestyle factors have been evaluated in the context of PD. Exposure to environmental pesticides is one of the risk factors that have more converging and consistent evidence. The introduction to pesticides after World War 2 – largely used to feed the fast-growing population – could partially explain the current rise of PD (Bloem et al., 2021). In the Agricultural Health Study, positive associations were shown between disease risk and exposure to pesticides and herbicides known to affect mitochondrial complex I (including the pesticide rotenone) or to cause oxidative stress (including the herbicide paraquat) (Ascherio and Schwarzschild, 2016). Furthermore, specific environmental factors were further demonstrated to be selectively toxic to dopaminergic neurons (Richardson et al., 2005). Welding and heavy metal exposure (e.g., iron, copper, lead, aluminum, and zinc) have also been studied although there is still no solid evidence that they are linked to PD (Belvisi et al., 2020a).

Negative associations with the risk of developing PD include smoking, coffee drinking, and physical activity, among others. Different epidemiological studies showed that PD risk decreases up to 70% with increasing duration of smoking and increases with time since quitting in ex-smokers (Ascherio and

Schwarzschild, 2016). A lower PD risk among coffee drinkers (30% lower) when compared with non-drinkers has also been shown in several prospective cohorts and appears to be due to caffeine consumption. This association is more robust in men than in women, probably due to an interaction between caffeine and postmenopausal hormones (Ascherio and Schwarzschild, 2016). In fact, some studies suggest that nicotine and caffeine may have a protective role by modulating dopaminergic transmission and competing with neurotoxins binding (Ascherio and Schwarzschild, 2016). However, this association could also be false, because smokers and coffee drinkers might have higher DA levels, which in turn explain their appetite via the brain reward system while preventing consumers from dropping below a critically low DA threshold that is required to manifest parkinsonism (Bloem et al., 2021). Similar considerations are valid to the apparent protective effects of physical activity, which could directly protect against neurodegeneration – a fact that is consistent with the results from studies using PD animal models – but which might also reflect a generally healthier lifestyle (Bloem et al., 2021). Some of the proposed mechanisms for this physical activity's neuroprotective effect are an increase in serum urate, an increase in the release of neurotrophic factors, and regulation of DA turnover (Ascherio and Schwarzschild, 2016).

Other factors such as traumatic brain injury, non-steroidal anti-inflammatory drugs, and calcium-channel blocker intake have also been suggested, although with limited evidence (Belvisi et al., 2020a). Overall, the literature regarding this topic can be controversial because many factors have never been replicated, confounders variables ad conflict results exist, and a credible mechanistic explanation is often rare. Therefore, intervention studies are needed to further explore causality.

1.2.Clinical presentation of Parkinson's disease

PD was first classified as a movement disorder with classical motor symptoms manifestation, resulting from the degeneration of dopaminergic nerve cells in the substantia nigra *pars compacta* (SNpc). Today, the clinical picture of the disease has changed, and PD is recognized as a multi-systemic neurodegenerative disorder with motor and non-motor symptoms originating from a profoundly disrupted neurotransmitter system (Kaur et al., 2019). As a result, PD is currently divided into three distinct phases (represented in Figure 1): i) the preclinical phase, in which the neurodegenerative process has already begun but has not yet caused any symptoms; ii) the prodromal phase, in which a neurodegenerative process in various parts of CNS and peripheral nervous system (PNS) is leading to the presence of clinical signs, but not enough to make a diagnosis; and iii) the clinical phase, in which cardinal motor symptoms become sufficiently evident to diagnose PD (Schaeffer et al., 2020).

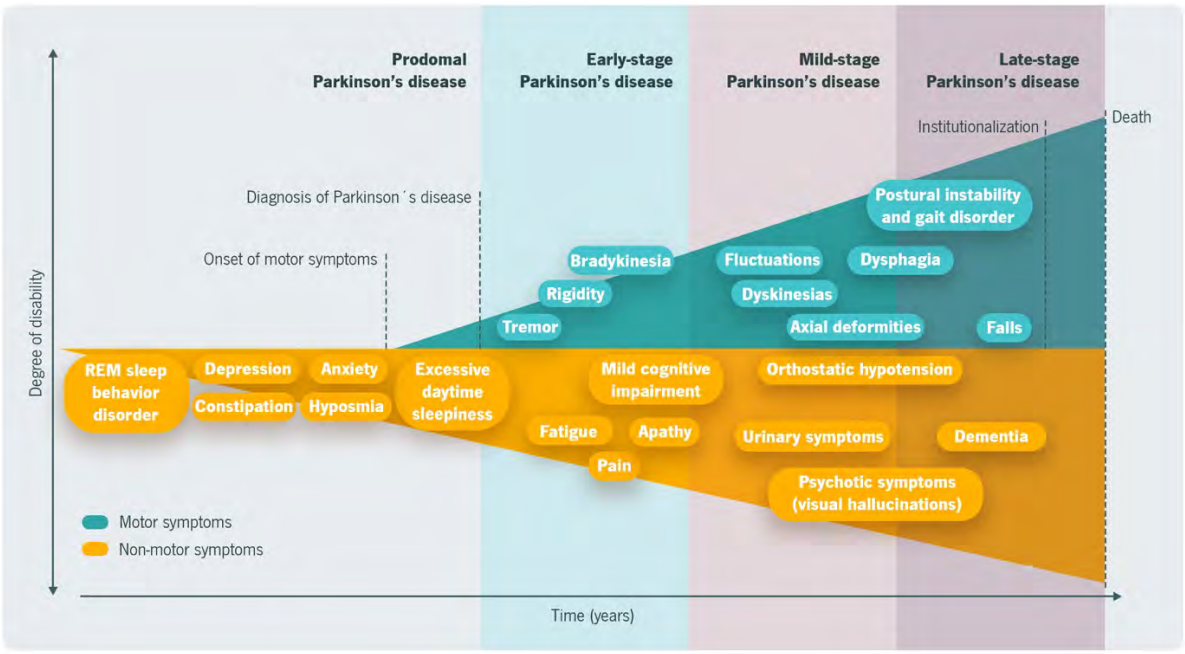


Figure 1. Clinical symptoms associated with Parkinson's disease progression. Diagnosis of PD occurs with the onset of motor symptoms (early-stage Parkinson's disease) normally in the late fifties but can be preceded by a prodromal phase of years or even decades, which is characterized by specific non-motor symptoms (prodromal Parkinson's disease). Non-motor symptoms become more prominent and noticeable as the disease progresses, but they can be present to varying degrees throughout all stages of PD. The combination of these non-motor problems with increasing severity of cardinal motor features, the development of L-DOPA-induced motor complications (mid-stage Parkinson's disease), and the evolution of poorly L-DOPA-responsive motor disabilities, such as postural instability, gait problems (including freezing), and dysphagia, all contribute to progressive disability from PD (late-stage Parkinson disease). Abbreviations: REM, rapid eye movement. Adapted from (Poewe et al., 2017).

1.2.1. Prodomal phase

Diagnosis of PD starts with the onset of motor symptoms but can be preceded by a prodromal period of up to 20 years (Kalia and Lang, 2015). This stage may allow for early detection of PD, leading to the initiation of prospective neuroprotective therapy to slow or prevent the onset of the disease. As a result, identifying individuals in this phase is a clinical and research priority (Hustad and Aasly, 2020). Despite many of the risk prodromal markers occurring frequently in PD patients, they also often appear in the general population which results in low specificity (Schaeffer et al., 2020). This principle forced the development of the "Research Criteria on Prodromal Parkinson's Disease", created by the Movement Disorder Society (MDS) in 2015 (Berg et al., 2015). The criteria firstly incorporate estimates of risk, based upon age, sex, and other documented PD risk factors, but this is not sufficient to determine an individual's probability to be in the prodromal phase of PD. The latter is based on estimates of

background risk combined with diagnostic measures of non-motor, subtle motor signs and, imaging markers expressed as likelihood ratios. Using Bayesian probability statistics, prodromal PD criteria defined by MDS refer to a high probability (>80% certainty) of the disease being present (Berg et al., 2015).

To date, the most important prodromal markers are clinical, as pre-clinical markers which reflect the neurodegenerative process associated with the absence of clinical symptoms have not yet been validated. One of the best described prodromal symptoms is idiopathic REM-sleep behavior disorder (RBD). RBD is a parasomnia characterized by the occurrence of atypical motor, behavioral or cognitive events, related to unlikable dreams and loss of normal REM-sleep muscle atonia (Tekriwal et al., 2017). This condition is by itself rare but quite specific, and cohort studies suggest that idiopathic RBD convert to PD and other synucleinopathies with a pheno-conversion risk of 15-35% between 2-5 years, which increases to 41%-90.9% if extending the follow-up period up to 12–25 years (Hustad and Aasly, 2020).

Hyposmia or olfactory dysfunction – partial or complete loss of the sense of smell – has been recognized as a highly frequent non-motor symptom in PD (about 80% of PD patients have impaired olfaction) and is often one of the earliest prodromal features to emerge (Hustad and Aasly, 2020). Recent evidence indicates that the likelihood ratio of olfactory dysfunction has been raised to 6.4 in the recently revised MDS prodromal criteria (Heinzel et al., 2019).

Another well-established non-motor symptom is constipation characterized by a decrease in stools frequency and/or difficulties in stool passage. Interestingly, α-synuclein inclusions can be found in the gastrointestinal tract 15-20 years before the diagnosis of PD, making constipation one of the earliest detectable prodromal features (Schaeffer et al., 2020). The likelihood ratio for constipation is currently 2.5 (Heinzel et al., 2019). Other important autonomic alterations under discussion as potential prodromal factors for PD are orthostatic hypotension, urinary and erectile dysfunctions (Schaeffer et al., 2020).

Depression and anxiety are common psychiatric symptoms of PD, and they are found to occur in 40-50% of PD patients (Goldman and Postuma, 2014). These conditions have a tremendous impact on quality of life, and although they become significantly more common in patients only about 2 years before PD diagnosis, data indicates that depressive disturbances can occur as a very early prodromal symptom, potentially starting up to 20 years before motor PD (Schaeffer et al., 2020).

In addition to non-motor symptoms, relatively subtle deterioration of the motor system can occur before the patient meets established motor criteria for a clinical diagnosis of PD (Maetzler and Hausdorff, 2012). The most promising prodromal motor signs include slightly voice changes, face akinesia, rigidity, gait dysfunctions, and reduced arm swing (Hustad and Aasly, 2020; Schaeffer et al., 2020), that interestingly are well-described in examined high-risk LRRK2 and idiopathic RBD cohorts (Mirelman et al., 2016, 2011; Postuma et al., 2019).

Molecular imaging techniques such as dopaminergic single-photon emission computed tomography (SPECT) or positron emission tomography (PET) techniques can also provide unique opportunities to evaluate functional changes in prodromal PD. Several studies reported dopaminergic abnormalities in ~40% of patients with idiopathic RBD, and patients with dopaminergic denervation were more prone to have hyposmia and constipation (Iranzo et al., 2010). The lead time of dopaminergic imaging markers is dubious, but different studies have led to estimated intervals of 10–20 years and 3–7 years (the results can change according to factors such as patient age and the type of radionucleotide used) (Postuma and Berg, 2016). Some magnetic resonance imaging (MRI) techniques are other promising tools for the visualization of early CNS changes. Decreased signal in locus coeruleus on neuromelanin-MRI sequences has been linked to RBD in individuals with and without PD, indicating that an impairment of the noradrenergic system can influence the generation of RBD symptoms. Other techniques with potential include white matter abnormalities documented on diffusion MRI, volumetry of the olfactory tract, and abnormalities of network function documented with resting-state functional MRI (Postuma and Berg, 2016; Schaeffer et al., 2020). Another considered technique is the SN ultrasound, where has been possible to detect abnormally high echogenicity in PD patients (Iranzo et al., 2014). In one population-based study, SN hyperechogenicity was associated with a 20-fold increase in the risk of PD. By contrast, a study of patients with idiopathic RBD did not show that hyperechogenicity has a clear predictive value (Postuma and Berg, 2016). Nonetheless, given the non-progression in hyperechogenicity, the lead time for this marker might be long, therefore there is a lack in long-term prospective studies. Moreover, this technique cannot be used in patients with insufficient bone window. For these reasons, whether this hyperechogenicity is a risk marker or a prodromal marker remains unclear (Postuma and Berg, 2016).

Due to extensive research into prodromal PD, the MDS criteria had a first update published in 2019 (Heinzel et al., 2019). Many of the predictive values (likelihood ratios) remain unchanged; the positive likelihood ratio notably increased for olfactory loss and decreased for SN hyperechogenicity; diabetes,

global cognitive deficit, physical inactivity, and low plasma urate levels in men entered the criteria as new markers.

Finally, although there are promising approaches in fluid and tissue biomarker research (e.g., detection of α-synuclein in cerebrospinal fluid (CSF) or the gastrointestinal tract, plasma urate levels in men, neurofilament light chain) currently there are no validated biomarkers to assist in diagnosing PD or determining its neuropathological progression (Hustad and Aasly, 2020).

1.2.2. Clinical phase

According to MDS criteria, PD clinical diagnosis is made on positive grounds based on a combination of symptoms or signs that should be present, and exclusion of symptoms or signs that should not be present (Bloem et al., 2021). The MDS-PD criteria include a two-step process, in which parkinsonism is firstly outlined, being defined by the presence of bradykinesia in combination with rigidity and/or rest tremor. After the parkinsonism diagnosis, the criteria then define whether this is attributable to PD, i.e., when absolute exclusion criteria are absent and red flags are balanced by supportive features (see BOX 1) (Marsili et al., 2018). Two levels of certainty are proposed: the diagnosis of clinically established PD that requires an absence of absolute exclusion criteria, presence of at least two supportive criteria, and no red flags; the diagnosis of clinically probable PD that requires an absence of absolute exclusion criteria, while the presence of red flags is admitted, but this should be counterbalanced by supportive criteria (Postuma et al., 2015). Identification of so-called red flags – specific signs that provide a relative argument against the presence of PD and propose the possible presence of an alternative pathology – can accelerate the diagnostic process, noting that no single red flag provides definitive assurance of a specific diagnosis (Bloem et al., 2021; Poewe et al., 2017).

PD is a heterogeneous disorder with variable clinical phenotypes and natural history, which led to an attempt to classify PD into subtypes. Although there is no consensus on the classification, PD subtypes have been traditionally identified based on clinical observations: i) tremor-dominant PD (with a relative absence of other motor symptoms) and characterized by a slower rate of progression and less functional disability; and ii) non-tremor-dominant PD (which includes phenotypes described as an akinetic-rigid syndrome and postural instability gait disorder) (Kalia and Lang, 2015; Thenganatt and Jankovic, 2014). Furthermore, the different PD subtypes are discussed to have distinct etiologies and pathogenesis. However, this classification has been incorporated very little into PD clinical research, and just a handful of the numerous studies that have looked at risk factors for PD have considered the

risk variables within subtypes. As a result, more research is needed to investigate this issue and address the lack of knowledge translation (Marras and Lang, 2013).

The majority of PD patients also develop non-motor symptoms, that contribute substantially to the disability of affected individuals (Bloem et al., 2021). Non-motor symptoms comprise sleep disturbance, cognitive impairment (including frontal executive dysfunction, memory retrieval deficits, dementia, and hallucinosis), disorders of mood and affect, autonomic dysfunction (mainly orthostatic hypotension, urogenital dysfunction, constipation, and hyperhidrosis), as well as sensory symptoms (most prominently hyposmia) and pain (Schapira et al., 2017). As already mentioned in the description of prodromal PD, some of these symptoms precede the onset of classic motor symptoms sometimes for several years.

Progression of PD involves a worsening of motor features, which initially can be attenuated with symptomatic therapies. However, there is a variety of complications due to long-term symptomatic treatment, including motor and non-motor fluctuations, dyskinesia, and psychosis (Bloem et al., 2021; Kalia and Lang, 2015), that will be discussed further below in this section. Some evidence suggests that a subset of patients with PD will progress to a late phase of the disease, in which disability is designated by levodopa-resistant motor and non-motor symptoms (Coelho and Ferreira, 2012). This late-stage PD includes axial motor symptoms like postural instability, freezing of gait, falls, dysphagia, and speech dysfunction. Dementia is particularly prevalent in this phase, affecting 83% of patients with PD that present 20 years of disease duration (Kalia and Lang, 2015).

BOX 1 | **Diagnostic criteria for Parkinson's disease**

Step 1: diagnosis of parkinsonian syndrome (core feature)
Presence of bradykinesia as a slowness of movement, decrementing amplitude and problematic fine motor control, plus one or more of the following features:

- Muscular rigidity
- 4-6 Hz rest tremor

Step 2: determining PD as the cause of parkinsonism
Two or more supportive criteria:

- Unilateral onset
- Persistent asymmetry affecting the side of onset most
- Rest tremor present
- Progressive disorder
- L-DOPA responsiveness and L-DOPA-induced dyskinesias
- Presence of either olfactory loss or cardiac sympathetic denervation on MIBG scintigraphy
- Clinical course of 10 years or more

Absence of absolute exclusion criteria (some examples):

- Unequivocal cerebellar abnormalities
- Presence of a cerebral tumor or communicating hydrocephalus
- Diagnosis of probable behavioral variant frontotemporal dementia or primary progressive aphagia
- History of repeated strokes, repeated head injury, and definite encephalitis
- Parkinsonian features restricted to the lower limbs for more than 3 years
- Normal functional neuroimaging of the presynaptic dopaminergic system

Red flags (some examples)

- Early falls
- Early bulbar dysfunction
- Bilateral symmetric parkinsonism
- Severe autonomic failure in the first 5 years of the disease (e.g., orthostatic hypotension, and severe urinary retention/incontinence
- Inspiratory respiratory dysfunction

1.3. Motor circuit pathophysiology

Dopaminergic neurons are part of the basal ganglia, a complex circuit that encompasses the striatum (comprising the caudate nucleus and putamen), the nucleus accumbens, the external and internal segments of the globus pallidus (GPe and GPi, respectively), the SN (divided in *pars compacta* and *pars reticulata* (SNpr)), and the subthalamic nucleus (STN). The principal input region of the basal ganglia is the striatum, which receives afferents from regions of the cerebral cortex and the intralaminar nuclei of the thalamus. The major output regions of the basal ganglia are the GPi and the SNpr, which project to the thalamus modulating the activity of cortical regions and to the brainstem (Magrinelli et al., 2016). The main neurotransmitter of the basal ganglia circuit is the inhibitory gamma-aminobutyric acid (GABA), while neurons of the STN use excitatory glutamate, and the ones present in SNpc use DA.

The classical model of the basal ganglia, developed in the late 1980s and early 1990s, formed our understanding of how DA contributes to motor output, and how the loss of dopaminergic neurons leads to basal ganglia-thalamocortical circuits dysfunction underlying PD motor symptoms (McGregor and Nelson, 2019). The correct functioning of the circuitry demands DA release in the striatum, with DA having a dual effect on the striatal projecting neurons – GABAergic output neurons also termed medium spiny neurons (MSNs) – depending on the subtype of DA receptor expressed in the MSNs (Magrinelli et al., 2016; McGregor and Nelson, 2019). The classical model thus divides striatal MSNs into direct and indirect pathway MSNs, based on their projection targets (Figure 2). Direct pathway MSNs project to basal ganglia output (Gpi/SNpr) and express D1-like DA receptors (increase neuronal excitability), and its activation is thought to decrease basal ganglia output, activating the thalamus, and leading to movement. On the other hand, indirect pathway MSNs project to basal ganglia via the GPe and STN and express D2-like DA receptors (exert inhibitory effect). Activation of this pathway leads to thalamus inhibition and consequently movement suppression. Considering that DA increases direct pathway MSNs and decreases indirect pathway MSNs activity, the DA loss present in PD, causes an imbalanced activity between the two pathways at the striatal level, prevailing the indirect pathway. This leads to excessive inhibition of thalamocortical and brainstem motor systems, interfering with normal speed of movement onset and execution (Galvan et al., 2015; Magrinelli et al., 2016; McGregor and Nelson, 2019). More specifically, extreme indirect pathway activity is thought to suppress GPe firing, increase STN activity, and drive an increase in GPi-mediated thalamic inhibition (McGregor and Nelson, 2019). The classical model and its prediction of increased STN and GPi activity in PD fit well with the efficacy of targeting and inhibiting these two nuclei with deep brain stimulation (DBS), which is the gold standard treatment for motor fluctuations and dyskinesia in advanced PD (Giugni and Okun, 2014).

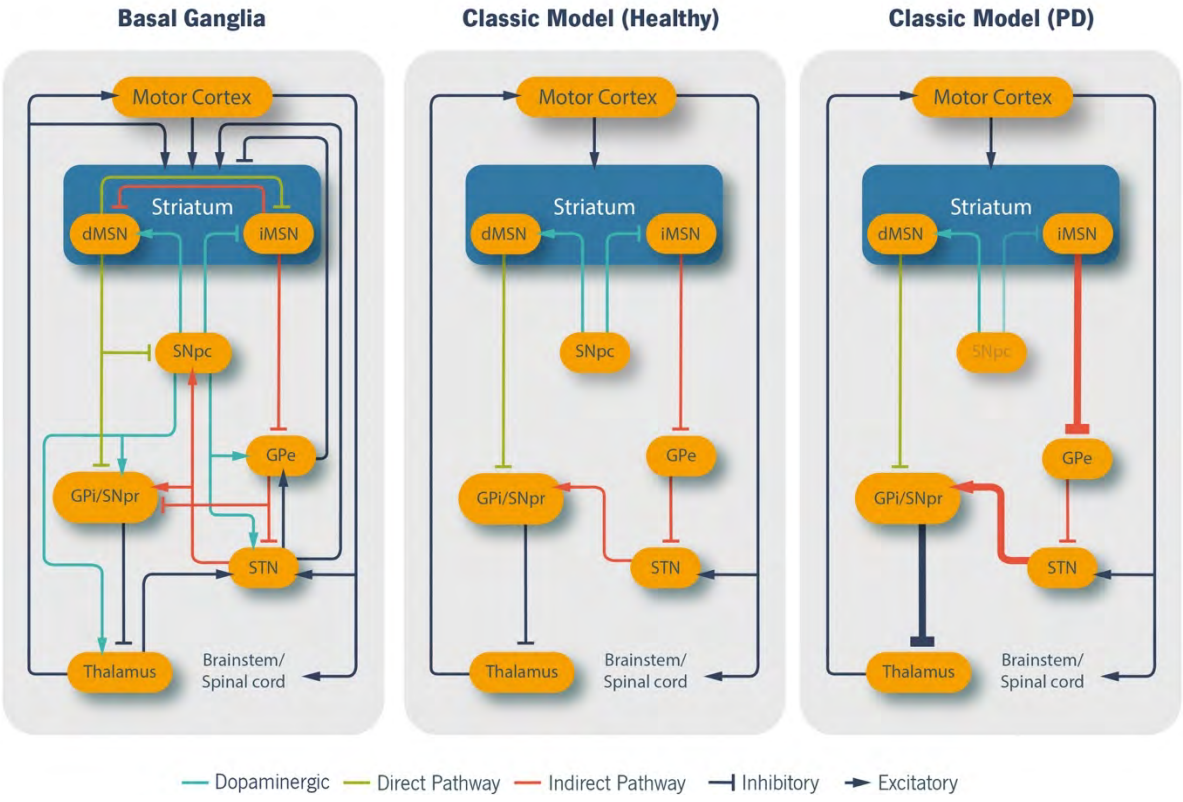


Figure 2. Motor circuitry in Parkinson's disease. The classical model (center) highlights the function of DA on direct and indirect route activity and motor output, simplifying basal ganglia connections (left). DA (clear blue) from the SNpc to the striatum activates direct pathway (green) MSNs and inhibits indirect pathway (red) MSNs in the healthy condition (center). This reduces GPi output, relieving inhibition in the thalamus and cortex and allowing for movement. Loss of SNpc DA produces hypoactivity of the direct pathway and hyperactivity of the indirect pathway in people with PD (right), resulting in excessive GPi output. As a result, movement is suppressed due to excessive inhibition of the thalamus and cortex. Abbreviations: DA, dopamine; GPe, external globus pallidus; GPi, internal globus pallidus; MSNs, medium spiny neurons; PD, Parkinson's disease; SNpc, substantia nigra *pars compacta*; SNpr, Substantia nigra *pars reticulata*. Adapted from (McGregor and Nelson, 2019).

Recently, additional connections have been added to this model like the hyperdirect pathway, a monosynaptic link between the cerebral cortex and the STN, which led to a new concept termed the center-surround model. This model assumes that to execute an action, similar or competing actions must be suppressed at the same time. Therefore, the activation of the hyperdirect pathway produces an enhancement of GPi firing, which in turn inhibit thalamus and cortex to suppress competing actions, thus suggesting a role in preventing premature responses by reinforcing indirect pathway activity (McGregor and Nelson, 2019; Poewe et al., 2017). These connections might also be a potent substrate for PD-related circuit dysfunction (McGregor and Nelson, 2019).

The accepted basal ganglia-thalamocortical indirect and direct pathways model provides important explanations for the origin of bradykinesia in PD but has difficulty in explaining other features such as rigidity, tremor, and some non-motor symptoms (Magrinelli et al., 2016). For instance, some studies already showed neuropathological changes and hyperactivation connectivity in the cerebellum of PD patients, which (Bostan et al., 2010; Jahanshahi et al., 2010; Wu and Hallett, 2013). If these changes represent a pathogenic or compensatory change is still a matter of debate, nonetheless, converging evidence indicates the possible role of the cerebellum in some PD symptoms including tremor (Helmich et al., 2012). Other issues of the classical model rely on the complex arrangement of MSNs that cannot only be explained by a simple direct-indirect pathway imbalance; a large number of basal ganglia neurotransmitters, neuromodulators, and their receptors go beyond GABA, glutamate, and DA; the model is based on the simple concept of firing rate and does not include firing patterns, synchronizations and coincidence. Therefore, future updated models are needed to incorporate a more complex basal ganglia circuitry (Magrinelli et al., 2016).

1.4. Neuropathology

Macroscopically, the idiopathic PD brain is normal with mild atrophy of the frontal cortex and ventricular dilation in some cases. The main typical morphological change is the loss of darkly pigmented area in the SNpc, which directly correlates with the death of dopaminergic neuromelanin-containing neurons in the SNpc (Dickson, 2012). In early-stage disease this neuronal loss is more restricted to the lateral ventral tier of the SNpc, containing the neurons that project to the dorsal putamen of the striatum, while other midbrain dopaminergic neurons are largely spared. It is stated that neuronal loss at the time of symptoms onset is around 30%, adjusted for age, and after the motor symptoms appear, the nigral dopaminergic loss is estimated to increase higher than 60% (Giguère et al., 2018; Kordower et al., 2013). This remarkable cell loss has as consequence the denervation of the nigrostriatal pathway, leading to reduce DA levels in the striatum. Nevertheless, it has been shown that at the early stages of PD, nerve cell death in SNpc is preceded by the loss of axon terminals projecting to the striatum, suggesting a retrograde mechanism of degeneration of the nigrostriatal pathway (Hernandez et al., 2019). Although from the development of neuroprotective therapies point of view it would be extremely important to understand where the degeneration starts exactly, today we still know very little about the molecular mechanisms underlying retrograde axon degeneration (Tagliaferro and Burke, 2016).

The other hallmark of PD is the presence of LBs, which are abnormal cytoplasmatic deposits present in neuronal cell bodies, accompanied by dystrophic neurites (Lewy neurites) that are mostly axonal (Gibb

and Lees, 1988). LBs are distinctive intracytoplasmic inclusions composed of a granular and fibrillar core with a surrounding halo, having as major component filamentous α-synuclein, a protein ubiquitously expressed in the brain, that acquires an amyloid-like filamentous structure and becomes abnormally phosphorylated and aggregated (Olanow and Brundin, 2013). A LB can have between 5 to 30 μm in diameter, and a single neuron can have more than one LB (Spillantini et al., 1998). Besides α-synuclein, the LBs incorporate other proteins such as ubiquitin, tau, parkin, heat shock proteins, oxidized/nitrated proteins, cytoskeletal proteins, proteasomal and lysosomal elements, among others (Xia, 2008).

Currently, it is known that the neuropathological picture of PD is not restricted to SNpc, with other non-dopaminergic nuclei affected including the locus coeruleus, raphe nucleus, dorsal motor nucleus of the vagus, reticular formation of the brain stem, basal nucleus of the Meyner, amygdala, and hippocampus. All these nuclei degenerate with LB pathology, suggesting a common pathogenic process with the one occurring in the SNpc, that might be responsible for the development of some non-motor symptoms (Dexter and Jenner, 2013). Indeed, evidence suggests that LB pathology spreads rostrocaudal, following a predictable stepwise sequence throughout the brain. This concept was introduced in 2003 by Braak and colleagues (Braak et al., 2003), indicating that the initial sites displaying LB lesions are the dorsal motor nucleus, the reticular formation, and the anterior olfactory nucleus (Stage 1 and 2) progressing in an upward direction to the midbrain (stage 3; where the typical clinical motor features begin to manifest) and from there to the locus coeruleus and the amygdala, subsequently extending to the temporal limbic cortex (stage 4), finally reaching the neocortex and high-order areas like prefrontal cortex and primary sensory and motor areas (stages 5 and 6). Clinically, this is thought to cause severe PD with significant gait problems and dementia (Dexter and Jenner, 2013). Nonetheless, the Braak system was later revised, proposing a "dual-hit hypothesis", where the α-synuclein spreading pattern may, in fact, be initiated in nasal and intestinal mucosal sites, specifically in the olfactory bulb and the enteric cell plexuses (Hawkes et al., 2007).

Despite the existence of considerable evidence supporting Braak's hypothesis, this staging system has been a target of controversy, as a significant portion of PD patients (~7-11%) do not follow the pattern described above (Rietdijk et al., 2017). Moreover, this hypothesis only considers LB-related pathology, disregarding neuronal loss that is also a hallmark of PD neuropathology, as well as it has been difficult to correlate the Braak stating with PD clinical manifestations (Jellinger, 2009; Surmeier et al., 2017). These drawbacks raised new hypotheses, and evidence suggests that α-synuclein aggregates can

spread from one neuron to another in a prion-like manner (Masuda-Suzukake et al., 2013; Volpicelli-Daley and Brundin, 2018). According to this, small amounts of fibrillar α-synuclein act as seeds that can trigger the conversion of normal/soluble α-synuclein into insoluble aggregates. *In vitro* studies demonstrated that recombinant α-synuclein can polymerize into amyloidogenic fibrils with similar morphologies and staining as those observed in disease-affected brains (Ma et al., 2019). Moreover, when treating SH-SY5Y cell lines with recombinant human α-synuclein short amyloid fibrils resulted in sustained aggregation and accumulation of endogenous α-synuclein (Aulić et al., 2014). In animal studies, young mice injected with aggregated α-synuclein or synthetic α-synuclein fibrils displayed spread α-synuclein inclusions throughout the brain resulting in early-onset motor symptoms, and reduced mice lifespan (Luk et al., 2012b; Mougenot et al., 2012). Synthetic α-synuclein fibrils injected in the striatum of wild-type mice also induced widespread Lewy-pathology: firstly, in neurons that directly project to the site of injection like SNpc, amygdala, and cortex, and then sparse aggregates also appear in neuron populations of the olfactory bulb and hippocampus (Luk et al., 2012a; Masuda-Suzukake et al., 2014, 2013). The formation of α-synuclein inclusions in the SNpc leads to the death of dopaminergic neurons, and as consequence motor deficits, demonstrating the development of the two hallmarks of PD neuropathology (Luk et al., 2012a).

Because olfactory bulb pathology is a condition of varied synucleinopathies, recent studies have also highlighted how α-synuclein fibrils injected into the olfactory bulb of wild-type mice can trigger a slowly progressing (described up to one year) α-synucleinopathy throughout the olfactory system and interconnected brain (Rey et al., 2016, 2013).

Indeed, several studies have been undertaken in recent years to confirm the similarities in mode of action between misfolded α-synuclein and prions. Even though there is a lot of evidence to support this hypothesis, all information on α-synuclein propagation comes from *in vitro* and experimental animal models, not from humans. Another difference is that PD is not rapidly progressive like prions. Moreover, it is also important to understand if the prion-like theory fits or not into Braak's hypothesis (Ma et al., 2019; Rietdijk et al., 2017). Addressing all these issues in the future it will have a major impact on the molecular understanding of pathogenesis in PD.

1.5. Mechanisms of neurodegeneration

Genetic forms of PD and postmortem studies have provided crucial clues to the mechanisms underlying the neuropathology of the disease. The α-synuclein aggregation has been in the center stage of the development of the disease, but a variety of other processes are assumed to be involved in the onset and progression of PD such as abnormal protein clearance, mitochondrial dysfunction, oxidative stress, and neuroinflammation (Figure 3).

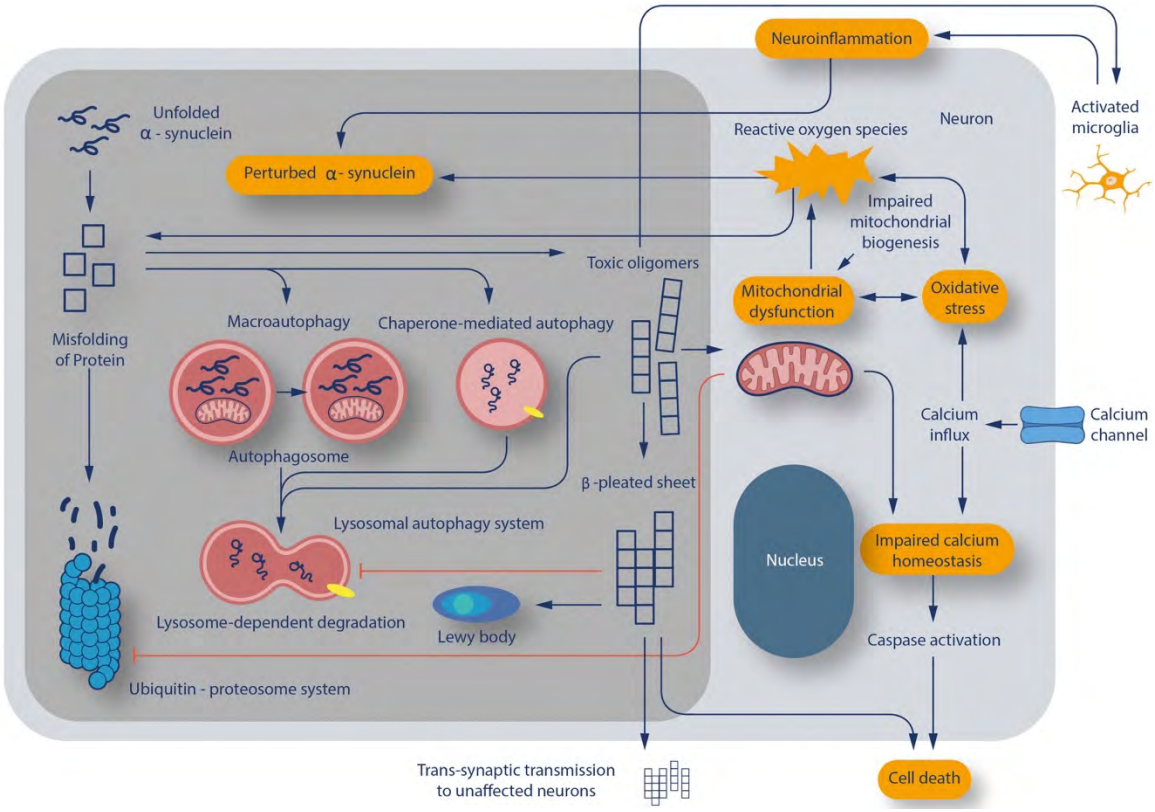


Figure 3. Molecular mechanisms involved in Parkinson's disease. Schematic diagram of the interplay between major molecular pathways that are implicated in the pathogenesis of the disease. Adapted from (Poewe et al., 2017).

1.5.1. α-synuclein misfolding and aggregation

α-synuclein is expressed throughout the body but has the highest expression levels within the brain. In neurons, α-synuclein is localized to nerve terminals, and although its normal neuronal function is still not fully understood, it is hypothesized that it occurs in the cytosol, possibly also in mitochondria and the nucleus, having a role in synaptic vesicle dynamics, mitochondrial function, intracellular trafficking and might be a potential chaperone (Vekrellis et al., 2011). Native α-synuclein is mainly unfolded in normal conditions, with no identifiable tertiary structure. However, α-synuclein folds into α-helical

structures when it interacts with negatively charged lipids, such as the phospholipids that make up cell membranes (Eliezer et al., 2001; Ulmer et al., 2005). This balance between unstructured monomeric forms and tetrameric α-helical oligomers, that are resistant to fibrilization under physiological conditions, emphasize the key point that the dynamic structure of α-synuclein may play role in PD pathogenesis. In PD, α-synuclein adopts a β-sheet-rich amyloid-like structure that is prone to aggregate. Aberrant α-synuclein function or structure may produce different oligomers, which may be toxic *per se*, or fibril into toxic species (Bartels et al., 2011; Wang et al., 2011). In fact, different species of α-synuclein are found in PD brains, including unfolded monomers, soluble oligomers, protofibrils, and high molecular weight insoluble fibrils (Barrett and Timothy Greenamyre, 2015).

The identification of mutations in SNCA, the gene encoding α-synuclein, causing heritable forms of PD, also strongly supports the notion that α-synuclein is a key player in PD. Similarly, GWAS revealed a single-nucleotide polymorphism associated with SNCA locus that alters the risk for idiopathic PD, which is linked with increased expression levels of α-synuclein (Nalls et al., 2014). Although the exact role of SNCA-associated mutations is still under investigation, it is known that some of them like A30P and A53T, can alter the rate at which α-synuclein oligomerizes and or/aggregates into LBs (Barrett and Timothy Greenamyre, 2015). In addition to genetic changes, α-synuclein is extensively post-translationally modified in PD. The modifications include nitration and phosphorylation – both found in LBs from PD patients - and modification by DA, mechanisms that are nicely reviewed by (Barrett and Timothy Greenamyre, 2015). An age-related progressive decline in proteolytic defense mechanisms within the brain could also influence the accumulation of α-synuclein (Poewe et al., 2017).

1.5.2. Dysfunctional protein clearance systems

The ubiquitin-proteasome system (UPS) and the Lysosomal autophagy system (LAS) are the two key protein clearance processes in cells that remove defective proteins (Dexter and Jenner, 2013). The UPS is primarily required for non-lysosomal degradation and removal of short-lived, misfolded, and damaged (e.g., due to oxidative stress) proteins. This is performed through a sequence of enzyme-mediated events that first recognize aberrant proteins and covalently bind them to multiple ubiquitin molecules as a destruction signal. Proteins are ubiquitinated, allowing them to be recognized, unfolded, deubiquitinated, and translocated into the proteasome's core, where they are destroyed (McNaught et al., 2001). On the other hand, autophagy is a cellular catabolic process that transports cytosolic components to the lysosome for destruction, including long-lived proteins, protein aggregates, and

defunct organelles. Dependent on the mechanisms by which the distinct components are delivered to the lysosome, LAS has been subdivided into three subtypes: macroautophagy, microautophagy, and chaperone-mediated autophagy (CMA). Briefly, in macroautophagy, intracellular components, such as cytosolic proteins, are absorbed by the autophagosome, which subsequently combines with the lysosome, causing the lysosome's contents to be broken down. Microautophagy, on the other hand, involves the lysosome consuming and destroying cytoplasmic components on its own. CMA is a more selective mechanism in which molecular chaperones identify and transport certain proteins to the lysosome for destruction (Pan et al., 2008; Rivero-Ríos et al., 2016). Damage to either the UPS or LAS is implicated in the pathophysiology of PD by contributing to the accumulation of dysfunctional proteins, particularly soluble misfolded α-synuclein (Ebrahimi-Fakhari et al., 2012; Lee et al., 2004).

Ubiquitin-proteasome system (UPS)

Evidence of proteasomal abnormalities in PD was provided by postmortem analysis, where the UPS' catalytic activity was found markedly reduced in the SNpc of PD brains (McNaught and Jenner, 2001). Similar findings were also reported in peripheral blood mononuclear cells of PD patients contrary to healthy controls (Ullrich et al., 2010). Additionally, structural proteasome alterations were also identified, including loss of α-subunit (the component that regulates and stabilized the proteasome complex), and lower expression of other molecules involved in the normal function of the UPS such as PA70mm and PA28 (proteasome activators) (McNaught et al., 2003, 2002a). UPS involvement was also supported by genetic studies through the identification of two PARK genes associated with monogenic PD encodes proteins involved in UPS function, namely, PRKN and UCH-L1 (Dexter and Jenner, 2013).

Following on from findings in human PD, the use of proteasomal inhibitors was discovered to selectively destroy dopaminergic neurons in cell culture studies (McNaught et al., 2002b; Xie et al., 2010). The initiation of cell death led to a cascade of events involving increases in oxidative and nitrative stress and damage, as well as alterations in mitochondrial function (Hyun et al., 2003). In animal models, marmosets injected with the toxin MPTP decreased enzyme activity in the UPS, in addition to diminished levels of the 26S subunit components (Zeng et al., 2006). Similarly, transgenic mice with proteasomal defects (knockout for 26S proteasome regulatory subunit 4) exhibited dopaminergic cell degeneration and observed LB-like inclusions in the brain (Bedford et al., 2008). Furthermore, the probable role of UPS has been validated numerous times and supported by microarray and

transcriptional studies on laser-captured microdissected nigral dopaminergic neurons from PD (Grünblatt et al., 2004).

Lysosomal autophagy system (LAS)

Similar to UPS, several lysosomal and autophagy-related components are dysfunctional or differently expressed in PD. The levels of autophagosome marker LC3-II were increased in nigral neurons of PD patients, indicating an accumulation of autophagic vacuoles (Dehay et al., 2010; Tanji et al., 2011). Furthermore, vital proteins of lysosomal membranes (LAMP1 and LAMP2A), and several molecular chaperones from the heat-shock protein family (such as hsc70 and hsp35) were found to be reduced (Alvarez-Erviti et al., 2010; Chu et al., 2009). Other findings supporting the hypothesis that malfunction in LAS might contribute to PD pathogenesis, were the identification of point mutations in PINK1 and PRKN, both of which are involved in the autophagic turnover of mitochondria (Dexter and Jenner, 2013). Furthermore, of particular interest is the discovery of a point mutation in the gene of the lysosomal protein ATP13A2 (PARK9), leading to an autosomal recessive atypical parkinsonian syndrome, referred to as Kufor–Rakeb syndrome (Williams et al., 2005). The Gaucher disease (leading to a 20- to 30-fold increase in the risk of developing PD), a lysosomal storage illness caused by mutations in the GBA gene, is another strand indicating lysosomal involvement in neuronal loss in PD. The lysosomal enzyme GCase, which catalyzes the conversion of the sphingolipid glucosylceramide to ceramide, is deficient as a result. In line with this, a GCase deficit has recently been discovered in the SN of patients with PD and GBA mutations, as well as those with idiopathic PD (Dexter and Jenner, 2013; Velayati et al., 2010).

Evidence from different disease models showed that for instance, silencing LAMP2A activity in a dopaminergic cell line, reduced chaperone-mediated autophagy and increased the half-life of α-synuclein. Altered handling of α-synuclein can also be induced by disruption/mutation of the lysosomal membrane protein ATPase (ATP13A2) (Usenovic et al., 2012). In addition, MPTP-treated mice presented depletion of lysosomes in dopaminergic cells secondary to the onset of oxidative stress that led to the accumulation of autophagosomes and cellular degeneration. The MPTP-induced toxicity was attenuated by pharmacological and genetic treatments that enhanced lysosomal formation (Dehay et al., 2012, 2010). Alterations in autophagy and mitophagy also occur in response to nigral neuronal degeneration induced by other neurotoxins such as 6-hydroxydopamine (6-OHDA) (Marin and Aguilar, 2011; Solesio et al., 2012).

1.5.3. Altered mitochondrial function

Mitochondrial impairments have been implicated in several neurodegenerative diseases and are considered a key element in the pathogenesis of both familial and idiopathic PD (Bose and Beal, 2016). One of the first pieces of evidence linking mitochondrial dysfunction and PD was the described deficiency of mitochondrial-complex I (a fundamental component of the electron transport chain) found through postmortem studies in the SNpc of PD brains (Schapira et al., 1990), that was also detectable in muscle and platelets of PD patients (Bindoff et al., 1991; Krige et al., 1992). The discovery of MPTP's neurotoxicity, and the follow-up studies showing that its oxidation is taken up by dopaminergic neurons and leads to complex I inhibition, reinforce the role of mitochondrial dysfunction in the context of PD (Elbaz et al., 2009). Moreover, other toxins like rotenone and paraquat also shown to damage mitochondrial complex I activity, inducing degeneration of dopaminergic neurons and parkinsonism in animal models and potentially in humans (Tanner et al., 2011). This converging evidence indicates that mitochondrial complex-I may be critical in driving dopaminergic cell death due to energy depletion (Moon and Paek, 2015).

The interest in the role of mitochondria also emerged from genetic investigations, since PINK1 and PRKN mutations have been associated with altered mitochondrial function, given their crucial role in selective degradation of defective mitochondria by mitophagy. These mutations can also lead to alterations of protein localization in mitochondria in PD, abnormalities in mitochondrial structure and function, and a decrease in complex I assembly and activity. Moreover, loss of function of DJ-1, but also PINK1 *and* PRKN, increases mitochondrial dysfunction by decreasing mitochondrial protection against oxidative stress (Schapira, 2008; Anthony H. V. Schapira, 2011).

The interaction between α-synuclein pathology and mitochondrial dysfunction has also been investigated in the context of PD, and accumulation of this protein is thought to interact with complex I, influencing mitochondria homeostasis (Poewe et al., 2017). Even though the mechanism behind α-synuclein actions remains to be fully elucidated, a recent study showed that oligomeric α-synuclein binds with high affinity to the mitochondrial receptor TOM20, leading to an impairment in protein import, and having as consequences deficient mitochondrial respiration, enhanced reactive oxygen species (ROS) production and loss of mitochondrial membrane potential (Di Maio et al., 2016). Another study reported that oligomeric α-synuclein negatively impacts complex-I-dependent respiration, by inducing selective oxidation of the ATP synthase and mitochondrial lipid peroxidation. These events lead to mitochondrial swelling, and ultimately to cell death (Ludtmann et al., 2018).

Other important findings were originated from transcriptome studies, showing that genes controlling cellular bioenergetics that are expressed in response to peroxisome proliferator-activated receptor-γ co-activator 1α (PGC-1α; a mitochondrial transcriptional regulator) are generally subexpressed in PD (Elstner et al., 2011). Loss of dopaminergic neurons *in vitro*, induced by rotenone and mutant α-synuclein was avoided duo to PGC-1α activation and linked with increase expression of nuclear-encoded subunits of the mitochondrial respiratory chain (Pacelli et al., 2011; Shin et al., 2011; Zheng et al., 2011). Moreover, the expression of mitochondrial DNA transcriptional factors (TFAM and TFB2M) is decreased in the SNpc of patients with idiopathic PD, possible because of impaired NRF1/2 signaling (Grünewald et al., 2016).

1.5.4. Neuroinflammation

It is currently accepted that neuroinflammation is a prominent characteristic of PD, and while initially thought to be a secondary phenomenon, today we know that inflammatory responses are important components of PD pathogenesis (Ransohoff, 2016). Microglial and complement activation, T-lymphocyte infiltration, and higher concentrations of pro-inflammatory cytokines have been observed in the SNpc and striatum of PD patients. Furthermore, compared to healthy subjects, increased microglial activation early in PD in the brainstem, basal ganglia, and frontotemporal cortices, with additional involvement of the parietal and occipital cortices in patients with PD dementia was also demonstrated (Edison et al., 2013; Gerhard et al., 2006; Hirsch and Hunot, 2009; Loeffler et al., 2006).

Several lines of evidence support a role for neuroinflammation mainly mediated by activated microglia. Microglia are phagocytic cells of the CNS's innate immune system that normally present a resting state but become activated in response to brain injury or immunological assault (Block et al., 2007). Superoxide and nitric oxide are produced by activated microglia, which contribute to oxidative and nitrative stress in the brain microenvironment. They can also contribute to neurodegeneration by creating harmful substances like glutamate and tumor necrosis factor-α (Dias et al., 2013). Initial studies with rodent models of PD using neurotoxins showed that inhibiting microglial activation resulted in a significant reduction of dopaminergic cell death in the SNpc, suggesting that microglia-induced inflammatory processes may be contributing to the degeneration of these cells (He et al., 2001; Wu et al., 2002). There is also a growing body of evidence that α-synuclein can directly activate microglia and promote inflammatory processes. In primary cultures, for example, α-synuclein activates microglia in a dose-dependent manner (Su et al., 2008).

Besides microglia, astrocytes might also be involved in PD pathogenesis. Astrocytes are the most common type of glial cell in the mammalian CNS, with a wide range of functional characteristics. Aside from providing structural support to neurons, astrocytes have a role in metabolic support and energy control by secreting neurotrophic substances, maintaining BBB integrity, and modulating synaptic transmission and neuronal excitability, among other functions (Domingues et al., 2020). Because so many key brain activities rely on proper astrocyte-neuron interactions, some abnormal circumstances are likely triggered by a malfunction or failure in this process at some level. This could be the case in PD, where astrocytes have been shown to play a key role in the onset and progression of the disease, as the distribution of α -synuclein-positive astrocytes is similar to the distribution of LBs (Charron et al., 2014). Furthermore, the loss of dopaminergic neurons in the SNpc is linked to an increase in the number of activated astrocytes (McGeer and McGeer, 2008). The density of astrocytes in the SNpc is low, which may difficult their ability to effectively maintain and preserve dopaminergic neurons. In line with this, some evidence shows that, in the context of PD, astrocytes become dysfunctional and lose their protective abilities, rather than exhibited reactive astrogliosis phenotype (Ramos-Gonzalez et al., 2021). For instance, interesting findings showed that astrocytes derived from induced pluripotent stem cells (iPSCs) presenting LRRK2 G2019S mutation, manifest increased expression of α-synuclein. This resulted in altered metabolism, disturbed Ca^{2+} homeostasis, and increased release of cytokines upon inflammatory stimulation (Sonninen et al., 2020).

Nonetheless, activated microglia and astrocytes were also found to have neuroprotective effects on dopaminergic neurons, for instance, by the secretion of neurotrophic factors (Domingues et al., 2020). Understanding this 'dual' role of glial cells could be crucial in developing new thoughts and insights for the treatment of PD. Moreover, whether neuroinflammatory responses are a direct cause of neurodegeneration or are triggered in reaction to neuronal injury, is still a matter of debate. As a result, immune system modification remains a promising topic for disease-modifying therapies.

1.5.5. Iron accumulation

Iron is necessary for nearly all cell types, including brain cells. For instance, it is an important co-factor for proteins involved in neural tissue proper function, such as the non-heme iron enzyme tyrosine hydroxylase (TH), that is required for catecholamine neurotransmitter production. Iron has a heterogeneous geographic distribution in normal brains, with higher concentrations in the GP, putamen, and SNpc of the basal ganglia. However, there is an abnormal progressive deposition of iron in the SNpc with aging and degenerative disorders like PD, as well as a rise in free iron concentration

(Dashtipour et al., 2015; Dias et al., 2013). Compared to controls, postmortem brain tissue from PD patients had higher amounts of iron in the SNpc (Dexter et al., 1991; Kosta et al., 2006). Nonetheless, the specific stage of PD at which iron changes occur is unknown. Moreover, high iron levels are either a cause or a result of neuronal death remains a topic of debate (Dashtipour et al., 2015; Dias et al., 2013). Iron is currently thought to be cytotoxic and capable of producing oxygen free radicals, which when combined with dopamine oxidation, can cause neurotoxicity (Dashtipour et al., 2015). Experimentally, feeding a high-iron diet to one-month-old weanling mice or stereotaxic iron infusion into the SNpc of rats causes a considerable rise in iron levels in the striatum, which is related to decreased total glutathione and increased hydroxyl radical levels (Sziráki et al., 1998). In addition, different studies demonstrated that iron chelators (responsible for lowering iron levels) protect against toxin-induced striatal lesions (Ben-Shachar et al., 1991; Lan and Jiang, 1997). Additionally, exposure of neonatal mice to iron results in PD-like neurodegeneration with age, with animals exhibiting striatal DA depletion and nigral neuronal loss by 12 and 24 months of age, respectively, and becoming more vulnerable to toxic injury (Kaur et al., 2007). Important of note is that iron does not readily cross the blood-brain barrier (BBB), therefore the accumulation of iron in some brain regions in PD could indicate that it has translocated from one anatomical place to another (Dashtipour et al., 2015).

Correlations between MRI signals and iron concentration have been established using a variety of imaging techniques. Several studies have recently attempted to test brain iron levels *in vivo* in patients with PD, with the majority of research indicating that patients with PD have more iron in their SN than non-affected control subjects. However, these findings have not been replicated between all studies, and no one study was able to determine an iron threshold value that can be used as a biomarker to differentiate between patients with PD and healthy controls (Dashtipour et al., 2015; Péran et al., 2010; Rossi et al., 2014).

1.5.6. Oxidative stress

Oxidative stress is a central concept underlying the loss of dopaminergic neurons, and compelling evidence has been showing that the formation of ROS is the final step of neuronal death regardless of the origin (Dexter and Jenner, 2013). Increased quantities of oxidized lipids, proteins, and DNA are found in the brain tissue of PD patients, indicating increased levels of oxidative stress (Bosco et al., 2006; Nakabeppu et al., 2007). However, the exact cause of oxidative stress is unknown. Iron accumulation in the SNpc, changes in calcium channel activity, altered proteolysis, changes in synuclein aggregation, and the presence of mutant proteins are all examples of how oxidative stress can

be induced in PD, with ROS formation originating from mitochondria being the most likely contributor to this process (Dexter and Jenner, 2013; Poewe et al., 2017).

Mutations in DJ-1, associated with autosomal recessive early-onset parkinsonism, are of particular interest because are linked to increased cellular oxidative stress. As previously mentioned, DJ-1 is a stress sensor, participating in a variety of signalling pathways including control of mitochondrial quality and reaction to oxidative stress (Dolgacheva et al., 2019). DJ-1 may protect neurons from oxidative stress-induced cell death by controlling mitochondrial homeostasis or by acting in the oxidative stress response as an antioxidant scavenger or as a redox sensor, according to data from *in vitro* models (Di Nottia et al., 2017). Additionally, knocking out DJ-1 in mice results in increased protein oxidation in stressed dopaminergic neurons of the SNpc (Dias et al., 2013).

Allied to all these issues, nigral dopaminergic neurons have also been suggested to be especially sensitive to oxidative stress due to different aspects: i) they present very long and unmyelinated axons with a high number of synapses, which implicates a lot of energy; ii) they engage in independent pacemaking including cytosolic calcium oscillations and calcium extrusion at the cost of energy; and iii) elevated cytosolic DA and its metabolites can result in harmful oxidative stress (Bolam and Pissadaki, 2012; Mosharov et al., 2009; Pissadaki and Bolam, 2013).

To summarize, significant progress has been achieved in identifying cellular and molecular mechanisms connected to the etiology of PD. Rather than pinpointing a single cause for neurodegeneration, these data underscore the disease's enormous complexity. The relationship between these pathways is yet unknown, and one of the goals of PD research is to discover out how they work together and interact.

2. Experimental models of Parkinson's disease

2.1. In vitro

In vitro studies can provide powerful tools to study the cascade of neurodegenerative events, and to better understand the cellular and molecular mechanisms underlying PD. Furthermore, modeling PD in a dish enables for rapid pathology development, easy pharmacological and genetic alterations, and large-scale testing in a relatively short period of time (Martínez-Morales and Liste, 2012). Different culture systems have been developed to study the pathogenies of PD, ranging from cell lines, primary and organotypic cultures to more advanced techniques such as PD-specific iPSCs models and 3D human brain organoids.

2.1.1. Cell lines, primary cultures and organotypic cultures

Traditional *in vitro* cell culture techniques typically implicate 2D monolayers in standard tissue-culture plates, petri dishes or coverslips (Slanzi et al., 2020). These are frequently based on immortalized cell lines such as pheochromocytoma (PC12) cells, human neuroblastoma cell line SH-SY5Y, Lund human mesencephalic (LUHMES) cells, among others. Although this type of cell lines can be easily genetically manipulated, offering high-throughput and reproducible testing, the use of these models is limited because of their high proliferative state which is in clear contrast with neuronal features (Ferrari et al., 2020).

Primary dopaminergic cultures and organotypic cultures, obtained from rodent brain tissue, have the potential to overcome many of the difficulties inherent to cell lines, since the neurons present within these cultures are similar to human ones in terms of morphology, physiology, and proliferation rates (Slanzi et al., 2020). Although the primary neurons are often contaminated with glial cells, which can be seen as an advantage, organotypic slice culture models maintain the *in vivo* cellular interactions and 3D structure of the host region that remain for weeks or even moths. Nonetheless, both systems can be used to model PD by for instance exposing them to toxic agents, thus providing important platforms to assess the neuroprotective effects of different agents (Slanzi et al., 2020; Stahl et al., 2009). Nonetheless, the variations among different culture preparation, the difficulty to maintain them and species-dependent differences, affects the reproducibility of the experiments (Ferrari et al., 2020; Slanzi et al., 2020).

2.1.2. Stem cell-derived neurons for Parkinson's modeling

In the realm of stem cell therapy and regenerative medicine, tremendous progress has been made in the last decade. The limited regeneration potential of the CNS, combined with the complicated clinical and histological aspects of PD, makes the development of acceptable disease models extremely difficult (Liu and Cheung, 2020). Stem cells are the key elements for all tissue and organ system of the body and mediate distinct roles in development, disease progression, and tissue repair processes. They are characterized by the capacity to renew themselves and to differentiate into more specialized cells, being classified according to their differentiation potential as follows: totipotent stem cells, that can create an entire organism; pluripotent stem cells, that give rise to all cell types from the three embryonic germ layers (mesoderm, ectoderm, and endoderm); and multipotent cells that can yield a more restricted subset of cell lineages (van der Kooy and Weiss, 2000). The first and best-described type of pluripotent

stem cells were embryonic stem cells (ESCs), derived from the inner cell mass of the blastocyst, being therefore very primitive (Fortier, 2005). Since their discovery in 1981, ESCs have been widely used to differentiate into distinct cell types aiming to treat diseases like diabetes, heart failure, and different neurodegenerative diseases (Vazin and Freed, 2010). Because of their properties, these cells have been used to generate dopaminergic neurons using a variety of methods ranging from the use of co-cultures with stromal cells, growth and transcription factors and morphogens, for study PD *in vitro*, cell-replacement therapies, and drug testing. However, ESCs require the destruction of the embryo which implies ethical and moral concerns in their isolation and further application (Vazin and Freed, 2010).

A big step in the field was the discovery of the Yamanaka factors (Oct3/4, Sox2, KIf4, and c-myc) that *via* retroviral delivery generated pluripotent stem cells from mouse fibroblasts (Takahashi and Yamanaka, 2006), being later reprogrammed in human somatic cells (Nakagawa et al., 2008; Yu et al., 2007). Nowadays, different protocols have been used to generate iPSCs from dermal fibroblasts, hematopoietic stem cells, adipocytes, and peripheral blood mononuclear cells (Gois Beghini et al., 2020). Moreover, Swistowski et al. (Swistowski et al., 2010) demonstrated that iPSC lines derived from different somatic cell populations were successfully grown in ESC-based protocols, having similar morphology, differentiation potential, and gene expression. Today, several highly efficient iPSC-reprogramming strategies are widely used to obtain a variety of cell types within the CNS, including neural precursor cells, glial and BBB cells (LaMarca et al., 2018).

One of the major challenges of using iPSCs for disease modeling and personalized medicine is to efficiently generate therapeutically target cells like functional neurons. In the case of PD, it is essential to obtain a specific, reproducible, and standardized differentiation protocol into midbrain dopaminergic neurons (Shi et al., 2017). The ability to generate them from iPSCs has proved to be particularly insightful, with current differentiation protocols using dual-SMAD inhibition followed by sonic Hedgehog (SHH) and fibroblast growth factor 8b (FGF8b) signaling, and subsequent maintenance in brain-derived neurotrophic factor (BDNF), glial cell line-derived neurotrophic factor (GDNF), ascorbic acid, and cAMP (Marotta et al., 2020). Importantly, multiple studies have been able to recapitulate key PD pathological features and shed light on new mechanistic pathways using patient-specific cell lines with relevant genetic backgrounds, allowing new opportunities for gene discovery and therapy (LaMarca et al., 2018; Marotta et al., 2020).

In fact, iPSC-derived dopaminergic neurons obtained from familial and idiopathic PD patients exhibited cellular abnormalities like de ones described in section 1.5, such as mitochondrial dysfunction, increased oxidative stress, impaired autophagy, and mitophagy, irregular DA metabolism, among others (Cobb et al., 2018; LaMarca et al., 2018). iPSC-derived neurons have been used in early-stage drug discovery pipelines, from testing a limited set of candidate compounds to mini-screens using a focused set of compounds through medium-scale screening. These studies have paved the way for the use of iPSC-derived cells as a reliable proxy for human disease, making it easier to build robust assays before screening large drug libraries (Little, Ketteler, Gissen, & Devine, 2019). Regarding PD, therapeutical strategies have currently shown potential in inhibiting overactive proteins, rescuing phenotypes with wildtype proteins, or using agonists to rescue the activity of associated proteins, as reviewed recently by Marotta and colleagues (Marotta et al., 2020).

Despite the numerous advantages of using iPSC technology, there are some key points that need to be addressed. One of them relies on the immaturity of iPSC-derived neurons, which may not be suitable to study an age-associated disorder like PD (Mohamed et al., 2019). Another thing that should be taken into consideration is the significant line-to-line variability across patients, and also within clonal populations of the same individual. This could be explained in part due to variations between experiments and distinct genetic backgrounds between Patients (Mohamed et al., 2019). Therefore, we should be critical in the interpretation of the results and find strategies to circumvent this variation. One of them is to take advantage of genome editing techniques, like CRISPR technology, to create isogenic lines, by either introducing a genetic mutation in a control line or correcting a mutation in a patient line (Mohamed et al., 2019). Another approach that can be used in iPSC-based studies, is to produce 3 or more independent batches of differentiation (Marotta et al., 2020). It is also important to highlight the need for standardized differentiation protocols, especially for efficient generation and validation of A9 dopaminergic neurons (Marotta et al., 2020). Finally, iPSC-derived neuronal cultures are extremely costly, due to the sheer cost of media, peptides, small molecules, supplements, and consumables that are required for iPSC maintenance and throughout the duration of neuronal differentiation.

2.1.3. Brain organoids

The CNS is a dynamic physiologic microenvironment where chemical and mechanical alterations continuously occur due to cell-cell and cell-extracellular matrix (ECM) interactions. Additionally, the neurodegeneration underlying PD is not a neuron-autonomous process, involving interaction between different cell types (Hirsch et al., 2013). Therefore, attempts have been made to create more accurate

in vitro models for different applications. To obtain neurons that have the same characteristics and behavior (e.g., formation of synapses, myelination, firing between neurons) as they have in the human body, it is crucial the presence of other cell populations in culture, such as astrocytes, microglia, oligodendrocytes, and other subtypes of neurons besides the desired ones (Mohamed et al., 2019). For that, we can take advantage of systems inspired by organs-on-chip work like co-culture systems and 3D organoid models. In this section, we will focus on human brain organoids and how can be used for modeling PD (Figure 4).

Generating brain organoids

In the near past, most stem cell culture systems were focused on single-cell populations, missing the complete set of cell types that compose an organ. However, since 2013 this starts to change with the development of organ-like 3D tissue cultures (Lancaster and Knoblich, 2014). The definition of organoid involves three main features, that are basic characteristics of an organ: contain organ-specific cell types (i.e., stem cells, neurons, and glial cells); capacity to recapitulate some functions of the organ (e.g., production of neurotransmitters); and ability to self-organize in a way that resembles *in vivo* (Lancaster and Knoblich, 2014). The ability of cells to self-organize was already observed in the early 1990s when Wilson et al. showed the potential of dissociated sea sponges to reaggregate into a whole organism (Wilson, 1907), which was later demonstrated in other organisms (Child, 1928; Wilson, 1911). Afterward, this dissociation-reaggregation process was demonstrated using cells from chick embryos (Moscona, 1957; Moscona and Moscona, 1952). Indeed, dissociated cells from vertebrate organs such as skin, liver, and kidney, can under the right conditions, organize into 3D aggregates to reconstitute the tissue (Weiss and Taylor, 1960).

The work of Yoshiki Sasai's lab was a pioneer in 3D neuronal tissue development using mouse and human stem cells. This work was inspired by the experiments established by Zhang and colleagues, showing the capacity of embryoid bodies (EBs) to generate clusters of neuroepithelial stem cells that self-organized to form neural rosettes (Zhang et al., 2001). They demonstrated that serum-free suspension of EBs aggregates forms more complex structures when allowed to grow in 3D for long periods, with the addition of specific inductive signals, eventually leading to dorsal forebrain generation (Eiraku et al., 2008; Watanabe et al., 2005). Later, the same group demonstrated the formation of self-organized optic up from a 3D culture mouse ESCs aggregates, displaying features of retinal architecture (Eiraku et al., 2011). These findings prompted advances in organoid technology, and the work of Sato et al. (Sato et al., 2009) in intestinal organoids have inspired the big step in brain organoid field.

Currently, brain organoid models have been widely used to study human brain disorders, and two different methodologies can be used to generate them: i) unguided methods, that are based on spontaneous morphogenesis and intrinsic differentiation ability of pluripotent stem cell aggregates, and ii) guided methods that require external patterning factors to induce differentiation in specific structures (Qian et al., 2019).

Unguided protocols: self-patterned organoids

The fundamental concept that drives unguided protocols for brain organoids is based on the fact that differentiation into neural outcomes occurs by default in the absence of external cues. Based on this principle, Lancaster et al. (Lancaster et al., 2013) develop a 3D culture system for deriving brain tissue to study microcephaly *in vitro,* the so-called cerebral organoids. In this work a simple medium for organoid culture was used, without the addition of any small molecule. Moreover, based on the methodology used to generate gastrointestinal organoids, EBs were embedded into matrigel matrix, a gelatinous protein mixture that resembles the epithelial basement membrane for structural support and more complex tissue growth by inducing the correct polarity signal. To increase gas and nutrient exchange, the cerebral organoids were plated in a spinning bioreactor or on orbital shaker plates, which also allowed the significant increase of organoids size in diameter. These conditions enabled organoids to develop several regional identities capable of communicating with each other, and cortical regions exhibited an organization analogous to the developing human brain at early stages (Lancaster et al., 2013).

High-throughput single-cell transcriptional profiling has further demonstrated that cerebral organoids can accomplish extensive development, as well as generate different types of cells such as neural progenitors, different types of neurons, and glial cells found in CNS, but also photosensitive cells found in the retina (Quadrato et al., 2017). Moreover, organoids undergo significant neuronal maturation, verified by the formation of dendritic spines and spontaneous neuronal networks similar to *in vivo*. Besides mapping cellular diversity, Quadrato et al. (Quadrato et al., 2017) measure organoid-to-organoid variability, identifying cell types that are reproducibly generated and others that appear more sporadically, partially attributing this variability to bioreactor batch effects. The problem of unguided protocols relies on the fact that spontaneous differentiation of pluripotent stem cells leads to arbitrary proportions and heterogeneous arrangements between organoid batches. Although this cell diversity in cerebral organoids has the advantage to mimic the interactions across different brain regions, the high variability can compromise quantitative studies (Qian et al., 2019).

Guided protocols: patterning organoids with small molecules

To model some types of diseases it is necessary to generate more regionally restricted organoids. To partially overcome the heterogeneity of classical cerebral organoids and restrict identity to a unique brain region, most of the protocols altered the composition of the medium to guide organoid differentiation into a specific fate. For that, signaling molecules and growth factors which had previously been used in 2D protocols, are used to instruct stem cells to form cells and tissues typical of some brain regions from the forebrain to midbrain to hindbrain (Qian et al., 2019).

Dual-SMAD inhibition is currently used to prepattern cells towards a neuroectodermal fate, using several combinations of SMAD pathway inhibitors (e.g., Dorsomorphin, SB-431542), which results in the development of organoids with forebrain identity (Kadoshima et al., 2013; Paşca et al., 2015; Qian et al., 2016). For instance, in Pasca et al. study (Paşca et al., 2015), using this principle and with the combination of basic fibroblast growth factor (bFGF) and epidermal growth factor (EGF), as well as the absence of extracellular scaffolding resulted in the generation of neural progenitors expressing dorsal telencephalic markers. Substituting these growth factors by BDNF and neurotrophic factor 3 (NT3), cortical spheroids were generated, resembled the mod-fetal prenatal brain. Moreover, cortical neurons were synaptically connected with a network of non-reactive astrocytes (Paşca et al., 2015). On the other hand, initial dual SMAD inhibition followed by exposure to SHH agonists promotes ventral forebrain identities (Qian et al., 2019). Following this principle, while maintaining some features of Lancaster protocol like matrigel embedding and agitation, Qian et al. (Qian et al., 2016) developed and compared different culture conditions at the same time using self-engineered miniaturized spinning bioreactors. The work aimed to reduce the heterogeneity of the cerebral organoids and generate different types of specific brain regions. Through the inhibition of transforming growth factor-beta (TGF-β) signaling and activation of WNT signaling, they originated forebrain organoids organized in defined multi-layered progenitor zones, used to model Zika virus exposure. Furthermore, forebrain organoids generate cortical neurons expressing markers found in the six layers of the human cortex, as well as GABAergic neuronal subtypes. Treating EBs with SHH and WNT3a, Qian and colleagues also produced organoids with hypothalamic identity (Qian et al., 2016). Additionally, Sakaguchi et al. (Sakaguchi et al., 2015) demonstrated the 3D generation of choroid plexus and medial pallium-like structures from human ESCs, through a modified neocortical induction method using transient exposure to WNT and bone morphogenetic protein (BMP). After long periods in culture, medial-pallium tissues gave rise to hippocampal neurons electrically functional with network formation. Cerebellar organoids have been

also successfully developed. Muguruma et al. (Muguruma et al., 2015) showed that self-organized neuroepithelium differentiates into functional Purkinje cells and that the addition of FGF-19 induces the generation of dorsoventrally polarized neural-tube-like structures at cerebellum level. Likewise, the addition of stromal cell-derived factor 1 (SDF-1) and FGF-19 to the cultures gave rise to the tree layer cytoarchitecture similar to developing human cerebellum. Finally, to generate midbrain organoids, most of the protocols are built on 2D methods for generating midbrain dopaminergic neurons, which will be discussed below in more detail.

Overall, besides chemical external factors that are removed or minimized to induce brain region-specific organoids, also physical signs like biomaterials can also be used to guide its formation as demonstrated by some studies (Lancaster et al., 2017). Spinning bioreactors have been also used to scale-up 3D cultures production, however, they consume higher volumes of culture medium, which can compromise protocols efficiency. To circumvent this problem, culture plates on orbital shakers have been used as an alternative to reduce costs and the need for massive machines within the incubator (Qian et al., 2019).

Midbrain organoids for Parkinson's disease modeling

Midbrain organoids have been considered a respectable system, especially to investigate the early stage of disease progression. For modeling PD, the major issue is the low abundance of dopaminergic neurons in cerebral organoids (between 0 and 5% over different batches), which is not suitable to study the disease (Nickels et al., 2020). Similar to dopaminergic 2D neuronal differentiation, human midbrain organoids (hMOs) are generated by patterning iPSCs to midbrain fate, either from human pluripotent stem cells (Jo et al., 2016; Kim et al., 2019; Qian et al., 2016) or already patterned neural stem cells (NSCs) (Monzel et al., 2017; Smits et al., 2019). Besides developing a protocol for organoids with forebrain and hypothalamus identity, Qian and colleagues also developed a method to produce hMOs (Qian et al., 2016). Inspired by the work of Kris et al. (Kriks et al., 2011), they induced the floor plate differentiation by activating SMAD inhibition, (SB431542 and LDN193189), WNT (GSK3β inhibitor: CHIR99021), and SHH (recombinant SHH and PMA) signaling and by adding FGF8 in the 3D cultures. After 18 days, hMOs exhibited neuroepithelium-like structures expressing NESTIN and floor plate precursor marker forkhead box A2 (FOXA2), but no dorsal markers such as paired box protein 6 (PAX6). On day 38 several TH-positive neurons were observed, and after 56 days in culture, the majority of them were positive for FOXA2 and DAT. Shortly after, another work came out describing the differentiation of human ESCs into organoids expressing specific markers of the human midbrain using the same guided self-organized principle described above towards a mesencephalic fate (Jo et al.,

2016). After 7 days in culture, emerging neural organoids expressed already markers of midbrain DA progenitors like FOXA2, orthodenticle homeobox 2 (OTX2), CORIN, and LIM homeobox transcription factor 1 alpha (LMX1A). Like other protocols described above, the spheroids were embedded in matrigel to promote growth and organization in 3D, but then were transferred to a tissue culture plate containing media supplemented with neurotrophic factors placed in an orbital shaker. Interestingly, after 35 days of growth, the hMOs exhibited three layers namely the ventral zone, an intermediate zone, and an outer neuronal layer, similar to the murine embryonic midbrain floor plate that eventually gives rise to midbrain dopaminergic neurons. The number of TH-positive neurons significantly increase by day 60, and some of them co-expressed with G-protein-regulated inward-rectifier potassium channel 2 (GIRK2), suggesting A9 neurons specification, that are subtypes of midbrain dopaminergic neurons forming the SNpc affected in PD (Jo et al., 2016). Moreover, they conducted a transcriptional analysis creating a gene expression profile for the organoid system and 2D-generated dopaminergic neurons. A cluster analysis comparing the differentially expressed genes indicated that hMOs share features of gene expression profiles of the human prenatal midbrain samples, which cannot be recapitulated using a conventional 2D derivation of dopaminergic neurons. In this work, they also detected electrically active and functionally mature midbrain dopaminergic neurons and DA production in hMOs, as well as neuromelanin-like granules that shared similarity to those isolated from human SN tissues (Jo et al., 2016).

The majority of brain organoids have been generated directly from iPSCs, but Monzel and colleagues (Monzel et al., 2017) showed that hMOs can also be derived from more fate restricted NSCs. This has the advantage that already patterned cells might differentiate more efficiently in the desired regions. For that, they used a human neuroepithelial stem cells (NESCs) culture system described by Reinhardt et al. (Reinhardt et al., 2013), to derive hMOs under dynamic conditions. Besides showing spatially patterned groups of dopaminergic neurons, hMOs exhibited robust astrocyte immunoreactivity after 60 days of differentiation, which are crucial for synapse formation and regular neuronal activity. Moreover, it was possible to detect synaptic connections, and hMOs were electrophilically functional which was verified by Ca^{2+} imaging and multielectrode array measurements. Additionally, hMOs achieved a robust differentiation into oligodendrocytes and an elevated degree of neurite myelination (Monzel et al., 2017).

Regarding PD modeling using hMOs, two studies have stood out focusing on LRRK2-G2019S specific mutation (Kim et al., 2019; Smits et al., 2019). Besides a decrease in the number of dopaminergic

neurons in mutant organoids and a reduction of neuronal complexity, more interesting findings were observed in both studies. For instance, Kim et al. (Kim et al., 2019) showed that mutant organoids were more susceptible to MPTP-induced cell death and abnormal localization of phosphorylated α-synuclein was present, which was reduced with LRRK2 kinase activity inhibition. Moreover, analysis of the protein-protein interaction network in mutant organoids revealed that TXNIP, a thiol-oxidoreductase, is functionally important in the development of LRRK2-associated PD in a 3D environment. On the other hand, Smits et al. (Smits et al., 2019), demonstrated a significant increase of FOXA2-positive cells in the patient-specific organoids, which indicates that this might be a compensatory response to an impaired specification of midbrain dopaminergic neurons promoted by the mutated *LRRK2* gene since FOXA2 is required for midbrain dopaminergic neurons generation. Another interesting study used an organoid model using iPSCs obtained from PD patients with an idiopathic form of the disease (Chlebanowska et al., 2020). In this work, mature organoids displayed expression of neuronal early and late markers, and it was observed a significantly higher level of midbrain floor plate progenitors, such as FOXA2 and LMX1A, as well as in later markers like TH in healthy controls. On the other hand, PTX3 gene expression, an important factor in development and survival of midbrain dopaminergic neurons was increased in PD patients. No differences were found regarding NURR1, responsible for the differentiation of early midbrain DA progenitors into mature TH-positive neurons. Importantly, hMOs were also shown to be valuable tools for studying PD using putative neurotoxic compounds. For instance, Monzel and colleagues (Monzel et al., 2020) described a pipeline for a machine learning-based analytical method, allowing for detailed image-based cell profiling and toxicity prediction in midbrain organoids treated with the 6-OHDA.

Only a few studies have used hMOs to explore the pathophysiology of PD so far, and still exist some limitations to the use of organoids as a model. Similar to 2D cultures, 3D neuronal organoids are also highly variable even if generated from the same clonal cell line, are time-consuming and expensive. Moreover, there is a need for improved vascularization to avoid neuronal death inside the organoids, and to test the ability of compounds to cross the BBB. Furthermore, because so much of the current development in organoid technology has been made with cortical and forebrain organoids, further work is needed to better characterize and standardize the differentiation of midbrain organoids that will be useful in PD research. Nonetheless, there is no doubt that they are a powerful technology, thus providing key insights into developmental characteristics that might be implicated in disease development and progression. Moreover, the use of organoids for drug discovery allows the possibility

for studying how therapeutics modulate multiple cell types in a more physiological 3D model (Marotta et al., 2020; Slanzi et al., 2020).

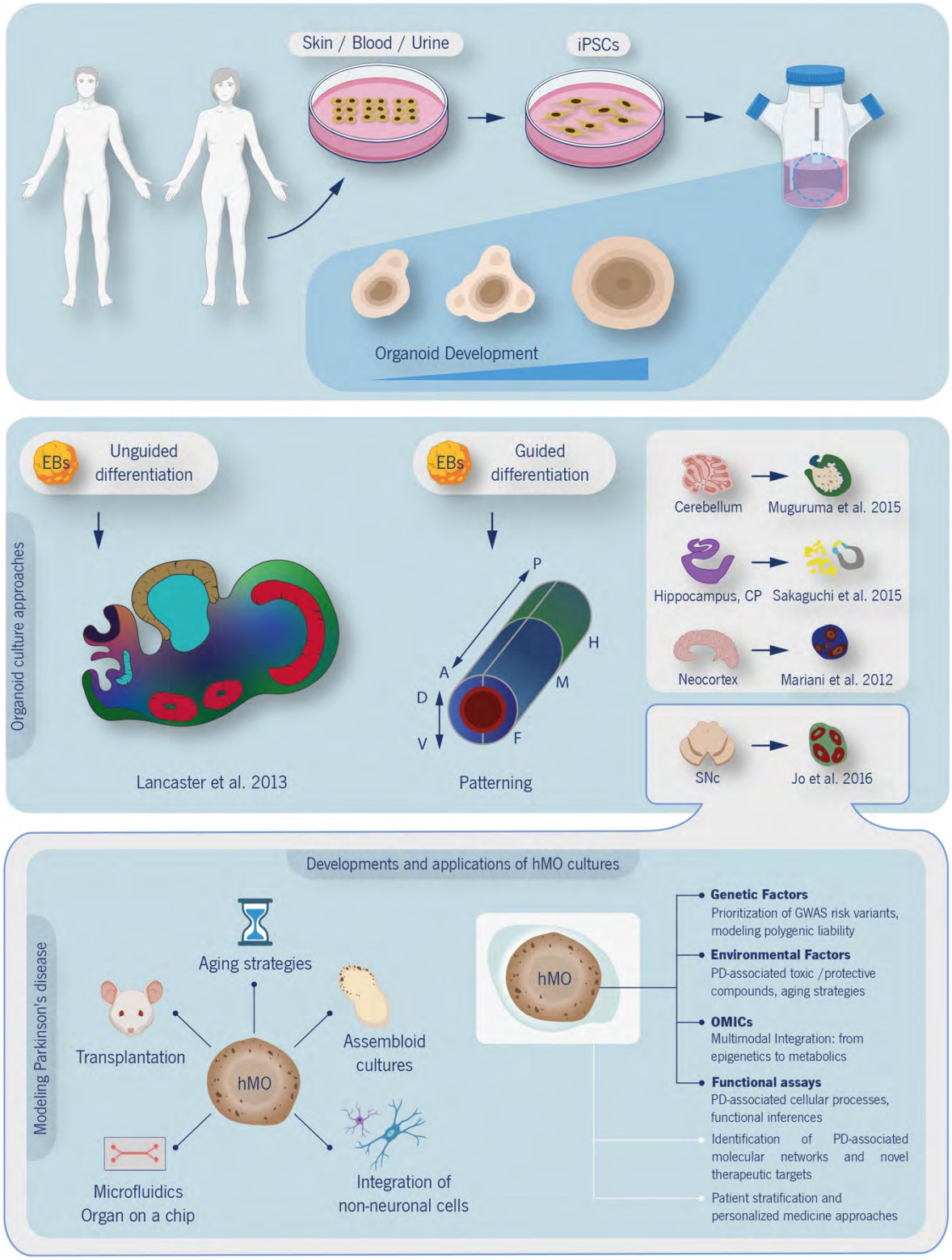


Figure 8. Organoid differentiation protocols and application of human midbrain-specific organoids (hMOs). Human iPSC-derived organoids can be used to study human brain development (top); Unguided organoid differentiation methods (middle) result in cerebral organoids that resemble the developing brain. With minimal external interference, iPSCs self-organize into heterogenous brain proxies with various brain areas. Small chemicals and growth factors are used in guided organoid techniques to influence stem cell fate in the desired anteroposterior and dorsoventral directions. This enables the creation of brain region-specific organoids that imitate different parts of the developing brain, such as the SNpc (middle). Aging strategies, fusions with other brain region organoids, co-cultures with non-neuronal lineage cells (e.g., microglia, endothelial cells), microfluidics or "organ on a chip" approaches, and *in vivo* transplantations (bottom left) are all possible developments of hMO cultures. Such approaches could lead to a greater understanding of the molecular basis of PD, as well as the identification of new treatment targets and the development of personalized medicine strategies (bottom right). Abbreviations: CP, choroid plexus; EBs, embryoid bodies; iPSCs, induced pluripotent stem cells; hMO, human midbrain-specific organoid; PD, Parkinson's disease; SNpc, substantia nigra *pars compacta*; A, anterior; P, posterior; D, dorsal; V, ventral; F, forebrain; M, midbrain; H, hindbrain. Adapted from (Arlotta, 2018; Galet et al., 2020).

2.2. In vivo

The PD clinical phenotype is as diverse as its etiology. While the motor and non-motor symptoms can be clinically detected, brain pathology can only be validated by studying post-mortem tissues (Konnova and Swanberg, 2018). As a result, experimental models are desperately needed to increase our understanding of PD and expand the currently limited therapeutic options. The selection of the experimental model is crucial since the research's translatability is dependent on the use of appropriate animal models to mimic the human situation. Face validity (animal models should display similar symptomatology to human PD), constructive validity (animal models should have similar alterations regarding cellular and molecular mechanisms underlying PD), and predictive validity (animal models should respond to treatments in a manner comparable to clinical treatment) should all be taken in consideration (Kin et al., 2019). Although neither of the available models captured all the disease clinical and behavioral aspects, they exhibited individual or multiple disease features. As a result, all animal models are important, and the best model must be determined based on the research questions.

Non-mammalian animals, rodents, and non-human primates are the three animal categories that are widely used to model human disorders, including PD. Each group has advantages and disadvantages that influence its eligibility for a particular experiment. Understanding species-specific distinctions aids in experimental design as well as the interpretation of behavioral findings and pathology (Konnova and Swanberg, 2018). Over the past decades, non-mammalian models such as drosophila and Caenorhabditis (C.) elegans have been used in a small proportion of experimental PD investigations.

However, they do present various advantages such as a rapid reproductive cycle, are easily genetic manipulated, present well-defined neuropathology, and behavior, as well as low maintenance costs which provide a valuable *in vivo* platform for drug screening (Lim, 2010). Although attractive, these models have several limitations, and the most important relies on their limited face validity (Konnova and Swanberg, 2018). On the other hand, non-human primates (e.g., macaques and common marmosets) because of their anatomic and genetic resemblance to humans, provide useful insights into PD pathogenesis. Only 10% of animal research on PD is undertaken in non-human primates, and they are frequently reserved for preclinical evaluation (Grow et al., 2016). Currently, non-human primate models are based on neurotoxic or viral vector-mediated PD pathology, which produces parkinsonian symptoms and behaviors comparable to those seen in patients, therefore, a measure similar to the Unified Parkinson's Disease Rating Scale (UPDRS) can be developed (Imbert et al., 2000). In addition, they can be very useful for neuroimaging studies (Emborg, 2007). Nonetheless, they are demanding in terms of resources and imply more complex ethical concerns. Finally, rodents are extensively studied across biomedical fields because they are easy to maintain under laboratory conditions and have associated robust experimental protocols, such as forms of drug administration, generation of transgenic strains, and behavioral assessments (Konnova and Swanberg, 2018). Thus, in this section, we will focus on the most used neurotoxic and genetic PD models in rodents.

2.2.1. Neurotoxic models

Among the various accepted experimental models of PD, neurotoxins have remained the most popular tools to produce selective neuronal death *in vivo* (Konnova and Swanberg, 2018). In this section, we will discuss what we believe are the most popular parkinsonian neurotoxins, namely 6-OHDA, MPTP, and models using pesticides and herbicides such as rotenone and paraquat.

6-OHDA

6-OHDA, an analog of DA, was the first neurotoxin found to cause degeneration of dopaminergic neurons in the SNPc, accompanied by marked postural bias and turning asymmetry in rats, more than fifty years ago (Ungerstedt, 1968). Since then, 6-OHDA is the neurotoxin *par excellence* to model PD in rodents and to test possible neuroprotective compounds (Bové and Perier, 2012). Although the exact mechanism by which 6-OHDA acts on dopaminergic neurons is unknown, it is stated that 6-OHDA is transported DAT into dopaminergic neurons and accumulates in mitochondria, blocking the action of mitochondrial respiratory chain complex I. Inhibition of monoamine oxidase A/B(MAO-A/B) enhanced

the inhibitory of 6-OHDA on complex I, and once inside the cells, 6-OHDA undertakes auto-oxidation or metabolic degradation and produces hydrogen peroxide, superoxide, and hydroxyl radicals. This process causes lipid peroxidation, protein oxidation, and DNA oxidation and finally results in mitochondrial dysfunction and oxidative stress (Hwang, 2013).

Because 6-OHDA is hydrophilic, it cannot penetrate the BBB and must be administered via direct injection in the medial forebrain bundle (MFB; a compacted area containing the ascending nigrostriatal fiber pathway), SNpc, or striatum, depending on the rate of lesion formation required. Injections into the SNpc or the MFB lead to more rapid cell death. In nigral injections, the degeneration of dopaminergic neurons takes place within 12 h preceding a significant loss of striatal terminals, which occurs 2–3 days later (Tieu, 2011). When injected into the MFB, 6-OHDA induces degeneration in striatal terminals before dopaminergic cell death occurs, with a complete loss of DA content achieved in the striatum within 3 weeks. The number of dopaminergic neurons in the SNpc decreases gradually, with a complete lesion (>90%) obtained after 5 weeks (Bové and Perier, 2012). By contrast, intrastriatal lesions cause slower retrograde degeneration of up to 70% of the dopaminergic neurons in 4-6 weeks, thereby allowing longitudinal follow-up of the lesion in a more progressive manner (Bové and Perier, 2012). Nonetheless, besides the site of injection, the magnitude and characteristics of neurodegeneration induced by 6-OHDA can be also significantly affected by lesion coordinates and neurotoxin dosages (Smith and Heuer, 2011).

6-OHDA can be applied unilaterally, allowing the use of the non-lesioned ipsilateral side as an internal control, leading to asymmetric motor deficits and rotational behavior. Because the unilateral lesion can be quantitatively assayed, the ability to assess the anti-PD properties of new therapeutic approaches is extremely advantageous. Moreover, unilateral models avoid the profound impairments in feeding, drinking, and ability of the animal to maintain the full health that results from bilateral lesions (Heuer et al., 2012). Nonetheless, bilateral lesions can be useful to mimic early-stage PD and replicate the manifestation of prodromal comorbidities like non-motor symptoms (Masini et al., 2021).

MPTP

MPTP is a frequently used neurotoxin for modeling PD and can be delivered acutely or chronically by different routes (Jackson-Lewis and Przedborski, 2007). Because MPTP is lipophilic can rapidly cross BBB, and once in glial cells, is metabolized by MAO-B, and converted to the active toxic cation 1-methyl-4 phenylpyridinium (MPP+). MPP+ is released from the nigral and striatal glial cells through the organic

cation transporter 3 into the extracellular space where it is taken up by the neighbouring dopaminergic neurons and terminals through DAT. After accumulation in dopaminergic neurons, MPP+ induces neurotoxicity by inhibiting complex I, resulting in ATP depletion and increased oxidative stress (Jagmag et al., 2016; Konnova and Swanberg, 2018).

MPTP-monkey model is the gold standard for preclinical testing of therapeutic strategies for PD, however, for many researchers, the reliability and accessibility of the mouse MPTP model makes it a popular choice in PD research (Jagmag et al., 2016; Konnova and Swanberg, 2018). On the other hand, rats are resistant to moderate doses of MPTP, while higher doses increase the mortality rates (Konnova and Swanberg, 2018). The extent of the lesion depends on mouse strain, the dosage, and the route of administration used (Konnova and Swanberg, 2018). Most commonly, mice received acute doses of MPTP by intraperitoneal (i.p.) injection which causes a loss of dopaminergic neurons, specifically in the SNpc rather than nearby regions such as the ventral tegmental area (VTA) (Blesa and Przedborski, 2014). The neurodegeneration occurs within hours and stabilizes within 7 days, and four injections of an acute dose (up to 20 mg/kg; 2-hour interval) cause 90% of striatal DA depletion and 70% loss of dopaminergic neurons in the SNpc without the formation of α-synuclein aggregates (Jackson-Lewis and Przedborski, 2007). Although MPTP-induced dopaminergic degeneration in mice correlates with motor deficits, they can recover within a few days post-acute injection, which might be a limitation for longitudinal behavioral studies. Alternatively, repeated daily i.p. injections of sub-acute doses result in delayed nigrostriatal neurodegeneration and leads to the progressive accumulation of α-synuclein inclusions and motor deficits (although not consistent within the literature) (Konnova and Swanberg, 2018; Zhang et al., 2017).

Pesticides and herbicides

Correlations between agrochemical exposure in populations and increased risk for PD have been difficult to conclude due to a lack of details on exposure to particular agents. Nonetheless, rotenone, paraquat, and maneb as been indicated as possible environmental causes of PD. So far, these pesticides and herbicides have been mostly used in rodents to try to model PD (Konnova and Swanberg, 2018).

Both rotenone and paraquat are thought to cause dopaminergic degeneration by inducing oxidative stress. Rotenone is found naturally in many plants and has been used as a broad-spectrum insecticide and pesticide. Similar to MPTP, it works by inhibiting complex I, but also inhibits cell proliferation by

inhibiting mitosis. This is accomplished by interfering with microtubule assembly and slowing the rate of GTP hydrolysis (Jagmag et al., 2016). The rotenone rat model has gained some attention due to its ability to cause dopaminergic degeneration, α-synuclein inclusions, and motor deficits (Betarbet et al., 2000). Daily i.p. injections of 3 mg/kg of rotenone for 6–10 days are sufficient to induce 45% loss of dopaminergic neurons in the SNpc, striatal DA depletion, and motor symptoms (Cannon et al., 2009). Moreover, rotenone can also induce non-motor symptoms such as sleep disturbances (García-García et al., 2005). Regarding paraquat, despite being structurally similar to MPP+, it is still unclear how paraquat penetrates the BBB despite its high polarity (PQ2+) (Jagmag et al., 2016; Konnova and Swanberg, 2018). Nonetheless, it is hypothesized that PQ2+ is not transported by DAT but is converted to a monocation radical PQ+ through redox cycling. PQ+ seems to be the active agent penetrating the dopaminergic neurons through DAT and exerting cytotoxicity, as shown in cultured cells and mice (Konnova and Swanberg, 2018). This neurotoxin has been shown to cause dopaminergic degeneration and like rotenone also induces the formation of LB pathology in dopaminergic neurons in rodents (Cicchetti et al., 2005; McCormack et al., 2002). However, large variability has been observed between studies (Jagmag et al., 2016). Paraquat has been used in combination with the fungicide maneb, which has also been shown to potentiate the effects of MPTP (Jagmag et al., 2016). Maneb *per se* has also been shown to decrease locomotor activity and produce nigral cell loss (Thrash et al., 2007).

2.2.2. Genetic-based models

The identification of several mutations causing familial forms of PD has led to the development of multiple animal models expressing similar genetic alterations. These models present a valuable opportunity for understanding the pathophysiological mechanisms leading to PD and may provide suitable models for preclinical testing of new therapies (Magen and Chesselet, 2010). As previously stated in this chapter, SNCA was the first gene to be linked to familial PD, and this, along with the discovery that the encoded protein α-synuclein aggregates in LB, resulted in a breakthrough in PD research. Since then, different studies have been conducted on α-synuclein models and pathology (Konnova and Swanberg, 2018). Several lines of α-synuclein-overexpressing mice have been generated, using a variety of promoters and transgenes (Koprich et al., 2017; Visanji et al., 2016). The same approach is also often used for other autosomal dominant genes like LRRK2 (Dawson et al., 2010; Magen and Chesselet, 2010; Ouchi et al., 2005). On the other hand, recessive mutations in PINK1, PRKN, and DJ-1 are usually modeled by knockout strategies, leading to the absence of the corresponding protein (Magen and Chesselet, 2010). In addition, the development of new genetic tools

also allows for the generation of new genetic-based models. One example is the use of viral vectors that can be used to introduce wild-type or mutated genes for targeted expression of a disease-associated protein (Konnova and Swanberg, 2018). Important of note, these models typically lack an extensive nigrostriatal degeneration, do not exhibit motor deficits, and when present, demands a long period, they are highly variable between studies and may also develop from non-PD related neuronal dysfunction (Dawson et al., 2010; Konnova and Swanberg, 2018). In the Table 2 we described some of the currently used genetic models and their related limitations.

Table 2. Characteristics, uses, and limitations of Parkinson's disease genetic-based models. Adapted from (Konnova and Swanberg, 2018)

Gene	PD model	Characteristics	Uses	Limitations
SNCA	Transgenic *Wilde-type and point mutations (A53T, A30P, E46K)*	Mice and rats Widespread of α-synuclein aggregation No dopaminergic neurodegeneration* Some motor deficits	Model familial mutations of SNCA Study α-synuclein function/propagation and synucleinopathies	May affect development
	Viral transfection *AAV and LV vectors*	Mice and rats α-synuclein aggregates Moderate dopaminergic neurodegeneration Moderate motor deficits	Delivered into SNpc Study α-synuclein function/propagation and synucleinopathies Potential preclinical use	Potential vector toxicity and interference of viral vector
	Preformed fibrils *Seeding of α-synuclein aggregates*	Mice and rats Widespread of α-synuclein aggregation Mild dopaminergic neurodegeneration Lack of motor deficits in rats, some in mice	Administered to the striatum Study α-synuclein function/propagation and synucleinopathies Can be combined with α-synuclein viral vector	Slow/weak onset of pathology
LRRK2	Wilde-type, G2019S, R1441C *Transgenic and viral vector-mediated*	Mice and rats Affects inclusion formation Little dopaminergic neurodegeneration Most lack motor deficits	Study the role of LRRK2, its interaction with α-synuclein, and toxicity of mutant LRRK2	Large gene size prevents the use of AAV vectors
UCH-L1	193M mutation	Mice No α-synuclein aggregates Dopaminergic neurodegeneration Mild motor deficits	Study the role of UHC-L1 Used in combination with α-synuclein and MPTP to study interaction	Relevance to pathogenies of PD is debated

PINK1 PRKN DJ-1	Transgenic KO, silencing, or overexpression using viral vectors	Mice and rats Affects aggregation in α-synuclein models Most give no dopaminergic neurodegeneration Lack clear motor deficits	Study the role of these genes Used in combination with α-synuclein overexpression or MPTP models to study interaction	Large number of identified mutations

AAV: adeno-associated virus; LV: lentivirus; *not consistent (depends on promotor and transgene expressed).

3. Current treatments and therapies in development for Parkinson's disease

PD is caused by the selective loss of neurons in the SNpc, resulting in DA depletion in the striatum. Because of that, dopaminergic drugs designed to replace DA's action in the depleted striatum are currently the mainstay of PD treatment (Zahoor et al., 2018). This can be accomplished with drugs that are converted to DA, activate the DA receptor, or block endogenous DA breakdown. There are currently no disease-modifying treatments for PD, with management strategy adapted to each individual patient severity and temporal nature of symptoms, as well as the existence of adverse effects (Zahoor et al., 2018).

3.1. Dopamine biosynthesis and metabolism

DA is not able to cross the BBB and is primarily synthesized in the dopaminergic neurons within the brain, with small amounts of DA also being produced in the medulla of the adrenal glands (Seeman, 2010). The DA synthesis and storage pathway involves several enzymes and co-factors, any one of which could be manipulated genetically to yield increased DA levels (Lawlor and During, 2004). The rate-limiting enzyme in DA production is TH, which converts the aminoacid tyrosine to L-dihydroxyphenylalanine (L-DOPA or levodopa). Then, L-DOPA is metabolized DA by aromatic amino acid decarboxylase (AADC) in the pre-synaptic terminal. After absorption into dopaminergic neurons or glial cells, DA is metabolized by the enzyme MAO, which catalyses oxidative deamination in the presence of flavin adenine dinucleotide (FAD) to create the reactive aldehyde 3,4-dihydroxyphenylacetaldehyde (DOPAL). DOPAL is inactivated by alcohol dehydrogenase (ADH) converting it to 3,4-dihydroxyphenylethanol (DOPET) or aldehyde dehydrogenase (ALDH) converting it to 3,4-dihydroxyphenylacetic acid (DOPAC). The enzyme catechol-O-methyl transferase (COMT) then degrades DOPAC to the physiologically inactive metabolite homovanillic acid (HVA) (Lawlor and During, 2004; Zahoor et al., 2018). Therefore, multiple components in this pathway have been targeted for the treatment of PD.

3.1.1. Dopaminergic pharmacological targets

Levodopa-based preparations have remained the core treatment for PD, and over time, practically all patients with PD will require its usage (Poewe et al., 2017). As mentioned above, contrary to DA, the DA precursor levodopa can cross BBB and can be administered as a therapy (AlDakheel et al., 2014). In general, the clinical effect of levodopa is immediate and can last for several hours, especially in the early stages of the disease. Nevertheless, as the disease progresses, the drug's effect usually wears off after a shorter period, demanding higher doses (Tambasco et al., 2017). Although effective, levodopa has significant side effects that are an important part of the patient's illness, especially in advanced disease. Some of its side effects are caused by DOPA decarboxylase's conversion of levodopa to DA outside the CNS (peripheral conversion). These side effects are reduced by combining levodopa with peripheral inhibitors of DOPA decarboxylase such as benserazide and carbidopa (Zahoor et al., 2018). Nonetheless, prolonged use can cause serious motor complications such as dyskinesias and severe on-off motor fluctuations. Dyskinesias are involuntary twisting hyperkinetic movements that typically occur when the drug is at its highest dose. The emergence of problematic dyskinesias may be treated by lowering the levodopa dose, implying that a difficult balance must be struck between optimizing motor symptom control and minimizing adverse side effects (Tambasco et al., 2017; Zahoor et al., 2018). The on-off phenomenon describes how patients with advanced PD may experience rapid fluctuations in their motor function, being well controlled during the "on" state, but when levodopa begins to lose its effect, known as “wearing-off”, the patient experienced severe parkinsonian motor features. These fluctuations can be especially difficult and severely restrict function (Tambasco et al., 2017). Gastrointestinal disturbances such as nausea and vomiting, as well as orthostatic hypotension, are other serious side effects. Moreover, due to the "off-target" effects of DA acting in extranigral brain regions, neuropsychiatric symptoms such as anxiety and hallucinations may ensue (Zahoor et al., 2018). More recently, continuous intestinal infusion of levodopa gel (Duodopa [AbbVie Limited] - a combination of levodopa and carbidopa) has been demonstrated to be more successful than oral levodopa in terms of reducing severe motor fluctuations, owing to more consistent levodopa absorption. However, the cost of this therapy makes it impractical to apply on a large scale (Oertel, 2017).

DA agonists were first introduced in PD therapy in the 1970s, and since then become an important medical therapy for motor symptomatology (Poewe et al., 2017). This class of drugs stimulates the activity of the DA system by binding to the dopaminergic receptors and, contrasting levodopa, do not need to be converted into DA. Initial members of DA agonists were ergoline derivatives, which also

activate serotonin receptors, and these became associated with pleuropulmonary and cardiac valvular fibrosis, which introduced important safety concerns (Poewe et al., 2017; Zahoor et al., 2018). Currently used agents, namely pramipexole, ropinirole, and piribedil (targeting D2 receptor family), as well as apomorphine, and rotigotine (targeting D1 receptor family), are non-ergoline drugs and do not present this activity (Poewe et al., 2017). DA agonists are frequently administered as initial therapy for PD, especially in younger individuals, since they allow for a delay in the administration of levodopa, which consequently may reduce the impact of the problematic motor problems mentioned earlier. However, they may cause other severe adverse effects such as constipation, peripheral enema, hallucinations, and sleepiness, with the most important one being the development of impulsive control disorder (Poewe et al., 2017; Zahoor et al., 2018).

Other PD medications work by inhibiting the enzymes involved in DA metabolism, which preserves its endogenous levels (Zahoor et al., 2018). One such class is the MAO-B inhibitors. Inhibition of MAO-B prolongs and increases synaptic DA concentrations and increases dopaminergic activity within the striatum. Their use relieves motor symptoms in PD patients, and similarly to DA agonists they can be used as an initial treatment option, to delay the need for levodopa therapy. They are also efficacious when added to L-DOPA in patients with motor fluctuations (Anthony H.V. Schapira, 2011). Commonly used MAO-B inhibitors include selegiline (Deprenyl, Eldepryl, Zelapar) and rasagiline (Azilect) (Zahoor et al., 2018). More recently, safinamide (Xadago) was also approved for use in the PD context, and its benefits in improving motor functions and fluctuations, and some non-motor symptoms, could have a valuable impact on patients' quality of life (Abbruzzese et al., 2021; Teixeira et al., 2018). Similarly, COMT inhibitors can also help to preserve endogenous DA levels by reducing its breakdown (Zahoor et al., 2018). Inhibition of this enzyme in the periphery will further enhance bioavailability and the half-life of L-DOPA, which is of particular benefit in patients who have developed motor fluctuations of the wearing-off type. COMT inhibitors are not generally prescribed as monotherapy, because they offer only limited effect on PD symptoms (Müller, 2015). Currently, three preparations are available for clinical use, namely entacapone (Comtan), tolcapone (Tasmar), and opicapone (Ongentys) (Poewe et al., 2017). COMT inhibitors can amplify levodopa-induced adverse effects, such as dyskinesias, and may demand a lower levodopa dose. Tolcapone is linked to a rare but substantial risk of hepatotoxicity, hence entacapone is usually recommended. Both MAO-B and COMT inhibitors include other side effects such as dry mouth, headaches, confusion, dizziness, among others (Zahoor et al., 2018).

3.2. Non-dopaminergic pharmacological targets

All the drugs mentioned thus far are intended to boost dopaminergic activity, however, non-dopaminergic pathways are exploited by a small number of medications used to treat PD. An example are anticholinergics, that operate as antagonists at cholinergic receptors, reducing the action of the neurotransmitter acetylcholine (Katzenschlager et al., 2002). Anticholinergic drugs may help restore and maintain the normal balance between DA and acetylcholine in the brain, which is disrupted when dopaminergic neurons are lost (Katzenschlager et al., 2002; Zahoor et al., 2018). Although their utility is restricted and they are currently prescribed infrequently, the central role of these drugs is in young patients at early stages of the disease for the relief of mild movement symptoms, particularly tremors and muscle stiffness (Zahoor et al., 2018).

Another example is amantadine (Symmetrel) that was initially created as an antiviral drug for treating flu, but it is now used for PD treatment. It is not fully understood how amantadine may have an anti-PD effect, but it acts as a weak glutamate antagonist at the N-methyl-d-aspartate receptor (NMDAR) (Sawada et al., 2010). It can be used to treat rigidity, rest tremor, and sometimes fatigue. Moreover, it also enables the administration of a lower dose of levodopa, lowering the risk of dyskinesias (Zahoor et al., 2018).

Importantly, in PD patients, some non-motor complaints can fluctuate in response to dopaminergic therapy, which can be even more incapacitating than the motor symptoms. The majority of non-motor symptoms do not respond to DA replacement medication, and some are aggravated or precipitated by it (Poewe et al., 2017). Cognitive dysfunction, depression, and autonomic failure are among the most prevalent and troublesome non-motor symptoms in PD (Chaudhuri and Schapira, 2009). Cholinesterase inhibitors can have a significant positive effect on cognitive difficulties in PD patients who also have dementia, an effect that may be connected to the significant loss of cholinergic projections from the nucleus basalis of Meynert (Connolly and Fox, 2014). Regarding depression, it is not clear if this condition in PD has the same pathogenic root as depression in the general population. Although patients may respond to all types of antidepressant medications, there is some evidence that tricyclic antidepressants are more effective than selective serotonin reuptake inhibitors, implying a stronger involvement for noradrenergic systems, however, this remains to be proven (Poewe et al., 2017; Weintraub and Burn, 2011). Autonomic dysfunction is also very common, mainly in late-stage PD, and pharmaceutical treatments are predominantly focused on autonomic nerve system targets. They include the mineralocorticoid fludrocortisone and adrenergic agents, the noradrenaline precursor

to treat orthostatic hypotension, antimuscarinics for urinary urgency or incontinence, and pro-kinetic to improve constipation (Perez-Lloret et al., 2013; Poewe et al., 2017).

3.3. Deep brain stimulation

DBS is an effective treatment for improving motor symptoms of PD among well-selected patients where the pharmacological treatment is no longer effective (Dallapiazza et al., 2018). Exclusion criteria include dementia, serious psychosis, and significant depression, and patients with early-onset PD are the most likely to benefit from DBS and are overrepresented in the operated group (Poewe et al., 2017). DBS is a surgical treatment that involves implanting electrodes in specific brain targets that produce high-frequency (100– 200 Hz) electrical stimulation to alter or disrupt neural transmission pathways (Dallapiazza et al., 2018; Hutchinson and Wick, 2016). The STN and the GPi are the most common DBS targets, and both are equally effective in controlling motor PD symptoms who are not medicated. STN DBS is effective in reducing postoperative levodopa requirements, whereas GPi DBS may have fewer negative effects on mood and cognition, particularly in older Patients (Dallapiazza et al., 2018). Interestingly, bilateral STN DBS reduces the UPDRS II (activities of daily living) and UPDRS III (motor) scores on average by 50-60% compared with the preoperative medical off-state (Poewe et al., 2017). Nevertheless, it is important to note that DBS requires high levels of expertise, imaging, and stereotaxic surgery, thereby limiting its widespread applicability (Dallapiazza et al., 2018). Moreover, the most important adverse events are intracranial bleedings and device complications (e.g., infections and lead misplacement), which account for permanent morbidity of >1-3% (Voges et al., 2007).

3.4. Gene therapy

The two principal strategies for gene therapy in PD are based on the viral vector-mediated expression of growth factors or neurotransmitter-synthesizing enzymes (Poewe et al., 2017; Stoker and Barker, 2020). Clinical trials using viral vector-mediated production of key enzymes in the DA production pathway namely lentiviral and AAV vectors expressing TH with co-factors and AADC are currently undergoing (Stoker and Barker, 2020), with two phase 1 trials already completed showing motor function improvements and good tolerance (Christine et al., 2019, 2009). Another phase 1 trial that was completed aimed to deliver glutamic acid decarboxylase, an essential enzyme for GABA synthesis that induces GABAergic inhibition of STN, thereby improving motor deficits (Kaplitt et al., 2007). Attention has also been given to the GDNF due to evidence suggesting its role in the protection of nigral dopaminergic neurons from death and promotion of regeneration of their axons following damage

(Poewe et al., 2017). A phase 1 experiment using the AAV2 vector to deliver GDNF to the putamen is now underway (ClinicalTrials.gov Identifier: NCT01621581).

3.5. Cell-based therapy

Currently, no disease-modifying treatments exist for PD. The current treatment involves the use of dopaminergic drugs to restore the striatal DA concentration, with consequent improvement in motor function. None of the available treatments do alter the course of the disease and do not treat the non-motor aspects of PD, and although these drugs offer significant symptomatic benefits, they also result in problematic side effects (Liu and Cheung, 2020). Therefore, for the past four decades, there has been much interest in the development of cell-based regenerative therapies, designed to treat the dopaminergic deficits of PD in a physiological manner (Poewe et al., 2017; Stoker and Barker, 2020). Pioneering studies in this field started in the 1990s and were based on cell-grafting with mesencephalic dopaminergic neurons precursors from allogenic fetal tissue into the striatum of PD patients (Lindvall et al., 1990; Piccini et al., 1999). While this was shown to be effective in some cases, with patients being able to discontinue dopaminergic medication for extended periods, rapidly became clear that the use of fetal tissue as a cell source implies logistical barriers due to their limited availability and standardization (Stoker and Barker, 2020). Nonetheless, although the clinical trials were halted, these findings prompted a new era of regenerative stem cell therapy research, and experimental stem cell therapy in PD animal models has developed intensely (Poewe et al., 2017). The fact that stem cells offer a renewable source of dopaminergic neuron progenitor cells, together with the discovery of iPSCs and the creation of robust dopaminergic neuron differentiation methods, have reignited the promise of cell-replacement treatment in terms of producing more robust and consistent therapeutic outcomes (Liu and Cheung, 2020; Shen et al., 2016). The current focus of research is on overcoming difficulties linked to scaling up cell production, ensuring safety, and fulfilling the growing regulatory expectations put on biological products. Moreover, a better understanding of PD pathogenesis will also benefit the next generation of cell-based therapies (Poewe et al., 2017). Several experimental studies have used cells from different origins to treat PD, such as ESCs, NSCs, iPSCs, and multipotent mesenchymal stem cells (MSCs) (Shen et al., 2016; Stoker and Barker, 2020). Some of the clinical trials that are now underway are summarized in Table 3.

Table 4. Current and planned trials of human stem cell-derived neuronal products

Cell source	Sponsor	Status
Dopaminergic neurons derived from human ESCs	BlueRock Therapeutics	Phase 1 NCT04802733
Mesencephalic neuronal precursor cells	Bundang CHA Hospital	Phase ½ NCT01860794
Embryonic dopamine cell implants	University of Colorado	Phase 3 NCT00038116
ESC-derived neural precursor cells	Chinese Academy of Sciences	Phase ½ NCT03119636
NSCs differentiated from MSCs	University of Jordan	Phase ½ NCT03684122
Umbilical cord derived-MSCs	Hebei Newtherapy Blo-Pharma technology Co., Ltd.	Phase 1 NCT03550183
Allogeneic bone marrow derived-MSCs	The University of Texas Health Science Center	Phase 2 NCT04506073
Autologous bone marrow derived-MSCs	Belarusian Medical Academy of Post-Graduate Education	Phase 2/3 NCT04146519
Adipose tissue derived-MSCs	Hope Biosciences Stem Cell Research Foundation	Phase 2 NCT04928287
Autologous peripheral nerve grafts	Craig van Horne, MD, PhD	Phase 1 NCT02369003
ESCs (RC17 cell line)	European STEM-PD trial	In set-up
Autologous iPSCs	Fujifilm cellular dynamics international	In set-up
Autologous iPSC-NSCs	Allife Medical Science and Technology Co., Ltd.	In set-up
ESCs (H9 cell line)	NYSTEM-PD	Pending decision from FDA

ESCs: embryonic stem cells; NSCs: neural stem cells; MSCs: mesenchymal stem cells; IPSCs: induced pluripotent stem cells.

4. Mesenchymal stem cells: focus on secretome as a cell-free therapy for Parkinson's disease

4.1. Mesenchymal stem cells

MSCs are currently one of the most extensively investigated therapeutic cellular products for clinical applications (Merimi et al., 2021). Alexander Friedenstein was the first to isolate MSCs from bone marrow, describing them as fibroblastoid cells with clonogenic potential and plastic culture adherence (Friedenstein et al., 1974). In the early 1990s, Arnold Caplan named them "mesenchymal stem cells" to describe the cells involved in embryonic bone and cartilage formation as well as repair and

maintenance in the adult (Caplan, 1991). Although following these discoveries, their nomenclature and origin remain highly debatable, MSCs have proven to be a promising tool for regenerative medicine (Wright et al., 2021). MSCs are described as multipotent progenitor cells with self-renewable capacity and a high ability to proliferate. The conventional source of MSCs is the bone marrow, however, more than 50 years of research on MSCs allowed their isolation from various tissues, such as adipose tissue, skin, dental pulp, corneal limbus, peripheral blood, umbilical cord tissue, muscles, lungs, menstrual blood, placental tissues, breast milk, and neonatal tissues (Merimi et al., 2021; Wright et al., 2021).

In 2005, the International Society for Cellular Therapy (ISCT) established the minimum criteria for defining *in vitro* human MSCs: i) MSCs must be plastic-adherent and display fibroblastoid morphology in standard culture conditions; ii) MSCs must present immunophenotypic expression of CD105, CD90, and CD73 and absence of expression of CD34, CD45, CD14, CD19, CD11b, CD79a, and HLA-DR surface molecules; and iii) MSCs must be able to differentiate into osteoblasts, chondroblasts, and adipocytes *in vitro* (Dominici et al., 2006). In 2019, ISCT updated their MSC definition recommended the following topics: i) include cells' tissue origin; ii) use of stromal cell nomenclature unless rigorous evidence for stemness is shown; and iii) including functional assays to define the therapeutic mechanism of action, although no tissue-specific guidelines were addressed (Viswanathan et al., 2019). Nevertheless, despite efforts to give a consistent characterization, MSCs are considered a heterogeneous cell population that is influenced by their origin properties (species, tissue source, and donor), as well as by culture conditions such as expansion media and passage number (Merimi et al., 2021).

The potential of MSCs has been attributed to their widespread availability throughout the human body, easy isolation, and expansion, as well as maintenance of viability and regenerative capacity after cryopreservation. Additionally, the low immunogenic and tumorigenic potential make them suitable for allogeneic transplantation approaches (Han et al., 2019; Pittenger et al., 2019). On the other hand, the therapeutic effects of transplanted MSCs were initially attributed to their differentiation capacity. Most of the studies emphasized the ability of stem cells to migrate to the sites of injury, integrate the damaged tissue and differentiate into specialized cells (Drago et al., 2013). However, adult tissue injury resolution, is a complex process that is unlikely to be solved by the MSC differentiation into specific lineages. Therefore, the focus on MSC therapeutical potential has switched in the last decade and it has been increasingly accepted that they induce tissue repair, immunological responses, and control inflammation due to its paracrine function (Pittenger et al., 2019).

4.2. The concept of secretome

The concept that cell-based therapies were the future for regenerative medicine started to change after the work of Gnecchi et al. in 2005 (Gnecchi et al., 2005). His work was the first to show that paracrine factors released from MSCs could promote tissue regeneration. This paracrine hypothesis has inspired an alternative outlook on the use of cell secretome in the most diverse areas of regenerative medicine, including regenerative neurology. The secretome is defined as a set of factors/molecules actively or passively released by a cell, tissue, or organism to the extracellular space (Skalnikova et al., 2011). These factors include, among others, soluble proteins (e.g., cytokines, chemokines, and growth factors), lipids, and extracellular vesicles (EVs; e.g., microvesicles, exosomes, and apoptotic bodies) (Marote et al., 2016; Vizoso et al., 2017).

The secretome of individual cells and tissues is specific, and changes in response to fluctuations in physiological states or pathological conditions (Vizoso et al., 2017). Nevertheless, several studies have been designating MSCs as trophic mediators of regenerative processes. It has been demonstrated that MSCs can secrete important trophic molecules such as BDNF, GDNF, FGF2, nerve growth factor (NGF), insulin-like growth factor-1 (IGF-1), vascular endothelial growth factor (VEGF), among others, that are capable of promoting cell survival, proliferation, differentiation, neurite and axonal outgrowth, and immunomodulation of microglial cells (Drago et al., 2013; Salgado et al., 2015; Teixeira et al., 2013; Vizoso et al., 2017). Moreover, these factors are likely responsible for the prevention of neuronal programmed cell death and glial scar formation in different neurological disorders. MSCs can also protect other cells from damaging oxygen free radicals through the production of antioxidants and anti-apoptotic molecules (Teixeira et al., 2013; Vizoso et al., 2017).

As mentioned above, in addition to soluble paracrine factors, recent findings have shown that EVs are also an important component of the secretome. EVs were primarily considered cellular debris or a way to excrete unneeded products from cells. However, in the past decade, it has been recognized that they perform crucial physiological roles in intercellular communication (Riazifar et al., 2017). EVs-mediated signals can be transmitted by the different biomolecule categories - protein, lipids, nucleic acids and sugars - and the unique package of this information provides both protection and simultaneous delivery of multiple different messengers even to distant sites of the vesicular origin (Lopez-Verrilli et al., 2016). Robust data indicate that EVs have similar protective properties as their cellular counterparts to condition and reprogram the surrounding microenvironment influencing a variety of endogenous responses, particularly in injured tissues (Koniusz et al., 2016). It has been shown that EVs can affect

other cells via the transfer of genetic cargo, transfer of receptors, and ultimately initiating pathways (Momen-Heravi et al., 2013). They can modify cell fate, function, and plasticity, and have the capacity to modulate the immune system and facilitate tissue regeneration (Koniusz et al., 2016).

The use of secretome in regenerative medicine holds several advantages over more conventional stem-cell-based applications regarding manufacturing, storage, handling, and their potential as a ready-to-go biologic product (Vizoso et al., 2017). Storage can be done for long periods without loss of product potency and quality (Bermudez et al., 2016, 2015). The time and cost of expansion and maintenance of cultured MSCs could be significantly reduced and secretome therapies could be immediately administered for the treatment of acute conditions like cerebral ischemia and trauma (Vizoso et al., 2017). Moreover, production in large quantities is possible under controlled laboratory conditions and the biological product could be modified to desired cell-specific effects (McKee and Chaudhry, 2017; Vizoso et al., 2017). Importantly, the use of the secretome derivatives could bypass potential issues associated with cell transplantation including the number of available cells for transplantation and its survival after this procedure (Tran and Damaser, 2015). Nevertheless, regulatory requirements for manufacturing and quality control will be necessary to establish the safety and efficacy profile of these products (Vizoso et al., 2017).

4.3. Mesenchymal stem cell therapeutical effects in Parkinson's disease

Several studies have been reported the therapeutical potential of MSCs in the context of PD (Figure 5), either by a direct secretion of bioactive molecules *in situ* after MSC transplantation, or by its direct exposure or injection in the form of conditioning medium (CM) (Marques et al., 2018).

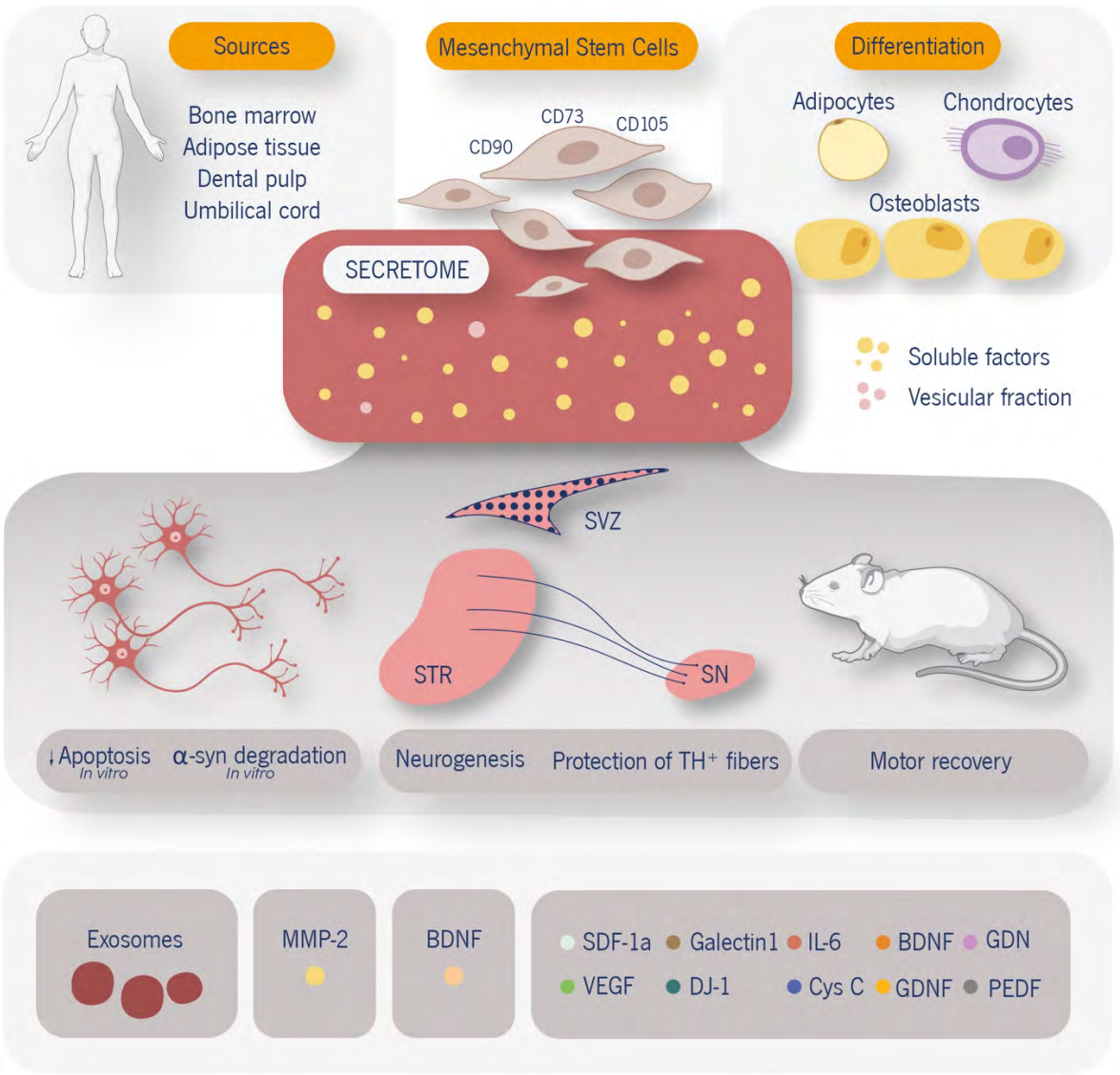


Figure 5. Mesenchymal stem cells and their therapeutical potential in Parkinson's disease. Schematic representation of MSC isolation sources, characterization, and overview of the impact of their secretome in the context of PD and the secreted factors underlying these effects. Abbreviations: SN, substantia nigra; STR, striatum; SVZ, subventricular zone; TH, tyrosine hydroxylase. Adapted from (Marques et al., 2018).

Several *in vitro* studies have identified MSC paracrine activity-neuroprotective effects, as well as the role of some secreted factors in the protection of neurotoxin-induced cytotoxicity. For instance, Wang and colleagues (Wang et al., 2010) showed that bone marrow-derived MSCs (BM-MSCs) exerted neuroprotection in 6-OHDA-exposed dopaminergic neurons, through antiapoptotic mechanisms promoted by the expression of SDF-1α. Moreover, MSC secretome also increased the viability of dopaminergic neurons of rat and human origins, having both neuroprotective and neurorescue activities against 6-OHDA. Prostaglandin E2 receptors have been identified as the main mediators of the MSC secretome effects (Parga et al., 2018). *In vivo*, the first report of MSC potential in the context of PD

demonstrated a behavioral recovery in apomorphine-induced rotations after Wharton's Jelly-derived MSCs (WJ-MSCs) transplantation in the striatum of a hemiparkinsonian rat model, suggesting trophic factor secretion as a mediator of the rescue of degenerating dopaminergic neurons in the SNpc (Weiss et al., 2006). Since then, different studies have been demonstrating the neuroprotection effects of MSCs on neuronal cell death decrease and motor function improvement in PD animal models, most of them using 6-OHDA as a model.

Over the past years, our lab has provided robust evidence of MSC secretome beneficial effects using a 6-OHDA severe PD model. We demonstrated that BM-MSC secretome was able to mediate a partial behavioral recovery in 6-OHDA lesioned rats supported by an increase of dopaminergic neurons and neuronal terminals in the SNpc and striatum, respectively (Teixeira et al., 2017). This work was then replicated, where a direct comparison between BM-MSC secretome injection and BM-MSC transplantation alone was performed (Mendes-Pinheiro et al., 2019). This work demonstrated a positive effect of the secretome at the functional and neuropathological level which was not observed in the BM-MSC-transplanted group. Interestingly, we reproduced the same results in another study where levodopa was also used, with no recovery observed with the PD gold standard treatment contrary to BM-MSC secretome. Additionally, we also showed that the use of full secretome is more advantageous than the use of its protein soluble or vesicular fractions (Vilaça-Faria et al., 2021). Proteomic analysis has consistently identified a myriad of neuroregulatory molecules with a possible role in the modulation of PD associated phenotypic alterations, namely DJ-1, cystatin C, glial-derived nexin, galectin-1, and pigment epithelium-derived factor (PEDF) (Mendes-Pinheiro et al., 2019; Pires et al., 2016; Teixeira et al., 2020), whereas growth factors, such as BDNF, GDNF and VEGF have been identified in MSC secretome by multiplex analysis (Teixeira et al., 2017), which probably mediate the above described effects.

Some studies also suggested the modulation of MSC secretion profile by exposure to neurotrophic factors, overexpression of a specific factor, or even combining MSC secretome with cell replacement strategies. For instance, Sadan and colleagues (Sadan et al., 2009), induced human BM-MSCs into neurotrophic factors-secreting cells, observing a remarkable attenuation of abnormal behavior, as wells as in the loss of TH immunoreactive nerve terminals when compared to the untreated MSC group, attributing these effects to the secretion of BDNF and GDNF. On the other hand, GDNF-transduced rat BM-MSCs provide localized neuroprotection in LPS and 6-OHDA PD animal models (Hoban et al., 2015; Moloney et al., 2010). Other studies were embryonic dopaminergic neurons (Shintani et al., 2007) or

NSCs (Yao et al., 2016) with BM-MSCs CM, induced grafting survival and functional improvement in a 6-OHDA PD rat model, respectively.

Besides neuroprotection effects, the action of MSCs and their secretome in neurogenic niches have also been described, by increasing the proliferation of endogenous NSCs into de dentate gyrus of immunodeficient mice (Munoz et al., 2005) or inducing both neuronal survival and differentiation within the adult rat hippocampus (Teixeira et al., 2015). In the context of disease, it was demonstrated that BM-MSCs transplanted in the striatum 6-OHDA-lesioned rats were able to survive and interact with the lesion site surroundings, enhancing the survival of dopaminergic terminals and neurogenesis in the subventricular zone (SVZ) in a sustained manner. The secretion of BDNF *in vivo* by BM-MSCs, was correlated with the activation of endogenous stem cells (Cova et al., 2010). Similar effects were also observed in the studies by Schwerk et al. using adipose tissue MSCs (ASCs) (Schwerk et al., 2015).

In addition, some studies also demonstrate the beneficial effects of MSCs on immunomodulation and aggregate clearance. Using co-cultures of microglia and mesencephalic neurons together with BM-MSCs, it was observed that there was a decrease in the microglia activation due to the release of anti-inflammatory molecules such as IL-6 and TGF-β, thereby protecting dopaminergic neurons from death (Kim et al., 2009). More recently in our group, using C. elegans it was possible to assess the impact of MSC secretome on α-synuclein accumulation and its induced dopaminergic degeneration. In a C. elegans strain overexpressing human wild-type α-synuclein in dopaminergic neurons, MSC secretome treatment was able to reduce the progressive dopaminergic cell loss. Moreover, the MSC secretome was also effective in reducing the number of aggregates in a model that expresses α-synuclein in the body wall muscle cells (Marques et al., 2021). Besides providing a direct implication of MSC secretome effects on neuroprotection from α-synuclein accumulation, these data also suggest a possible effect of MSC secretome on the degradation of α-synuclein aggregates. This function might be either associated with an indirect activity of MSC secretome on α-synuclein degradation, mediated by the modulation lysosomal autophagy system or through a direct proteolytic activity of enzymes contained in MSC secretome, such as metalloproteinase 2 protein (MMP-2), as recently demonstrated by Oh and colleagues (Oh et al., 2017).

5. Conclusions

PD is a neurological disorder affecting millions of people worldwide with evolving layers of complexity. Together, the various forms of PD create fast-growing health-care issues with enormous global impact (Bloem et al., 2021). It has long been characterized by the classical motor features of parkinsonism associated with LBs and loss of dopaminergic neurons in the SNpc. However, the symptomatology of PD is today recognized as heterogeneous, with clinically significant non-motor features that are equally disabled. The cause of PD remains unknown but seems to result from a complicated interplay of genetic and environmental factors affecting numerous fundamental cellular processes (Bloem et al., 2021; Poewe et al., 2017). PD is treatable, however, the standard treatments available are infective in delaying or stopping disease progression. Current scientific research is focused on the identification of disease biomarkers allowing correct and timely diagnosis, and on developing effective disease modifying therapies (Dawson and Dawson, 2019). The use of stem cells cell-based strategy has emerged as a potential alternative therapy for PD, and among several promising stem cell sources, MSCs have stand out as a valid therapeutic option. Earlier research attributed the therapeutic effects of MSCs to their engrafting and differentiation capacity, however, it has been recognized that the main effects of MSCs are probably mediated by paracrine mechanisms. More importantly, recent studies brought attention to the wide array of bioactive factors produced by MSCs, which may play an important role in the regulation of numerous physiological processes, such as the ability to promote dopaminergic neurons survival, stimulate neurogenesis, decrease neuroinflammation, and promote functional recovery in *in vivo* models (D'angelo et al., 2020; Marques et al., 2018; Teixeira et al., 2013; Vizoso et al., 2017). Thus, MSC-derived secretome may be used as a potential therapeutic approach or as adjuvant therapy for PD symptoms and to counteract the disease progression.

References

Abbas MM, Xu Z, Tan LCS. 2018. Epidemiology of Parkinson's Disease-East Versus West. *Mov Disord Clin Pract* **5**:14–28. doi:10.1002/mdc3.12568

Abbruzzese G, Barone P, Lopiano L, Stocchi F. 2021. The current evidence for the use of safinamide for the treatment of parkinson's disease. *Drug Des Devel Ther* **15**:2507–2517. doi:10.2147/DDDT.S302673

AlDakheel A, Kalia L V., Lang AE. 2014. Pathogenesis-Targeted, Disease-Modifying Therapies in Parkinson Disease. *Neurotherapeutics* **11**:6–23. doi:10.1007/s13311-013-0218-1

Alvarez-Erviti L, Rodriguez-Oroz MC, Cooper JM, Caballero C, Ferrer I, Obeso JA, Schapira AHV. 2010. Chaperone-mediated autophagy markers in Parkinson disease brains. *Arch Neurol* **67**:1464–1472. doi:10.1001/archneurol.2010.198

Ariga H, Takahashi-Niki K, Kato I, Maita H, Niki T, Iguchi-Ariga SMM. 2013. Neuroprotective Function of DJ-1 in Parkinson's Disease. *Oxid Med Cell Longev* **2013**:1–9. doi:10.1155/2013/683920

Arlotta P. 2018. Organoids required! A new path to understanding human brain development and disease. *Nat Methods* **15**:27–29. doi:10.1038/nmeth.4557

Armstrong MJ, Okun MS. 2020. Diagnosis and Treatment of Parkinson Disease. *JAMA* **323**:548. doi:10.1001/jama.2019.22360

Ascherio A, Schwarzschild MA. 2016. The epidemiology of Parkinson's disease: risk factors and prevention. *Lancet Neurol* **15**:1257–1272. doi:10.1016/S1474-4422(16)30230-7

Aulić S, Le TTN, Moda F, Abounit S, Corvaglia S, Casalis L, Gustincich S, Zurzolo C, Tagliavini F, Legname G. 2014. Defined α-synuclein prion-like molecular assemblies spreading in cell culture. *BMC Neurosci* **15**:69. doi:10.1186/1471-2202-15-69

Barrett PJ, Timothy Greenamyre J. 2015. Post-translational modification of α-synuclein in Parkinson's disease. *Brain Res* **1628**:247–253. doi:10.1016/j.brainres.2015.06.002

Bartels T, Choi JG, Selkoe DJ. 2011. α-Synuclein occurs physiologically as a helically folded tetramer that resists aggregation. *Nature* **477**:107–111. doi:10.1038/nature10324

Bedford L, Hay D, Devoy A, Paine S, Powe DG, Seth R, Gray T, Topham I, Fone K, Rezvani N, Mee M, Soane T, Layfield R, Sheppard PW, Ebendal T, Usoskin D, Lowe J, Mayer RJ. 2008. Depletion of 26S proteasomes in mouse brain neurons causes neurodegeneration and lewy-like inclusions resembling human pale bodies. *J Neurosci* **28**:8189–8198. doi:10.1523/JNEUROSCI.2218-08.2008

Belvisi D, Pellicciari R, Fabbrini A, Costanzo M, Pietracupa S, De Lucia M, Modugno N, Magrinelli F, Dallocchio C, Ercoli T, Terravecchia C, Nicoletti A, Solla P, Fabbrini G, Tinazzi M, Berardelli A, Defazio G. 2020a. Risk factors of Parkinson disease. *Neurology* **95**:e2500–e2508. doi:10.1212/WNL.0000000000010813

Belvisi D, Pellicciari R, Fabbrini G, Tinazzi M, Berardelli A, Defazio G. 2020b. Modifiable risk and protective factors in disease development, progression and clinical subtypes of Parkinson's disease: What do prospective studies suggest? *Neurobiol Dis* **134**:104671. doi:10.1016/j.nbd.2019.104671

Ben-Shachar D, Eshel G, Finberg JPM, Youdim MBH. 1991. The Iron Chelator Desferrioxamine (Desferal) Retards 6-Hydroxydopamine-Induced Degeneration of Nigrostriatal Dopamine Neurons. *J Neurochem* **56**:1441–1444. doi:10.1111/j.1471-4159.1991.tb11444.x

Berg D, Postuma RB, Adler CH, Bloem BR, Chan P, Dubois B, Gasser T, Goetz CG, Halliday G, Joseph L, Lang AE, Liepelt-Scarfone I, Litvan I, Marek K, Obeso J, Oertel W, Olanow CW, Poewe W, Stern M, Deuschl G. 2015. MDS research criteria for prodromal Parkinson's disease. *Mov Disord* **30**:1600–1611. doi:10.1002/mds.26431

Bermudez MA, Sendon-Lago J, Eiro N, Trevino M, Gonzalez F, Yebra-Pimentel E, Giraldez MJ, Macia M, Lamelas ML, Saa J, Vizoso F, Perez-Fernandez R. 2015. Corneal epithelial wound healing and bactericidal effect of conditioned medium from human uterine cervical stem cells. *Invest Ophthalmol Vis Sci* **56**:983–992. doi:10.1167/iovs.14-15859

Bermudez MA, Sendon-Lago J, Seoane S, Eiro N, Gonzalez F, Saa J, Vizoso F, Perez-Fernandez R. 2016. Anti-inflammatory effect of conditioned medium from human uterine cervical stem cells in uveitis. *Exp Eye Res* **149**:84–92. doi:10.1016/j.exer.2016.06.022

Betarbet R, Sherer TB, MacKenzie G, Garcia-Osuna M, Panov A V., Greenamyre JT. 2000. Chronic systemic pesticide exposure reproduces features of Parkinson's disease. *Nat Neurosci* **3**:1301–1306. doi:10.1038/81834

Bindoff LA, Birch-Machin MA, Cartlidge NEF, Parker WD, Turnbull DM. 1991. Respiratory chain abnormalities in skeletal muscle from patients with Parkinson's disease. *J Neurol Sci* **104**:203–208. doi:10.1016/0022-510X(91)90311-T

Blesa J, Przedborski S. 2014. Parkinson's disease: Animal models and dopaminergic cell vulnerability. *Front Neuroanat* **8**:155. doi:10.3389/fnana.2014.00155

Block ML, Zecca L, Hong J-S. 2007. Microglia-mediated neurotoxicity: uncovering the molecular mechanisms. *Nat Rev Neurosci* **8**:57–69. doi:10.1038/nrn2038

Bloem BR, Okun MS, Klein C. 2021. Parkinson's disease. *Lancet* **397**:2284–2303. doi:10.1016/S0140-6736(21)00218-X

Bolam JP, Pissadaki EK. 2012. Living on the edge with too many mouths to feed: Why dopamine neurons die. *Mov Disord* **27**:1478–1483. doi:10.1002/mds.25135

Bosco DA, Fowler DM, Zhang Q, Nieva J, Powers ET, Wentworth P, Lerner RA, Kelly JW. 2006. Elevated levels of oxidized cholesterol metabolites in Lewy body disease brains accelerate α-synuclein fibrilization. *Nat Chem Biol* **2**:249–253. doi:10.1038/nchembio782

Bose A, Beal MF. 2016. Mitochondrial dysfunction in Parkinson's disease. *J Neurochem* **139**:216–231. doi:10.1111/jnc.13731

Bostan AC, Dum RP, Strick PL. 2010. The basal ganglia communicate with the cerebellum. *Proc Natl Acad Sci U S A* **107**:8452–6. doi:10.1073/pnas.1000496107

Bové J, Perier C. 2012. Neurotoxin-based models of Parkinson's disease. *Neuroscience* **211**:51–76. doi:10.1016/j.neuroscience.2011.10.057

Braak H, Del Tredici K, Rüb U, de Vos RAI, Jansen Steur ENH, Braak E. 2003. Staging of brain pathology related to sporadic Parkinson's disease. *Neurobiol Aging* **24**:197–211. doi:10.1016/s0197-4580(02)00065-9

Cannon JR, Tapias V, Na HM, Honick AS, Drolet RE, Greenamyre JT. 2009. A highly reproducible rotenone model of Parkinson's disease. *Neurobiol Dis* **34**:279–290. doi:10.1016/j.nbd.2009.01.016

Caplan AI. 1991. Mesenchymal stem cells. *J Orthop Res* **9**:641–650. doi:10.1002/jor.1100090504

Cerri S, Mus L, Blandini F. 2019. Parkinson's Disease in Women and Men: What's the Difference? *J Parkinsons Dis* **9**:501–515. doi:10.3233/JPD-191683

Charron G, Doudnikoff E, Canron MH, Li Q, Ve´ga C, Marais S, Baufreton J, Vital A, Oliet SHR, Bezard E. 2014. Astrocytosis in parkinsonism: Considering tripartite striatal synapses in physiopathology? *Front Aging Neurosci* **6**:258. doi:10.3389/fnagi.2014.00258

Chaudhuri KR, Schapira AH. 2009. Non-motor symptoms of Parkinson's disease: dopaminergic pathophysiology and treatment. *Lancet Neurol* **8**:464–474. doi:10.1016/S1474-4422(09)70068-7

Child CM. 1928. Axial Development in Aggregates of Dissociated Cells from Corymorpha palma. *Physiol Zool* **1**:419–461. doi:10.1086/physzool.1.3.30151056

Chlebanowska P, Tejchman A, Sułkowski M, Skrzypek K, Majka M. 2020. Use of 3D Organoids as a Model to Study Idiopathic Form of Parkinson's Disease. *Int J Mol Sci* **21**. doi:10.3390/ijms21030694

Christine CW, Bankiewicz KS, Van Laar AD, Richardson RM, Ravina B, Kells AP, Boot B, Martin AJ, Nutt J, Thompson ME, Larson PS. 2019. Magnetic resonance imaging–guided phase 1 trial of putaminal AADC gene therapy for Parkinson's disease. *Ann Neurol* **85**:704–714. doi:10.1002/ana.25450

Christine CW, Starr PA, Larson PS, Eberling JL, Jagust WJ, Hawkins RA, Vanbrocklin HF, Wright JF, Bankiewicz KS, Aminoff MJ. 2009. Safety and tolerability of putaminal AADC gene therapy for Parkinson disease. *Neurology* **73**:1662–1669. doi:10.1212/WNL.0b013e3181c29356

Chu Y, Dodiya H, Aebischer P, Olanow CW, Kordower JH. 2009. Alterations in lysosomal and proteasomal markers in Parkinson's disease: Relationship to alpha-synuclein inclusions. *Neurobiol Dis* **35**:385–398. doi:10.1016/j.nbd.2009.05.023

Cicchetti F, Lapointe N, Roberge-Tremblay A, Saint-Pierre M, Jimenez L, Ficke BW, Gross RE. 2005. Systemic exposure to paraquat and maneb models early Parkinson's disease in young adult rats. *Neurobiol Dis* **20**:360–371. doi:10.1016/j.nbd.2005.03.018

Cobb MM, Ravisankar A, Skibinski G, Finkbeiner S. 2018. iPS cells in the study of PD molecular pathogenesis. *Cell Tissue Res* **373**:61–77. doi:10.1007/s00441-017-2749-y

Coelho M, Ferreira JJ. 2012. Late-stage Parkinson disease. *Nat Rev Neurol* **8**:435–442. doi:10.1038/nrneurol.2012.126

Connolly B, Fox SH. 2014. Treatment of Cognitive, Psychiatric, and Affective Disorders Associated with Parkinson's Disease. *Neurotherapeutics* **11**:78–91. doi:10.1007/s13311-013-0238-x

Cova L, Armentero M-T, Zennaro E, Calzarossa C, Bossolasco P, Busca G, Lambertenghi Deliliers G, Polli E, Nappi G, Silani V, Blandini F. 2010. Multiple neurogenic and neurorescue effects of human mesenchymal stem cell after transplantation in an experimental model of Parkinson's disease. *Brain Res* **1311**:12–27. doi:10.1016/j.brainres.2009.11.041

D'angelo M, Cimini A, Castelli V. 2020. Insights into the effects of mesenchymal stem cell-derived secretome in Parkinson's disease. *Int J Mol Sci* **21**:5241. doi:10.3390/ijms21155241

Dallapiazza RF, De Vloo P, Fomenko A, Lee DJ, Hamani C, Munhoz RP, Hodaie M, Lozano AM, Fasano A, Kalia SK. 2018. Considerations for Patient and Target Selection in Deep Brain Stimulation Surgery for Parkinson's Disease In: Stoker TB, Greenland JC, editors. Parkinson's Disease: Pathogenesis and Clinical Aspects. Codon Publications. pp. 145–160. doi:10.15586/codonpublications.parkinsonsdisease.2018.ch8

Dashtipour K, Liu M, Kani C, Dalaie P, Obenaus A, Simmons D, Gatto NM, Zarifi M. 2015. Iron Accumulation Is Not Homogenous among Patients with Parkinson's Disease. *Parkinsons Dis* **2015**:324843. doi:10.1155/2015/324843

Dawson TM, Ko HS, Dawson VL. 2010. Genetic Animal Models of Parkinson's Disease. *Neuron* **66**:646–661. doi:10.1016/j.neuron.2010.04.034

Dawson VL, Dawson TM. 2019. Promising disease-modifying therapies for Parkinson's disease. *Sci Transl Med* **11**:eaba1659. doi:10.1126/scitranslmed.aba1659

Deas E, Plun-Favreau H, Wood NW. 2009. PINK1 function in health and disease. *EMBO Mol Med* **1**:152–165. doi:10.1002/emmm.200900024

Dehay B, Bové J, Rodríguez-Muela N, Perier C, Recasens A, Boya P, Vila M. 2010. Pathogenic lysosomal depletion in Parkinson's disease. *J Neurosci* **30**:12535–12544. doi:10.1523/JNEUROSCI.1920-10.2010

Dehay B, Ramirez A, Martinez-Vicente M, Perier C, Canron MH, Doudnikoff E, Vital A, Vila M, Klein C, Bezard E. 2012. Loss of P-type ATPase ATP13A2/PARK9 function induces general lysosomal deficiency and leads to Parkinson disease neurodegeneration. *Proc Natl Acad Sci U S A* **109**:9611–9616. doi:10.1073/pnas.1112368109

Dexter DT, Carayon A, Javoy-agid F, Agid Y, Wells FR, Daniel SE, Lees AJ, Jenner P, Marsden CD. 1991. Alterations in the levels of iron, ferritin and other trace metals in parkinson's disease and other neurodegenerative diseases affecting the basal ganglia. *Brain* **114**:1953–1975. doi:10.1093/brain/114.4.1953

Dexter DT, Jenner P. 2013. Parkinson disease: from pathology to molecular disease mechanisms. *Free Radic Biol Med* **62**:132–144. doi:10.1016/j.freeradbiomed.2013.01.018

Di Maio R, Barrett PJ, Hoffman EK, Barrett CW, Zharikov A, Borah A, Hu X, McCoy J, Chu CT, Burton EA, Hastings TG, Greenamyre JT. 2016. α-Synuclein binds to TOM20 and inhibits mitochondrial protein import in Parkinson's disease. *Sci Transl Med* **8**:342ra78. doi:10.1126/scitranslmed.aaf3634

Di Nottia M, Masciullo M, Verrigni D, Petrillo S, Modoni A, Rizzo V, Di Giuda D, Rizza T, Niceta M, Torraco A, Bianchi M, Santoro M, Bentivoglio AR, Bertini E, Piemonte F, Carrozzo R, Silvestri G. 2017. DJ-1 modulates mitochondrial response to oxidative stress: clues from a novel diagnosis of PARK7. *Clin Genet* **92**:18–25. doi:10.1111/cge.12841

Dias V, Junn E, Mouradian MM. 2013. The Role of Oxidative Stress in Parkinson's Disease. *J Parkinsons Dis* **3**:461–491. doi:10.3233/JPD-130230

Dickson DW. 2012. Parkinson's Disease and Parkinsonism: Neuropathology. *Cold Spring Harb Perspect Med* **2**:a009258–a009258. doi:10.1101/cshperspect.a009258

Dolgacheva LP, Berezhnov A V., Fedotova EI, Zinchenko VP, Abramov AY. 2019. Role of DJ-1 in the mechanism of pathogenesis of Parkinson's disease. *J Bioenerg Biomembr* **51**:175–188. doi:10.1007/s10863-019-09798-4

Domingo A, Klein C. 2018. Genetics of Parkinson's disease In: Geschwind DH, Paulson HL, Klein C, editors. Handbook of Clinical Neurology: Volume 147, Neurogenetics, Part I. Elsevier. pp.221-227. doi:10.1016/B978-0-444-63233-3.00014-2

Domingues A V., Pereira IM, Vilaça-Faria H, Salgado AJ, Rodrigues AJ, Teixeira FG. 2020. Glial cells in Parkinson´s disease: protective or deleterious? *Cell Mol Life Sci* **77**:5171–5188. doi:10.1007/s00018-020-03584-x

Dominici M, Le Blanc K, Mueller I, Slaper-Cortenbach I, Marini F., Krause DS, Deans RJ, Keating A, Prockop D, Horwitz EM. 2006. Minimal criteria for defining multipotent mesenchymal stromal cells. The International Society for Cellular Therapy position statement. *Cytotherapy* **8**:315–317. doi:10.1080/14653240600855905

Dorsey ER, Elbaz A, Nichols E, Abd-Allah F, Abdelalim A, Adsuar JC, Ansha MG, Brayne C, Choi J-YJ, Collado-Mateo D, Dahodwala N, Do HP, Edessa D, Endres M, Fereshtehnejad S-M, Foreman KJ, Gankpe FG, Gupta R, Hankey GJ, Hay SI, Hegazy MI, Hibstu DT, Kasaeian A, Khader Y, Khalil I, Khang Y-H, Kim YJ, Kokubo Y, Logroscino G, Massano J, Mohamed Ibrahim N, Mohammed MA, Mohammadi A, Moradi-Lakeh M, Naghavi M, Nguyen BT, Nirayo YL, Ogbo FA, Owolabi MO, Pereira DM, Postma MJ, Qorbani M, Rahman MA, Roba KT, Safari H, Safiri S, Satpathy M, Sawhney M, Shafieesabet A, Shiferaw MS, Smith M, Szoeke CEI, Tabarés-Seisdedos R, Truong NT, Ukwaja KN, Venketasubramanian N, Villafaina S, Weldegwergs K gidey, Westerman R, Wijeratne T, Winkler AS, Xuan BT, Yonemoto N, Feigin VL, Vos T, Murray CJL. 2018a. Global, regional, and national burden of Parkinson's disease, 1990–2016: a systematic analysis for the Global Burden of Disease Study 2016. *Lancet Neurol* **17**:939–953. doi:10.1016/S1474-4422(18)30295-3

Dorsey ER, Sherer T, Okun MS, Bloem BR. 2018b. The Emerging Evidence of the Parkinson Pandemic. *J Parkinsons Dis* **8**:S3–S8. doi:10.3233/JPD-181474

Drago D, Cossetti C, Iraci N, Gaude E, Musco G, Bachi A, Pluchino S. 2013. The stem cell secretome and its role in brain repair. *Biochimie* **95**:2271–2285. doi:10.1016/j.biochi.2013.06.020

Ebrahimi-Fakhari D, Wahlster L, McLean PJ. 2012. Protein degradation pathways in Parkinson's disease: curse or blessing. *Acta Neuropathol* **124**:153–172. doi:10.1007/s00401-012-1004-6

Edison P, Ahmed I, Fan Z, Hinz R, Gelosa G, Ray Chaudhuri K, Walker Z, Turkheimer FE, Brooks DJ. 2013. Microglia, amyloid, and glucose metabolism in parkinson's disease with and without dementia. *Neuropsychopharmacology* **38**:938–949. doi:10.1038/npp.2012.255

Eiraku M, Takata N, Ishibashi H, Kawada M, Sakakura E, Okuda S, Sekiguchi K, Adachi T, Sasai Y. 2011. Self-organizing optic-cup morphogenesis in three-dimensional culture. *Nature* **472**:51–56. doi:10.1038/nature09941

Eiraku M, Watanabe K, Matsuo-Takasaki M, Kawada M, Yonemura S, Matsumura M, Wataya T, Nishiyama A, Muguruma K, Sasai Y. 2008. Self-Organized Formation of Polarized Cortical Tissues from ESCs and Its Active Manipulation by Extrinsic Signals. *Cell Stem Cell* **3**:519–532. doi:10.1016/j.stem.2008.09.002

Elbaz A, Clavel J, Rathouz PJ, Moisan F, Galanaud J-P, Delemotte B, Alpérovitch A, Tzourio C. 2009. Professional exposure to pesticides and Parkinson disease. *Ann Neurol* **66**:494–504. doi:10.1002/ana.21717

Eliezer D, Kutluay E, Bussell R, Browne G. 2001. Conformational properties of α-synuclein in its free and lipid-associated states. *J Mol Biol* **307**:1061–1073. doi:10.1006/jmbi.2001.4538

Elstner M, Morris CM, Heim K, Bender A, Mehta D, Jaros E, Klopstock T, Meitinger T, Turnbull DM, Prokisch H. 2011. Expression analysis of dopaminergic neurons in Parkinson's disease and aging links transcriptional dysregulation of energy metabolism to cell death. *Acta Neuropathol* **122**:75–86. doi:10.1007/s00401-011-0828-9

Emamzadeh F. 2016. Alpha-synuclein structure, functions, and interactions. *J Res Med Sci* **21**:29. doi:10.4103/1735-1995.181989

Emborg ME. 2007. Nonhuman Primate Models of Parkinson's Disease. *ILAR J* **48**:339–355. doi:10.1093/ilar.48.4.339

Esteves AR, Cardoso SM. 2017. LRRK2 at the Crossroad Between Autophagy and Microtubule Trafficking. *Neurosci* **23**:16–26. doi:10.1177/1073858415616558

Ferrari E, Cardinale A, Picconi B, Gardoni F. 2020. From cell lines to pluripotent stem cells for modelling Parkinson's Disease. *J Neurosci Methods* **340**:108741. doi:10.1016/j.jneumeth.2020.108741

Fortier LA. 2005. Stem Cells: Classifications, Controversies, and Clinical Applications. *Vet Surg* **34**:415–423. doi:10.1111/j.1532-950X.2005.00063.x

Friedenstein AJ, Deriglasova UF, Kulagina NN, Panasuk AF, Rudakowa SF, Luria EA, Ruadkow IA. 1974. Precursors for fibroblasts in different populations of hematopoietic cells as detected by the in vitro colony assay method. *Exp Hematol* **2**:83–92.

Galet B, Cheval H, Ravassard P. 2020. Patient-Derived Midbrain Organoids to Explore the Molecular Basis of Parkinson's Disease. *Front Neurol* **11**:1005. doi:10.3389/fneur.2020.01005

Galvan A, Devergnas A, Wichmann T. 2015. Alterations in neuronal activity in basal ganglia-thalamocortical circuits in the parkinsonian state. *Front Neuroanat* **9**:5. doi:10.3389/fnana.2015.00005

García-García F, Ponce S, Brown R, Cussen V, Krueger JM. 2005. Sleep disturbances in the rotenone animal model of Parkinson disease. *Brain Res* **1042**:160–168. doi:10.1016/j.brainres.2005.02.036

Gerhard A, Pavese N, Hotton G, Turkheimer F, Es M, Hammers A, Eggert K, Oertel W, Banati RB, Brooks DJ. 2006. In vivo imaging of microglial activation with [11C](R)-PK11195 PET in idiopathic Parkinson's disease. *Neurobiol Dis* **21**:404–412. doi:10.1016/j.nbd.2005.08.002

Gibb WRG, Lees AJ. 1988. The relevance of the Lewy body to the pathogenesis of idiopathic Parkinson's disease. *J Neurol Neurosurg Psychiatry* **15**:745–752. doi: 10.1136/jnnp.51.6.745

Giguère N, Burke Nanni S, Trudeau L-E. 2018. On Cell Loss and Selective Vulnerability of Neuronal Populations in Parkinson's Disease. *Front Neurol* **9**:455. doi:10.3389/fneur.2018.00455

Giugni JC, Okun MS. 2014. Treatment of advanced Parkinson's disease. *Curr Opin Neurol* **27**:450–460. doi:10.1097/WCO.0000000000000118

Gnecchi M, He H, Liang OD, Melo LG, Morello F, Mu H, Noiseux N, Zhang L, Pratt RE, Ingwall JS, Dzau VJ. 2005. Paracrine action accounts for marked protection of ischemic heart by Akt-modified mesenchymal stem cells. *Nat Med* **11**:367–368. doi:10.1038/nm0405-367

Gois Beghini D, Iwao Horita S, Cascabulho CM, Anastácio Alves L, Henriques-Pons A. 2020. Induced Pluripotent Stem Cells: Hope in the Treatment of Diseases, including Muscular Dystrophies. *Int J Mol Sci* **21**:5467. doi:10.3390/ijms21155467

Goldman JG, Postuma R. 2014. Premotor and nonmotor features of Parkinson's disease. *Curr Opin Neurol* **27**:434–441. doi:10.1097/WCO.0000000000000112

Grow DA, McCarrey JR, Navara CS. 2016. Advantages of nonhuman primates as preclinical models for evaluating stem cell-based therapies for Parkinson's disease. *Stem Cell Res* **17**:352–366. doi:10.1016/j.scr.2016.08.013

Grünblatt E, Mandel S, Jacob-Hirsch J, Zeligson S, Amariglo N, Rechavi G, Li J, Ravid R, Roggendorf W, Riederer P, Youdim MBH. 2004. Gene expression profiling of parkinsonian substantia nigra pars compacta; alterations in ubiquitin-proteasome, heat shock protein, iron and oxidative stress regulated proteins, cell adhesion/cellular matrix and vesicle trafficking genes. *J Neural Transm* **111**:1543–1573. doi:10.1007/s00702-004-0212-1

Grünewald A, Rygiel KA, Hepplewhite PD, Morris CM, Picard M, Turnbull DM. 2016. Mitochondrial DNA Depletion in Respiratory Chain–Deficient Parkinson Disease Neurons. *Ann Neurol* **79**:366–378. doi:10.1002/ana.24571

Han Yu, Li X, Zhang Y, Han Yuping, Chang F, Ding J. 2019. Mesenchymal Stem Cells for Regenerative Medicine. *Cells* **8**:886. doi:10.3390/cells8080886

Hawkes CH, Del Tredici K, Braak H. 2007. Parkinson's disease: a dual-hit hypothesis. *Neuropathol Appl Neurobiol* **33**:599–614. doi:10.1111/j.1365-2990.2007.00874.x

He Y, Appel S, Le W. 2001. Minocycline inhibits microglial activation and protects nigral cells after 6-hydroxydopamine injection into mouse striatum. *Brain Res* **909**:187–193. doi:10.1016/S0006-8993(01)02681-6

Heinzel S, Berg D, Gasser T, Chen H, Yao C, Postuma RB. 2019. Update of the MDS research criteria for prodromal Parkinson's disease. *Mov Disord* **34**:1464–1470. doi:10.1002/mds.27802

Helmich RC, Hallett M, Deuschl G, Toni I, Bloem BR. 2012. Cerebral causes and consequences of parkinsonian resting tremor: a tale of two circuits? *Brain* **135**:3206–3226. doi:10.1093/brain/aws023

Hernandez LF, Obeso I, Costa RM, Redgrave P, Obeso JA. 2019. Dopaminergic Vulnerability in Parkinson Disease : The Cost of Humans ' Habitual Performance. *Trends Neurosci* **42**:375–383. doi:10.1016/j.tins.2019.03.007

Heuer A, Smith GA, Lelos MJ, Lane EL, Dunnett SB. 2012. Unilateral nigrostriatal 6-hydroxydopamine lesions in mice I: Motor impairments identify extent of dopamine depletion at three different lesion sites. *Behav Brain Res* **228**:30–43. doi:10.1016/j.bbr.2011.11.027

Hirsch EC, Hunot S. 2009. Neuroinflammation in Parkinson's disease: a target for neuroprotection? *Lancet Neurol* **8**:382–397. doi:10.1016/S1474-4422(09)70062-6

Hirsch EC, Jenner P, Przedborski S. 2013. Pathogenesis of Parkinson's disease. *Mov Disord* **28**:24–30. doi:10.1002/mds.25032

Hoban DB, Howard L, Dowd E. 2015. GDNF-secreting mesenchymal stem cells provide localized neuroprotection in an inflammation-driven rat model of Parkinson's disease. *Neuroscience* **303**:402–411. doi:10.1016/j.neuroscience.2015.07.014

Hustad E, Aasly JO. 2020. Clinical and Imaging Markers of Prodromal Parkinson's Disease. *Front Neurol* **11**:395. doi:10.3389/fneur.2020.00395

Hutchinson K, Wick JY. 2016. Deep Brain Stimulation and Medication Management in Parkinson's Disease. *Consult Pharm* **31**:73–84. doi:10.4140/TCP.n.2016.73

Hwang O. 2013. Role of Oxidative Stress in Parkinson's Disease. *Exp Neurobiol* **22**:11–17. doi:10.5607/en.2013.22.1.11

Hyun DH, Lee MH, Halliwell B, Jenner P. 2003. Proteasomal inhibition causes the formation of protein aggregates containing a wide range of proteins, including nitrated proteins. *J Neurochem* **86**:363–373. doi:10.1046/j.1471-4159.2003.01841.x

Imbert C, Bezard E, Guitraud S, Boraud T, Gross CE. 2000. Comparison of eight clinical rating scales used for the assessment of MPTP-induced parkinsonism in the Macaque monkey. *J Neurosci Methods* **96**:71–76. doi:10.1016/S0165-0270(99)00184-3

Iranzo A, Lomeña F, Stockner H, Valldeoriola F, Vilaseca I, Salamero M, Molinuevo JL, Serradell M, Duch J, Pavía J, Gallego J, Seppi K, Högl B, Tolosa E, Poewe W, Santamaria J. 2010. Decreased striatal dopamine transporter uptake and substantia nigra hyperechogenicity as risk markers of synucleinopathy in patients with idiopathic rapid-eye-movement sleep behaviour disorder: a prospective study. *Lancet Neurol* **9**:1070–1077. doi:10.1016/S1474-4422(10)70216-7

Iranzo A, Stockner H, Serradell M, Seppi K, Valldeoriola F, Frauscher B, Molinuevo JL, Vilaseca I, Mitterling T, Gaig C, Vilas D, Santamaria J, Högl B, Tolosa E, Poewe W. 2014. Five-year follow-up of substantia nigra echogenicity in idiopathic REM sleep behavior disorder. *Mov Disord* **29**:1774–1780. doi:10.1002/mds.26055

Jackson-Lewis V, Przedborski S. 2007. Protocol for the MPTP mouse model of Parkinson's disease. *Nat Protoc* **2**:141–151. doi:10.1038/nprot.2006.342

Jagmag SA, Tripathi N, Shukla SD, Maiti S, Khurana S. 2016. Evaluation of Models of Parkinson's Disease. *Front Neurosci* **9**:503. doi:10.3389/fnins.2015.00503

Jahanshahi M, Jones CRG, Zijlmans J, Katzenschlager R, Lee L, Quinn N, Frith CD, Lees AJ. 2010. Dopaminergic modulation of striato-frontal connectivity during motor timing in Parkinson's disease. *Brain* **133**:727–745. doi:10.1093/brain/awq012

Jellinger KA. 2009. A critical evaluation of current staging of α-synuclein pathology in Lewy body disorders. *Biochim Biophys Acta - Mol Basis Dis* **1792**:730–740. doi:10.1016/j.bbadis.2008.07.006

Jo J, Xiao Y, Sun AX, Cukuroglu E, Tran H-D, Göke J, Tan ZY, Saw TY, Tan C-P, Lokman H, Lee Y, Kim D, Ko HS, Kim S-O, Park JH, Cho N-J, Hyde TM, Kleinman JE, Shin JH, Weinberger DR, Tan EK, Je HS, Ng H-H. 2016. Midbrain-like Organoids from Human Pluripotent Stem Cells Contain Functional Dopaminergic and Neuromelanin-Producing Neurons. *Cell Stem Cell* **19**:248–257. doi:10.1016/j.stem.2016.07.005

Kadoshima T, Sakaguchi H, Nakano T, Soen M, Ando S, Eiraku M, Sasai Y. 2013. Self-organization of axial polarity, inside-out layer pattern, and species-specific progenitor dynamics in human ES cell-derived neocortex. *Proc Natl Acad Sci* **110**:20284–20289. doi:10.1073/pnas.1315710110

Kalia L V., Lang AE. 2015. Parkinson's disease. *Lancet* **386**:896–912. doi:10.1016/S0140-6736(14)61393-3

Kaplitt MG, Feigin A, Tang C, Fitzsimons HL, Mattis P, Lawlor PA, Bland RJ, Young D, Strybing K, Eidelberg D, During MJ. 2007. Safety and tolerability of gene therapy with an adeno-associated virus (AAV) borne GAD gene for Parkinson's disease: an open label, phase I trial. *Lancet* **369**:2097–2105. doi:10.1016/S0140-6736(07)60982-9

Katzenschlager R, Sampaio C, Costa J, Lees A. 2002. Anticholinergics for symptomatic management of Parkinson´s disease. *Cochrane Database Syst Rev* **2**:CD003735. doi:10.1002/14651858.CD003735

Kaur D, Peng J, Chinta SJ, Rajagopalan S, Di Monte DA, Cherny RA, Andersen JK. 2007. Increased murine neonatal iron intake results in Parkinson-like neurodegeneration with age. *Neurobiol Aging* **28**:907–913. doi:10.1016/j.neurobiolaging.2006.04.003

Kaur R, Mehan S, Singh S. 2019. Understanding multifactorial architecture of Parkinson's disease: pathophysiology to management. *Neurol Sci* **40**:13–23. doi:10.1007/s10072-018-3585-x

Kim H, Park HJ, Choi H, Chang Y, Park H, Shin J, Kim Junyeop, Lengner CJ, Lee YK, Kim Jongpil. 2019. Modeling G2019S-LRRK2 Sporadic Parkinson's Disease in 3D Midbrain Organoids. *Stem Cell Reports* **12**:518–531. doi:10.1016/j.stemcr.2019.01.020

Kim Y-J, Park H-J, Lee G, Bang OY, Ahn YH, Joe E, Kim HO, Lee PH. 2009. Neuroprotective effects of human mesenchymal stem cells on dopaminergic neurons through anti-inflammatory action. *Glia* **57**:13–23. doi:10.1002/glia.20731

Kin K, Yasuhara T, Kameda M, Date I. 2019. Animal Models for Parkinson's Disease Research: Trends in the 2000s. *Int J Mol Sci* **20**:5402. doi:10.3390/ijms20215402

Koniusz S, Andrzejewska A, Muraca M, Srivastava AK, Janowski M, Lukomska B. 2016. Extracellular Vesicles in Physiology, Pathology, and Therapy of the Immune and Central Nervous System, with Focus on Extracellular Vesicles Derived from Mesenchymal Stem Cells as Therapeutic Tools. *Front Cell Neurosci* **10**:109. doi:10.3389/fncel.2016.00109

Konnova EA, Swanberg M. 2018. Animal Models of Parkinson's Disease In: Stoker TB, Greenland JC, editors. Parkinson's Disease: Pathogenesis and Clinical Aspects. Codon Publications. pp. 83–106. doi:10.15586/codonpublications.parkinsonsdisease.2018.ch5

Koprich JB, Kalia L V., Brotchie JM. 2017. Animal models of α-synucleinopathy for Parkinson disease drug development. *Nat Rev Neurosci* **18**:515–529. doi:10.1038/nrn.2017.75

Kordower JH, Olanow CW, Dodiya HB, Chu Y, Beach TG, Adler CH, Halliday GM, Bartus RT. 2013. Disease duration and the integrity of the nigrostriatal system in Parkinson's disease. *Brain* **136**:2419–2431. doi:10.1093/brain/awt192

Kosta P, Argyropoulou MI, Markoula S, Konitsiotis S. 2006. MRI evaluation of the basal ganglia size and iron content in patients with Parkinson's disease. *J Neurol* **253**:26–32. doi:10.1007/s00415-005-0914-9

Krige D, Carroll MT, Cooper JM, Marsden CD, Schapira AH V. 1992. Platelet mitochondria function in Parkinson's disease. *Ann Neurol* **32**:782–788. doi:10.1002/ana.410320612

Kriks S, Shim JW, Piao J, Ganat YM, Wakeman DR, Xie Z, Carrillo-Reid L, Auyeung G, Antonacci C, Buch A, Yang L, Beal MF, Surmeier DJ, Kordower JH, Tabar V, Studer L. 2011. Dopamine neurons derived from human ES cells efficiently engraft in animal models of Parkinson's disease. *Nature* **480**:547-551. doi:10.1038/nature10648

LaMarca EA, Powell SK, Akbarian S, Brennand KJ. 2018. Modeling Neuropsychiatric and Neurodegenerative Diseases With Induced Pluripotent Stem Cells. *Front Pediatr* **6**:82. doi:10.3389/fped.2018.00082

Lan J, Jiang DH. 1997. Desferrioxamine and vitamin E protect against iron and MPTP-induced neurodegeneration in mice. *J Neural Transm* **104**:469–481. doi:10.1007/BF01277665

Lancaster MA, Corsini NS, Wolfinger S, Gustafson EH, Phillips AW, Burkard TR, Otani T, Livesey FJ, Knoblich JA. 2017. Guided self-organization and cortical plate formation in human brain organoids. *Nat Biotechnol* **35**:659–666. doi:10.1038/nbt.3906

Lancaster MA, Knoblich JA. 2014. Organogenesis in a dish: Modeling development and disease using organoid technologies. *Science* **345**:1247125. doi:10.1126/science.1247125

Lancaster MA, Renner M, Martin C-A, Wenzel D, Bicknell LS, Hurles ME, Homfray T, Penninger JM, Jackson AP, Knoblich JA. 2013. Cerebral organoids model human brain development and microcephaly. *Nature* **501**:373–379. doi:10.1038/nature12517

Langston J, Ballard P, Tetrud J, Irwin I. 1983. Chronic Parkinsonism in humans due to a product of meperidine-analog synthesis. *Science* **219**:979–980. doi:10.1126/science.6823561

Lawlor PA, During MJ. 2004. Gene therapy for Parkinson's disease. *Expert Rev Mol Med* **6**:1–18. doi:10.1017/S146239940400746X

Lee HJ, Khoshaghideh F, Patel S, Lee SJ. 2004. Clearance of α-Synuclein Oligomeric Intermediates via the Lysosomal Degradation Pathway. *J Neurosci* **24**:1888–1896. doi:10.1523/JNEUROSCI.3809-03.2004

Lim K-L. 2010. Non-mammalian animal models of Parkinson's disease for drug discovery. *Expert Opin Drug Discov* **5**:165–176. doi:10.1517/17460440903527675

Lindvall O, Brundin P, Widner H, Rehncrona S, Gustavii B, Frackowiak R, Leenders KL, Sawle G, Rothwell JC, Marsden CD, et al. 1990. Grafts of fetal dopamine neurons survive and improve motor function in Parkinson's disease. *Science* **247**:574–577.

Liu Z, Cheung H-H. 2020. Stem Cell-Based Therapies for Parkinson Disease. *Int J Mol Sci* **21**:8060. doi:10.3390/ijms21218060

Loeffler DA, Camp DM, Conant SB. 2006. Complement activation in the Parkinson's disease substantia nigra: An immunocytochemical study. *J Neuroinflammation* **3**:29. doi:10.1186/1742-2094-3-29

Lopez-Verrilli MA, Caviedes A, Cabrera A, Sandoval S, Wyneken U, Khoury M. 2016. Mesenchymal stem cell-derived exosomes from different sources selectively promote neuritic outgrowth. *Neuroscience* **320**:129–139. doi:10.1016/j.neuroscience.2016.01.061

Ludtmann MHR, Angelova PR, Horrocks MH, Choi ML, Rodrigues M, Baev AY, Berezhnov A V., Yao Z, Little D, Banushi B, Al-Menhali AS, Ranasinghe RT, Whiten DR, Yapom R, Dolt KS, Devine MJ, Gissen P, Kunath T, Jaganjac M, Pavlov E V., Klenerman D, Abramov AY, Gandhi S. 2018. α-synuclein oligomers interact with ATP synthase and open the permeability transition pore in Parkinson's disease. *Nat Commun* **9**:2293. doi:10.1038/s41467-018-04422-2

Luk KC, Kehm V, Carroll J, Zhang B, O'Brien P, Trojanowski JQ, Lee VM-Y. 2012a. Pathological α-Synuclein Transmission Initiates Parkinson-like Neurodegeneration in Nontransgenic Mice. *Science* **338**:949–953. doi:10.1126/science.1227157

Luk KC, Kehm VM, Zhang B, O'Brien P, Trojanowski JQ, Lee VMY. 2012b. Intracerebral inoculation of pathological α-synuclein initiates a rapidly progressive neurodegenerative α-synucleinopathy in mice. *J Exp Med* **209**:975–986. doi:10.1084/jem.20112457

Ma J, Gao J, Wang J, Xie A. 2019. Prion-Like Mechanisms in Parkinson's Disease. *Front Neurosci* **13**:552. doi:10.3389/fnins.2019.00552

Maetzler W, Hausdorff JM. 2012. Motor signs in the prodromal phase of Parkinson's disease. *Mov Disord* **27**:627–633. doi:10.1002/mds.24973

Magen I, Chesselet M-F. 2010. Genetic mouse models of Parkinson's disease: The state of the art In:Bjorklund A, Cenci MA, editors. Progress in Brain Research: Volume 184, Recents Advances in

Parkinson's Disease: Translational and Clinical Research. Elsevier. pp. 53–87. doi:10.1016/S0079-6123(10)84004-X

Magrinelli F, Picelli A, Tocco P, Federico A, Roncari L, Smania N, Zanette G, Tamburin S. 2016. Pathophysiology of Motor Dysfunction in Parkinson's Disease as the Rationale for Drug Treatment and Rehabilitation. *Parkinsons Dis* **2016**:1–18. doi:10.1155/2016/9832839

Marin C, Aguilar E. 2011. In vivo 6-OHDA-induced neurodegeneration and nigral autophagic markers expression. *Neurochem Int* **58**:521–526. doi:10.1016/j.neuint.2011.01.010

Marote A, Teixeira FG, Mendes-Pinheiro B, Salgado AJ. 2016. MSCs-Derived Exosomes: Cell-Secreted Nanovesicles with Regenerative Potential. *Front Pharmacol* **7**:231. doi:10.3389/fphar.2016.00231

Marotta N, Kim S, Krainc D. 2020. Organoid and pluripotent stem cells in Parkinson's disease modeling: an expert view on their value to drug discovery. *Expert Opin Drug Discov* **15**:427–441. doi:10.1080/17460441.2020.1703671

Marques CR, Marote A, Mendes-Pinheiro B, Teixeira FG, Salgado AJ. 2018. Cell secretome based approaches in Parkinson's disease regenerative medicine. *Expert Opin Biol Ther* **18**:1235–1245. doi:10.1080/14712598.2018.1546840

Marques CR, Pereira-Sousa J, Teixeira FG, Sousa RA, Teixeira-Castro A, Salgado AJ. 2021. Mesenchymal stem cell secretome protects against alpha-synuclein-induced neurodegeneration in a Caenorhabditis elegans model of Parkinson's disease. *Cytotherapy* **23**:894–901. doi:10.1016/j.jcyt.2021.04.002

Marras C, Lang A. 2013. Parkinson's disease subtypes: lost in translation? *J Neurol Neurosurg Psychiatry* **84**:409–415. doi:10.1136/jnnp-2012-303455

Marsili L, Rizzo G, Colosimo C. 2018. Diagnostic Criteria for Parkinson's Disease: From James Parkinson to the Concept of Prodromal Disease. *Front Neurol* **9**. doi:10.3389/fneur.2018.00156

Martínez-Morales PL, Liste I. 2012. Stem Cells as In Vitro Model of Parkinson's Disease. *Stem Cells Int* **2012**:980941. doi:10.1155/2012/980941

Masini D, Plewnia C, Bertho M, Scalbert N, Caggiano V, Fisone G. 2021. A Guide to the Generation of a 6-Hydroxydopamine Mouse Model of Parkinson's Disease for the Study of Non-Motor Symptoms. *Biomedicines* **9**:598. doi:10.3390/biomedicines9060598

Masuda-Suzukake M, Nonaka T, Hosokawa M, Kubo M, Shimozawa A, Akiyama H, Hasegawa M. 2014. Pathological alpha-synuclein propagates through neural networks. *Acta Neuropathol Commun* **2**:88. doi:10.1186/s40478-014-0088-8

Masuda-Suzukake M, Nonaka T, Hosokawa M, Oikawa T, Arai T, Akiyama H, Mann DMA, Hasegawa M. 2013. Prion-like spreading of pathological α-synuclein in brain. *Brain* **136**:1128–1138. doi:10.1093/brain/awt037

McCormack AL, Thiruchelvam M, Manning-Bog AB, Thiffault C, Langston JW, Cory-Slechta DA, Di Monte DA. 2002. Environmental risk factors and Parkinson's disease: Selective degeneration of nigral dopaminergic neurons caused by the herbicide paraquat. *Neurobiol Dis* **10**:119–127. doi:10.1006/nbdi.2002.0507

McGeer PL, McGeer EG. 2008. Glial reactions in Parkinson's disease. *Mov Disord* **23**:474–483. doi:10.1002/mds.21751

McGregor MM, Nelson AB. 2019. Circuit Mechanisms of Parkinson's Disease. *Neuron* **101**:1042–1056. doi:10.1016/j.neuron.2019.03.004

McKee C, Chaudhry GR. 2017. Advances and challenges in stem cell culture. *Colloids Surf B Biointerfaces* **159**:62–77. doi:10.1016/j.colsurfb.2017.07.051

McNaught KSP, Belizaire R, Isacson O, Jenner P, Olanow CW. 2003. Altered proteasomal function in sporadic Parkinson's disease. *Exp Neurol* **179**:38–46. doi:10.1006/exnr.2002.8050

McNaught KSP, Belizaire R, Jenner P, Olanow CW, Isacson O. 2002a. Selective loss of 20S proteasome α-subunits in the substantia nigra pars compacta in Parkinson's disease. *Neurosci Lett* **326**:155–158. doi:10.1016/S0304-3940(02)00296-3

McNaught KSP, Jenner P. 2001. Proteasomal function is impaired in substantia nigra in Parkinson's disease. *Neurosci Lett* **297**:191–194. doi:10.1016/S0304-3940(00)01701-8

McNaught KSP, Mytilin C, JnoBaptiste R, Yabut J, Shashidharan P, Jenner P, Olanow CW. 2002b. Impairment of the ubiquitin-proteasome system causes dopaminergic cell death and inclusion body formation in ventral mesencephalic cultures. *J Neurochem* **81**:301–306. doi:10.1046/j.1471-4159.2002.00821.x

McNaught KSP, Olanow CW, Halliwell B, Isacson O, Jenner P. 2001. Failure of the ubiquitin–proteasome system in Parkinson's disease. *Nat Rev Neurosci* **2**:589–594. doi:10.1038/35086067

Mendes-Pinheiro B, Anjo SI, Manadas B, Da Silva JD, Marote A, Behie LA, Teixeira FG, Salgado AJ. 2019. Bone Marrow Mesenchymal Stem Cells' Secretome Exerts Neuroprotective Effects in a Parkinson's Disease Rat Model. *Front Bioeng Biotechnol* **7**:294. doi:10.3389/fbioe.2019.00294

Merimi M, El-Majzoub R, Lagneaux L, Moussa Agha D, Bouhtit F, Meuleman N, Fahmi H, Lewalle P, Fayyad-Kazan M, Najar M. 2021. The Therapeutic Potential of Mesenchymal Stromal Cells for

Regenerative Medicine: Current Knowledge and Future Understandings. *Front Cell Dev Biol* **9**:661532. doi:10.3389/fcell.2021.661532

Mirelman A, Bernad-Elazari H, Thaler A, Giladi-Yacobi E, Gurevich T, Gana-Weisz M, Saunders-Pullman R, Raymond D, Doan N, Bressman SB, Marder KS, Alcalay RN, Rao AK, Berg D, Brockmann K, Aasly J, Waro BJ, Tolosa E, Vilas D, Pont-Sunyer C, Orr-Urtreger A, Hausdorff JM, Giladi N. 2016. Arm swing as a potential new prodromal marker of Parkinson's disease. *Mov Disord* **31**:1527–1534. doi:10.1002/mds.26720

Mirelman A, Gurevich T, Giladi N, Bar-Shira A, Orr-Urtreger A, Hausdorff JM. 2011. Gait alterations in healthy carriers of the LRRK2 G2019S mutation. *Ann Neurol* **69**:193–197. doi:10.1002/ana.22165

Mohamed N-V, Larroquette F, Beitel LK, Fon EA, Durcan TM. 2019. One Step Into the Future: New iPSC Tools to Advance Research in Parkinson's Disease and Neurological Disorders. *J Parkinsons Dis* **9**:265–281. doi:10.3233/JPD-181515

Moloney TC, Rooney GE, Barry FP, Howard L, Dowd E. 2010. Potential of rat bone marrow-derived mesenchymal stem cells as vehicles for delivery of neurotrophins to the Parkinsonian rat brain. *Brain Res* **1359**:33–43. doi:10.1016/j.brainres.2010.08.040

Momen-Heravi F, Balaj L, Alian S, Mantel PY, Halleck AE, Trachtenberg AJ, Soria CE, Oquin S, Bonebreak CM, Saracoglu E, Skog J, Kuo WP. 2013. Current methods for the isolation of extracellular vesicles. *Biol Chem* **394**:1253–1262. doi:10.1515/hsz-2013-0141

Monzel AS, Hemmer K, Kaoma T, Smits LM, Bolognin S, Lucarelli P, Rosety I, Zagare A, Antony P, Nickels SL, Krueger R, Azuaje F, Schwamborn JC. 2020. Machine learning-assisted neurotoxicity prediction in human midbrain organoids. *Parkinsonism Relat Disord* **75**:105–109. doi:10.1016/j.parkreldis.2020.05.011

Monzel AS, Smits LM, Hemmer K, Hachi S, Moreno EL, van Wuellen T, Jarazo J, Walter J, Brüggemann I, Boussaad I, Berger E, Fleming RMT, Bolognin S, Schwamborn JC. 2017. Derivation of Human Midbrain-Specific Organoids from Neuroepithelial Stem Cells. *Stem Cell Reports* **8**:1144–1154. doi:10.1016/j.stemcr.2017.03.010

Moon HE, Paek SH. 2015. Mitochondrial Dysfunction in Parkinson's Disease. *Exp Neurobiol* **24**:103–116. doi:10.5607/en.2015.24.2.103

Moscona A. 1957. Formation of Lentoids by Dissociated Retinal Cells of the Chick Embryo. *Science* **125**:598–599. doi:10.1126/science.125.3248.598

Moscona A, Moscona H. 1952. The dissociation and aggregation of cells from organ rudiments of the early chick embryo. *J Anat* **86**:287–301.

Mosharov E V, Larsen KE, Kanter E, Phillips KA, Wilson K, Schmitz Y, Krantz DE, Kobayashi K, Edwards RH, Sulzer D. 2009. Interplay between Cytosolic Dopamine, Calcium, and α-Synuclein Causes Selective Death of Substantia Nigra Neurons. *Neuron* **62**:218–229. doi:10.1016/j.neuron.2009.01.033

Mougenot A-L, Nicot S, Bencsik A, Morignat E, Verchère J, Lakhdar L, Legastelois S, Baron T. 2012. Prion-like acceleration of a synucleinopathy in a transgenic mouse model. *Neurobiol Aging* **33**:2225–2228. doi:10.1016/j.neurobiolaging.2011.06.022

Muguruma K, Nishiyama A, Kawakami H, Hashimoto K, Sasai Y. 2015. Self-Organization of Polarized Cerebellar Tissue in 3D Culture of Human Pluripotent Stem Cells. *Cell Rep* **10**:537–550. doi:10.1016/j.celrep.2014.12.051

Müller T. 2015. Catechol-O-methyltransferase inhibitors in Parkinson's disease. *Drugs* **75**:157–174. doi:10.1007/s40265-014-0343-0

Munoz JR, Stoutenger BR, Robinson AP, Spees JL, Prockop DJ. 2005. Human stem/progenitor cells from bone marrow promote neurogenesis of endogenous neural stem cells in the hippocampus of mice. *Proc Natl Acad Sci U S A* **102**:18171–18176. doi:10.1073/pnas.0508945102

Nakabeppu Y, Tsuchimoto D, Yamaguchi H, Sakumi K. 2007. Oxidative damage in nucleic acids and Parkinson's disease. *J Neurosci Res* **85**:919–934. doi:10.1002/jnr.21191

Nakagawa M, Koyanagi M, Tanabe K, Takahashi K, Ichisaka T, Aoi T, Okita K, Mochiduki Y, Takizawa N, Yamanaka S. 2008. Generation of induced pluripotent stem cells without Myc from mouse and human fibroblasts. *Nat Biotechnol* **26**:101–106. doi:10.1038/nbt1374

Nalls MA, N P, CM L, CB D, DG H, M Saad, AL D, E K, J B, M Sharma, C S, MF K, S A, C L, C E, H S, X L, H P, JH L, R; C, Gro, AB. S. 2014. Large-scale meta-analysis of genome-wide association data identifies six new risk loci for Parkinson's disease. *Nat Genet* **46**:989–993. doi:10.1038/ng.3043.Large-scale

Nickels SL, Modamio J, Mendes-Pinheiro B, Monzel AS, Betsou F, Schwamborn JC. 2020. Reproducible generation of human midbrain organoids for in vitro modeling of Parkinson's disease. *Stem Cell Res* **46**:101870. doi:10.1016/j.scr.2020.101870

O'Regan G, DeSouza R-M, Balestrino R, Schapira AH. 2017. Glucocerebrosidase Mutations in Parkinson Disease. *J Parkinsons Dis* **7**:411–422. doi:10.3233/JPD-171092

Oertel WH. 2017. Recent advances in treating Parkinson's disease. *F1000Research* **6**:260. doi:10.12688/f1000research.10100.1

Oh SH, Kim HN, Park HJ, Shin JY, Kim DY, Lee PH. 2017. The Cleavage Effect of Mesenchymal Stem Cell and Its Derived Matrix Metalloproteinase-2 on Extracellular α-Synuclein Aggregates in Parkinsonian Models. *Stem Cells Transl Med* **6**:949–961. doi:10.5966/sctm.2016-0111

Olanow CW, Brundin P. 2013. Parkinson's Disease and Alpha Synuclein: Is Parkinson's Disease a Prion-Like Disorder? *Mov Disord* **28**:31–40. doi:10.1002/mds.25373

Ouchi Y, Yoshikawa E, Sekine Y, Futatsubashi M, Kanno T, Ogusu T, Torizuka T. 2005. Microglial activation and dopamine terminal loss in early Parkinson's disease. *Ann Neurol* **57**:168–175. doi:10.1002/ana.20338

Pacelli C, De Rasmo D, Signorile A, Grattagliano I, di Tullio G, D'Orazio A, Nico B, Comi G Pietro, Ronchi D, Ferranini E, Pirolo D, Seibel P, Schubert S, Gaballo A, Villani G, Cocco T. 2011. Mitochondrial defect and PGC-1α dysfunction in parkin-associated familial Parkinson's disease. *Biochim Biophys Acta - Mol Basis Dis* **1812**:1041–1053. doi:10.1016/j.bbadis.2010.12.022

Pan T, Kondo S, Le W, Jankovic J. 2008. The role of autophagy-lysosome pathway in neurodegeneration associated with Parkinson's disease. *Brain* **131**:1969–1978. doi:10.1093/brain/awm318

Parga JA, García-Garrote M, Martínez S, Raya Á, Labandeira-García JL, Rodríguez-Pallares J. 2018. Prostaglandin EP2 Receptors Mediate Mesenchymal Stromal Cell-Neuroprotective Effects on Dopaminergic Neurons. *Mol Neurobiol* **55**:4763–4776. doi:10.1007/s12035-017-0681-5

Parkinson J. 2002. An Essay on the Shaking Palsy. *J Neuropsychiatry Clin Neurosci* **14**:223–236. doi:10.1176/jnp.14.2.223

Paşca AM, Sloan SA, Clarke LE, Tian Y, Makinson CD, Huber N, Kim CH, Park J-Y, O'Rourke NA, Nguyen KD, Smith SJ, Huguenard JR, Geschwind DH, Barres BA, Paşca SP. 2015. Functional cortical neurons and astrocytes from human pluripotent stem cells in 3D culture. *Nat Methods* **12**:671–678. doi:10.1038/nmeth.3415

Péran P, Cherubini A, Assogna F, Piras F, Quattrocchi C, Peppe A, Celsis P, Rascol O, Démonet JF, Stefani A, Pierantozzi M, Pontieri FE, Caltagirone C, Spalletta G, Sabatini U. 2010. Magnetic resonance imaging markers of Parkinson's disease nigrostriatal signature. *Brain* **133**:3423–3433. doi:10.1093/brain/awq212

Perez-Lloret S, Rey MV, Pavy-Le Traon A, Rascol O. 2013. Emerging drugs for autonomic dysfunction in Parkinson's disease. *Expert Opin Emerg Drugs* **18**:39–53. doi:10.1517/14728214.2013.766168

Piccini P, Brooks DJ, Björklund A, Gunn RN, Grasby PM, Rimoldi O, Brundin P, Hagell P, Rehncrona S, Widner H, Lindvall O. 1999. Dopamine release from nigral transplants visualized in vivo in a Parkinson's patient. *Nat Neurosci* **2**:1137–1140. doi:10.1038/16060

Pickrell AM, Youle RJ. 2015. The Roles of PINK1, Parkin, and Mitochondrial Fidelity in Parkinson's Disease. *Neuron* **85**:257–273. doi:10.1016/j.neuron.2014.12.007

Pires AO, Mendes-Pinheiro B, Teixeira FG, Anjo SI, Ribeiro-Samy S, Gomes ED, Serra SC, Silva NA, Manadas B, Sousa N, Salgado AJ. 2016. Unveiling the Differences of Secretome of Human Bone Marrow Mesenchymal Stem Cells, Adipose Tissue-Derived Stem Cells, and Human Umbilical Cord Perivascular Cells: A Proteomic Analysis. *Stem Cells Dev* **25**:1073–1083. doi:10.1089/scd.2016.0048

Pissadaki EK, Bolam JP. 2013. The energy cost of action potential propagation in dopamine neurons: clues to susceptibility in Parkinson's disease. *Front Comput Neurosci* **7**:13. doi:10.3389/fncom.2013.00013

Pittenger MF, Discher DE, Péault BM, Phinney DG, Hare JM, Caplan AI. 2019. Mesenchymal stem cell perspective: cell biology to clinical progress. *npj Regen Med* **4**:22. doi:10.1038/s41536-019-0083-6

Poewe W, Seppi K, Tanner CM, Halliday GM, Brundin P, Volkmann J, Schrag A-E, Lang AE. 2017. Parkinson disease. *Nat Rev Dis Prim* **3**:17013. doi:10.1038/nrdp.2017.13

Polymeropoulos MH, Lavedan C, Leroy E, Ide SE, Dehejia A, Dutra A, Pike B, Root H, Rubenstein J, Boyer R, Stenroos ES, Chandrasekharappa S, Athanassiadou A, Papapetropoulos T, Johnson WG, Lazzarini AM, Duvoisin RC, Di Iorio G, Golbe LI, Nussbaum RL. 1997. Mutation in the alpha-synuclein gene identified in families with Parkinson's disease. *Science* **276**:2045–7. doi:10.1126/science.276.5321.2045

Postuma RB, Berg D. 2016. Advances in markers of prodromal Parkinson disease. *Nat Rev Neurol* **12**:622–634. doi:10.1038/nrneurol.2016.152

Postuma RB, Berg D, Stern M, Poewe W, Olanow CW, Oertel W, Obeso J, Marek K, Litvan I, Lang AE, Halliday G, Goetz CG, Gasser T, Dubois B, Chan P, Bloem BR, Adler CH, Deuschl G. 2015. MDS clinical diagnostic criteria for Parkinson's disease. *Mov Disord* **30**:1591-1601. doi:10.1002/mds.26424

Postuma RB, Iranzo A, Hu M, Högl B, Boeve BF, Manni R, Oertel WH, Arnulf I, Ferini-Strambi L, Puligheddu M, Antelmi E, Cochen De Cock V, Arnaldi D, Mollenhauer B, Videnovic A, Sonka K, Jung K-Y, Kunz D, Dauvilliers Y, Provini F, Lewis SJ, Buskova J, Pavlova M, Heidbreder A, Montplaisir JY, Santamaria J, Barber TR, Stefani A, St.Louis EK, Terzaghi M, Janzen A, Leu-Semenescu S, Plazzi G, Nobili F, Sixel-Doering F, Dusek P, Bes F, Cortelli P, Ehgoetz Martens K, Gagnon J-F, Gaig C, Zucconi M, Trenkwalder C, Gan-Or Z, Lo C, Rolinski M, Mahlknecht P, Holzknecht E, Boeve AR, Teigen LN, Toscano G, Mayer G, Morbelli S, Dawson B, Pelletier A. 2019. Risk and predictors of dementia and parkinsonism in idiopathic REM sleep behaviour disorder: a multicentre study. *Brain* **142**:744–759. doi:10.1093/brain/awz030

Qian X, Nguyen HN, Song MM, Hadiono C, Ogden SC, Hammack C, Yao B, Hamersky GR, Jacob F, Zhong C, Yoon K, Jeang W, Lin L, Li Y, Thakor J, Berg DA, Zhang C, Kang E, Chickering M, Nauen D, Ho C-Y, Wen Z, Christian KM, Shi P-Y, Maher BJ, Wu H, Jin P, Tang H, Song H, Ming G. 2016. Brain-Region-Specific Organoids Using Mini-bioreactors for Modeling ZIKV Exposure. *Cell* **165**:1238–1254. doi:10.1016/j.cell.2016.04.032

Qian X, Song H, Ming G. 2019. Brain organoids: advances, applications and challenges. *Development* **146**:dev166074. doi:10.1242/dev.166074

Quadrato G, Nguyen T, Macosko EZ, Sherwood JL, Min Yang S, Berger DR, Maria N, Scholvin J, Goldman M, Kinney JP, Boyden ES, Lichtman JW, Williams ZM, McCarroll SA, Arlotta P. 2017. Cell diversity and network dynamics in photosensitive human brain organoids. *Nature* **545**:48–53. doi:10.1038/nature22047

Ramos-Gonzalez P, Mato S, Chara JC, Verkhratsky A, Matute C, Cavaliere F. 2021. Astrocytic atrophy as a pathological feature of Parkinson's disease with LRRK2 mutation. *npj Park Dis* **7**:31. doi:10.1038/s41531-021-00175-w

Ransohoff RM. 2016. How neuroinflammation contributes to neurodegeneration. *Science* **353**:777–783. doi:10.1126/science.aag2590

Reinhardt P, Glatza M, Hemmer K, Tsytsyura Y, Thiel CS, Höing S, Moritz S, Parga JA, Wagner L, Bruder JM, Wu G, Schmid B, Röpke A, Klingauf J, Schwamborn JC, Gasser T, Schöler HR, Sterneckert J. 2013. Derivation and Expansion Using Only Small Molecules of Human Neural Progenitors for Neurodegenerative Disease Modeling. *PLoS One* **8**:e59252. doi:10.1371/journal.pone.0059252

Rey NL, Petit GH, Bousset L, Melki R, Brundin P. 2013. Transfer of human α-synuclein from the olfactory bulb to interconnected brain regions in mice. *Acta Neuropathol* **126**:555–573. doi:10.1007/s00401-013-1160-3

Rey NL, Steiner JA, Maroof N, Luk KC, Madaj Z, Trojanowski JQ, Lee VMY, Brundin P. 2016. Widespread transneuronal propagation of α-synucleinopathy triggered in olfactory bulb mimics prodromal Parkinson's disease. *J Exp Med* **213**:1759–1778. doi:10.1084/jem.20160368

Riazifar M, Pone EJ, Lotvall J, Zhao W. 2017. Stem Cell Extracellular Vesicles: Extended Messages of Regeneration. *Annu Rev Pharmacol Toxicol* **57**:125–154. doi:10.1146/annurev-pharmtox-061616-030146

Richardson JR, Quan Y, Sherer TB, Greenamyre JT, Miller GW. 2005. Paraquat Neurotoxicity is Distinct from that of MPTP and Rotenone. *Toxicol Sci* **88**:193–201. doi:10.1093/toxsci/kfi304

Rietdijk CD, Perez-Pardo P, Garssen J, van Wezel RJA, Kraneveld AD. 2017. Exploring Braak's Hypothesis of Parkinson's Disease. *Front Neurol* **8**:37. doi:10.3389/fneur.2017.00037

Rivero-Ríos P, Madero-Pérez, J, Fernández B, Hilfiker S. 2016. Targeting the Autophagy/Lysosomal Degradation Pathway in Parkinsons Disease. *Curr Neuropharmacol* **14**:238–249. doi:10.2174/1570159x13666151030103027

Rossi ME, Ruottinen H, Saunamäki T, Elovaara I, Dastidar P. 2014. Imaging Brain Iron and Diffusion Patterns. A Follow-up Study of Parkinson's Disease in the Initial Stages. *Acad Radiol* **21**:64–71. doi:10.1016/j.acra.2013.09.018

Rui Q, Ni H, Li D, Gao R, Chen G. 2018. The Role of LRRK2 in Neurodegeneration of Parkinson Disease. *Curr Neuropharmacol* **16**:1348–1357. doi:10.2174/1570159X16666180222165418

Sadan O, Bahat-Stromza M, Barhum Y, Levy YS, Pisnevsky A, Peretz H, Ilan AB, Bulvik S, Shemesh N, Krepel D, Cohen Y, Melamed E, Offen D. 2009. Protective Effects of Neurotrophic Factor–Secreting Cells in a 6-OHDA Rat Model of Parkinson Disease. *Stem Cells Dev* **18**:1179–1190. doi:10.1089/scd.2008.0411

Sakaguchi H, Kadoshima T, Soen M, Narii N, Ishida Y, Ohgushi M, Takahashi J, Eiraku M, Sasai Y. 2015. Generation of functional hippocampal neurons from self-organizing human embryonic stem cell-derived dorsomedial telencephalic tissue. *Nat Commun* **6**:8896. doi:10.1038/ncomms9896

Salgado AJ, Sousa JC, Costa BM, Pires AO, Mateus-Pinheiro A, Teixeira FG, Pinto L, Sousa N. 2015. Mesenchymal stem cells secretome as a modulator of the neurogenic niche: basic insights and therapeutic opportunities. *Front Cell Neurosci* **9**:249. doi:10.3389/fncel.2015.00249

Sato T, Vries RG, Snippert HJ, van de Wetering M, Barker N, Stange DE, van Es JH, Abo A, Kujala P, Peters PJ, Clevers H. 2009. Single Lgr5 stem cells build crypt-villus structures in vitro without a mesenchymal niche. *Nature* **459**:262–265. doi:10.1038/nature07935

Sawada H, Oeda T, Kuno S, Nomoto M, Yamamoto K, Yamamoto M, Hisanaga K, Kawamura T. 2010. Amantadine for dyskinesias in parkinson's disease: A randomized controlled trial. *PLoS One* **5**:6–12. doi:10.1371/journal.pone.0015298

Schaeffer E, Postuma RB, Berg D. 2020. Prodromal PD: A new nosological entity In: Bjorklund A, Cenci MA, editors. Progress in Brain Research: Volume 252, Recent Advances in Parkinson's Disease. Elsevier. pp. 331–356. doi:10.1016/bs.pbr.2020.01.003

Schapira AH. 2008. Mitochondria in the aetiology and pathogenesis of Parkinson's disease. *Lancet Neurol* **7**:97–109. doi:10.1016/S1474-4422(07)70327-7

Schapira Anthony H.V. 2011. Monoamine oxidase B inhibitors for the treatment of parkinsons disease: A review of symptomatic and potential disease-modifying effects. *CNS Drugs* **25**:1061–1071. doi:10.2165/11596310-000000000-00000

Schapira AHV, Chaudhuri KR, Jenner P. 2017. Non-motor features of Parkinson disease. *Nat Rev Neurosci* **18**:435–450. doi:10.1038/nrn.2017.62

Schapira AHV, Cooper JM, Dexter D, Clark JB, Jenner P, Marsden CD. 1990. Mitochondrial Complex I Deficiency in Parkinson's Disease. *J Neurochem* **54**:823–827. doi:10.1111/j.1471-4159.1990.tb02325.x

Schapira Anthony H. V. 2011. Mitochondrial Pathology in Parkinson's Disease. *Mt Sinai J Med A J Transl Pers Med* **78**:872–881. doi:10.1002/msj.20303

Schwerk A, Altschüler J, Roch M, Gossen M, Winter C, Berg J, Kurtz A, Steiner B. 2015. Human adipose-derived mesenchymal stromal cells increase endogenous neurogenesis in the rat subventricular zone acutely after6-hydroxydopamine lesioning. *Cytotherapy* **17**:199–214. doi:10.1016/j.jcyt.2014.09.005

Seeman P. 2010. Historical Overview: Introduction to the Dopamine Receptors In: Neve KA, editor. The Dopamine Receptors. Totowa, NJ: Humana Press. pp. 1–21. doi:10.1007/978-1-60327-333-6_1

Shen Y, Huang J, Liu L, Xu X, Han C, Zhang G, Jiang H, Li J, Lin Z, Xiong N, Wang T. 2016. A Compendium of Preparation and Application of Stem Cells in Parkinson's Disease: Current Status and Future Prospects. *Front Aging Neurosci* **8**:117. doi:10.3389/fnagi.2016.00117

Shi Y, Inoue H, Wu JC, Yamanaka S. 2017. Induced pluripotent stem cell technology: A decade of progress. *Nat Rev Drug Discov* **16**:115–130. doi:10.1038/nrd.2016.245

Shin J-H, Ko HS, Kang H, Lee Y, Lee Y-I, Pletinkova O, Troconso JC, Dawson VL, Dawson TM. 2011. PARIS (ZNF746) Repression of PGC-1α Contributes to Neurodegeneration in Parkinson's Disease. *Cell* **144**:689–702. doi:10.1016/j.cell.2011.02.010

Shintani A, Nakao N, Kakishita K, Itakura T. 2007. Protection of dopamine neurons by bone marrow stromal cells. *Brain Res* **1186**:48–55. doi:10.1016/j.brainres.2007.09.086

Sidransky E. 2004. Gaucher disease: complexity in a "simple" disorder. *Mol Genet Metab* **83**:6–15. doi:10.1016/j.ymgme.2004.08.015

Sidransky E, Lopez G. 2012. The link between the GBA gene and parkinsonism. *Lancet Neurol* **11**:986–998. doi:10.1016/S1474-4422(12)70190-4

Skalnikova H, Motlik J, Gadher SJ, Kovarova H. 2011. Mapping of the secretome of primary isolates of mammalian cells, stem cells and derived cell lines. *Proteomics* **11**:691–708. doi:10.1002/pmic.201000402

Slanzi A, Iannoto G, Rossi B, Zenaro E, Constantin G. 2020. In vitro Models of Neurodegenerative Diseases. *Front Cell Dev Biol* **8**:328. doi:10.3389/fcell.2020.00328

Smith GA, Heuer A. 2011. 6-OHDA Toxin Model in Mouse In Walz W, editor. Neuromethods: Volume 61, Animal Models of Movement Disorders. Human Press. pp. 281–297. doi:10.1007/978-1-61779-298-4_14

Smits LM, Reinhardt L, Reinhardt P, Glatza M, Monzel AS, Stanslowsky N, Rosato-Siri MD, Zanon A, Antony PM, Bellmann J, Nicklas SM, Hemmer K, Qing X, Berger E, Kalmbach N, Ehrlich M, Bolognin S, Hicks AA, Wegner F, Sterneckert JL, Schwamborn JC. 2019. Modeling Parkinson's disease in midbrain-like organoids. *npj Park Dis* **5**:5. doi:10.1038/s41531-019-0078-4

Soldner F, Stelzer Y, Shivalila CS, Abraham BJ, Latourelle JC, Barrasa MI, Goldmann J, Myers RH, Young RA, Jaenisch R. 2016. Parkinson-associated risk variant in distal enhancer of α-synuclein modulates target gene expression. *Nature* **533**:95–99. doi:10.1038/nature17939

Solesio ME, Saez-atienzar S, Jordán J, Galindo MF. 2012. Characterization of mitophagy in the 6-hydoxydopamine Parkinson's disease model. *Toxicol Sci* **129**:411–420. doi:10.1093/toxsci/kfs218

Sonninen TM, Hämäläinen RH, Koskuvi M, Oksanen M, Shakirzyanova A, Wojciechowski S, Puttonen K, Naumenko N, Goldsteins G, Laham-Karam N, Lehtonen M, Tavi P, Koistinaho J, Lehtonen Š. 2020. Metabolic alterations in Parkinson's disease astrocytes. *Sci Rep* **10**:14474. doi:10.1038/s41598-020-71329-8

Spillantini MG, Crowther RA, Jakes R, Hasegawa M, Goedert M. 1998. Synuclein in filamentous inclusions of Lewy bodies from Parkinson's disease and dementia with Lewy bodies. *Proc Natl Acad Sci* **95**:6469–6473. doi:10.1073/pnas.95.11.6469

Stahl K, Skare Ø, Torp R. 2009. Organotypic Cultures as a Model of Parkinson´s Disease. A Twist to an Old Model. *Sci World J* **9**:811–821. doi:10.1100/tsw.2009.68

Stoker TB, Barker RA. 2020. Recent developments in the treatment of Parkinson's Disease. *F1000Research* **9**:F1000. doi:10.12688/f1000research.25634.1

Su X, Maguire-Zeiss KA, Giuliano R, Prifti L, Venkatesh K, Federoff HJ. 2008. Synuclein activates microglia in a model of Parkinson's disease. *Neurobiol Aging* **29**:1690–1701. doi:10.1016/j.neurobiolaging.2007.04.006

Surmeier DJ, Obeso JA, Halliday GM. 2017. Parkinson's Disease Is Not Simply a Prion Disorder. *J Neurosci* **37**:9799–9807. doi:10.1523/JNEUROSCI.1787-16.2017

Swistowski A, Peng J, Liu Q, Mali P, Rao MS, Cheng L, Zeng X. 2010. Efficient Generation of Functional Dopaminergic Neurons from Human Induced Pluripotent Stem Cells Under Defined Conditions. *Stem Cells* **28**:1893–1904. doi:10.1002/stem.499

Sziráki I, Mohanakumar KP, Rauhala P, Kim HG, Yeh KJ, Chiueh CC. 1998. Manganese: A transition metal protects nigrostriatal neurons from oxidative stress in the iron-induced animal model of Parkinsonism. *Neuroscience* **85**:1101–1111. doi:10.1016/S0306-4522(97)00660-X

Tagliaferro P, Burke RE. 2016. Retrograde Axonal Degeneration in Parkinson Disease. *J Parkinsons Dis* **6**:1–15. doi:10.3233/JPD-150769

Takahashi K, Yamanaka S. 2006. Induction of Pluripotent Stem Cells from Mouse Embryonic and Adult Fibroblast Cultures by Defined Factors. *Cell* **126**:663–676. doi:10.1016/j.cell.2006.07.024

Tambasco N, Romoli M, Calabresi P. 2017. Levodopa in Parkinson's Disease: Current Status and Future Developments. *Curr Neuropharmacol* **16**:1239–1252. doi:10.2174/1570159x15666170510143821

Tanji K, Mori F, Kakita A, Takahashi H, Wakabayashi K. 2011. Alteration of autophagosomal proteins (LC3, GABARAP and GATE-16) in Lewy body disease. *Neurobiol Dis* **43**:690–697. doi:10.1016/j.nbd.2011.05.022

Tanner CM, Kame F, Ross GW, Hoppin JA, Goldman SM, Korell M, Marras C, Bhudhikanok GS, Kasten M, Chade AR, Comyns K, Richards MB, Meng C, Priestley B, Fernandez HH, Cambi F, Umbach DM, Blair A, Sandler DP, Langston JW. 2011. Rotenone, paraquat, and Parkinson's disease. *Environ Health Perspect* **119**:866–872. doi:10.1289/ehp.1002839

Teixeira FG, Carvalho MM, Neves-Carvalho A, Panchalingam KM, Behie LA, Pinto L, Sousa N, Salgado AJ. 2015. Secretome of mesenchymal progenitors from the umbilical cord acts as modulator of neural/glial proliferation and differentiation. *Stem Cell Rev* **11**:288–297. doi:10.1007/s12015-014-9576-2

Teixeira FG, Carvalho MM, Panchalingam KM, Rodrigues AJ, Mendes-Pinheiro B, Anjo S, Manadas B, Behie LA, Sousa N, Salgado AJ. 2017. Impact of the Secretome of Human Mesenchymal Stem Cells on Brain Structure and Animal Behavior in a Rat Model of Parkinson's Disease. *Stem Cells Transl Med* **6**:634–646. doi:10.5966/sctm.2016-0071

Teixeira FG, Carvalho MM, Sousa N, Salgado AJ. 2013. Mesenchymal stem cells secretome: a new paradigm for central nervous system regeneration? *Cell Mol Life Sci* **70**:3871–3882. doi:10.1007/s00018-013-1290-8

Teixeira FG, Gago MF, Marques P, Moreira PS, Magalhães R, Sousa N, Salgado AJ. 2018. Safinamide: a new hope for Parkinson's disease? *Drug Discov Today* **23**:736–744. doi:10.1016/j.drudis.2018.01.033

Teixeira FG, Vilaça-Faria H, Domingues A V., Campos J, Salgado AJ. 2020. Preclinical Comparison of Stem Cells Secretome and Levodopa Application in a 6-Hydroxydopamine Rat Model of Parkinson's Disease. *Cells* **9**:315. doi:10.3390/cells9020315

Tekriwal A, Kern DS, Tsai J, Ince NF, Wu J, Thompson JA, Abosch A. 2017. REM sleep behaviour disorder: prodromal and mechanistic insights for Parkinson's disease. *J Neurol Neurosurg Psychiatry* **88**:445–451. doi:10.1136/jnnp-2016-314471

Thenganatt MA, Jankovic J. 2014. Parkinson Disease Subtypes. *JAMA Neurol* **71**:499. doi:10.1001/jamaneurol.2013.6233

Thrash B, Uthayathas S, Karuppagounder SS, Suppiramaniam V, Dhanasekaran M. 2007. Paraquat and maneb induced neurotoxicity. *Proc West Pharmacol Soc* **50**:31–42.

Tieu K. 2011. A Guide to Neurotoxic Animal Models of Parkinson's Disease. *Cold Spring Harb Perspect Med* **1**:a009316–a009316. doi:10.1101/cshperspect.a009316

Tran C, Damaser MS. 2015. Stem cells as drug delivery methods: application of stem cell secretome for regeneration. *Adv Drug Deliv Rev* **82–83**:1–11. doi:10.1016/j.addr.2014.10.007

Trinh J, Zeldenrust FMJ, Huang J, Kasten M, Schaake S, Petkovic S, Madoev H, Grünewald A, Almuammar S, König IR, Lill CM, Lohmann K, Klein C, Marras C. 2018. Genotype-phenotype relations for the Parkinson's disease genes SNCA, LRRK2, VPS35: MDSGene systematic review. *Mov Disord* **33**:1857–1870. doi:10.1002/mds.27527

Tysnes O-B, Storstein A. 2017. Epidemiology of Parkinson's disease. *J Neural Transm* **124**:901–905. doi:10.1007/s00702-017-1686-y

Ullrich C, Mlekusch R, Kuschnig A, Marksteiner J, Humpel C. 2010. Ubiquitin Enzymes, Ubiquitin and Proteasome Activity in Blood Mononuclear Cells of MCI, Alzheimer and Parkinson Patients. *Curr Alzheimer Res* **7**:549–555. doi:10.2174/156721020455864205O

Ulmer TS, Bax A, Cole NB, Nussbaum RL. 2005. Structure and dynamics of micelle-bound human α-synuclein. *J Biol Chem* **280**:9595–9603. doi:10.1074/jbc.M411805200

Ungerstedt U. 1968. 6-Hydroxy-Dopamine Induced Degeneration of Central Monoamine Neurons. *Eur J Pharmacol* **5**:107–110. doi:10.1016/0014-2999(68)90164-7

Usenovic M, Tresse E, Mazzulli JR, Taylor JP, Krainc D. 2012. Deficiency of ATP13A2 leads to lysosomal dysfunction, α-synuclein accumulation, and neurotoxicity. *J Neurosci* **32**:4240–4246. doi:10.1523/JNEUROSCI.5575-11.2012

van der Kooy D, Weiss and S. 2000. Why Stem Cells? *Science* **287**:1439–1441. doi:10.1126/science.287.5457.1439

Vazin T, Freed WJ. 2010. Human embryonic stem cells: Derivation, culture, and differentiation: A review. *Restor Neurol Neurosci* **28**:589–603. doi:10.3233/RNN-2010-0543

Vekrellis K, Xilouri M, Emmanouilidou E, Rideout HJ, Stefanis L. 2011. Pathological roles of α-synuclein in neurological disorders. *Lancet Neurol* **10**:1015–1025. doi:10.1016/S1474-4422(11)70213-7

Velayati A, Yu WH, Sidransky E. 2010. The Role of Glucocerebrosidase Mutations in Parkinson Disease and Lewy Body Disorders. *Curr Neurol Neurosci Rep* **10**:190–198. doi:10.1007/s11910-010-0102-x

Vilaça-Faria H, Marote A, Lages I, Ribeiro C, Mendes-Pinheiro B, Domingues AV, Campos J, Lanceros-Mendez S, Salgado AJ, Teixeira FG. 2021. Fractionating stem cells secretome for Parkinson's disease modeling: Is it the whole better than the sum of its parts? *Biochimie* **189**:87–98. doi:10.1016/j.biochi.2021.06.008

Visanji NP, Brotchie JM, Kalia L V., Koprich JB, Tandon A, Watts JC, Lang AE. 2016. α-Synuclein-Based Animal Models of Parkinson's Disease: Challenges and Opportunities in a New Era. *Trends Neurosci* **39**:750–762. doi:10.1016/j.tins.2016.09.003

Viswanathan S, Shi Y, Galipeau J, Krampera M, Leblanc K, Martin I, Nolta J, Phinney DG, Sensebe L. 2019. Mesenchymal stem versus stromal cells: International Society for Cell & Gene Therapy (ISCT®) Mesenchymal Stromal Cell committee position statement on nomenclature. *Cytotherapy* **21**:1019–1024. doi:10.1016/j.jcyt.2019.08.002

Vizoso F, Eiro N, Cid S, Schneider J, Perez-Fernandez R. 2017. Mesenchymal Stem Cell Secretome: Toward Cell-Free Therapeutic Strategies in Regenerative Medicine. *Int J Mol Sci* **18**:1852. doi:10.3390/ijms18091852

Voges J, Hilker R, Bötzel K, Kiening KL, Kloss M, Kupsch A, Schnitzler A, Schneider GH, Steude U, Deuschl G, Pinsker MO. 2007. Thirty days complication rate following surgery performed for deep-brain-stimulation. *Mov Disord* **22**:1486–1489. doi:10.1002/mds.21481

Volpicelli-Daley L, Brundin P. 2018. Prion-like propagation of pathology in Parkinson diseasePhysiology & Behavior. pp. 321–335. doi:10.1016/B978-0-444-63945-5.00017-9

Wang F, Yasuhara T, Shingo T, Kameda M, Tajiri N, Yuan WJ, Kondo A, Kadota T, Baba T, Tayra JT, Kikuchi Y, Miyoshi Y, Date I. 2010. Intravenous administration of mesenchymal stem cells exerts therapeutic effects on parkinsonian model of rats: Focusing on neuroprotective effects of stromal cell-derived factor-1α. *BMC Neurosci* **11**:52. doi:10.1186/1471-2202-11-52

Wang W, Perovic I, Chittuluru J, Kaganovich A, Nguyen LTT, Liao J, Auclair JR, Johnson D, Landeru A, Simorellis AK, Ju S, Cookson MR, Asturias FJ, Agar JN, Webb BN, Kang CH, Ringe D, Petsko GA, Pochapsky TC, Hoang QQ. 2011. A soluble α-synuclein construct forms a dynamic tetramer. *Proc Natl Acad Sci U S A* **108**:17797–17802. doi:10.1073/pnas.1113260108

Watanabe K, Kamiya D, Nishiyama A, Katayama T, Nozaki S, Kawasaki H, Watanabe Y, Mizuseki K, Sasai Y. 2005. Directed differentiation of telencephalic precursors from embryonic stem cells. *Nat Neurosci* **8**:288–296. doi:10.1038/nn1402

Weintraub D, Burn DJ. 2011. Parkinson's disease: The quintessential neuropsychiatric disorder. *Mov Disord* **26**:1022–1031. doi:10.1002/mds.23664

Weiss ML, Medicetty S, Bledsoe AR, Rachakatla RS, Choi M, Merchav S, Luo Y, Rao MS, Velagaleti G, Troyer D. 2006. Human umbilical cord matrix stem cells: preliminary characterization and effect of transplantation in a rodent model of Parkinson's disease. *Stem Cells* **24**:781–92. doi:10.1634/stemcells.2005-0330

Weiss P, Taylor AC. 1960. Reconstitution of complete organs from single-cell suspensions of chick embryos in advanced stages of differentiation. *Proc Natl Acad Sci* **46**:1177–1185. doi:10.1073/pnas.46.9.1177

Williams DR, Hadeed A, Najim al-Din AS, Wreikat AL, Lees AJ. 2005. Kufor Rakeb disease: Autosomal recessive, levodopa-responsive Parkinsonism with pyramidal degeneration, supranuclear gaze palsy, and dementia. *Mov Disord* **20**:1264–1271. doi:10.1002/mds.20511

Wilson H V. 1911. On the behavior of the dissociated cells in hydroids, alcyonaria, and Asterias. *J Exp Zool* **11**:281–338. doi:10.1002/jez.1400110304

Wilson H V. 1907. A New Method by Which Sponges May Be Artificially Reared. *Science* **25**:912–915. doi:10.1126/science.25.649.912

Wright A, Arthaud-Day ML, Weiss ML. 2021. Therapeutic Use of Mesenchymal Stromal Cells: The Need for Inclusive Characterization Guidelines to Accommodate All Tissue Sources and Species. *Front Cell Dev Biol* **9**:632717. doi:10.3389/fcell.2021.632717

Wu DC, Jackson-Lewis V, Vila M, Tieu K, Teismann P, Vadseth C, Choi DK, Ischiropoulos H, Przedborski S. 2002. Blockade of microglial activation is neuroprotective in the 1-methyl-4-phenyl-1,2,3,6-tetrahydropyridine mouse model of Parkinson disease. *J Neurosci* **22**:1763–1771. doi:10.1523/jneurosci.22-05-01763.2002

Wu T, Hallett M. 2013. The cerebellum in Parkinson's disease. *Brain* **136**:696–709. doi:10.1093/brain/aws360

Xia Q. 2008. Proteomic identification of novel proteins associated with Lewy bodies. *Front Biosci* **13**:3850. doi:10.2741/2973

Xie W, Li X, Li C, Zhu W, Jankovic J, Le W. 2010. Proteasome inhibition modeling nigral neuron degeneration in Parkinson's disease. *J Neurochem* **115**:188–199. doi:10.1111/j.1471-4159.2010.06914.x

Yao Y, Huang C, Gu P, Wen T. 2016. Combined MSC-secreted factors and neural stem cell transplantation promote functional recovery of PD rats. *Cell Transplant* **25**:1101–1113. doi:10.3727/096368915X689938

Yu J, Vodyanik MA, Smuga-Otto K, Antosiewicz-Bourget J, Frane JL, Tian S, Nie J, Jonsdottir GA, Ruotti V, Stewart R, Slukvin II, Thomson JA. 2007. Induced Pluripotent Stem Cell Lines Derived from Human Somatic Cells. *Science* **318**:1917–1920. doi:10.1126/science.1151526

Zahoor I, Shafi A, Haq E. 2018. Pharmacological Treatment of Parkinson's Disease In: Stoker TB, Greenland JC, editors. Parkinson's Disease: Pathogenesis and Clinical Aspects. Codon Publications. pp. 129–144. doi:10.15586/codonpublications.parkinsonsdisease.2018.ch7

Zeng BY, Iravani MM, Lin ST, Irifune M, Kuoppamäki M, Al-Barghouthy G, Smith L, Jackson MJ, Rose S, Medhurst AD, Jenner P. 2006. MPTP treatment of common marmosets impairs proteasomal enzyme activity and decreases expression of structural and regulatory elements of the 26S proteasome. *Eur J Neurosci* **23**:1766–1774. doi:10.1111/j.1460-9568.2006.04718.x

Zhang QS, Heng Y, Mou Z, Huang JY, Yuan YH, Chen NH. 2017. Reassessment of subacute MPTP-treated mice as animal model of Parkinson's disease. *Acta Pharmacol Sin* **38**:1317–1328. doi:10.1038/aps.2017.49

Zhang S-C, Wernig M, Duncan ID, Brüstle O, Thomson JA. 2001. In vitro differentiation of transplantable neural precursors from human embryonic stem cells. *Nat Biotechnol* **19**:1129–1133. doi:10.1038/nbt1201-1129

Zheng B, Liao Z, Locascio JJ, Lesniak KA, Roderick SS, Watt ML, Eklund AC, Zhang-James Y, Kim PD, Hauser MA, Grünblatt E, Moran LB, Mandel SA, Riederer P, Miller RM, Cantuti-Castelvetri I, Young AB, Vance JM, Davis RL, Hedreen JC, Adler CH, Beach TG, Graeber MB, Middleton FA, Rochet J-C, Scherzer CR. 2010. PGC-1α, A Potential Therapeutic Target for Early Intervention in Parkinson's Disease. *Sci Transl Med* **2**:52ra73. doi: 10.1126/scitranslmed.3001059

CHAPTER 2

Research aims

Parkinson's disease (PD) is a recognizable clinical syndrome with a range of causes and clinical presentations. PD represents a fast-growing neurodegenerative condition affecting millions of people worldwide with no cure. Due to its complexity and unknown etiology, disease-modifying therapies able to slow, halt or reverse PD underlying neurodegeneration are a large unmet need in the field. Mesenchymal stem cells (MSCs) are a population of adult stem cells that have been put forward as a promising therapeutic approach for PD. Despite being a powerful tool for clinical applications, they present limitations in terms of delivery, safety, and variability of therapeutic response. Conversely, the secretome of MSCs mainly composed of soluble factors and vesicles could represent a valid alternative to their use. Thus, the main goal of this thesis was to address the neuroprotective effects of bone marrow-derived MSCs (BM-MSCs) using different models of PD, as follows:

- Modulate neuronal degeneration in midbrain-specific organoids aiming to foster dopaminergic repair using the secretome of BM-MSCs. **– Chapter 3**

- Establish a unilateral intrastriatal 6-Hydroxydopamine (6-OHDA) PD mouse model, exploring motor and non-motor phenotypes, performing histological and neurochemical characterization, as well as investigating the participation of glial responses. **– Chapter 4**

- Evaluate the effects of BM-MSC secretome in the established PD mouse model at the behavioral and histological level, comparing two different routes of secretome administration: intracerebral injections *versus* multiple systemic administration. **– Chapter 5**

CHAPTER 3

Modeling Parkinson's disease in human midbrain-specific organoids to study the neuroprotective potential of mesenchymal stem cell secretome

Bárbara Mendes-Pinheiro[1,2,3], Nickels S[3], Anna Monzel[3], Ibrahim Boussaad[3], Sofia C. Serra[1,2], Ana Marote[1,2], Rejko Kruger[3], António J. Salgado[1,2*] & Jens C. Schwamborn[3*]. (2022). Modeling Parkinson's disease in human midbrain-specific organoids to study the neuroprotective potential of mesenchymal stem cell secretome.

*These authors share senior authorship.

[1]Life and Health Sciences Research Institute (ICVS), School of Medicine, University of Minho, Campus de Gualtar, 4710-057 Braga, Portugal;

[2]ICVS/3B's - PT Government Associate Laboratory, 4805-017 Guimarães, Portugal;

[3]Luxembourg Centre for Systems and Biomedicine (LCSB), University of Luxembourg, L-4367 Belvaux, Luxembourg.

Abstract

Parkinson's disease (PD) is characterized by the loss of dopaminergic neurons from the substantia *nigra pars compacta* leading to the denervation of the nigrostriatal tract and a significant reduction of dopamine at the striatal level. The exact mechanism behind dopaminergic cell death is still not completely understood, therefore, *in vitro* studies can provide powerful tools for the investigation of cellular and molecular features underlying PD. Three-dimensional cell culture models represent an innovative technique to recapitulate some aspects of the complexity and physiology of the human brain, holding great potential for its application in modeling neurological disorders including PD. Moreover, these systems can further be used as platforms for studying the neuroprotective effects of newly developed therapeutic tools such as the secretome of mesenchymal stem cells (MSCs). Therefore, we used regionally patterned neuroepithelial stem cells to derive human midbrain-specific organoids (hMOs). This midbrain organoid system was further used to test the neuroprotective effects of bone marrow-derived MSCs (BM-MSCs) secretome, taking advantage of two different models: i) neurotoxin-induced PD model by exposing the hMOs to 6-hydroxydopamine (6-OHDA), which induces selective dopaminergic cell death and treating them with BM-MSC secretome immediately after toxin exposure; ii) genetic PD model through the generation of isogenic hMOs with DJ-1 mutation, performing the treatments since the beginning of the differentiation. Herein we demonstrated that these organoids recapitulated key hallmarks of the PD pathology, such as reduced amounts of midbrain dopaminergic neurons. Moreover, the secretome of BM-MSCs was able to protect from the dopaminergic neuronal loss, as well as from induced fragmentation of dopaminergic neurites, being these effects more evident in the genetic model.

1. Introduction

Parkinson's disease (PD) is the second most common age-related neurodegenerative disorder and is characterized by the progressive loss of the nigrostriatal dopaminergic neurons. PD is a highly heterogeneous disease, with patients displaying considerable disparities in the age of onset, adherence to Braak staging, neurotransmitter system changes, and symptom presentation (Bloem et al., 2021; Poewe et al., 2017). The cause of PD is still unclear but is recognized as a multifactorial disease, involving an interplay between aging, genetic predisposition, and environmental factors. The majority of people suffering from this disorder have idiopathic PD, however, approximately 10% of the cases can be attributed to known genetic factors (Pang et al., 2019). Among these genes, mutations in SNCA (encoding α-synuclein), leucine-rich repeat kinase 2 (LRRK2), PTEN-induced putative kinase (PINK1), parkin, PARK7 (encoding DJ-1), and glucocerebrosidase (GBA) have been associated with inherent forms of parkinsonism (Domingo and Klein, 2018). The identification of these proteins and the complex pathogenesis caused by its mutations allowed the discovery of neurodegeneration pathways, that can be common between inherited and idiopathic PD. Nonetheless, as a result of this heterogeneity, the cause of PD could entail a variety of molecular and cellular pathways that have yet to be fully elucidated. Therefore, the use of *in vitro* models provides unique opportunities for assessing molecular pathologies and for the identification of novel therapeutic strategies (Lázaro et al., 2017). The discovery of induced pluripotent stem cells (iPSCs) revolutionized the stem cell field and consequently the biomedical research, allowing the use of human models to study a variety of diseases, including PD (Cobb et al., 2018). Since then, an increasing number of iPSC lines have been generated, including iPSCs from patients with mutations in familial PD genes, as well as from patients with sporadic PD, or even lines where a pathogenic mutation in a control line was introduced or corrected in a patient line using genome editing techniques (Mohamed et al., 2019).

Traditionally, iPSCs have been cultured using 2D methods that do not fully represent complex tissues like the human brain. In recent years, the generation of 3D *in vitro* models of complete organs – the so-called organoids – emerged as promising disease models (Smits and Schwamborn, 2020). These complex *in vitro* systems mimic the organ architecture and function and have been shown to model different neurological disorders (Lancaster and Knoblich, 2014). Current studies demonstrated that organoids can produce different cell types including stem cells, neurons, and glial cells, forming defined structural layers and ventricular-like structures, as well as the capacity to recapitulate some aspects of disease pathology. Concerning PD, only a few studies used human midbrain-specific organoids (hMOs),

however, they proved that organoids can offer important insights involved in PD progression. Moreover, hMOs can be highly relevant for studying the role of PD familial genes, as they present high amounts of TH-expressing dopaminergic neurons, and can produce neuromelanin, contrary to the common laboratory animal models (Monzel et al., 2017). Importantly, these systems can further be used as platforms for studying the neuroprotective or neurogenerative effects of newly developed therapeutic tools.

In the last years, compelling evidence has brought attention to the array of bioactive molecules produced by mesenchymal stem cells (MSCs), defined as secretome (Marques et al., 2018; Teixeira et al., 2013; Vizoso et al., 2017). Proteomic analysis has identified a myriad of molecules with a possible role in the modulation of PD associated phenotypic alterations (Mendes-Pinheiro et al., 2019; Pires et al., 2016), whereas growth factors, such as BDNF, GDNF, and VEGF have been identified in MSC secretome by multiplex analysis (Teixeira et al., 2017). Nevertheless, the designing of innovative disease-modifying therapies for PD requires the use of experimental models that better recapitulate disease pathomechanisms underlying dopaminergic degeneration. In this work, we took advantage of a previously described neuroepithelial stem cell (NESC) culture system (Reinhardt et al., 2013) and differentiated these cells under dynamic conditions into hMOs (Monzel et al., 2017; Nickels et al., 2020; Smits et al., 2019). Two different experiments were conducted to test the neuroprotective effects of bone marrow-derived MSCs (BM-MSCs) secretome. In the first approach, ventralized hMOs were exposed to 6-hydroxydopamine (6-OHDA), which induces selective dopaminergic cell death, and treated with BM-MSCs secretome immediately after toxin exposure. In the second approach, we generated isogenic hMOs with DJ-1 mutation, exposing them to BM-MSC secretome from the beginning of the differentiation process. We demonstrated that these organoids recapitulated key hallmarks of the PD pathology, such as reduced amounts of midbrain dopaminergic neurons, as well as, that the secretome of BM-MSCs was able to protect from the dopaminergic neuronal loss, and from induced fragmentation of dopaminergic neurites, being these effects more evident in the genetic model.

2. Materials and methods

2.1. Neuroepithelial stem cell derivation and generation of midbrain organoids

All work with human stem cells was done after approval of the national ethics board, Comité National d'Ethique de Recherche (CNER), under the approval numbers 201305/04 and 201901/01 (Model 1;

(Nickels et al., 2020)) and approved by the ethics committee of the University of Tübingen (Model 2, (Krebiehl et al., 2010)).

Model 1: Neurotoxin-induced model (6-OHDA)

iPSCs were generated as described in the study of Reinhardt et al., (Reinhardt et al., 2013) or bought from Coriel, and derivation of human ventralized NESCs (hvNESCs) from iPSCs via embryonic body formation is described in detail in the study of Smits et al. (Smits et al., 2019). Three different wild-type lines were used, namely K7 (derived from fibroblasts from an 81-year-old female), T12 (derived from a 53-year-old female), and COR (derived from a 55-year-old male) (supplementary Figure S1a). Briefly, hvNESCs were maintained for up to 15 passages (after their generation from iPSCs) under maintenance medium, splitted at a confluency of 80% using Accutase (ThermoFisher Scientific, USA), and seeded 600 000 cells per well on a Geltrex (ThermoFisher Scientific) coated 6-well plates. N2B27 maintenance media consisted of equal parts of DMEM/F12 (ThermoFisher Scientific) and Neurobasal (ThermoFisher Scientific) supplemented with L-glutamine (1:100; ThermoFisher Scientific), penicillin-streptomycin (Pen-Strep, 1:100; ThermoFisher Scientific), N2 (1:200; ThermoFisher Scientific), and B27 (–Vitamin A, 1:100; ThermoFisher Scientific). N2B27 was freshly supplemented with 3 μM CHIR 99021 (CHIR; Axon Medchem, Netherlands), 2.5 μM SB-431542 (SB; Ascent Scientific, UK), 100 nM LDN-193189 (LDN; Sigma, USA), 0.5 μM SAG (Merck, USA), and 200 μM ascorbic acid (AA; Sigma).

To generate the hMOs from hvNESCs, 9000 cells were seeded per well into ultra-low attachment 96-well round-bottom plates (Corning, USA) and kept under maintenance conditions for colony formation for 8 days. Patterning I medium consists of maintenance medium without SB and LDN. For patterning II medium, the concentration of CHIR was reduced to 0.7 μM. On day 8, the 3D colonies were embedded into Geltrex droplets (Zagare et al., 2021) and cultivated into non-treated 24-well tissue culture plates (CELLTREAT, USA) in N2B27 differentiation media (one organoid was kept per well). Differentiation media consist in N2B27 media supplemented with 200 μM AA, 500 μM dibutyryl cAMP (db-cAMP, Sigma), 10 ng/ml brain-derived neurotrophic factor (BDNF; Peprotech, UK), 10 ng/ml glial cell line-derived neurotrophic factor (GDNF; Peprotech), 1 ng/ml transforming growth factor β3 (TGF-β3; Peprotech), 10 μM DAPT (R&D Systems, USA), and 2.5 ng/ml Activin A (Peprotech). The organoids were placed on an orbital shaker rotating at 80 rpm, and media was changed every third day for more 22 days (Figure 1a).

Model 2: Genetic model (DJ-1 mutation)

hNESCs were differentiated from iPSCs using a previously described protocol (Reinhardt et al., 2013). Isogenic hMOs were derived from the control line 17608/6 (C4) and the isogenic line 17608/6A8 (C4Mut) (supplementary Figure S2a), in which the pathogenic c.192G>C (exonic splicing mutation in PARK7 gene) mutation was inserted via CRISPR-Cas9 technology, as previously described in detail (Boussaad et al., 2020). hNESCs were cultured on Geltrex-coated plates in N2B27 media supplemented with 3 μM CHIR, 0.75 μM purmorphamine (PMA; Enzo Life Sciences, USA), and 150 μM AA. The generation of hMOs was performed as previously described (Monzel et al., 2017). Briefly, hNESCs were plated from single cell suspension following accutase treatment and cultured for 6 days in ultra-low attachment 96-well plates in N2B27 maintenance media. On day 8, the hNESC colonies were embedded into droplets of Geltrex, and cultured in non-treated tissue culture 24-well plates. On day 10, the differentiation into midbrain dopaminergic neurons was initiated with N2B27 media supplemented with 10 ng/ml BDNF, 10 ng/ml GDNF, 500 μM db-cAMP, 200 μM AA, and 1 ng/ml TGF-β3. 1 μM PMA was added to this medium for an additional 6 days. On day 14, organoids were placed under shanking conditions. On day 16, PMA was removed from the media, and media was changed every 3 to 4 days. The hMOs were kept in culture for a maximum of 35 days (Figure 4a).

2.2. 6-OHDA treatment

For experiment 1, 6-OHDA was used to induce dopaminergic cell death. 6-OHDA treatment was performed on day 30 of culture. At this time-point, robust neuronal differentiation has been achieved in the hMO cultures. 6-OHDA hydrobromide (100 μM, calculated from freebase weight; 162957, Sigma) was prepared on ice in the dark and dissolved in N2 media without growth factors (DMEM/F12 with 1% N2, 1% PenStrep, and 1% Glutamax (Gibco, USA)). B27 was not added to the media, to not reduce the effect of 6-OHDA, due to its antioxidant capacity. Because of the instability and rapid auto-oxidation of 6-OHDA, a double-treatment was performed (two consecutive days for 24 h).

2.3. BM-MSC culture, secretome collection and concentration

Human bone marrow-derived MSCs (BM-MSCs; Lonza, Switzerland) were thawed and seeded into T75 cm^2 tissue culture flasks and expanded in MesenCult™-ACF Plus Medium (STEMCELL Technologies, Canada). The medium was renewed every 3 days and upon confluence, cells were dissociated using Animal Component-Free Cell Dissociation Kit (STEMCELL Technologies), according to the

manufacturer's instructions. The BM-MSCs used in this work were phenotypically characterized by our laboratory, being positive for the standard MSC markers CD73, CD90, and CD105, and negative for CD45 and HLA-DR. The functional characterization was also evaluated by chondrogenic, osteogenic, and adipogenic differentiation (unpublished data).

The secretome of BM-MSCs was collected in passage 8 (P8) under the form of conditioned medium according to protocols already established in our laboratory (Fraga et al., 2013; Teixeira et al., 2016). Briefly, 5 000 cells/cm^2 were seeded for the *in vitro* experiments and expanded for 72h in MesenCult™-ACF Plus Medium. On the conditioning day, cells were washed 5 times with PBS without Ca^{2+}/Mg^{2+} (Invitrogen, USA) and incubated with Neurobasal A medium (TermoFisher Scientific) supplemented with 1% kanamycin (Life Technologies, USA). After 24 h, the media containing the factors secreted by BM-MSCs were collected and centrifuged at 1200 rpm for 10 min at 4°C to remove any cell debris. For the model 2, the secretome was 100× concentrated by centrifugation using a 5 kDa cut-off concentrator (Vivaspin, GE Healthcare, UK), and frozen at -80 °C until used.

2.4. Secretome treatments

Model 1: Neurotoxin-induced model (6-OHDA)

After neurotoxin exposure, 6-OHDA was removed, and the wells were incubated with the following conditions for 6 days (with one media change; Figure 1a): differentiation medium N2B27 (Control+), Neurobasal A medium (basal medium without any supplementation; Control-), and BM-MSC conditioned medium (Secretome).

Model 2: Genetic model (DJ-1 mutation)

The C4 hMOs and C4Mut hMOs were treated with BM-MSC secretome since the first day of differentiation process (day 10). The secretome was added to the cultures as a supplement in every medium change (100× concentrated) for 25 days (Figure 4a).

2.5. Immunofluorescence staining

To verify the expression of neural progenitor markers within hvNESCs and hNESCs in both models, immunocytochemistry was performed as followed: cells were fixed for 20 min with 4% paraformaldehyde (PFA) in phosphate buffered saline (PBS) and washed twice with PBS. Permeabilization and blocking were performed simultaneously using 0.1% Triton X-100 (Sigma), 1% BSA

(Sigma), and 10% fetal calf serum (FCS) in PBS for 45 min. The cells were washed with 0.1% BSA in PBS, and the primary antibodies (supplementary Table S1) were applied overnight at 4 °C in 0.1% BSA in PBS. On the next day, the cells were washed with 0.1% BSA in PBS and incubated with secondary antibodies for 1 h at room temperature (RT). All secondary antibodies were conjugated to Alexa Fluor fluorochromes (Invitrogen). Finally, cells were washed 3 times with 0.1% BSA in PBS-T (0.005% Tween-20; Sigma), including a Hoechst 33342 (ThermoFisher Scientific) counterstaining for nuclei in the second washing step. Cells were mounted using Vectashield (Vector Labs, USA) and images were taken using the 60× objective of the confocal microscope (Zeiss LSM 710, Germany).

Regarding organoids' staining, at the end of experiments, hMOs were fixed with 4 % PFA overnight at RT and washed 3x with PBS for 15 min. Then, hMOs were embedded in 3% low-melting point agarose in PBS and incubated for 20 min at 40 °C, followed by 30 min incubation at RT. 80 µm sections were cut using a vibratome (Leica VT1000s, Germany), and sections were separated into "border" and "center" sections. The sections were permeabilized and blocked with 0.5 % Triton X-100, 2.5 % normal goat serum (Invitrogen), 2.5% BSA, and 0.1% sodium azide. Sections were incubated on a shaker for 48 h at 4°C with primary antibodies in the blocking buffer containing 0.1% Triton X-100 at the following dilutions: anti-TH from rabbit (1:1000; ab112, Abcam, UK), anti-TUJ1 from mouse (1:600; 801201, BioLegend, USA) and anti-MAP2 from chicken (1:1000; ab5392, Abcam). After incubation with the primary antibodies, sections were washed three times in 0.01% Triton X-100 and incubated with the secondary antibodies (1:1000), including a Hoechst 33342 counterstaining for nuclei in blocking buffer with 0.01% Triton X-100. All secondary antibodies (Invitrogen) were conjugated to Alexa Fluor fluorochromes. Fluorescence images were acquired on an Operetta confocal microscope (Perkin Elmer) with a 20× objective (16-20 area scans, 25 z-planes).

The same immunofluorescent protocol was applied to verify the presence of astrocytic markers, as well as the midbrain identity of hMOs using other primary antibodies besides TH (supplementary Table S1). Images were taken using the 20× or 40× objectives of the Zeiss LSM 710 confocal microscope.

2.6. Image analysis

Immunofluorescence 3D images of hMOs were analyzed in Matlab (Version 2017b, Mathworks) as previously described in detail (Monzel et al., 2020). The in-house developed image analysis algorithms automate the segmentation of nuclei and neurons, with structure-specific feature extraction. High-

content image analysis workflow and the features that is possible to extract are represented in the supplementary material section: Figure S3 and Table S2.

2.7. Statistical analysis

A confidence interval of 95% was assumed for all statistical tests. The assumption of normality was tested for all continuous variables through evaluation of the frequency distribution histogram, the values of skewness and kurtosis, and through the Shapiro-Wilk test. The assumption of homoscedasticity was tested through Levene's test. Both assumptions were met by all tested continuous variables. All continuous data are shown as the mean as mean ± SEM. For the evaluation of mean differences between samples with one independent variable, one-way ANOVA was used, followed by multiple comparisons analysis through Tukey's post hoc test or Dunnett's test to compare each treatment with a single control. For the comparison of means between two groups, a Student's t-test for independent samples was used. Statistical analysis and graphic representation were using the GraphPad Prism ver.8.0c (GraphPad Software; La Jolla, USA).

3. Results

3.1. Model 1: Neurotoxin-induced model (6-OHDA)

Generation, self-organization and neuronal differentiation of hMOs

Previously described hvNESCs (Nickels et al., 2020; Smits et al., 2019) were used as the starting population for the generation of hMOs. Typically, hvNESCs express the neural progenitor markers Nestin, SOX2, SOX1, but also express midbrain floorplate markers like FOXA2 before organoid generation (supplementary Figure S1). Then, cells were seeded on round-bottomed ultra-low-adhesion 96-well plates, enabling the cells to form 3D colonies, and cultured in the presence of small molecules to induce midbrain specification. On day 8, 3D colonies were embedded into droplets of Geltrex for structural support, and the guided differentiation into hMOs was initiated under dynamic conditions (Figure 1A). All experiments were conducted with three different and independent hvNESC lines, individually derived from three different and independent human iPSC lines. During the first 12 days of culture, the hMOs rapidly increased in size and reached a mean core size of 1.25 mm (±0.19 mm, n = 5) in diameter after 20 days (Figure 1B). After 30 days in culture, some hMOs were collected to assess self-organization and neuronal differentiation. We observed that hMOs present a stem cell niche in the center and the dopaminergic neurons are distributed asymmetrically within the organoids (Figure 2A).

Besides the observed robust differentiation into dopaminergic neurons, hMOs maintained the expression of midbrain floorplate markers FOXA2 and EN1 (Figure 2B). Additionally, we demonstrate the presence of dopamine (DA) and an evident co-expression of GIRK2 with TH, revealing the presence of the A9 subtype midbrain dopaminergic neurons (Figure 2C). These stainings revealed the formation of a complex neuronal network and are in line with the previously published results (Monzel et al., 2017; Nickels et al., 2020; Smits et al., 2019), demonstrating the specificity and reproducibility of these cultures. During the development of the fetal human brain, neural tube-derived cells not only differentiate into neurons but also into glia cells, including astrocytes and oligodendrocytes (Kriegstein and Alvarez-Buylla, 2009). Thus, we also investigated the presence of astrocyte markers in the hMOs, however, no robust differentiation in astrocytes was observed at day 30 (we only observed some S100β+ and GFAP+ astrocytes in one specific location of the organoids; supplementary Figure S4). This is in agreement with brain development where glial differentiation temporally follows neuronal differentiation, therefore, a significant increase of astrocytes would be expected to be observe on more mature organoids (~day 60) as previously shown (Monzel et al., 2017)

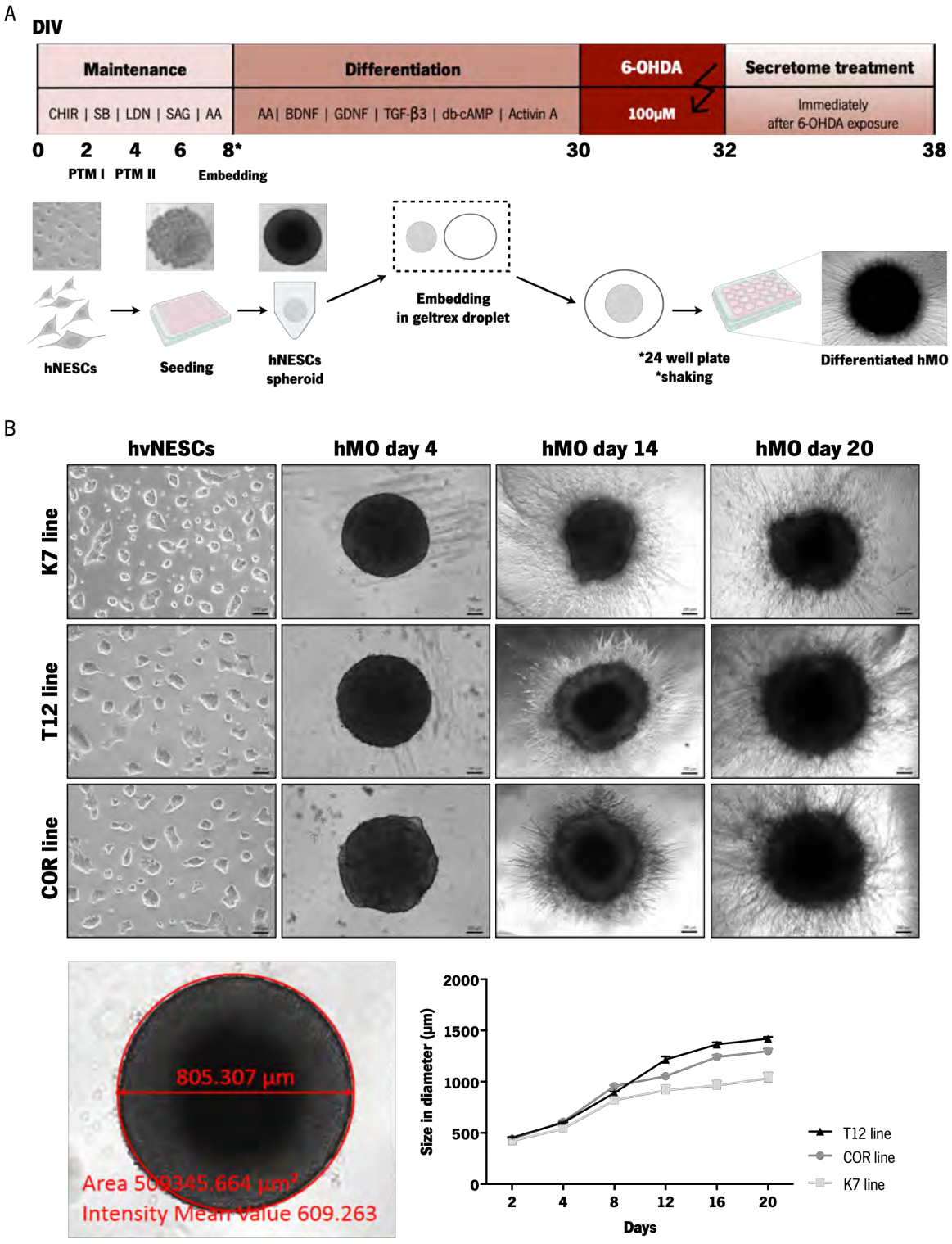


Figure 1. Derivation of hMOs from hvNESCs. A) Schematic representation of the procedure of hMO culture system and the generation of the neurotoxin-induced PD model to assess the neuroprotective effects of BM-MSC secretome; **B)** Growth of hMOs in culture: brightfield images of hMOs generated from hvNESCs at different days in culture (scale bar represents 100 and 200 μm), and the diameter size of hMOs per organoid line from day 2 to day 20. Error bars represent mean ± SEM.

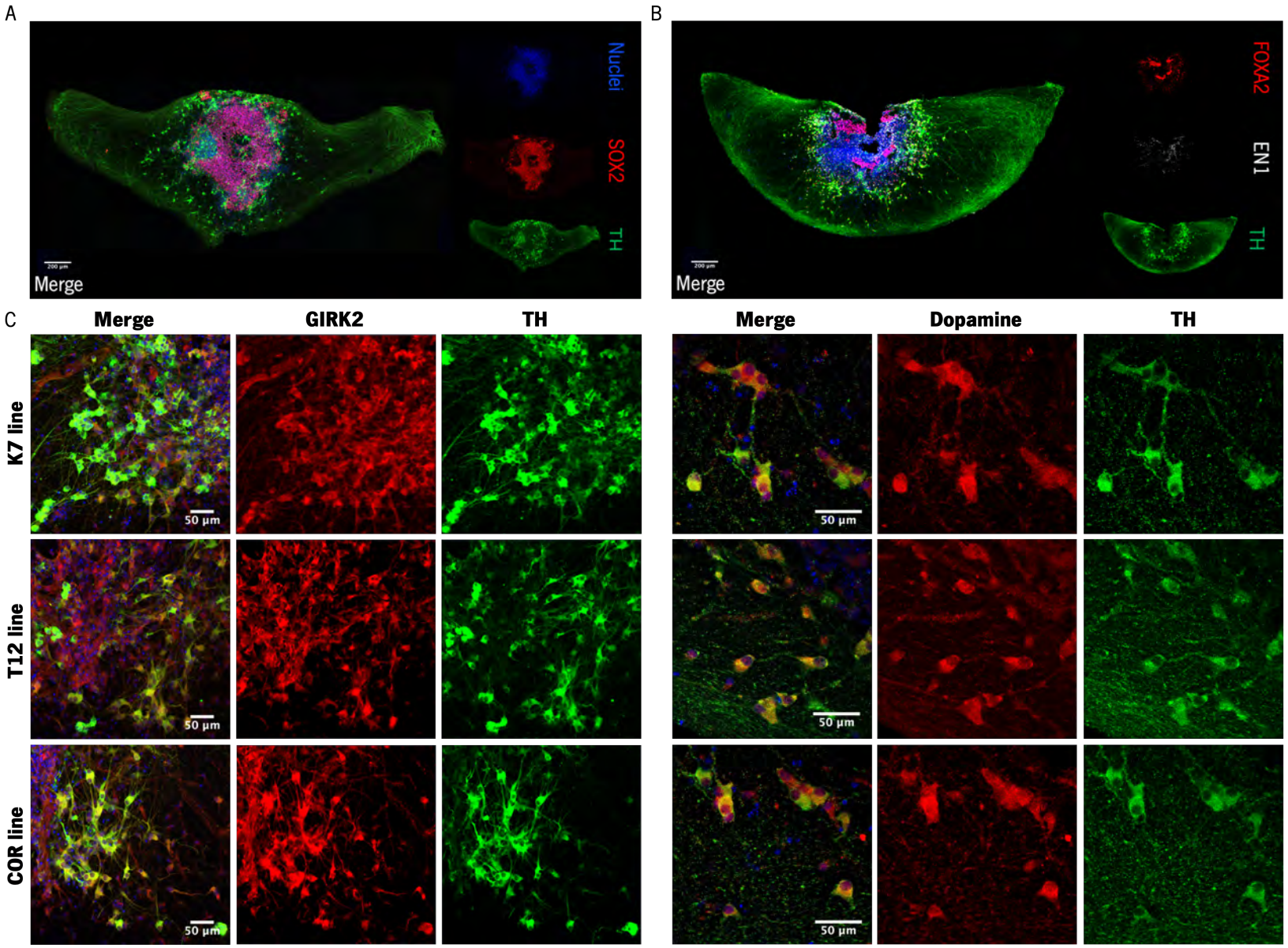

A
Nuclei
SOX2
TH
Merge
B
FOXA2
EN1
TH
Merge
C
Merge
GIRK2
TH
Merge
Dopamine
TH
K7 line
T12 line
COR line
50 µm

Figure 2. Characterization of hMOs at day 30 of the differentiation protocol. A) hMOs self-organization: stem cell niche in the middle (marked with SOX2 in red) and the dopaminergic neurons distributed asymmetrically (marked with TH at green); **B)** hMOs still express midbrain floorplate markers like FOXA2 and EN1 at day 30 in culture, and **(C)** other midbrain markers besides TH such as dopamine, and GIRK2 (a marker of A9 neurons affected in PD), revealing the high specification for the midbrain.

Effects of BM-MSC secretome

Afterwards, we used the hMO cultures as a platform to generate an *in vitro* PD model to study the neuroprotective effects of BM-MSC secretome. For that, hMOs were exposed to 6-OHDA (100 μM) for 2 days to induce dopaminergic degeneration, and then incubated during 6 days with total BM-MSC secretome (1x) immediately after 6-OHDA exposure (Figure 1A). Then, we examined the effects of 6-OHDA and the respective treatments on the neuronal network within hMOs using image-based cell profiling. After 6-OHDA treatments, the amount of TUJ+ neurons remained unaltered ($F_{(5,138)} = 1.280$, $p = 0.235$; Figure 3A). When we looked for TH+ dopaminergic neurons, both secretome and the basal medium (Control-) were able to maintain the cultures in the same conditions when compared to the organoids exposed to the differentiation medium (Control+), however, a significant decrease in TH+ cells was observed for the 6-OHDA-treated organoids ($F_{(5,138)} = 10.73$, $p < 0.001$; Figure 3C), which validates the purpose of this optimized midbrain organoid system as a potential model for PD. Nevertheless, an almost significant trend ($F_{(2,69)} = 2.55$, $p = 0.08$) in the increase of TH+ dopaminergic neurons was observed for 6-OHDA organoids treated with BM-MSC secretome when compared to the non-treated 6-OHDA organoids (Control-). A significant decrease of MAP2+ neurons was also observed after 6-OHDA exposure ($F_{(5,138)} = 10.22$, $p < 0.001$; Figure 3B). 6-OHDA is a highly oxidizable dopamine analog, which can be captured through the dopamine transporter (DAT) (Blandini and Armentero, 2012). As MAP2, DAT is a mature neuronal marker contrary to TUJ1 which is a marker of early committed neurons; therefore, we hypothesized that MAP2+ neurons could be more sensitive to 6-OHDA effects. We also computed a 3D mask for TH+ cells and generated a 3D skeleton of the dopaminergic network to extract features such as nodes (dendritic and axonal points of branching) and links (total number of branches), as well as neurite fragmentation. 6-OHDA treatment led to a decrease in the complexity of the dopaminergic neurons (links: $F_{(5,138)} = 33.56$, $p < 0.001$; nodes: $F_{(5,138)} = 35.13$, $p < 0.001$; Figure 3E, F) and an increase of fragmented neurites ($F_{(5,138)} = 10.87$, $p < 0.001$; Figure 3D). Interestingly, we observed that the hMOs treated with BM-MSC secretome present significant less fragmentation when compared to the non-treated group ($F_{(2,69)} = 6.17$, $p < 0.01$; Figure 3D). Representative images of the immunostainings are represented in Figure 4.

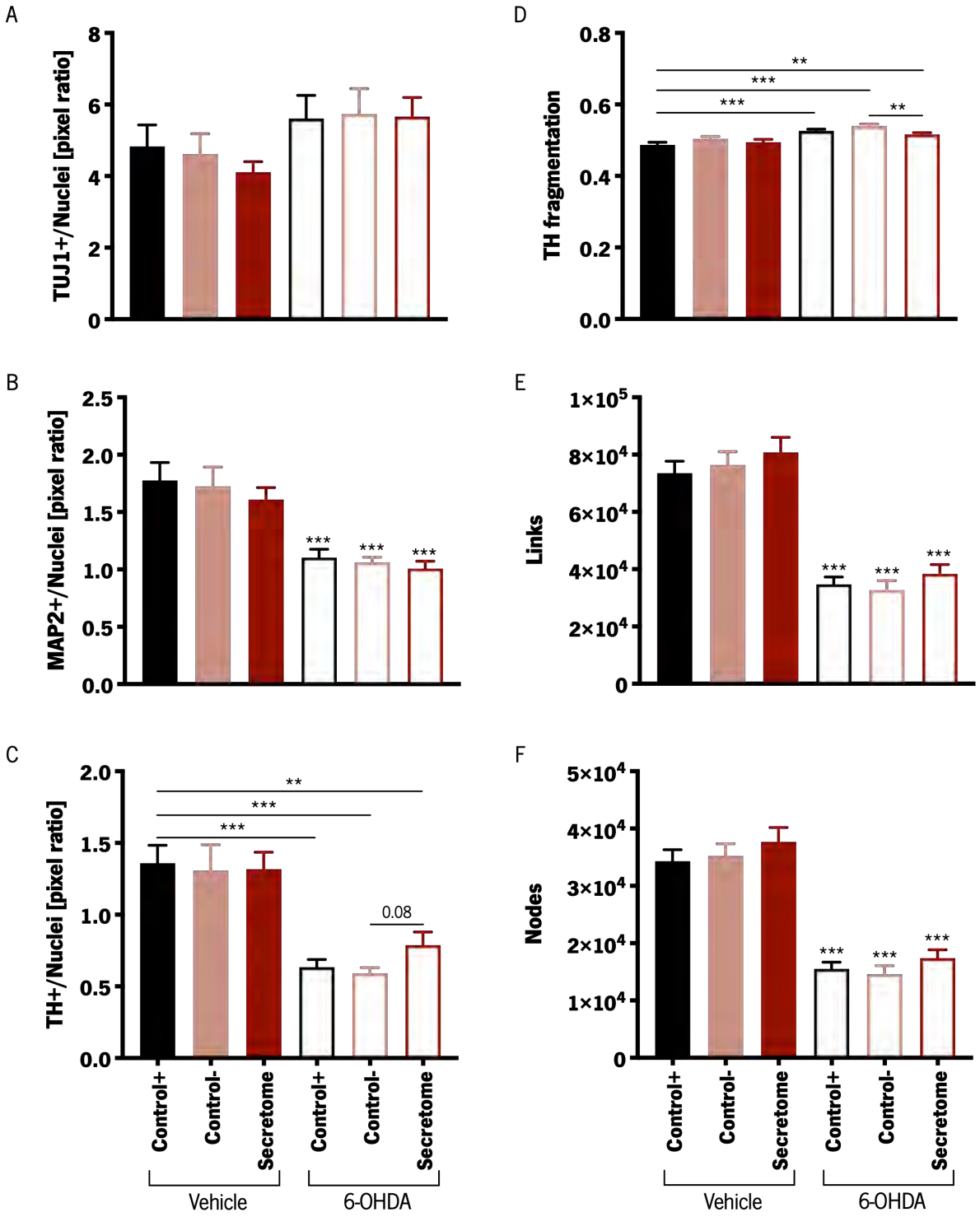


Figure 3. Effects of BM-MSC secretome in the 6-OHDA-induced PD model. Extracted features from high-content image analysis to evaluate the effects of 6-OHDA exposure and the respective treatments, namely in the overall amount of **A)** TUJ+ neurons, **B)** MAP2+ neurons, **C)** TH+ dopaminergic neurons; and on neuronal complexity, namely **D)** TH fragmentation, **E)** links, and **F)** nodes. Control+: differentiation medium N2B27; Control-: basal medium without any supplementation; Secretome: BM-MSC conditioned medium. Two-independent experiments (24 sections (border and center sections) analyzed/group). Data are presented as mean ± SEM. **p < 0.01, ***p < 0.01.

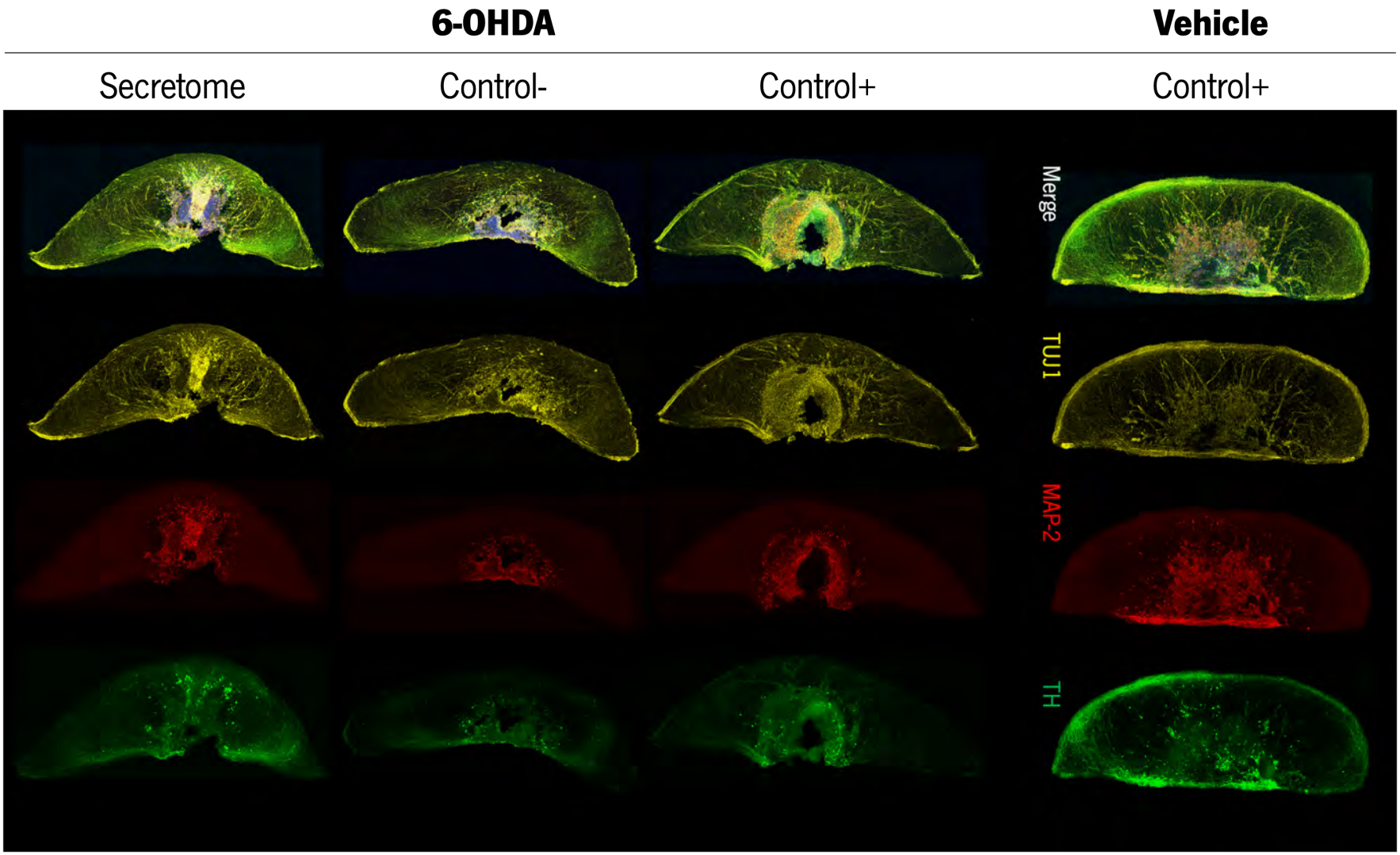

6-OHDA
Vehicle
Secretome
Control-
Control+
Control+
Merge
TUJ1
MAP-2
TH

Figure 4. Representative images of the 6-OHDA-induced degeneration and BM-MSC secretome treatment effects. Representative maximum intensity projection of confocal images (20x magnification) of hMOs, showing TUJ1 (yellow), MAP2 (red), and TH (green) staining.

3.2. Model 1: Genetic model (DJ-1 mutation)

Generation of hMOs

To analyze if mutant DJ-1 induces a disease-related phenotype, we generated isogenic hMOs that were derived from the control C4 line and the isogenic C4Mut line, in which the pathogenic c.192G>C mutation was inserted via CRISPR-Cas9 technology as previously described (Boussaad et al., 2020). hNESCs expressed the typical neural progenitor markers Nestin, SOX2, and PAX6 (supplementary Figure S2), and after generation of hNESCs spheroids, they were cultured iin the presence of the GSK3b inhibitor CHIR99021 to stimulate the canonical WNT signaling pathway, and the SHH pathway was activated using PMA. 3D colonies were kept in maintenance medium for10 days and subsequently differentiated into hMOs as represented in Figure 5A. Similar to the approach 1, during the first 14 days of culture the hMOs rapidly increased in size and reached a mean core size of 1.42 mm (±0.05 mm, n = 6) for the C4 line and 1.35 mm (±0.09 mm, n=6) for the C4Mut line in diameter after 26 days (Figure 5B), demonstrating no major differences in size between the wild-type and mutated lines.

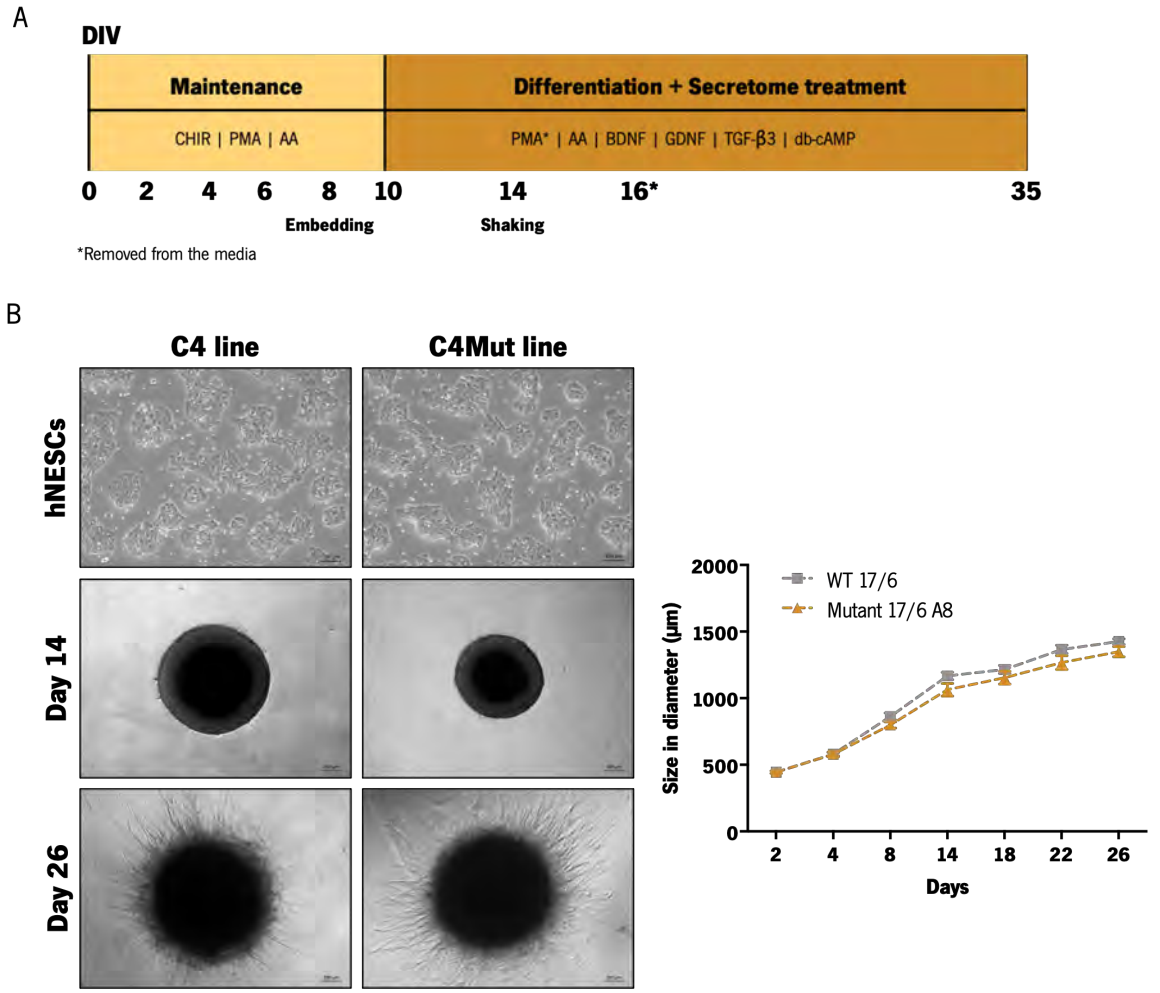


Figure 5. Derivation of isogenic hMOs derived from the control C4 (wild-type line) and C4Mut (mutant line) hNESCs. A) Schematic representation of the procedure of hMO culture system and the generation of the genetic PD model to assess the neuroprotective effects of BM-MSC secretome; **B)** Growth of hMOs in culture: brightfield images of hMOs generated from hNESCs at day 14 and day 26 in culture (scale bar represents 100 and 200 µm), and the diameter size of hMOs per organoid line from day 2 to day 26. Error bars represent mean ± SEM.

Effects of BM-MSC secretome

Contrary to model 1, herein we treated the hMOs cultures with BM-MSC secretome along the differentiation process until day 35, for a total duration of 25 days (Figure 5A). The secretome was added to the cultures as a supplement (100× concentrated) in every medium change. To evaluate the effects of BM-MSC secretome in this experiment, we performed the same analysis described above for the neurotoxin-induced model. No differences were observed when comparing the C4Mut organoids or the secretome treatment to the control condition (non-treated C4 organoids) in terms of the number of overall neurons as detected by TUJ1 and MAP2 staining (TUJ1: $F_{(3, 60)} = 0.51$, $p = 0.674$; MAP2: $F_{(3, 106)} = 0.47$, $p = 0.704$; Figure 6A, B). However, the number of TH+ dopaminergic neurons was significantly

decreased in the C4Mut organoids ($F_{(3, 106)} = 2.94$, $p < 0.05$; Figure 6C). Comparing the treated C4Mut hMOs with the non-treated ones, there as a rescue of this specific dopaminergic phenotype of DJ-1 loss after BM-MSC secretome treatment ($t_{(48)} = 2.46$, $p < 0.05$; Figure 6C). No major differences were found in terms of dopaminergic complexity (links: $F_{(3, 106)} = 1.88$, $p = 0.137$; nodes: $F_{(3, 106)} = 2.52$, $p = 0.062$); Figure 6E, F), though we observed a significant increase in the fragmentation of the TH+ dopaminergic neurites in the nontreated C4Mut organoids ($F_{(3, 106)} = 8.70$, $p < 0.001$; Figure 6D), that was also ameliorated with secretome treatment ($t_{(48)} = 2.12$, $p < 0.05$ Figure 6D). Representative images of the immunostainings are represented in Figure 7.

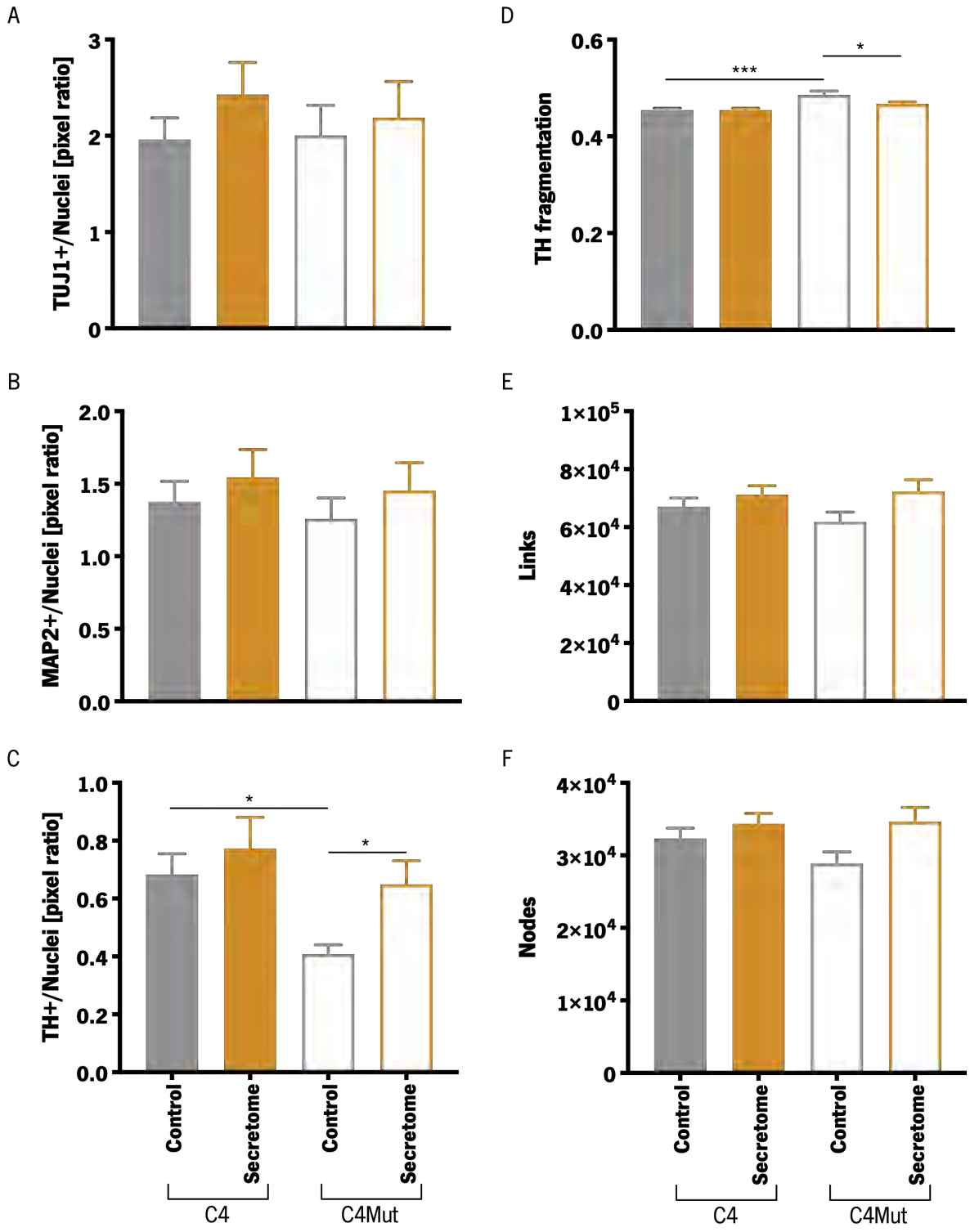


Figure 6. Effects of BM-MSC secretome in the DJ-1 genetic PD model. Extracted features from high-content image analysis to evaluate the effects of DJ-1-related phenotypes and the respective treatments, namely in the overall amount of **A)** TUJ+ neurons, **B)** MAP2+ neurons, **C)** TH+ dopaminergic neurons; and on neuronal complexity, namely **D)** TH fragmentation, **E)** links, and **F)** nodes. Control+: Differentiation medium N2B27; Secretome: BM-MSC conditioned medium. Two-independent experiments (24-30 sections (border and center sections) analyzed/group). Data are presented as mean ± SEM. *$p < 0.05$, ***$p < 0.001$.

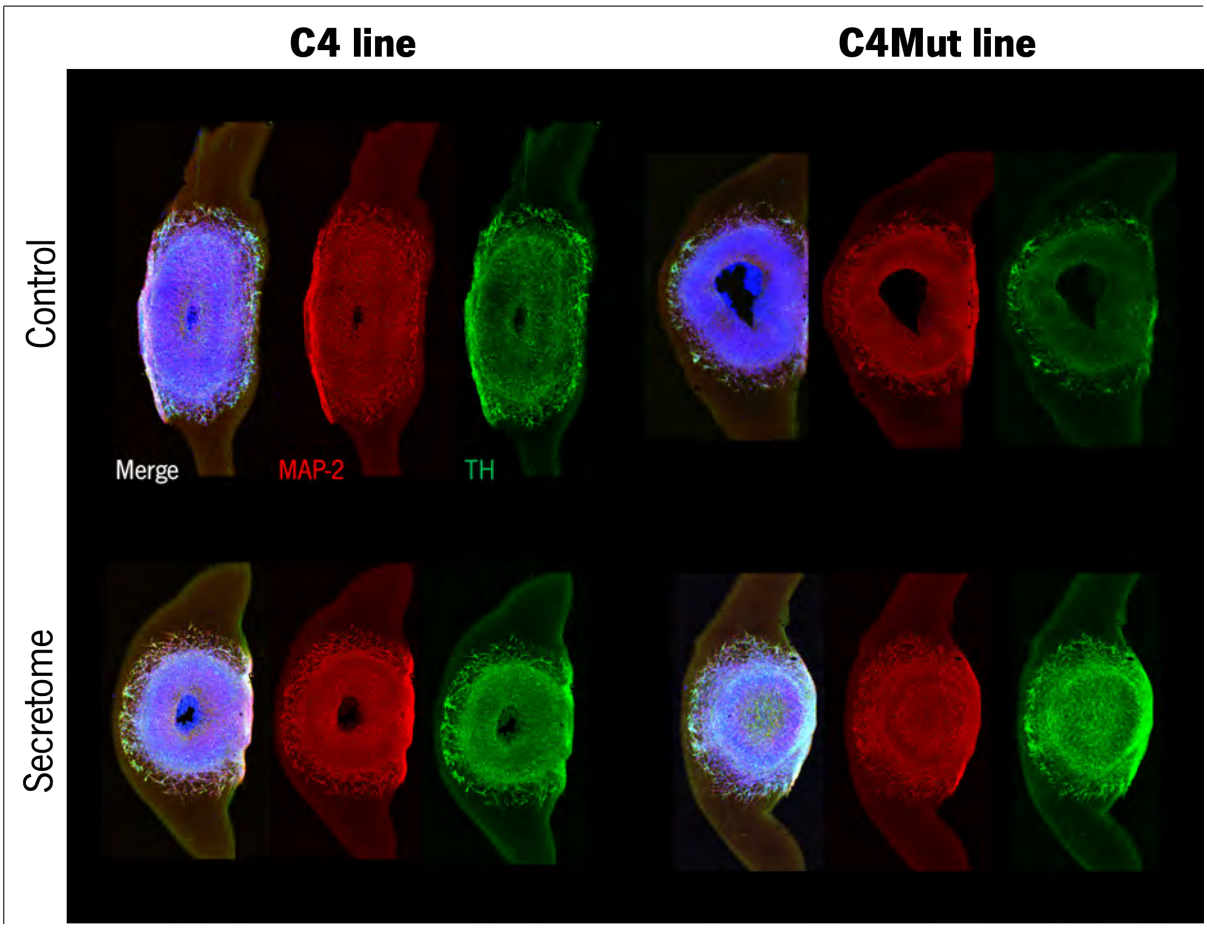


Figure 7. Representative images of the DJ-1-related phenotypes in hMOs and BM-MSC secretome treatment effects. Representative maximum intensity projection of confocal images (20x magnification) of hMOs, showing MAP2 (red), and TH (green) staining.

4. Discussion

One of the most significant limitations in neuroscience is the lack of advanced experimental *in vitro* models that truly mimic the complexity of the human brain. In the case of PD, disease modeling and drug development require high amounts of disease-relevant cells, such as midbrain dopaminergic neurons, that can be produced in a rapid and reproducible way (Smits and Schwamborn, 2020). The development of iPSC technology is transforming PD research since it allows for the differentiation and proliferation of human dopaminergic neurons *in vitro*, which has enormous potential not only for modeling PD but also for identifying novel therapies (Mohamed et al., 2019). However, in recent years, there was a need to refine the *in vitro* techniques to recapitulate some aspects of the complexity and physiology of the human midbrain. In 2013, Lancaster described a novel 3D model recapitulating different areas of the human brain: the cerebral organoid (Lancaster et al., 2013). Since then, other forms of brain organoids have been created based on modifications to Lancaster's initial methodology.

Initially, no growth factors were added to the culture, and the cells self-differentiated. However, different laboratories are already directly driving stem cells towards certain cell lineages (Qian et al., 2019).

In this work, we presented a human brain organoid system that is highly specific to the midbrain. The hMOs contain spatially organized groups of dopaminergic neurons, making them an attractive model for PD research. We were able to generate hMOs with considerable size (up to 2 mm in diameter), and we reproducibly generate hMOs based on iPSC lines that come from individuals of different ages. Important of note, contrary to all other human brain organoid systems, we used as starting population hNESCs and not iPSCs, which allow us to achieve a direct differentiation more efficiently as discussed by Nickels and colleagues (Nickels et al., 2020). The abundance of neurons with midbrain dopaminergic identity demonstrates that this protocol is entirely focused on the midbrain. These neurons are asymmetrically distributed in a discrete cluster, which mimics a unique feature of the human brain, where the soma of dopaminergic neurons resides in the substantia nigra.

The main objective of this work was to take advantage of this organoid culture system to explore the neuroprotective effects of BM-MSC secretome using two different approaches. These powerful tools were combined with the use of automated high-content microscope to extract structure-specific features to evaluate treatment effects. In model 1, we aimed to reproduce the work of Monzel and colleagues (Monzel et al., 2020) by developing a neurotoxin-induced PD organoid model. We were able to induce approximately the same level of dopaminergic degeneration with 100 μM of 6-OHDA, and incubation of 6-OHDA hMOs with BM-MSC secretome immediately after 6-OHDA exposure was able to slightly increase TH+ dopaminergic neurons (Figure 3C). Axon viability is critical for maintaining neural connectivity, which is central to neural functionality. Many neurodegenerative diseases like PD appear to involve extensive axonal degeneration that often precedes somatic loss in affected neural populations. Dystrophic axons were operationally defined as any TH immunoreactive fiber or fragment that exhibited at least one of three characteristics of degenerating axons, including axonal swelling (increased axonal diameter), fragmentation, and/or axonal spheroids (discrete swollen regions that are rounded) (Kneynsberg et al., 2016). After 6-OHDA exposure we observed an increase of neuronal fragmentation (clearly beaded and broken fibers; supplementary Figure S5). Interestingly, the BM-MSC secretome was able to protect 6-OHDA induced fragmentation of dopaminergic neurites when compared to the untreated group (Figure 3D). Different studies already reported the neuroprotective effects of MSC secretome from different sources *in vitro*, however, all these studies were done using dopaminergic cell line cultures or murine differentiated neural stem cells (Kim et al., 2009; Parga et al., 2018; Wang et

al., 2010; Yalvaç et al., 2013). In contrast, in this work, we used a more complex model, with a higher percentage of dopaminergic neurons, and even with a remarkable decrease of these cells after 6-OHDA exposure, we were able to observe a protective effect of BM-MSC secretome.

On the other hand, the neuroprotective effects of BM-MSC secretome were more robust in model 2. In this experiment, we generated isogenic hMOs with DJ-1 mutation, which is associated with an early-onset form of PD. DJ-1 is the third gene associated with autosomal recessive PD, and it is mutated in about 1%–2% of early-onset PD cases. Given that DJ-1-linked PD seems to be rare, very few patients have been reported in the literature. However, about 10 different point mutations and exonic deletions have been described, mostly in the homozygous or compound heterozygous state (Klein and Westenberger, 2012). Moreover, DJ-1 is involved in several functions including oxidative stress responses, anti-apoptotic signaling, and protein quality control, which are described to be dysregulated in the context of PD. Additionally, DJ-1 is required for correct mitochondrial morphology and function, being involved in the degradation of dysfunctional mitochondria via autophagy. Cells with mutated DJ-1 are also unable to eliminate ROS sources, leading to cell death (Strobbe et al., 2018). The addition of BM-MSC secretome since the beginning of the differentiation resulted in a significant rescue of the phenotype associated with DJ-1 mutant hMOs, namely in an increase of the number of dopaminergic neurons and a decrease of their fragmentation (Figure 6). Remarkably, DJ-1 has been identified in previous proteomic analyses of BM-MSC secretome (Mendes-Pinheiro et al., 2019; Pires et al., 2016). Nevertheless, it remains to be elucidated whether this DJ-1 mutant phenotype rescue is solely attributed to the reestablishment of DJ-1 levels in the model, or rather to a combined activity of other antioxidant molecules present in BM-MSC secretome, such as Thioredoxin or Peroxiredoxin-1 that have been shown to have a protective role in dopaminergic induced cell death (Arodin et al., 2014; Lee et al., 2008), and that have been consistently identified in our proteomic analysis as well.

The differences between both models regarding the effects of BM-MSC secretome could rely on the way that treatment was given to the cultures. In the genetic PD model, the treatment was done for a period of 25 days of the differentiation process and the secretome was administered 100× concentrated, while 6-OHDA exposed hMOs were incubated with non-concentrated secretome wherein the secreted factors may not be in the same amount as in the concentrated secretome. Importantly, these data further support the therapeutic potential of BM-MSC secretome, demonstrating its neuroprotective effects in human advanced *in vitro* dopaminergic degeneration models. Nevertheless, future studies are required to identify the molecular players underlying these neuroprotective effects.

Although brain organoids represent a tremendous promise in the field, several key points that need to be addressed in the next years. The major limitations of the current brain organoid systems are the absence of vascular and microglial cells. On one hand, the absence of vasculature might limit the growth of organoids beyond a certain size and the appearance of dead cells in the center of the organoids, on the other hand, microglial cells are actively involved in the development and maturation of neurons, mediating important functions that provide a supportive environment to neurons, including synaptic pruning, and the clearance of dead cells and misfolded proteins (Joe et al., 2018; Monzel et al., 2017; Qian et al., 2019; Smits and Schwamborn, 2020). Nonetheless, very recent data showed that macrophage precursors can be efficiently co-cultured with hMOs, integrating into the tissue and differentiating into microglia in 3D. Moreover, organoids containing microglia show a down-regulation of oxidative stress-related genes and differences in genes related to synaptic remodeling and action potential, as well as a more spontaneous action potential firing (Sabate-Soler et al., 2022). In line with this, the presence of astrocytes is also crucial for the formation of synapses and regular neuronal activity (Joe et al., 2018). Therefore, it would be interesting in the future to test the secretome of BM-MSCs in the same midbrain organoid system with all these players involved. Despite these drawbacks, the midbrain organoid system used here could represent the first step toward a more human patient-specific and personalized area of advanced disease modeling and therapeutic development.

Author contributions

Conceptualization, B.M.-P., A.J.S., and J.C.S.; methodology, B.M.-P., S.N., and A.M.; validation, B.M.-P., A.J.S., and J.C.S.; formal analysis, B.M.-P., and A.M.; data curation, B.M.-P.; investigation, B.M.-P., S.N., I.B., S.C.S., A.M.; resources, R.K., A.J.S., and J.C.S.; writing—original draft preparation, B.M.-P.; writing-review and editing, B.M.-P., A.J.S., and J.C.S.; supervision, A.J.S.; project administration, A.J.S., and J.C:S.; funding acquisition, A.J.S, and J.C.S.

Funding

This work was supported by the Foundation for Science and Technology (FCT) through the PhD Fellowship attributed to B.M.P. (SFRH/BD/120124/2016). J.C.S. lab is supported by the Fonds National de la Recherche (FNR) Luxembourg (INTER/MERA/17/11760144, FNR/PoC16/11559169). Furthermore, the project is part of the The National Centre of Excellence in Research on Parkinson's Disease (NCER-PD) which is funded by the Luxembourg National Research Fund (FNR/NCER13/BM/11264123). This project has received funding from the European Union's Horizon

2020 research and innovation programme H2020-FETPROACT-2018-01 under grant agreement No 824070.

Conflicts of interest

J.C.S. is co-founder and shareholder of the biotech company OrganoTherapeutics, which is using midbrain organoids for drug development in PD. All other authors declare no conflict of interest.

References

Arodin L, Miranda-Vizuete A, Swoboda P, Fernandes AP. 2014. Protective effects of the thioredoxin and glutaredoxin systems in dopamine-induced cell death. *Free Radic Biol Med* **73**:328–336. doi:10.1016/j.freeradbiomed.2014.05.011

Blandini F, Armentero MT. 2012. Animal models of Parkinson's disease. *FEBS J* **279**:1156–1166. doi:10.1111/j.1742-4658.2012.08491.x

Bloem BR, Okun MS, Klein C. 2021. Parkinson's disease. *Lancet* **397**:2284–2303. doi:10.1016/S0140-6736(21)00218-X

Boussaad I, Obermaier CD, Hanss Z, Bobbili DR, Bolognin S, Glaab E, Wołyńska K, Weisschuh N, De Conti L, May C, Giesert F, Grossmann D, Lambert A, Kirchen S, Biryukov M, Burbulla LF, Massart F, Bohler J, Cruciani G, Schmid B, Kurz-Drexler A, May P, Duga S, Klein C, Schwamborn JC, Marcus K, Woitalla D, Vogt Weisenhorn DM, Wurst W, Baralle M, Krainc D, Gasser T, Wissinger B, Krüger R. 2020. A patient-based model of RNA mis-splicing uncovers treatment targets in Parkinson's disease. *Sci Transl Med* **12**:eaau3960. doi:10.1126/scitranslmed.aau3960

Cobb MM, Ravisankar A, Skibinski G, Finkbeiner S. 2018. iPS cells in the study of PD molecular pathogenesis. *Cell Tissue Res* **373**:61–77. doi:10.1007/s00441-017-2749-y

Domingo A, Klein C. 2018. Genetics of Parkinson's disease In: Geschwind DH, Paulson HL, Klein C, editors. Handbook of Clinical Neurology: Volume 147, Neurogenetics, Part I. Elsevier. pp.221-227. doi:10.1016/B978-0-444-63233-3.00014-2

Fraga JS, Silva NA, Lourenço AS, Gonçalves V, Neves NM, Reis RL, Rodrigues AJ, Manadas B, Sousa N, Salgado AJ. 2013. Unveiling the effects of the secretome of mesenchymal progenitors from the umbilical cord in different neuronal cell populations. *Biochimie* **95**:2297–2303. doi:10.1016/j.biochi.2013.06.028

Joe E-H, Choi D-J, An J, Eun J-H, Jou I, Park S. 2018. Astrocytes, Microglia, and Parkinson's Disease. *Exp Neurobiol* **27**:77–87. doi:10.5607/en.2018.27.2.77

Kim Y-J, Park H-J, Lee G, Bang OY, Ahn YH, Joe E, Kim HO, Lee PH. 2009. Neuroprotective effects of human mesenchymal stem cells on dopaminergic neurons through anti-inflammatory action. *Glia* **57**:13–23. doi:10.1002/glia.20731

Klein C, Westenberger A. 2012. Genetics of Parkinson's Disease. *Cold Spring Harb Perspect Med* **2**:a008888. doi:10.1101/cshperspect.a008888

Kneynsberg A, Collier TJ, Manfredsson FP, Kanaan NM. 2016. Quantitative and semi-quantitative measurements of axonal degeneration in tissue and primary neuron cultures. *J Neurosci Methods* **266**:32–41. doi:10.1016/j.jneumeth.2016.03.004

Krebiehl G, Ruckerbauer S, Burbulla LF, Kieper N, Maurer B, Waak J, Wolburg H, Gizatullina Z, Gellerich FN, Woitalla D, Riess O, Kahle PJ, Proikas-Cezanne T, Krüger R. 2010. Reduced basal autophagy and impaired mitochondrial dynamics due to loss of Parkinson's disease-associated protein DJ-1. *PLoS One* **5**:e9367. doi:10.1371/journal.pone.0009367

Kriegstein A, Alvarez-Buylla A. 2009. The Glial Nature of Embryonic and Adult Neural Stem Cells. *Annu Rev Neurosci* **32**:149–184. doi:10.1146/annurev.neuro.051508.135600

Lancaster MA, Knoblich JA. 2014. Organogenesis in a dish: Modeling development and disease using organoid technologies. *Science* **345**:1247125. doi:10.1126/science.1247125

Lancaster MA, Renner M, Martin C-A, Wenzel D, Bicknell LS, Hurles ME, Homfray T, Penninger JM, Jackson AP, Knoblich JA. 2013. Cerebral organoids model human brain development and microcephaly. *Nature* **501**:373–379. doi:10.1038/nature12517

Lázaro DF, Pavlou MAS, Outeiro TF. 2017. Cellular models as tools for the study of the role of alpha-synuclein in Parkinson's disease. *Exp Neurol* **298**:162–171. doi:10.1016/j.expneurol.2017.05.007

Lee YM, Park SH, Shin DI, Hwang JY, Park B, Park YJ, Lee TH, Chae HZ, Jin BK, Oh TH, Oh YJ. 2008. Oxidative modification of peroxiredoxin is associated with drug-induced apoptotic signaling in experimental models of Parkinson disease. *J Biol Chem* **283**:9986–9998. doi:10.1074/jbc.M800426200

Marques CR, Marote A, Mendes-Pinheiro B, Teixeira FG, Salgado AJ. 2018. Cell secretome based approaches in Parkinson's disease regenerative medicine. *Expert Opin Biol Ther* **18**:1235–1245. doi:10.1080/14712598.2018.1546840

Mendes-Pinheiro B, Anjo SI, Manadas B, Da Silva JD, Marote A, Behie LA, Teixeira FG, Salgado AJ. 2019. Bone Marrow Mesenchymal Stem Cells' Secretome Exerts Neuroprotective Effects in a Parkinson's Disease Rat Model. *Front Bioeng Biotechnol* **7**:294. doi:10.3389/fbioe.2019.00294

Mohamed N-V, Larroquette F, Beitel LK, Fon EA, Durcan TM. 2019. One Step Into the Future: New iPSC Tools to Advance Research in Parkinson's Disease and Neurological Disorders. *J Parkinsons Dis* **9**:265–281. doi:10.3233/JPD-181515

Monzel AS, Hemmer K, Kaoma T, Smits LM, Bolognin S, Lucarelli P, Rosety I, Zagare A, Antony P, Nickels SL, Krueger R, Azuaje F, Schwamborn JC. 2020. Machine learning-assisted neurotoxicity prediction in human midbrain organoids. *Parkinsonism Relat Disord* **75**:105–109. doi:10.1016/j.parkreldis.2020.05.011

Monzel AS, Smits LM, Hemmer K, Hachi S, Moreno EL, van Wuellen T, Jarazo J, Walter J, Brüggemann I, Boussaad I, Berger E, Fleming RMT, Bolognin S, Schwamborn JC. 2017. Derivation of Human Midbrain-Specific Organoids from Neuroepithelial Stem Cells. *Stem Cell Reports* **8**:1144–1154. doi:10.1016/j.stemcr.2017.03.010

Nickels SL, Modamio J, Mendes-Pinheiro B, Monzel AS, Betsou F, Schwamborn JC. 2020. Reproducible generation of human midbrain organoids for in vitro modeling of Parkinson's disease. *Stem Cell Res* **46**:101870. doi:10.1016/j.scr.2020.101870

Pang SY-Y, Ho PW-L, Liu H-F, Leung C-T, Li L, Chang EES, Ramsden DB, Ho S-L. 2019. The interplay of aging, genetics and environmental factors in the pathogenesis of Parkinson's disease. *Transl Neurodegener* **8**:23. doi:10.1186/s40035-019-0165-9

Parga JA, García-Garrote M, Martínez S, Raya Á, Labandeira-García JL, Rodríguez-Pallares J. 2018. Prostaglandin EP2 Receptors Mediate Mesenchymal Stromal Cell-Neuroprotective Effects on Dopaminergic Neurons. *Mol Neurobiol* **55**:4763–4776. doi:10.1007/s12035-017-0681-5

Pires AO, Mendes-Pinheiro B, Teixeira FG, Anjo SI, Ribeiro-Samy S, Gomes ED, Serra SC, Silva NA, Manadas B, Sousa N, Salgado AJ. 2016. Unveiling the Differences of Secretome of Human Bone Marrow Mesenchymal Stem Cells, Adipose Tissue-Derived Stem Cells, and Human Umbilical Cord Perivascular Cells: A Proteomic Analysis. *Stem Cells Dev* **25**:1073–1083. doi:10.1089/scd.2016.0048

Poewe W, Seppi K, Tanner CM, Halliday GM, Brundin P, Volkmann J, Schrag A-E, Lang AE. 2017. Parkinson disease. *Nat Rev Dis Prim* **3**:17013. doi:10.1038/nrdp.2017.13

Qian X, Song H, Ming G. 2019. Brain organoids: advances, applications and challenges. *Development* **146**:dev166074. doi:10.1242/dev.166074

Reinhardt P, Glatza M, Hemmer K, Tsytsyura Y, Thiel CS, Höing S, Moritz S, Parga JA, Wagner L, Bruder JM, Wu G, Schmid B, Röpke A, Klingauf J, Schwamborn JC, Gasser T, Schöler HR, Sterneckert J. 2013. Derivation and Expansion Using Only Small Molecules of Human Neural

Progenitors for Neurodegenerative Disease Modeling. *PLoS One* **8**:e59252. doi:10.1371/journal.pone.0059252

Sabate-Soler S, Nickels SL, Saraiva C, Berger E, Dubonyte U, Barmpa K, Lan YJ, Kouno T, Jarazo J, Robertson G, Sharif J, Koseki H, Thome C, Shin JW, Cowley SA, Schwamborn JC. 2022. Microglia integration into human midbrain organoids leads to increased neuronal maturation and functionality. *bioRxiv* 2022.01.21.477192. doi:10.1101/2022.01.21.477192

Smits LM, Reinhardt L, Reinhardt P, Glatza M, Monzel AS, Stanslowsky N, Rosato-Siri MD, Zanon A, Antony PM, Bellmann J, Nicklas SM, Hemmer K, Qing X, Berger E, Kalmbach N, Ehrlich M, Bolognin S, Hicks AA, Wegner F, Sterneckert JL, Schwamborn JC. 2019. Modeling Parkinson's disease in midbrain-like organoids. *npj Park Dis* **5**:5. doi:10.1038/s41531-019-0078-4

Smits LM, Schwamborn JC. 2020. Midbrain Organoids: A New Tool to Investigate Parkinson's Disease. *Front Cell Dev Biol* **8**:1–12. doi:10.3389/fcell.2020.00359

Strobbe D, Robinson AA, Harvey K, Rossi L, Ferraina C, De Biase V, Rodolfo C, Harvey RJ, Campanella M. 2018. Distinct mechanisms of pathogenic DJ-1 mutations in mitochondrial quality control. *Front Mol Neurosci* **11**:1–15. doi:10.3389/fnmol.2018.00068

Teixeira FG, Carvalho MM, Panchalingam KM, Rodrigues AJ, Mendes-Pinheiro B, Anjo S, Manadas B, Behie LA, Sousa N, Salgado AJ. 2017. Impact of the Secretome of Human Mesenchymal Stem Cells on Brain Structure and Animal Behavior in a Rat Model of Parkinson's Disease. *Stem Cells Transl Med* **6**:634–646. doi:10.5966/sctm.2016-0071

Teixeira FG, Carvalho MM, Sousa N, Salgado AJ. 2013. Mesenchymal stem cells secretome: a new paradigm for central nervous system regeneration? *Cell Mol Life Sci* **70**:3871–3882. doi:10.1007/s00018-013-1290-8

Teixeira FG, Panchalingam KM, Assunção-Silva R, Serra SC, Mendes-Pinheiro B, Patrício P, Jung S, Anjo SI, Manadas B, Pinto L, Sousa N, Behie LA, Salgado AJ. 2016. Modulation of the Mesenchymal Stem Cell Secretome Using Computer-Controlled Bioreactors: Impact on Neuronal Cell Proliferation, Survival and Differentiation. *Sci Rep* **6**:27791. doi:10.1038/srep27791

Vizoso F, Eiro N, Cid S, Schneider J, Perez-Fernandez R. 2017. Mesenchymal Stem Cell Secretome: Toward Cell-Free Therapeutic Strategies in Regenerative Medicine. *Int J Mol Sci* **18**:1852. doi:10.3390/ijms18091852

Wang F, Yasuhara T, Shingo T, Kameda M, Tajiri N, Yuan WJ, Kondo A, Kadota T, Baba T, Tayra JT, Kikuchi Y, Miyoshi Y, Date I. 2010. Intravenous administration of mesenchymal stem cells exerts

therapeutic effects on parkinsonian model of rats: Focusing on neuroprotective effects of stromal cell-derived factor-1α. *BMC Neurosci* **11**:52. doi:10.1186/1471-2202-11-52

Yalvaç ME, Yarat A, Mercan D, Rizvanov AA, Palotás A, Şahin F. 2013. Characterization of the secretome of human tooth germ stem cells (hTGSCs) reveals neuro-protection by fine-tuning micro-environment. *Brain Behav Immun* **32**:122–130. doi:10.1016/j.bbi.2013.03.007

Zagare A, Gobin M, Monzel AS, Schwamborn JC. 2021. A robust protocol for the generation of human midbrain organoids. *STAR Protoc* **2**:100524. doi:10.1016/j.xpro.2021.100524

SUPPLEMENTARY MATERIAL

Modeling Parkinson's disease in human midbrain-specific organoids to study the neuroprotective potential of mesenchymal stem cell secretome

A

WT Name	Age of sampling	Sex	References	Database Number
K7	81	F	iPSCs Reinhardt et al., 2013	200
T12	53	F	iPSCs Reinhardt et al., 2013	232
COR	55	M	iPSCs Coriell GM23338	225

B

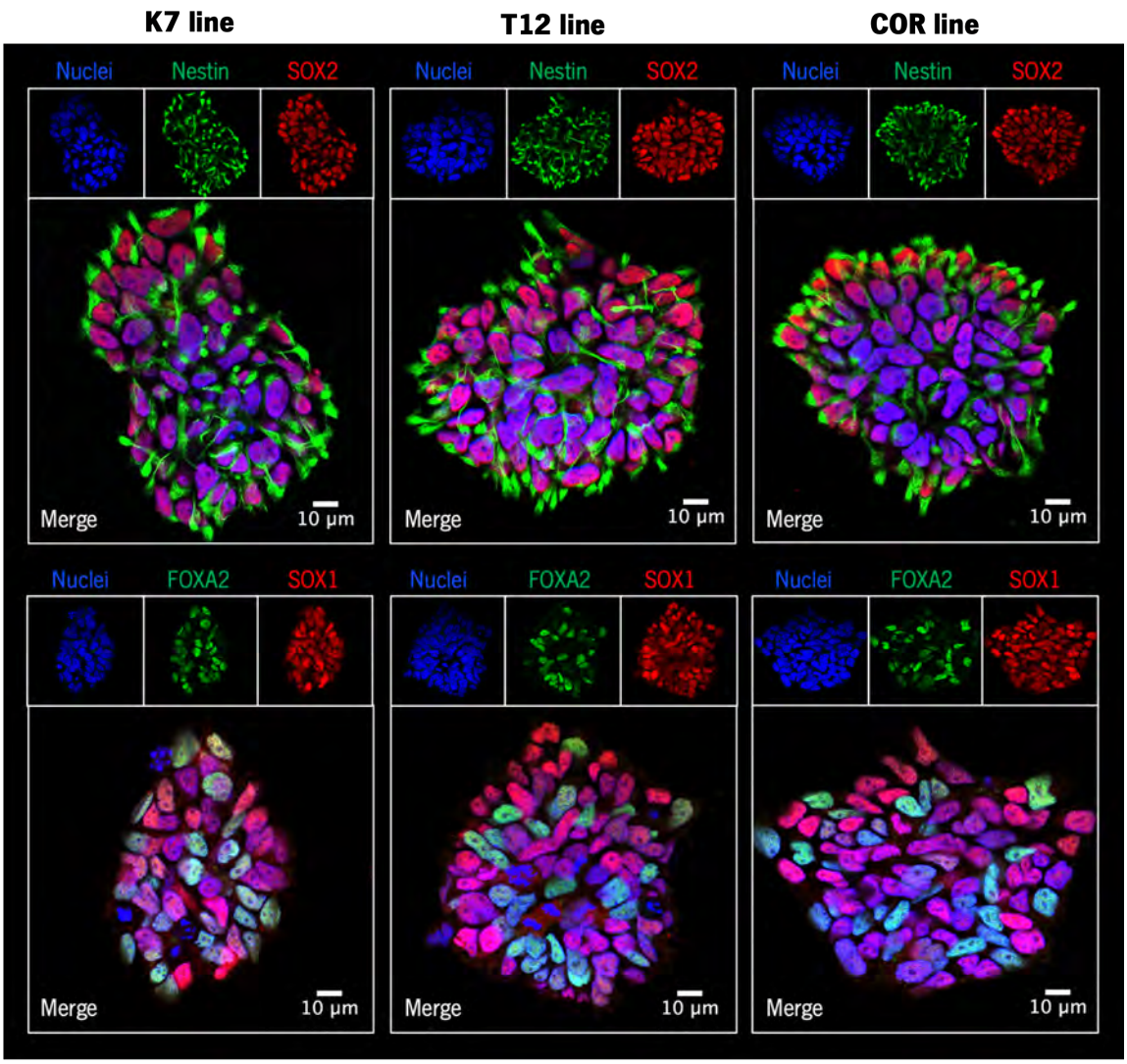


Figure S1. Human ventralized neuroepithelial stem cells used in Model 1. A) Cell lines used in this study to generate hMOs (passage 14); **B)** Representative images of hvNESC morphology and expression of neuronal progenitor (Nestin, SOX1, and SOX2) and midbrain floorplate markers (FOXA2).

A

Line	Mutation	Age of sampling	Sex	Reference
17608/6 (C4)	Wild-type	67	M	Boussaad et al., 2020
17608/6A8 (C4Mut)	Splicing mutation	67	M	

B

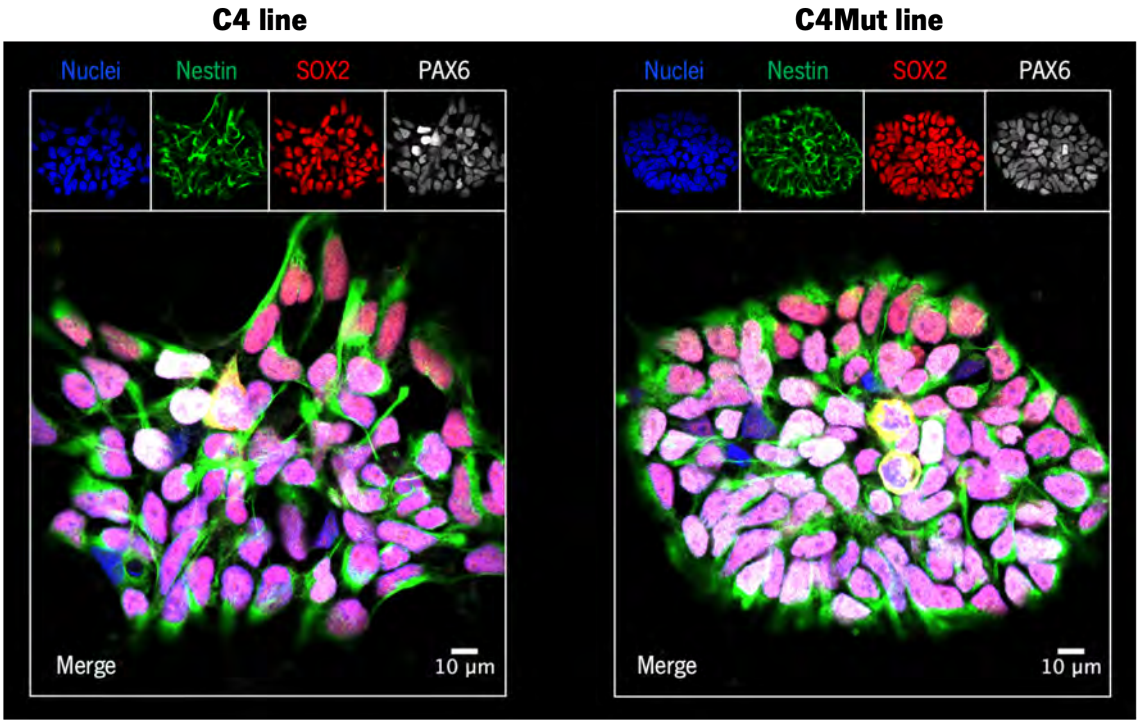


Figure S2. Human neuroepithelial stem cells used in Model 2. A) Cell lines used in this study to generate hMOs (passage 17 for C4 line and passage 15 for C4Mut line; **B)** Representative images of hNESC morphology and expression of neuronal progenitor markers (Nestin, SOX2, and PAX6).

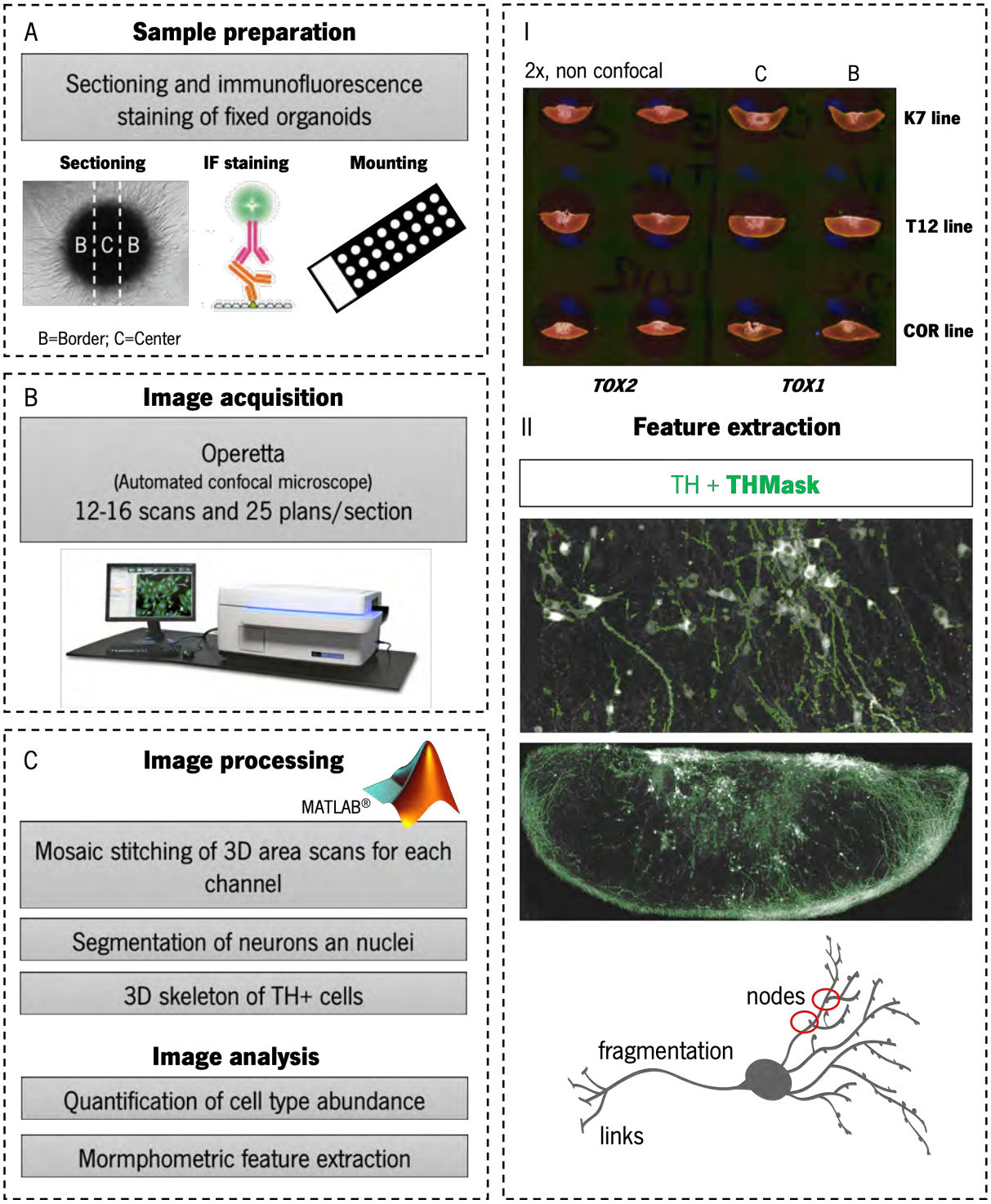


Figure S3. High-content image analysis workflow. **A)** Sample preparation: organoids were sectioned and prior to immnuofluorescence staining separated into border and center sections. Organoid sections were mounted on an object slide containing a grid for automated image acquisition; **B)** Image acquisition: 12-16 area scans in 25 planes were acquired using an automated confocal microscope (operetta); **C)** Images were exported in MATLAB and area scans were stitched. On the obtained 3D image, masks were generated for dopaminergic neurons in order to quantify cell type abundance and morphometric features; **I)** 2x non confocal image representation of organoid slices; **II)** Feature extraction: Dopaminergic

neuronal complexity was quantified by extracting cellular features such as TH mask, neurite nodes, links, and fragmentation. Adapted from (Monzel et al., 2020).

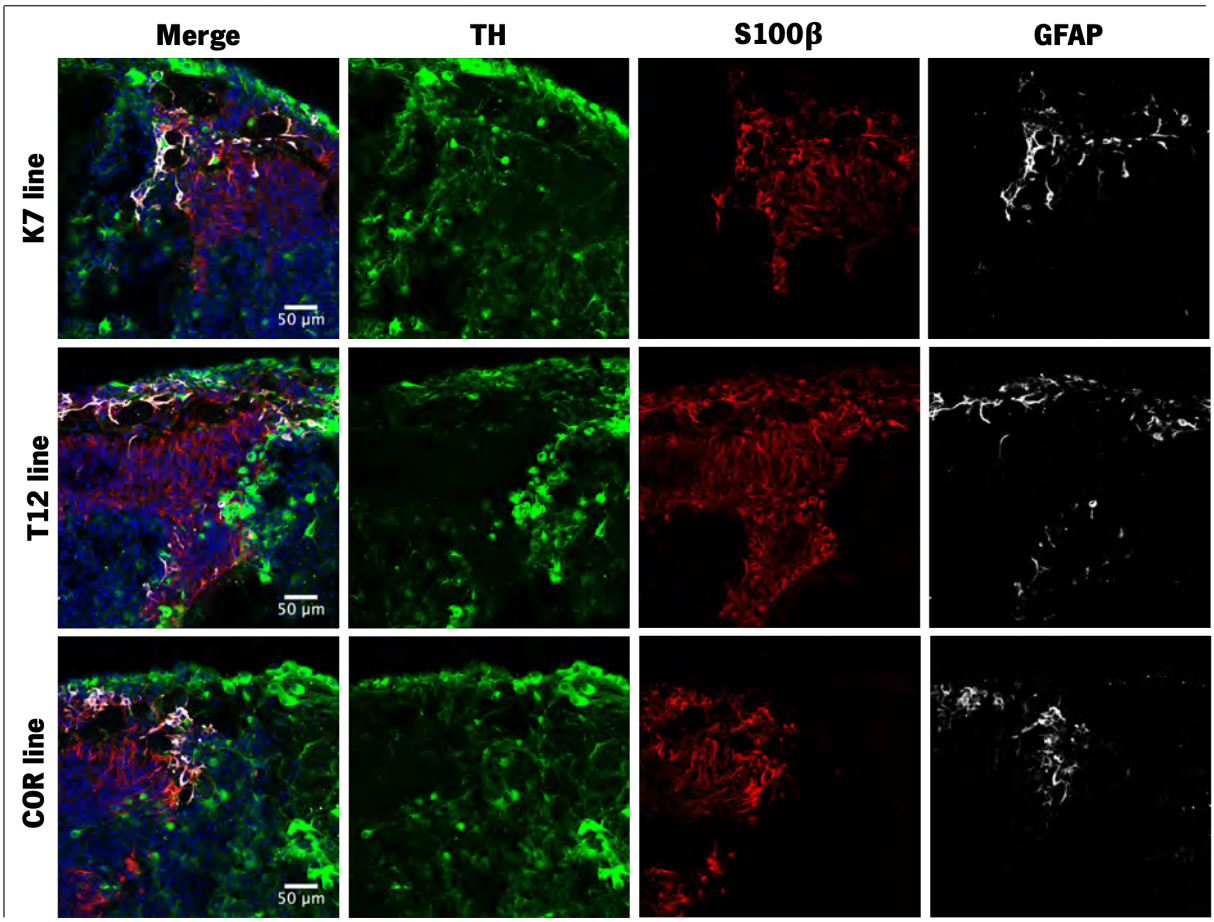


Figure S4. Characterization of glial differentiation at day 30 of the differentiation protocol. Immunofluorescence staining for astrocytic markers S100β (red) and GFAP (white) and for dopaminergic neuronal marker TH (green).

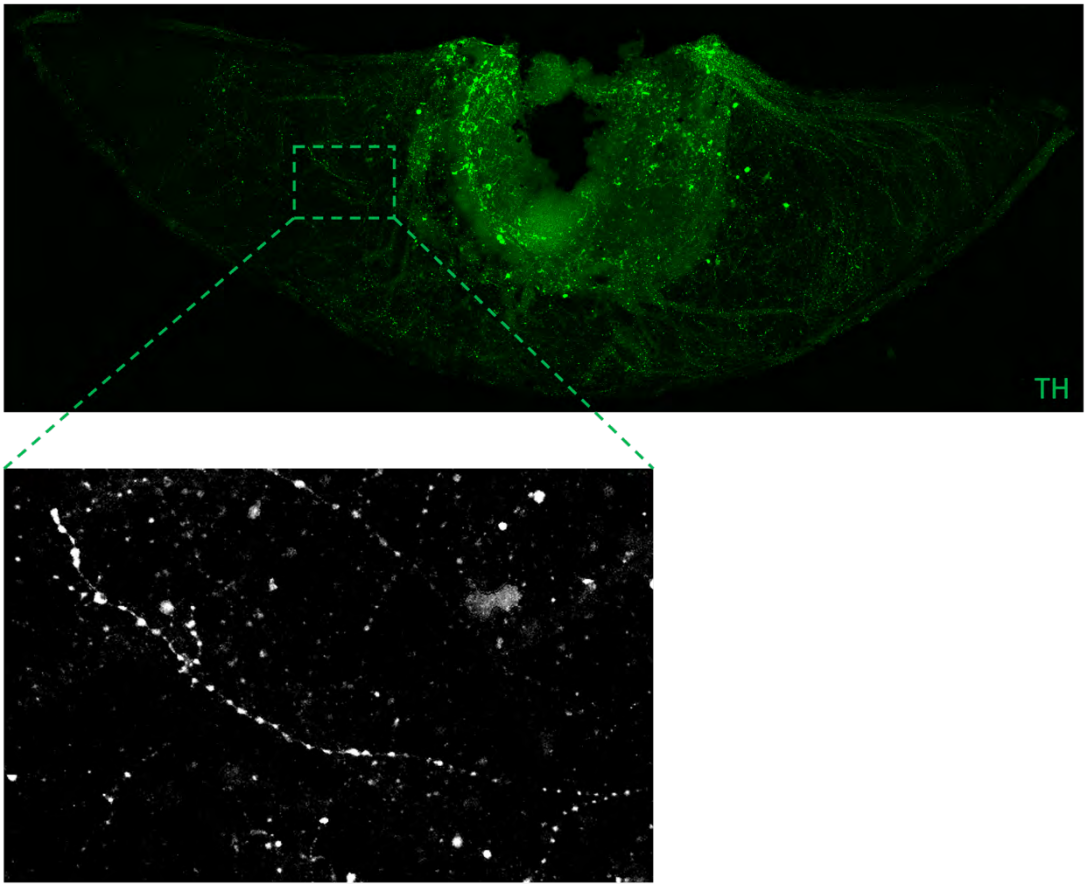


Figure S5. Example of a fragmented neurite after 6-OHDA treatment. It is possible to observe a clearly beaded and broken fiber marked with TH in the hMO exposed to the neurotoxin.

Table S1. List of primary antibodies

Antibody	Specie	Dilution	Source	Reference
Dopamine	rabbit	1:500	ImmuSmol	IS1005
EN1	goat	1:300	Santa Cruz	sc-46101
FOXA2	mouse	1:250	Santa Cruz	sc-101060
GFAP	chicken	1:500	Millipore	AB5541
GIRK2	goat	1:200	Abcam	ab65096
Nestin	mouse	1:100	Millipore	MAB5326
PAX6	rabbit	1:300	Covance	PRB-278P
SOX1	goat	1:100	R&D systems	AF3369
SOX2	goat	1:100	R&D systems	AF2018
S100β	mouse	1:100	Sigma	S2532
TH	chicken	1:1000	Abcam	ab76442

Table S2. Features from image analysis. Adapted from (Smits et al, 2019)

Feature	Description
Nuclei mask	Count of nuclear positive pixels
Nuclei dead mask	Count of nuclear dead pixels
Nuclei dead/nuclei	Count of nuclear dead pixels / Hoechst
TUJ1 mask	Count of TUJ1 mask pixels
TUJ1+/Nuclei	Sum of TUJ1+ pixels / Hoechst
MAP2 mask	Count of MAP2 mask pixels
MAP2+/Nuclei	Sum of MAP2+ pixels / Hoechst
TH mask	Count of TH mask pixels
TH+/Nuclei	Sum of TH+ pixels / Hoechst
TH percentage	Percentage of TH+ cells in the perinuclear zone of segmented nuclei
TH skeleton	Count of TH skeleton pixel (red). Skeleton is calculated using a thinning function resulting in a simplified representation of the neuronal branching. The skeleton allows identifying nodes and links 
Nodes	Total number of points located at a bifurcation of neuronal branching (red points), generated from the TH skeleton 
Links	Total number of connecting segments originated from the nodes (red lines), generated from the TH skeleton 
TH fragmentation	Surface to volume ratio of TH mask

CHAPTER 4

Unilateral intrastriatal 6-hydroxydopamine lesion in mice: a closer look into non-motor phenotype and glial response

This chapter is based on the following publication:

Bárbara Mendes-Pinheiro[1,2], Carina Soares-Cunha[1,2], Ana Marote[1,2], Eduardo Loureiro-Campos[1,2], Jonas Campos[1,2], Sandra Barata-Antunes[1,2], Daniela Monteiro-Fernandes[1,2], Diogo Santos[1,2], Sara Duarte-Silva[1,2], Luísa Pinto[1,2], António J. Salgado[1,2]. (2021). Unilateral 6-hydroxydopamine lesion in mice: a closer look into non-motor phenotype and glial response. *Int J Mole Sci* **22**:11530. doi: 10.3390/ijms222111530

[1]Life and Health Sciences Research Institute (ICVS), School of Medicine, University of Minho, Campus de Gualtar, 4710-057 Braga, Portugal;
[2]ICVS/3B's - PT Government Associate Laboratory, 4805-017 Guimarães, Portugal.

#Correspondance: António J. Salgado asalgado@med.uminho.pt

International Journal of
Molecular Sciences

MDPI

Article

Unilateral Intrastriatal 6-Hydroxydopamine Lesion in Mice: A Closer Look into Non-Motor Phenotype and Glial Response

Bárbara Mendes-Pinheiro [1,2], Carina Soares-Cunha [1,2], Ana Marote [1,2], Eduardo Loureiro-Campos [1,2], Jonas Campos[1,2], Sandra Barata-Antunes [1,2], Daniela Monteiro-Fernandes [1,2], Diogo Santos [1,2], Sara Duarte-Silva [1,2], Luísa Pinto [1,2] and António José Salgado [1,2,*]

1 Life and Health Sciences Research Institute (ICVS), School of Medicine, Campus de Gualtar, University of Minho, 4710-057 Braga, Portugal; id7153@alunos.uminho.pt (B.M.-P.); carinacunha@med.uminho.pt (C.S.-C.); anamarote@med.uminho.pt (A.M.); id7472@alunos.uminho.pt (E.L.-C.); id9533@alunos.uminho.pt (J.C.); id7405@alunos.uminho.pt (S.B.-A.); id8942@alunos.uminho.pt (D.M.-F.); a77974@alunos.uminho.pt (D.S.); sarasilva@med.uminho.pt (S.D.-S.); luisapinto@med.uminho.pt (L.P.)
2 ICVS/3B's—PT Government Associate Laboratory, 4805-017 Guimarães, Portugal
* Correspondence: asalgado@med.uminho.pt; Tel.: +351-253-60-49-47

Citation: Mendes-Pinheiro, B.; Soares-Cunha, C.; Marote, A.; Loureiro-Campos, E.; Campos, J.; Barata-Antunes, S.; Monteiro-Fernandes, D.; Santos, D.; Duarte-Silva, S.; Pinto, L.; et al. Unilateral Intrastriatal 6-OHDA Lesion in Mice: A Closer Look into Non-Motor Phenotype and Glial Response. *Int. J. Mol. Sci.* **2021**, *22*, x. https://doi.org/10.3390/xxxxx

Academic Editor(s):

Received: date
Accepted: date
Published: date

Publisher's Note: MDPI stays neutral with regard to jurisdictional claims in published maps and institutional affiliations.

Copyright: © 2021 by the authors. Submitted for possible open access publication under the terms and conditions of the Creative Commons Attribution (CC BY) license (http://creativecommons.org/licenses/by/4.0/).

Abstract: Parkinson's disease (PD) is a prevalent movement disorder characterized by the progressive loss of dopaminergic neurons in substantia nigra pars compacta (SNpc). The 6-hydroxydopamine (6-OHDA) lesion is still one of the most widely used techniques for modeling Parkinson's disease (PD) in rodents. Despite commonly used in rats, it can be challenging to reproduce a similar lesion in mice. Moreover, there is a lack of characterization of the extent of behavioral deficits and of the neuronal loss/neurotransmitter system in unilateral lesion mouse models. In this study, we present an extensive behavioral and histological characterization of a unilateral intrastriatal 6-OHDA mouse model. Our results indicate significant alterations in balance and fine motor coordination, voluntary locomotion, and in the asymmetry's degree of forelimb use in 6-OHDA lesioned animals, accompanied by a decrease in self-care and motivational behavior, common features of depressive-like symptomatology. These results were accompanied by a decrease in tyrosine hydroxylase (TH)-labelling and dopamine levels within the nigrostriatal pathway. Additionally, we also identify a marked astrocytic reaction, as well as proliferative and reactive microglia in lesioned areas. These results confirm the use of unilateral intrastriatal 6-OHDA mice for the generation of a mild model of nigrostriatal degeneration and further evidences the recapitulation of key aspects of PD, thereby being suitable for future studies beholding new therapeutical interventions for this disease.

Keywords: Parkinson's disease; 6-OHDA; unilateral; striatum; dopaminergic degeneration; motor behavior; non-motor behavior; glial response

1. Introduction

Parkinson's disease (PD) is the second most common age-related neurodegenerative disorder, affecting around six million people worldwide [1]. Motor symptoms, such as bradykinesia, rest tremor and rigidity, are the core of PD clinical features that develop due to the progressive loss of dopaminergic (DA) neurons in the substantia nigra pars compacta (SNpc) [2]. This neuronal loss is accompanied by the presence of cytoplasmatic inclusions or Lewy bodies (LBs), mainly composed of α-synuclein protein, that possibly propagates between synaptically-connected areas in a prion-like manner [3]. Moreover, non-motor symptoms like sleep disturbances, intestinal dysfunction, cognitive decline, anxiety and depression, have also been increasingly recognized as major determinants of patient's quality of life and overall disability [4]. The etiology of PD is still unclear, but it is recognized as a multifactorial disease, involving an interplay between aging, genetic

predisposition, and environmental factors [5]. After decades of research, no cure or neuroprotective treatment for PD is available. Although there are treatments to reduce the main symptoms and maintain life quality of the patients, none of them are capable to delay or stop the degeneration of DA neurons [6]. Efforts have been made to develop alternative therapeutical approaches, and for that, the use of PD pre-clinical models is a critical step to test new disease-modifying strategies.

Current PD animal models have been classically generated by targeting the nigrostriatal pathway with toxins or genetic interventions that mimic motor deficits [7]. Since its identification more than 50 years ago, 6-hydroxydopamine (6-OHDA) is still widely used to reproduce PD [8]. The compound 6-OHDA is a catecholamine selective neurotoxin, which assesses the cytosol of DA neurons through dopamine (DA) reuptake transporters, leading to mitochondrial respiratory dysfunction and consequently oxidative stress-induced toxicity and neuroinflammation, which ultimately causes cell death [9]. It is known that the model induced by 6-OHDA does not reproduce all PD features, such as the formation of LBs (an important hallmark of the disease), but notwithstanding this limitation, the relative selectivity of 6-OHDA has been behind its attractiveness to model the classic motor PD symptoms. Moreover, compared with other toxins, such as 1-methyl-4-phenyl-1,2,3,6-tetrahydropyridine (MPTP), 6-OHDA produces robust and relatively stable lesions, without spontaneous recovery [10]. Significant differences in 6-OHDA doses, volumes injected and sites/coordinates of injection are found throughout the literature, which have an impact on the size, location, rate of neurotoxin uptake and therefore in dopaminergic cell survival and behavioral outcomes [11]. When injected into the medial forebrain bundle (MFB) or SNpc, 6-OHDA induces a more complete and rapid lesion in the nigrostriatal pathway, with neurons starting to degenerate within 24 h [12]. On the other hand, if delivered into the striatum, 6-OHDA induces a slow protracted retrograde degeneration, and consequently a more progressive and stable depletion of DA neurons. Therefore, this route of administration offers some advantages over the other regions, since a progressive and less extensive lesion is more relevant in the context of PD [12,13]. Additionally, whereas 6-OHDA lesion in rats is well-described, the generation of 6-OHDA mouse models can be quite challenging, since mice are more prone to high post-lesion mortality and weight loss, therefore requiring intense post-operative care and vigilance [11,14]. Nevertheless, the unilateral administration of 6-OHDA can prevent the high mortality rate observed in bilateral lesions in mice, allowing the use of dosages able to induce motor phenotype, without compromising animals' well-being [14–18]. Indeed, due to their easier genetic manipulation, the establishment of PD mouse models is key for analyzing the increasingly recognized interplay between genetic and environmental factors. Therefore, these models should recapitulate not only PD-associated motor deficits, but also non-motor phenotypes and other histological alterations than nigrostriatal degeneration, such as glial response. Nevertheless, the assessment of non-motor phenotypes in mice is challenging, especially in unilateral lesions, which might explain the few studies exploring this behavioral dimension in 6-OHDA models. The most reported non-motor phenotypes are anxiety- and depressive-like behavior, which may be more directly implicated in the effects of 6-OHDA lesion in the nigrostriatal pathway [4]. For instance, Bonito-Oliva and colleagues showed that a 6-OHDA lesion into the dorsal striatum resulted in impairment of gait dynamics, accompanied by olfactory deficit, and depression- and anxiety-like behavior [19].

Besides behavioral assessment, the inclusion of glial response analysis is also an important readout of PD models. For several years, the function of glial cells in the central nervous system (CNS) was not fully understood, and they were seen only as supporters of neurons, being important in the maintenance of their viability. Today we know that astrocytes and microglia have a variety of functions in both an intact and injured brain [20]. For instance, astrocytes maintain glutamate, ion and water homeostasis, provide growth factors and metabolites to neurons, and have other functions such as energy storage, mitochondria biogenesis, scar formation, defense against oxidative stress, among

others [21]. On the other hand, microglia are involved in synaptic organization, control of neuronal excitability, myelin turnover, phagocytic debris removal, or respond to injury by expressing inflammatory cytokines [22]. Thus, their loss or functional alteration may be directly linked to brain diseases. Glial responses in PD are considered to exhibit dual effects in the neurodegenerative process. Although glial cells are essential for CNS homeostasis, and their activation may benefit DA neurons at early PD stages, the continued and excessive activation of glia can be damaging to neurons and contribute to PD pathogenesis and progression [23].

In the present study, we have reproduced the previously described unilateral intrastriatal 6-OHDA mouse model and performed an extensive behavioral characterization, including both motor and non-motor assessments. In addition, we evaluated neurochemical and histological alterations, including glial activation along the nigrostriatal pathway. This unilateral intrastriatal 6-OHDA model induces a mild degeneration, which is reflected not only in significant motor deficits, but also in subtle non-motor alterations. Moreover, this model is marked by a strong glial response, even 14 weeks after lesion. Therefore, it recapitulates both behavioral and histological phenotypes of PD, thereby being relevant for pre-clinical studies of neuroprotective drugs.

2. Results

2.1. Motor Performance Characterization

In this work, we performed several motor behavioral tests to characterize a unilateral intrastriatal 6-OHDA PD mouse model, three and eleven weeks after lesion. Data from the behavioral tasks are schemed in Figure 1, while the results of the statistical analyses are presented in Table S1.

The beam balance test was performed to assess balance and fine motor coordination (Figure 1a). Animals were trained in the square beam (12 mm), and on the day of the test, two more beams with a higher level of difficulty were presented to the animals (round beams of 17 mm and 11 mm). 6-OHDA-lesioned animals had a worse performance in all beams, after 3 and 11 weeks post-lesion when compared to the control group. Motor coordination and strength were assessed using the motor swimming test (MST). Presence of the 6-OHDA lesion significantly increased swimming latency of the animals throughout the time course of the experiment (Figure 1b). To monitor locomotor activity, the pole test was also used. 6-OHDA-lesioned animals showed impairments in this test, with 6-OHDA-lesioned animals taking more time to reach the cage (Figure 1c). However, the time that animals took to initiate the movement (latency to turn downward) was similar in both groups (data not shown). The cylinder test measures the spontaneous forelimb use during the exploration of a vertical cylinder wall. Weight-bearing wall touches using contralateral and ipsilateral forelimbs were counted to evaluate the limb use asymmetry after 6-OHDA unilateral lesion. The results showed that 6-OHDA-lesioned animals predominantly use the paw ipsilateral to the lesion (left paw) in exploration of the cylinder walls, compared to the vehicle group (Figure 1d). Spontaneous activity was characterized in terms of horizontal movement in an arena (number of squares crossed), and at the same time the gait of the animals was qualitatively evaluated (scored by the experimenter as normal and abnormal). Horizontal activity was significantly altered by 6-OHDA administration, and some 6-OHDA-lesioned animals showed abnormal gait quality (qualitative assessment, Figure 1e). The rotameter test, using apomorphine, was performed at the end of the motor behavioral assessment to gain insight on functional integrity of the dopaminergic system. Statistical analysis revealed that 6-OHDA lesioned mice displayed significantly more contralateral rotations when compared to the control group (Figure 1f). Rotameter also showed that 88.5% of 6-OHDA group were truly injured after toxin injections. In the animals without turning behavior after apomorphine injections, abnormal involuntary movements were observed, indicating that these animals were also effectively lesioned. Overall, this demonstrates the high success of 6-OHDA injections at the striatum brain

region. Overall, all performed tests were found to be sensitive to DA-depleting lesions of the nigrostriatal pathway.

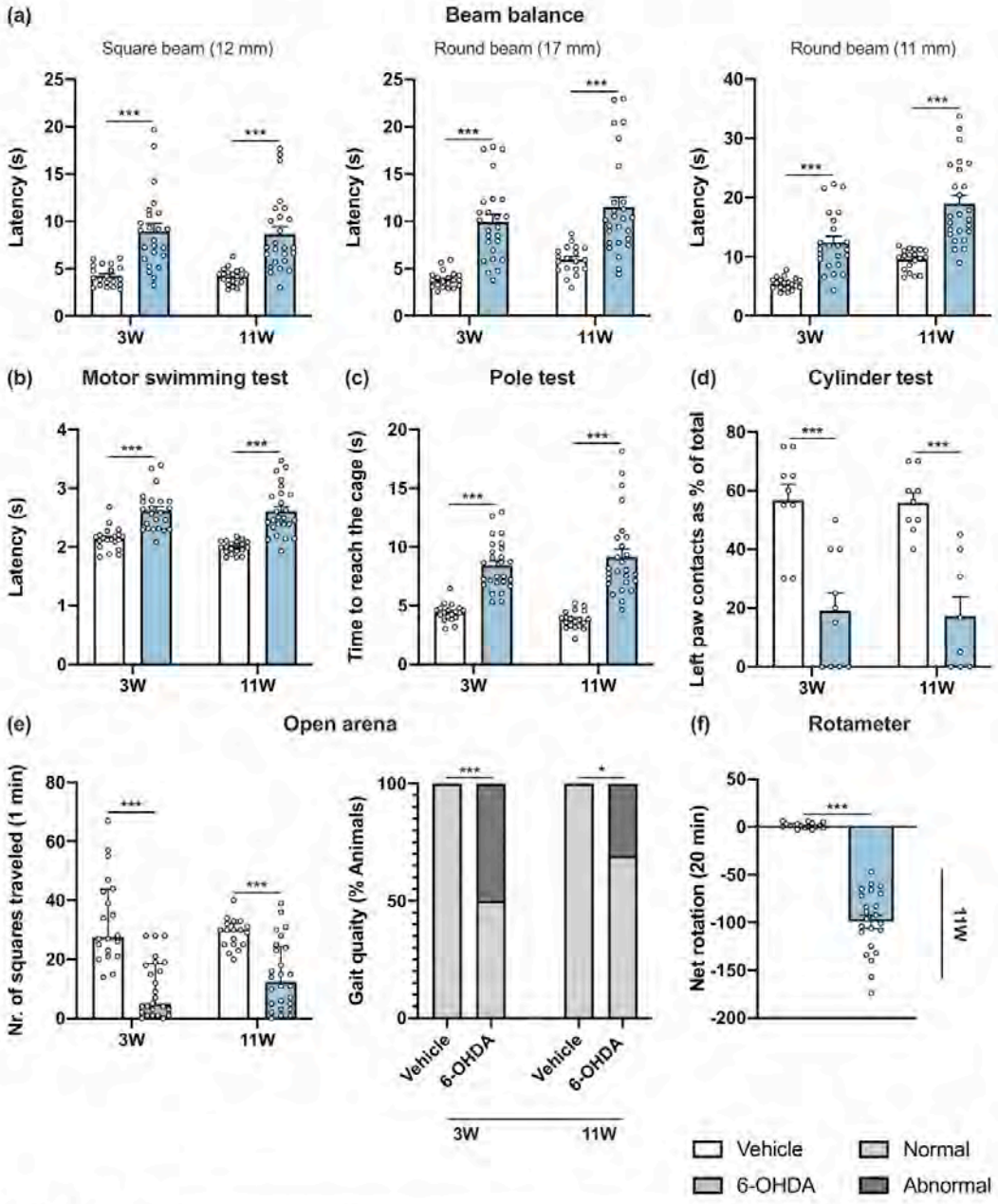


Figure 1. 6-OHDA intrastriatal lesion effects on motor behavioral tasks. Overall, all performed tests were found to be sensitive to DA-depleting lesions of the nigrostriatal pathway, 3 and 11 weeks after intrastriatal 6-OHDA injections. 6-OHDA-lesioned mice presented significant impairments in general motor paradigms observed after beam balance (**a**), motor swimming (**b**) and pole (**c**) tests evaluation. The cylinder test (**d**) revealed that 6-OHDA animals use the left (lesioned) forelimb significantly less when compared to the vehicle group (Student's t-test; statistical summary in Table S1; data are presented as mean ± SEM). At the open arena (**e**), it was observed that 6-OHDA injections had a negative impact on the horizontal exploratory activity and animal's gait quality. The rotameter test (**f**) revealed the success of intrastriatal 6-OHDA lesions with the majority of animals displaying turning behavior after apomorphine administration (Mann–

Whitney U test; statistical summary Table S1; data are presented as mean ± IQR). Vehicle n = 19–20, 6-OHDA n = 23–26; except for cylinder test—vehicle n = 8–9, 6-OHDA n = 8–10. * $p < 0.05$, *** $p < 0.001$. Abbreviations: 6-OHDA, 6-hydroxydopamine.

2.2. Effect of Intrastriatal 6-OHDA Lesion in Anxiety- and Depressive-Like Behavior

Although motor behavioral deficits are commonly reported in 6-OHDA PD models, non-motor features are less frequently addressed and are greatly inconsistent, because of the differences between protocols that can influence the reported outcomes [4]. Therefore, at the end of motor characterization at the last time-point we examined the mice for anxiety- and depressive-like phenotypes.

Mice were examined for anxiety-like behavior in the open field (OF) test. No significant differences were found between groups in the time spent in the anxiogenic center of the arena (Figure 2a). Additionally, no anxious-like signs were confirmed using the elevated-plus maze (EPM) test. During the five-minute test, vehicle and 6-OHDA-lesioned mice spent approximately the same amount of time in opened arms (Figure 2b). The effect produced by striatal 6-OHDA lesion on depressive-like behavior was examined in the forced swim test (FST). We found that 6-OHDA-lesioned animals spent less time immobile in comparison to the vehicle group (Figure 2c), demonstrating that 6-OHDA injections do not have an effect in behavior despair of lesioned animals. On the other hand, the sucrose splash test (SST) paradigm was used to evaluate self-care and motivational behavior, an important feature of depressive-like behavior. Although no differences between groups were found in the latency to initiate grooming (data not shown), 6-OHDA-lesioned mice spent significantly less time grooming after applying a sucrose solution to their coat (Figure 2d). Taken together, these data demonstrated that unilateral striatal 6-OHDA lesion points toward increases in depressive-like behavior, with no indication of alterations in anxiety-like behavior.

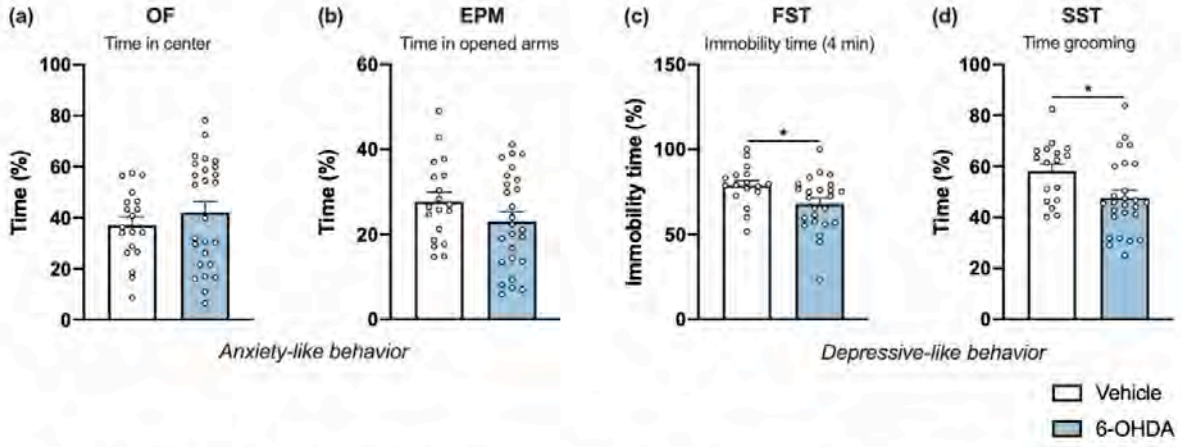


Figure 2. Impact of 6-OHDA intrastriatal lesion on anxiety- and depressive-like behavior. Compared to vehicle, 6-OHDA-lesioned group showed no signs for increased anxiety as seen by the similar time in the center of the OF arena (**a**) and the similar time in the open arms of the EPM (**b**). Regarding depressive-like behavior, in FST (**c**) 6-OHDA-lesioned mice displayed less time immobile but had an increase in time they spent grooming in SST (**d**), when compared to the vehicle group (Student's t-test; statistical summary in Table S1; data are presented as mean ± SEM). Vehicle n = 17–19, 6-OHDA n = 24–26. * $p < 0.05$. Abbreviations: EPM, elevated-plus maze; FST, forced swim test; OF, open field; SST, splash-sucrose test; 6-OHDA, 6-hydroxydopamine.

2.3. Histogical and Neurochemical Characterization of Intrastriatal 6-OHDA Lesion

At the end of the in vivo experiment, animals were divided into two tissue-processing groups: whole brain fixing for subsequent sectioning and immunohistochemistry, or macrodissection of specific brain regions for neurochemical analysis.

For histological assessment, tyrosine hydroxylase (TH) immunohistochemistry in the striatum, SNpc and ventral tegmental area (VTA) was performed. Representative examples of successful lesions are shown in Figure 3b in all these regions. TH+ cells were counted in the SNpc and VTA; and TH+ labelling was measured in the striatum—separated into dorsal striatum and nucleus accumbens (NAc). Both histological analyses in the lesioned hemisphere were compared and presented as percentage of contralateral side. The 6-OHDA injections caused a significant reduction of TH+ labelling in the dorsal striatum on the side of the lesion when compared to the vehicle group (Figure 3c). In the NAc, TH+ labelling was also significantly reduced, although to a lesser extent than dorsal striatal density (Figure 3d). From the results, analysis also revealed statistical differences in the number of TH+ neurons in the SNpc between groups (Figure 3e). Moreover, although intrastriatal lesions mainly affect dopaminergic neurons of the SNpc, they also lead to a decrease in VTA DA neurons, which constitute the mesolimbic pathway and innervate the nucleus accumbens. However, loss of VTA DA neurons does not exceed the 20% that is normally reported in other studies using a similar lesion (Figure 3f) [24].

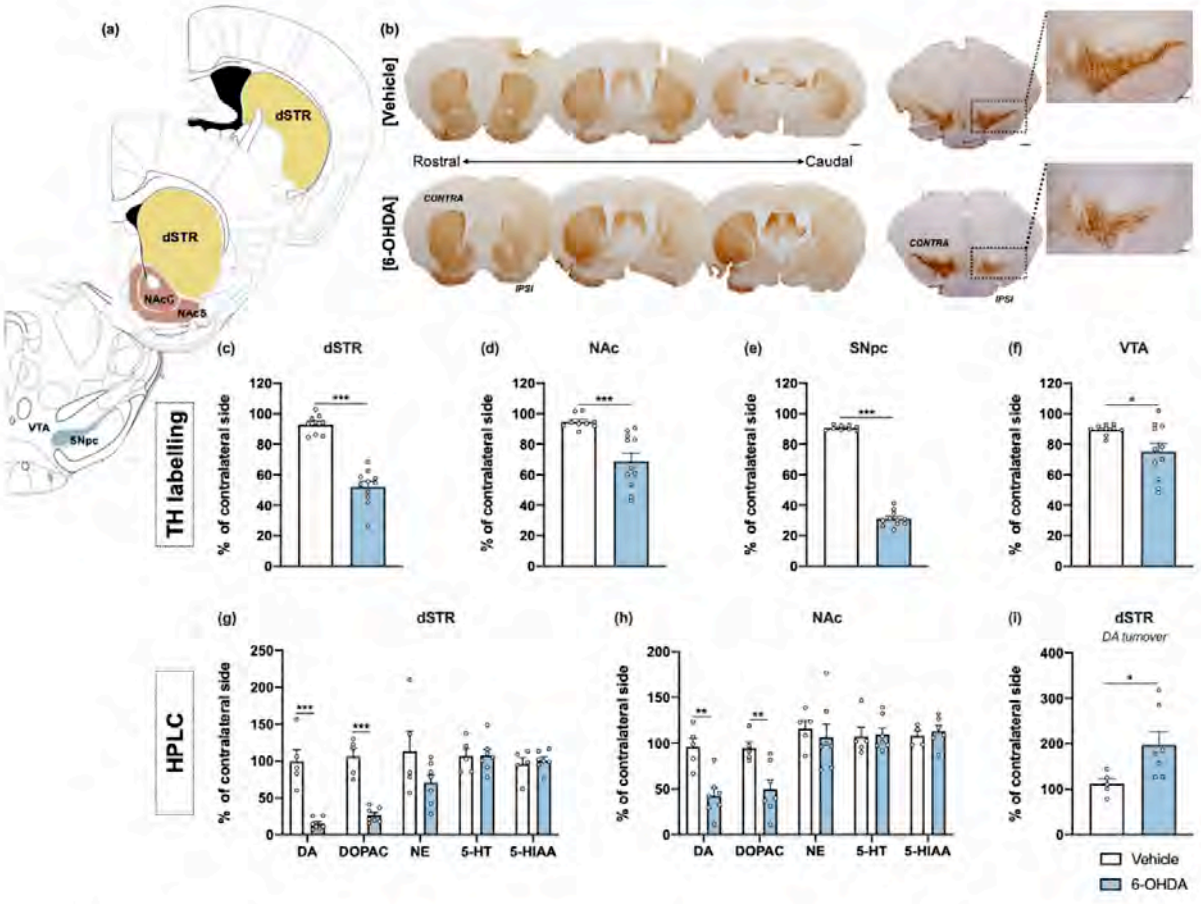


Figure 3. Histological and neurochemical characterization of intrastriatal 6-OHDA lesions. Representative image of the brain regions analyzed (**a**), using coronal sections of the mice's brains. Brightfield photomicrographs of representative coronal brain sections stained for TH (**b**). Compared to the vehicle group, 6-OHDA animals presented marked reduction of TH+ labelling into the dorsal striatum (**c**) and NAc (**d**), as well as significant loss of TH+ cells in the SNpc (**e**) and VTA (**f**). HPLC quantification, combined with electrochemical detection, showed a significant decrease of DA and its metabolite DOPAC in both dorsal striatum (**g**) and NAc (**h**), after 6-OHDA administration. No differences were found between

groups for the monoamines and its derivates (NE, 5-HT, and 5-HIAA), for both regions (**g**), (**h**). For the dorsal striatum, the reduced levels of DA were accompanied with an increased DA turnover in this brain region (**i**) (Student's t-test; statistical summary in Table S1; data are presented as mean ± SEM and as % of contralateral side). For histological analysis vehicle n = 9, 6-OHDA n = 11; for HPLC vehicle = 4–5, 6-OHDA n = 6–7. * $p < 0.05$, ** $p < 0.01$, *** $p < 0.001$. Scale bar = 1 mm. Abbreviations: dSTR, dorsal striatum; DA, dopamine; DOPAC, 3,4-dihydroxyphenylacetic acid; NAcC, nucleus accumbens core; NAcS: nucleus accumbens shell; NE, norepinephrine; SNpc, substantia nigra pars compacta; TH, tyrosine hydroxylase; VTA, ventral tegmental area; 5-HIAA, 5-hydroxyindoleacetic acid; 5-HT, serotonin; 6-OHDA, 6-hydroxydopamine.

Regarding neurochemical analysis, high-performance liquid chromatography (HPLC) measurements were performed for specific monoamines and their derivatives in the major projection targets of DA neurons—dorsal striatum and NAc. 6-OHDA animals presented significant decreases of DA and its metabolite 3,4-dihydroxyphenylacetic acid (DOPAC) in both areas (Figure 3g,h). In parallel with DA reduced levels, we observed an increased turnover of DA in the dorsal striatum (Figure 3i), indicated by the increased ratio of DA metabolite (DOPAC) to DA, which was not verified in the NAc region. No differences were found between groups for norepinephrine, serotonin (5-HT) and its metabolite 5-hydroxyndoleacetic acid (5-HIAA), for both areas (Figure 3g,h). The raw data regarding histological and neurochemical characterization is presented in detail in Supplementary Figure S1. Overall, the results indicate 6-OHDA induces a mild neurotoxic effect, mainly limited to the dorsal striatum and its dopaminergic afferents from the SNpc.

2.4. Glial Cell Reactivity in Lesioned Areas

Tissue sections from dorsal striatum and SNpc were stained with anti-GFAP antibody to visualize astrocytic cells (Figure 4a). Results showed a significant increase of astrocyte reactivity in 6-OHDA lesioned mice when compared to the vehicle group for both areas (after measuring the area occupied by GFAP+ cells and its processes; Figure 4b,c). A similar analysis was also performed for microglia, through IBA1 staining (Figure 5a). Contrary to astrocytes, no differences were found between groups in IBA1+ area (Figure 5b,e). However, we observed a significant increase of IBA1+ cells in both dorsal striatum and SNpc (Figure 5c,f). Moreover, to understand if IBA1+ cells were more activated (less ramified) in 6-OHDA lesioned mice, microglial branching pattern was evaluated using skeleton analysis (Figure S2). Interestingly, results revealed that the total branch length of IBA1+ cells was significantly decreased after 6-OHDA lesion for both lesioned areas (Figure 5d,g). The raw data regarding glial cell reactivity characterization is presented in detail in Supplementary Figure S3. Altogether, these results reveal a marked astrocytic response in this model, as well as microglial proliferation and activation, that is still present even 14 weeks after 6-OHDA injections.

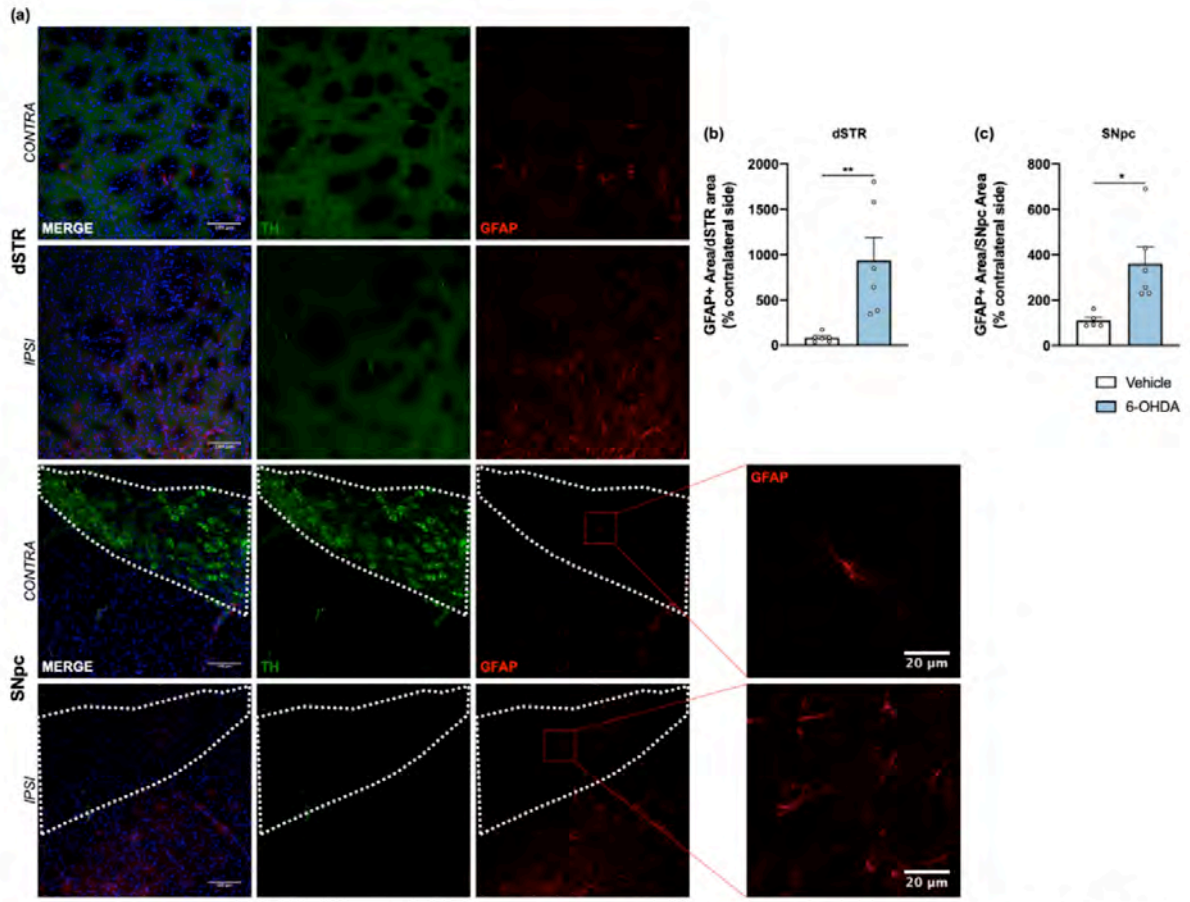


Figure 4. Astroglial reaction after 6-OHDA intrastriatal lesion. Confocal representative photomicrographs (**a**) showing labelling of DA neurons (green) and of astrocytic cells (red) from the dorsal striatum and SNpc, of contra- and ipsilateral sides of 6-OHDA-lesioned mice. Quantification of area coverage by GFAP+ staining showed a significant astrocytic reaction in the ipsilateral lesioned areas (**b**), (**c**) of 6-OHDA mice. Area coverage was acquired from each 20x magnification image, and for SNpc, the area was delineated considering the dopaminergic neurons labelled for TH (Student's t-test; statistical summary in Table S1; data are presented as mean ± SEM and as % of contralateral side). Vehicle n = 4–5, 6-OHDA n = 6–7 (four slices/animal). * $p < 0.05$, ** $p < 0.01$. Scale bars = 100 µm and 20 µm. Abbreviations: DA, dopamine; dSTR, dorsal striatum; GFAP, glial fibrillary acidic protein; SNpc, substantia nigra pars compacta; TH, tyrosine hydroxylase; 6-OHDA, 6-hydroxydopamine.

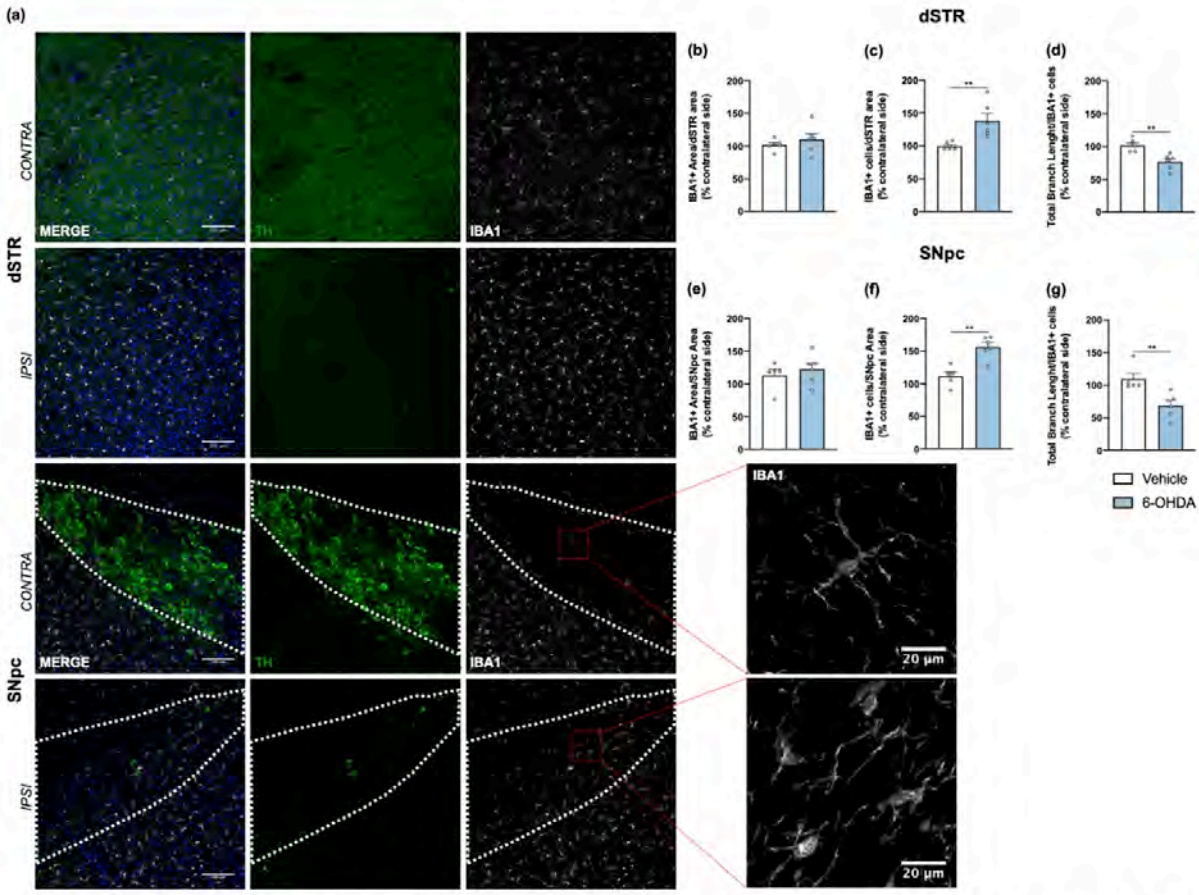


Figure 5. Microglial response after 6-OHDA intrastriatal lesion. Confocal representative photomicrographs (**a**) showing labelling of DA neurons (green) and of microglial cells (grey) from the dorsal striatum and SNpc, of contra- and ipsilateral sides of 6-OHDA-lesioned mice. No differences were found between groups after quantification of area coverage by IBA1+ staining in the dorsal striatum (**b**) and SNpc (**e**). A significant increase of IBA1+ cells (**c**,**f**), as well as a significant decrease of IBA1+ total branch length (**d**,**g**) in the ipsilateral areas of 6-OHDA group was observed, indicating the presence of proliferative and activated microglia. All measurements were performed in acquired 20× magnification images, and for SNpc, the area was delineated considering the dopaminergic neurons labelled for TH (Student's t-test; statistical summary in Table S1; data are presented as mean ± SEM and as % of contralateral side). Vehicle n = 4–5, 6-OHDA n = 6–7 (four slices/animal). ** $p < 0.01$. Scale bars = 100 µm and 20 µm . Abbreviations: DA, dopamine; dSTR, dorsal striatum; SNpc, substantia nigra pars compacta; TH, tyrosine hydroxylase; 6-OHDA, 6-hydroxydopamine.

3. Discussion

In this study, we report a complete behavioral, histological, and neurochemical characterization of a unilateral intrastriatal 6-OHDA mouse model, which evidences its value for mimicking a mild degeneration phenotype. Unilateral lesions in the striatum, as the one herein described, are a valuable tool for reproducing a less severe degeneration, since the striatum is a larger brain region than MFB and SNpc, and therefore it is easier to deliver 6-OHDA stereotactically, enhancing the lesion success in mice. Indeed, all animals injected with 6-OHDA were effectively lesioned, as evidenced by the turning behavior in the rotameter test, as well as by the loss of DA neurons in the nigrostriatal pathway revealed by TH staining in the striatum and SNpc, and DA levels quantification in the striatum. Moreover, this type of quantification benefits from the lesion's unilaterality, as side-specific behaviors, as well as lesioned and intact hemispheres of the brain, can be more easily compared [11]. Finally, in contrast to bilateral 6-OHDA administration, unilateral

lesions avoid profound impairments in feeding, drinking and animals' general health. In our study, the survival rate was greater than 70%, a value that could be further increased using enhanced post-operative care in future studies [25].

Regarding motor phenotype, our assessment revealed significant long-term alterations in general motor performance paradigms (Figure 1), namely deficits in balance and fine motor coordination in the beam balance test, MST and pole test. Impaired forelimb use was also revealed in the cylinder test, which is a standard test to identify unilateral lesions in rats. Spontaneous activity was evaluated in an open arena, revealing compromised horizontal movement and abnormal gait pattern, characterized by dragging of the lower part of the body (walking with the body closer to the floor) and exhibited a backwards positioning of the left (lesioned) hindlimb. These behavioral outcomes are in line with other studies using similar lesions in mice [14,15,17]. Although we did not perform some classical tests used in PD animal models, such as the rotarod and staircase tests, in this work we demonstrate that other tests that normally are used in bilateral lesions (e.g., beam balance, MST and pole tests), are also sensitive to intrastriatal unilateral lesions. Moreover, these tests are more straightforward, without requiring food restriction (e.g., required in the staircase test), especially difficult in mice, and long periods of baseline assessment, and are also less dependent of animals' motivation to perform the task, a common problem faced in the rotarod test.

Concerning drug induced rotational behavior, which is often used for confirming the lesion success in unilateral models, from the total 26 animals to which 6-OHDA was administered, 23 animals presented turning behavior (i.e., increased number of contralateral rotations) after apomorphine administration, thereby confirming the successful depletion of DA on the lesioned side (Figure 1f). Although, at least in rats, it is described that a denervation beyond 90% is necessary to induce consistent hypersensitivity and apomorphine rotation [26], 0.1 mg/kg dose of apomorphine used in this study induced turning behavior without the development of significant stereotyped behavior. Indeed, our histological and neurochemical analysis disclosed a significant degeneration at the nigrostriatal pathway and striatal DA depletion in 6-OHDA lesioned animals, which was lower than 90% that is usually reported for MFB and SNpc lesions [12]. We observed approximately 40% loss of TH+ labelling in the dorsal striatum and 60% loss of TH+ cells from the SNpc, as well as a less pronounced degeneration in VTA and NAc, which is in line with previous studies [14,15,27]. Of note, although we have used a slightly higher 6-OHDA dosage (18 µg) than usually reported (up to 12 µg), it did not seem to have a major impact on the extent of nigrostriatal degeneration. Interestingly, in the dorsal striatum, we observed that reduced levels of DA were accompanied by an increase in the DOPAC/DA ratio, indicating that remaining DA neurons may present an increased activity. In fact, an increase in DA turnover has been hypothesized as a compensatory mechanism for dopaminergic neuronal loss in early PD stages, which may increase the formation of reactive molecules (e.g., hydrogen peroxide and DA quinone) that arise from DA metabolism, and thus further contribute to dopaminergic loss in the long term, due to the reduced antioxidant capacity of SNpc [28–31]. Therefore, our study demonstrates that important neurochemical aspects of PD progression can also be recapitulated in this unilateral intrastriatal 6-OHDA model, offering opportunities for further studies of how DA metabolites affect the degenerative process.

In addition to classical motor symptoms, PD patients display incapacitating neuropsychiatric manifestations, such as apathy, depression, and anxiety, which are under-recognized and consequently undertreated [4,32]. Accordingly, these non-motor phenotypes are also less studied in PD animal models, especially in mice [4]. Indeed, to our knowledge, this is the first report on the neuropsychiatric effects of unilateral intrastriatal 6-OHDA injections in mice. Previous studies using bilateral intrastriatal 6-OHDA mouse models have consistently shown significant effects on anxiety- and depressive-like behaviors [4,19]. Nevertheless, our results on the OF and EPM tests show no signs of anxiety-like behavior, even though 6-OHDA lesioned animals present a decrease in the distance

travelled in the EPM and OF, as well as an increased time resting, which can confound the interpretation of the results. It is known that locomotor activity in the OF depends not only on motor skills, but also on the motivation to explore a novel arena; two behavioral dimensions in which the striatum is critically involved [33]. The dorsal striatum is essential for motor control and motor learning, whereas the ventral striatum, particularly NAc, is a key structure of emotional and motivation processing, modulating the reward system and acting as the limbic–motor interface [34]. As mentioned above, TH+ labelling in VTA and NAc is significantly affected after 6-OHDA injections. Moreover, the levels of DA and its metabolite DOPAC, measured using HPLC, were also significantly reduced in the NAc of 6-OHDA-lesioned mice (Figure 3h). Therefore, it is possible that the lesion of mesocorticolimbic network may contribute to decrease the drive to explore, as supported by other studies [35–37], and thus, have an impact on the performance of the tests herein described. Moreover, previous reports of anxiety-like behavior on bilateral intrastriatal mouse models are observed in animals with a reduced level of motor deficits because of the low dosage of 6-OHDA used, which can also contribute to a better readout on EPM and OF tests. On the other hand, our results on the SST reveal a decreased grooming behavior in 6-OHDA lesioned animals (Figure 2d), which is interpreted as a decrease in self-care and considered similar to motivational deficit and apathetic behavior observed in depressive patients [38]. This result may be explained by the partial, yet significant, degeneration of the VTA, a structure that is involved in emotional activities (e.g., motivation, reward, and addiction), and that is reported to be affected (decreased neuronal number) in severely depressed patients [39,40]. The VTA has also been implicated in PD pathophysiology, though with relative sparing of neurodegeneration, possibly due to the diverse neuronal populations found in VTA, lower expression of DA transporter, and differences in cytosolic DA levels and calcium channel expression [41]. Contrarily to this significant effect on the SST, the FST showed similar latency to immobility between control and lesioned animals (data not shown), and a subtle decrease in the immobility time of 6-OHDA lesioned animals (Figure 2c). This result is not in line with previous reports using bilateral striatal lesions in mice, which showed an increase in the immobility time for 6-OHDA-lesion animals—considered as a measure of behavioral despair [19,25]. However, FST could also be interpreted as a measure of learned-helplessness, a depressive-like paradigm that has been shown to be affected in unilateral intrastriatal 6-OHDA lesions in rats [42].

Finally, since glial activity is an important event of 6-OHDA toxicity [43], the present study also investigated alterations in glial cells within this unilateral intrastriatal 6-OHDA mouse model. Consistently with previous findings [44–47], we observed a significant increase in the area occupied by GFAP+ cells (specific for astrocytes) in the ipsilateral dorsal striatum and SNpc of 6-OHDA-lesioned animals (Figure 4), as well as a significant increase of IBA1+ cells in lesioned areas, indicative of microglial proliferation, with a significant decrease of IBA1+ total branch length, which suggests an activated phenotype. Of note, this evaluation of glial reactivity was only performed 14 weeks after 6-OHDA administration, whereas previous studies report this assessment at earlier timepoints (up to 6 weeks after 6-OHDA lesion), which may indicate the importance of glial response for 6-OHDA model stability and probably contributes to block behavioral compensation normally observed after moderate neurodegeneration. Indeed, in our study, there was a strong correlation between the number of IBA1+ in SNpc and the loss of TH+ neurons in this region, as well as between IBA1+ cells activation and the loss of dopaminergic fibers in the dorsal striatum (see Supplementary Materials, Figure S4 and Table S2). The specific role of astrocytes and microglia in the context of PD remains unclear, with both the excessive reaction and loss of normal activity of astrocytes being proposed as possible causes of the high vulnerability of the DA neurons. Astrocytes can stimulate or prevent neuronal damage, and the loss of balance could be essential for the onset and progression of PD [47]. An interesting study showed that fluorocitrate, that causes activation, prolonged dysfunction, and death of astrocytes, accelerated neuronal degeneration in SNpc induced by

6-OHDA. Stereological analysis indicated decreased TH+ neuronal density already seven days after combined treatment with 6-OHDA and fluorocitrate, while the effect of 6-OHDA alone was only partial [48]. Furthermore, several postmortem and PET studies revealed the presence of reactive microglia both in the striatum and SNpc, and also the expression of proinflammatory molecules such as IFN-γ, TNF-α and IL-1β [49,50]. The deleterious role of these inflammatory mediators on DA neuron's survival has been demonstrated in several experimental in vitro and in vivo models. For instance, the toxicity of lipopolysaccharide (LPS) to DA neurons was only observed in vitro in the presence of microglia [51]. In vivo, after 6-OHDA administration, some studies suggest that activation of microglia precedes DA neuronal cell loss [52,53]. These findings, and the fact that the SNpc region is particularly rich in microglia [54], strongly suggest that these cells may play a crucial role in PD pathogenesis. However, it is important to keep in mind that microglial activation is not always detrimental (for example, microglia plays a crucial role in phagocytic removal of cell debris and dead neurons), and its neuroprotective effects in CNS diseases, including PD, have gained special attention in recent years [55].

Overall, the unilateral intrastriatal 6-OHDA mouse model presented in this study highlights several aspects of the PD neurodegenerative process. Our protocol showed to be sensitive to voluntary simple motor behavior tasks and an attractive tool for the behavioral and mechanistic investigation of non-motor symptoms. Nevertheless, the degeneration in the nigrostriatal system may not be sufficient to mimic the still poorly understood neuropathological substrates of non-motor symptomatology in PD patients. Therefore, in the future, animal models should move in the same direction of clinical findings regarding PD pathophysiology. Moreover, in this study, the degeneration in the nigrostriatal pathway was accompanied by a reactive glial response in lesioned areas, which is an important feature of PD neuroinflammation process. In our view, this animal model is a powerful tool, that can be applied to future studies looking at therapeutic interventions.

4. Materials and Methods

4.1. Animals

A cohort of 55 male and female C57/BL6J mice aged 10–12 weeks (21–28 g) were used in this study. The sample size needed was calculated using the G*Power tool, assuming an effect size of 0.8 (Cohen's d), with a statistical power of 0.8 and a confidence interval of 95%. Animals were housed in groups of 5–6 animals in filtered-topped polysulfone cages (Techniplast, Buguggiate, Italy), with corncob bedding (Scobis Due, Mucedola, Settimo Milanese, Italy) in a SPF animal facility. All animals were maintained in the following conditions: artificial 12:12 h dark/light cycle with lights on at 08:00 h, room temperature (RT) of 21 ± 1 °C, relative humidity of 50–60%, with food (standard diet 4RF21; Mucedola, Settimo Milanese, Italy) and water ad libitum. All experiments were conducted in compliance with local regulations on animal care and experimentation (European Union Directive 2010/63/EU), and with consent from the Portuguese national authority for animal research, Direção Geral de Alimentação e Veterinária (ID: DGAV 005,454 23/04/2025, Lisbon, Portugal) and Ethical Subcommittee in Life and Health Sciences (SECVS; ID: SECVS-142/2016, University of Minho, Braga, Portugal).

4.2. Experimental Design

The sequence of the experiments carried out in this study is graphically outlined in Figure 6. Unilateral lesions in the dopaminergic system were achieved by injecting 6-OHDA at dorso-lateral striatum. Animals underwent surgical procedures for 6-OHDA lesions, and the degree of the lesion was assessed in a series of motor behavioral tests (balance beam, motor swimming test, pole test, spontaneous activity evaluation in open arena, cylinder test, and rotameter test). Behavioral assessment was performed 3 and 11 weeks after lesion surgery to evaluate possible progression of the lesion along time. In the last time-point of analysis, the open field, elevated plus maze, forced-swim test, and

sucrose splash test were also conducted to identify the presence of non-motor symptoms in this model. At the end of behavioral assessment, animals were oscised, and brains dissected and processed for TH histological analysis, neurochemical analysis, and evaluation of glial reaction in lesioned areas (these data were analyzed under blinded conditions). In this study, the experimental groups have both males and females, since differences between sexes in terms of motor behavioral phenotypes and histological analysis was not observed (see Supplementary Materials, Figure S3 and Table S2).

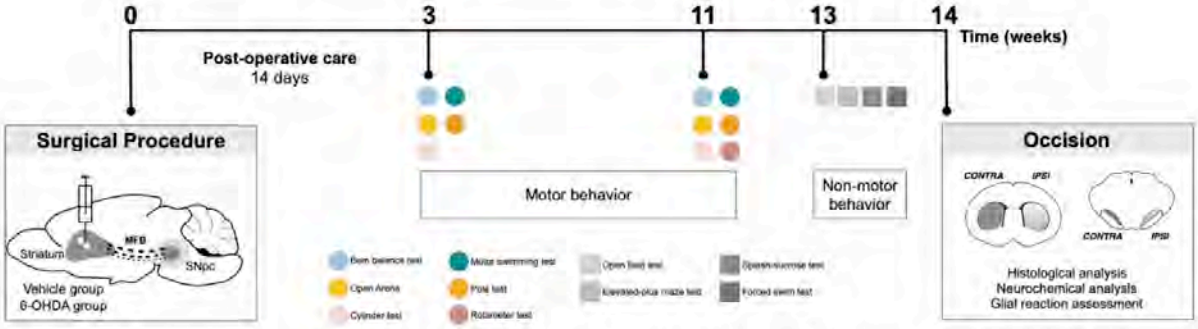


Figure 6. Experimental design. Schematic representation and temporal sequence of performed tasks throughout the experiment.

4.3. Lesion Procedure (6-Hydroxidopamine Injections)

Mice were intraperitoneally (i.p.) anesthetized with ketamine-medetomidine [75 mg/kg; 1 mg/kg] diluted in 0.9% NaCl. Once anesthetized, animals were positioned on a stereotaxic frame (Stoelting, Kiel, WI, USA), and unilateral lesions were achieved by injection of 6-OHDA hydrochloride (H4381, Merck, Darmstadt, Germany) in the right hemisphere using a 10 µl Hamilton syringe (DDBioLaB, Barcelona, Spain). The neurotoxin was used at a concentration of 6 µg/µl (calculated from free base weight) dissolved in a solution of 0.9% NaCl in 0.2 mg/mL ascorbic acid. 6-OHDA was administrated into the dorsolateral striatum (2 × 1.5 µl) at a rate of 300 nl/min, at the following stereotaxic coordinates (relative to bregma, in mm): (i) AP = +1.0, ML = −2.1, DV = −2.9; (ii) AP = +0.3, ML = −2.3, DV = −2.9. After each injection, the needle was left in place there for 5 min for diffusion and to avoid any backflow. The control group was injected in the same conditions with the neurotoxin vehicle. Anesthesia was reversed using atipamezole (1 mg/mL). Animals were randomly assigned into both experimental groups.

4.4. Post-Operative Care

Post-operative mortality is generally high in 6-OHDA mice models, and animals can suffer from a variety of complications (Table S3) [11,25]. However, this can be overcome by continuous health assessment and intensive post-operative care after lesion surgery. Thus, health status of each animal was assessed during the first 14 days post-surgery, and mice that reached the human endpoints [56] were euthanized. During the recovery, animals were housed in a warmed room and post-operative care was performed twice a day.

Following surgery, animals received 0.1 mg/kg injections of buprenorphine (i.p.) every 6 h for 5 days to avoid pain, and 5 mg/kg carprofen subcutaneously (s.c.) every 24 h for 3 days. Animals received 1 mL injections (s.c.) of sterile and warm saline twice daily to mitigate dehydration, and if needed, they were fed by hand with providing Nutri-plus Gel (Virbac, Nice, France) into the mouth via 1 mL syringe. Until the animals got used to the energy supplement, s.c. injections of 1 mg/kg/day Duphalyte (Zoetis, Parsippany-Troy Hills, NJ, USA) were also administered. Mice were weighed every day in the first week post-surgery, and then once a week until the end of the experiment (Figure S5). The

mortality rate of mice in the 6-OHDA group was 25.7% (9 animals were lost during the experiment).

4.5. Behavioral Assessment

Prior to each behavioral test, mice were habituated to the testing room for 20 min. Behavioral tests were conducted in the order outlined in (Figure 6) and as described below.

4.5.1. Beam Balance

This test was performed as previously described [57]. Animals were trained for 3 days on the square beam (12 mm), and at day 4 they were tested on the training beam and on two round beams (17 mm and 11 mm). The time the animal took to cross the beam was registered, and time was discounted whenever the animal stopped. If the animal fell or turned around, this was considered a failed trial. Each animal had the opportunity to fail 2 times on each beam.

4.5.2. Motor Swimming Test (FST)

For MST, mice were trained for 2 consecutive days (3 trials per animal) to traverse a clear Perspex water tank (100 cm long) to a safe black platform at the end. Mice were tested for 3 consecutive days (2 trials/animal), and the latency to cross the water was measured from 60 cm distance. Water temperature was monitored and set to 23 °C using a thermostat [57].

4.5.3. Pole Test

Mice were placed facing up on top of a pole (37.5 cm long) located in their cages. The time the animals took to reach the cage was registered. If the animal fell or did not turn down after 5 min, this was considered a failed trial. Time values were registered on 3 consecutive days (2 trials/animal) [58].

4.5.4. Open Arena

Mice were transferred to a 15-labeled-square arena (55 cm × 33 cm × 18 cm) and the number of squares travelled in the arena for 1 min was counted. Gait quality was also scored as normal or abnormal, by the same experimenter [59].

4.5.5. Cylinder Test

To perform this test, mice were placed individually in a transparent cylinder (11.5 cm diameter) and were video recorded for 5 min to record the laterality of forelimb use of the animals when exploring the cylinder wall. A mirror was placed behind the cylinder at an angle to allow the record of the forelimb movements along 360°. The videos were analyzed in slow motion and frame-by-frame to score the rears, and the number of wall contacts performed independently with the left and the right forepaw were counted to a total number of 20 wall contacts per mice and session. This test was performed during the night cycle when animals are more active to explore [14,60].

4.5.6. Rotameter Test

To estimate the dopaminergic denervation after 6-OHDA injections, the rotameter test using apomorphine was performed. For that, animals received a s.c. injection of 0.1 mg/kg apomorphine hydrochloride (A4393, Merck) dissolved in 1% ascorbic acid, 0.9% NaCl. Each mouse was placed in a glass cylinder, and full turns were counted in the ipsilateral and contralateral directions during 20 min. Data are expressed as total net contralateral rotations (representing the difference between the total number of contralateral and ipsilateral rotations). Mice received 2 apomorphine injections over the preceding days to avoid any potential wind-up effect [61].

4.5.7. Open Field (OF) Test

For the OF test, animals were placed at the center of an illuminated square arena (43.2 cm × 43.2 cm), enclosed by a 30.5 cm high wall. Their movements were tracked for 5 min, using a 16-beam infrared system (MedAssociates Inc, Twin City, GA, USA), and data was analysed using the Activity Monitor software (MedAssociates Inc). The distance and time at the center/periphery were considered as measurements of anxiety-like behavior [62].

4.5.8. Elevated-Plus Maze (EPM) Test

The EPM apparatus (ENV—560, MedAssociates Inc) was composed of two opposite open arms (50.8 cm × 10.2 cm) and two closed arms (50.8 cm × 10.2 cm × 40.6 cm) elevated 72.4 cm above the floor and softly illuminated. Each mouse was placed into the center of the maze (10 cm × 10 cm), facing one of the two open arms, and its behavior was video recorded for 5 min. Trials were recorded using an infrared photobeam system, and the percentage of time spent in each of the three compartments (open, close, center) was measured through the EthoVision XT 11.5 tracking system (Ethovision, Noldus Information Technologies, Leesburg, VA, USA). The propensity to avoid the open arms was considered as an index of anxiety [63].

4.5.9. Forced Swim Test (FST)

FST was performed as previously described [64]. For that, each animal was individually placed in glass cylinders filled with water (23 °C; depth 30 cm) during 6 min. All sessions were video-recorded, and the immobility time was measured. Mice were considered immobile when remained passively floating or doing minimal movements need to maintain the head above the water surface. The first 2 min of the trial were considered as a habituation period and the last 4 min as the test period.

4.5.10. Splash-Sucrose Test (SST)

To perform this test, a 10% sucrose solution was sprayed on the dorsal coat of mice in their home cage. The latency to initiate a grooming behavior, as well as the duration of grooming, was recorded during 5 min. The sucrose solution was chosen as a releaser and a persisting factor of grooming due to its viscosity [65].

4.6. Histological Assessment

After behavioral assessment, animals were deeply anesthetized with a mixture of ketamine (150 mg/kg) plus medetomidine (0.3 mg/Kg), and a cohort of animals of each group was transcardially perfused with a 4% paraformaldehyde in PBS. Brains were collected and immediately embedded in OCT and frozen at −80 °C for further processing in the cryostat. Coronal sections were then cut at 40 µm and representative sections of striatum and SNpc were selected for free-floating immunohistochemistry to visualize dopaminergic innervation. In brief, the endogenous peroxidases activity was stopped using 3% hydrogen peroxidase for 20 min RT, followed by permeabilization in 0.1% PBS-T for 10 min (3 times) and blockage in PBS 10% newborn calf serum (NBCS) for 2 h. Sections were then incubated with anti-TH from rabbit (1:1000; AB152, Merck) overnight at 4 °C. The next day, sections were incubated with a biotinylated secondary antibody (TP-125-BN, ThermoFisher Scientific, Waltham, MA, USA), followed by strepptavidine-peroxidase solution (TP-125-HR; ThermoFisher Scientific) for 30 min at RT. Antigen revelation was done using 3-3′-diaminobenzidine tetrahydrochloride (DAB; 25 mg DAB in 50 mL Tris–HCl 0.05 M with 12.5 µL H_2O_2, pH 7.6; D5905, Merck). Sections were mounted on slides, and after 24 h drying in the dark, they were mounted using Entellan (Merck, Darmstadt, Germany).

TH+ labelling in the dorsal striatum and NAc were imaged using brightfield illumination (SZX16, Olympus, Tokyo, Japan) and the mean grey value was measured using the ImageJ software (v1.48, National Institute of Health, Stapleton, NY, USA) as previously

described in detail [66], taking into account the anatomic landmarks represented in Figure 3a. Briefly, the measurements are taken from specified ROIs positioned in the specific areas (dorsal striatum and NAc), and the signal from measurements of background (mean intensity from ROIs positioned in cortical areas) is subtracted. TH+ cells in the SNpc and VTA were visualized and counted using a brightfield microscope (BX51, Olympus) equipped with a digital camera (PixeLINK PL-A622, CANIMPEX Enterprises, Zurich, Switzerland). Through the Visiomorph software (v2.12.3.0, Visiopharm, Horsholm, Denmark), the boundaries of the SNpc and VTA areas were drawn, and total TH+ cells were counted in both hemispheres. Data is presented as the percentage (%) of contralateral side (intact side). Raw data relative to histology results are represented in Figure S1a.

4.7. Neurochemical Analysis

Macrodissection was performed in a set of animals of each group after decapitation and brain snap-freezing in liquid nitrogen. Brain areas of interest were rapidly dissected using a brain slicer, observing anatomical landmarks. Samples were snap-frozen (dry ice) and stored at −80 °C for further experiments.

Quantification of catecholamine levels in the striatum and nucleus accumbens (NAc) was performed by high-performance liquid chromatography, combined with electrochemical detection (HPLC/EC) using a Gilson instrument (Gilson, Mettmenstetten, Switzerland), fitted with an analytical column (Supleco Supelcosil LC-18 3 mM; flow rate: 1.0 mL/min). Left and right striatum and NAc were weighted and then incubated with 0.2 N perchloric acid, sonicated (5 min on ice) and centrifuged at 5000× *g*. The resulting supernatant was filtered through a Spin-X HPLC column (Costar, ThermoFisher Scientific) to remove debris and 150 µL aliquots were injected into the HPLC system, using a mobile phase of 0.7 M aqueous potassium phosphate (pH 3.0) in 10% methanol, 1-heptanesulfonic acid (222 mg/L) and Na-EDTA (40 mg/L). A standard curve using known concentrations of all monoamines was run each day. Monoamine's concentration in each side were calculated using the standard curve and normalized to the amount of tissue from which they were extracted. Data is presented as the percentage (%) of contralateral side (intact side). Raw data relative to HPLC results are represented in Figure S1b.

4.8. Immunofluroescense and Detection of Glial Cells

For detection of glial fibrillary acidic protein (GFAP) and ionized calcium binding adaptor molecule 1 (Iba-1), representative sections of striatum and SNpc were permeabilized in 0.3% PBS-Triton X-100 (PBS-T) for 10 min (3 times), followed by blockage using 0.3% PBS-T with 10% NBCS for 1 h. Sections were then incubated with the following primary antibodies: anti-TH from mouse (1-1000; MAB318, Merck), anti-GFAP from goat (1-200; ab53554, Abcam, Cambridge, UK) and anti-Iba-1 from rabbit (1-750; 019-19741, Wako, Bellwood, VA, USA), diluted in 3% PBS-T with 2% NBCS overnight at 4 °C. After washing, tissue sections were incubated with the secondary antibodies (Alexa Fluor: 488 donkey anti-mouse, 594 donkey anti-goat and 647 donkey anti-rabbit; ThermoFisher Scientific), diluted in 3% PBS-T for 2 h at RT. Nuclei were stained with 4-6-diamidino-2-phenylindole-dhydrochloride (DAPI, 1:1000; ThermoFisher Scientific) for 10 min at RT. Afterwards, coverslips were mounted on glass slides using PermaFluor (ThermoFisher Scientific).

For image acquisition, two imaging workflows were developed for the scanning of SNpc and striatal areas, respectively. Photomicrographs from triple immunofluorescence stains were acquired with a confocal laser scanning microscope (Olympus FV3000) and are representative of 4 slices per animal. To standardize image acquisition and minimize inter-sample variation, all photos were taken at a sampling speed of 2 µs/pixel and pinhole aperture of 132 µm, using lasers 405 (Blue), 488 (Green), 594 (Red) and 647 (Grey), and scanned with a 3.5 micron step-size over the Z-plan. Striatal images were acquired along the dorsal–ventral and medial–lateral axis, and tiles encompassing the whole SNpc area were imaged using a motorized XY scanning stage equipped with a 20× objective

(UPlanSApo NA 0.75). Images had a resolution of 1.257 px/micron and a voxel size of 0.795 × 0.795 μm^3. Individual acquisition settings for each marker of interest can be found in Table S4.

4.9. Image Analyis of Glial Reaction

Photomicrographs containing the four channels were analyzed using a semi-automated workflow on ImageJ software. Measurements of the area occupied by astrocytes (GFAP-positive stain), as well as counts and branching patterns (skeleton analysis) for microglial cells were assessed in both lesioned areas. Images were first processed to produce projections along the *Z*-axis, and ROIs were implemented with the polygon tool to segment the striatal and nigral areas. Automatic and manual intensity-based thresholding was applied to segment microglial and astrocytic cells, respectively. The area occupied by the GFAP staining was measured and normalized against the control from both the SNpc and striatum ROIs. Manual counting of microglial cells (Iba-1-positive cells) was performed using the multi-point tool from the (Cell-Counter) plugin. Microglial branching was assessed with the skeletonize tool after the application of an unsharp mask and the close function. Total branch length was normalized by the number of microglial cells within each image [67]. Data are presented as the percentage (%) of contralateral side (intact side). Raw data relative to glia reaction image analysis results are represented in Figure S3.

4.10. Statistical Analysis

Statistical analysis was performed using GraphPad Prism v.8.0c (GraphPad Software, San Diego, CA, USA). A significance level of $\alpha = 0.05$ was chosen for all the comparisons. The assumption of normality was tested for all continuous variables through evaluation of the frequency distribution histogram, the values of skewness and kurtosis and through the Shapiro–Wilk test. All continuous data are shown as the mean ± SEM. For the comparison of means between two groups, a Student's t-test for independent samples was used, when data was continuous; for discrete data, a Mann–Whitney U test was carried out and data presented as mean ± IQR. A critical value for significance of $p < 0.05$ was used throughout the study. For Supplementary Figures S2 and S3, a Pearson correlation and two-way ANOVA analysis were performed, respectively. Statistical summary of all conducted analysis is presented in Tables S1 and S2.

Supplementary Materials: The following are available online at www.mdpi.com/xxx/s1.

Author Contributions: Conceptualization, B.M.-P., A.M., S.D.-S., L.P. and A.J.S.; methodology, B.M.-P., C.S.-C., A.M., E.L.-C., J.C., S.B.-A., D.M.-F., D.S., S.D.-S. and L.P.; validation, B.M.-P. and A.J.S.; formal analysis, B.M.-P., J.C., D.S. and S.D.-S.; data curation, B.M.-P.; investigation, B.M.-P., C.S.-C., A.M., E.L.-C., J.C., S.B.-A., D.M.-F., D.S. and S.D.-S.; resources, A.J.S.; writing—original draft preparation, B.M.-P.; writing—review and editing, B.M.-P., A.M., J.C. and A.J.S.; supervision, L.P. and A.J.S.; project administration, A.J.S.; funding acquisition, A.J.S. All authors have read and agreed to the published version of the manuscript.

Funding: This work was supported by the Foundation for Science and Technology (FCT) through PhD Fellowships attributed to B.M.P. (SFRH/BD/120124/2016), E.L.C. (SFRH/BD/131278/2017), J.C. (SFRH/BD/5813/2020), S.B.A. (PD/BDE/135568/2018), D.M.F. (SFRH/BD/147947/2019), and CEEC attributed to C.S.C. (CEECIND/03887/2017), S.D.S. (CEECIND/00685/2020), and L.P. (CEECIND/02855/2020). ICVS Scientific Microscopy Platform, member of the national infrastructure PPBI—Portuguese Platform of Bioimaging PPBI-POCI-01-0145-FEDER-022122; National funds, through the FCT—project UIDB/50026/2020 and UIDP/50026/2020; the projects NORTE-01-0145-FEDER-000013 and NORTE-01-0145-FEDER-000023, supported by Norte Portugal Regional Operational Programme (NORTE 2020), under the PORTUGAL 2020 Partnership Agreement, through the European Regional Development Fund (ERDF); Competitiveness Internationalization Operational Programme (POCI), and by National funds, through the FCT, under the scope of the project POCI-01-0145-FEDER-032619.

Institutional Review Board Statement: The animal study was reviewed and approved by Direção Geral de Alimentação e Veterinária (ID: DGAV 005454 23/04/2025, Lisbon, Portugal) and Ethical Subcommittee in Life and Health Sciences (SECVS; ID: SECVS-142/2016, University of Minho, Braga, Portugal).

Informed Consent Statement: Not applicable.

Data Availability Statement: Data is contained within the article or supplementary material.

Acknowledgments: The authors would like to acknowledge to Andreas Heuer for the important input regarding mice post-operative care.

Conflicts of Interest: The authors declare no conflict of interest.

References

1. Dorsey, E.R.; Sherer, T.; Okun, M.S.; Bloem, B.R. The Emerging Evidence of the Parkinson Pandemic. *J. Parkinsons. Dis.* **2018**, *8*, S3–S8.
2. Magrinelli, F.; Picelli, A.; Tocco, P.; Federico, A.; Roncari, L.; Smania, N.; Zanette, G.; Tamburin, S. Pathophysiology of Motor Dysfunction in Parkinson's Disease as the Rationale for Drug Treatment and Rehabilitation. *Parkinsons. Dis.* **2016**, *2016*, 9832839.
3. Ma, J.; Gao, J.; Wang, J.; Xie, A. Prion-Like Mechanisms in Parkinson's Disease. *Front. Neurosci.* **2019**, *13*, 552.
4. Magnard, R.; Vachez, Y.; Carcenac, C.; Krack, P.; David, O.; Savasta, M.; Boulet, S.; Carnicella, S. What can rodent models tell us about apathy and associated neuropsychiatric symptoms in Parkinson's disease? *Transl. Psychiatry* **2016**, *6*, e753.
5. Ball, N.; Teo, W.-P.; Chandra, S.; Chapman, J. Parkinson's Disease and the Environment. *Front. Neurol.* **2019**, *10*, 218.
6. Iarkov, A.; Barreto, G.E.; Grizzell, J.A.; Echeverria, V. Strategies for the Treatment of Parkinson's Disease: Beyond Dopamine. *Front. Aging Neurosci.* **2020**, *12*, 4.
7. Kin, K.; Yasuhara, T.; Kameda, M.; Date, I. Animal Models for Parkinson's Disease Research: Trends in the 2000s. *Int. J. Mol. Sci.* **2019**, *20*, 5402.
8. Buhidma, Y.; Rukavina, K.; Chaudhuri, K.R.; Duty, S. Potential of animal models for advancing the understanding and treatment of pain in Parkinson's disease. *NPJ Park. Dis.* **2020**, *6*, 1.
9. Duty, S.; Jenner, P. Animal models of Parkinson's disease: A source of novel treatments and clues to the cause of the disease. *Br. J. Pharmacol.* **2011**, *164*, 1357–1391.
10. Kim, tieu A guide to neurotoxic animal models of parkinson´s disease. *Cold Spring Harb. Perspect. Med.* **2011**, *1*, a009316.
11. Smith, G.A.; Heuer, A. 6-OHDA toxin model in mouse. In *Animal Models of Movement Disorders*; Humana Press: Tortowa, NJ, USA, 2011.
12. Bové, J.; Perier, C. Neurotoxin-based models of Parkinson's disease. *Neuroscience* **2012**, *211*, 51–76.
13. Cannon, J.R.; Greenamyre, J.T. Neurotoxic in vivo models of Parkinson's disease. *Prog. Brain Res.* **2010**, *184*, 17–33.
14. Heuer, A.; Smith, G.A.; Lelos, M.J.; Lane, E.L.; Dunnett, S.B. Unilateral nigrostriatal 6-hydroxydopamine lesions in mice I: Motor impairments identify extent of dopamine depletion at three different lesion sites. *Behav. Brain Res.* **2012**, *228*, 30–43.
15. Bagga, V.; Dunnett, S.B.; Fricker, R.A. The 6-OHDA mouse model of Parkinson's disease—Terminal striatal lesions provide a superior measure of neuronal loss and replacement than median forebrain bundle lesions. *Behav. Brain Res.* **2015**, *288*, 107–117.
16. Stott, S.R.W.; Barker, R.A. Time course of dopamine neuron loss and glial response in the 6-OHDA striatal mouse model of Parkinson's disease. *Eur. J. Neurosci.* **2014**, *39*, 1042–1056.
17. Lundblad, M.; Picconi, B.; Lindgren, H.; Cenci, M.A. A model of l-DOPA-induced dyskinesia in 6-hydroxydopamine lesioned mice: Relation to motor and cellular parameters of nigrostriatal function. *Neurobiol. Dis.* **2004**, *16*, 110–123.
18. Alvarez-Fischer, D.; Henze, C.; Strenzke, C.; Westrich, J.; Ferger, B.; Höglinger, G.U.; Oertel, W.H.; Hartmann, A. Characterization of the striatal 6-OHDA model of Parkinson's disease in wild type and α-synuclein-deleted mice. *Exp. Neurol.* **2008**, *210*, 182–193.
19. Bonito-Oliva, A.; Masini, D.; Fisone, G. A mouse model of non-motor symptoms in Parkinson's disease: Focus on pharmacological interventions targeting affective dysfunctions. *Front. Behav. Neurosci.* **2014**, *8*, 290.
20. Domingues, A.V.; Pereira, I.M.; Vilaça-Faria, H.; Salgado, A.J.; Rodrigues, A.J.; Teixeira, F.G. Glial cells in Parkinson´s disease: Protective or deleterious? *Cell. Mol. Life Sci.* **2020**, *77*, 5171–5188.
21. Kim, Y.; Park, J.; Choi, Y.K. The Role of Astrocytes in the Central Nervous System Focused on BK Channel and Heme Oxygenase Metabolites: A Review. *Antioxidants* **2019**, *8*, 121.
22. Bachiller, S.; Jiménez-Ferrer, I.; Paulus, A.; Yang, Y.; Swanberg, M.; Deierborg, T.; Boza-Serrano, A. Microglia in Neurological Diseases: A Road Map to Brain-Disease Dependent-Inflammatory Response. *Front. Cell. Neurosci.* **2018**, *12*, 488.
23. Vivekanantham, S.; Shah, S.; Dewji, R.; Dewji, A.; Khatri, C.; Ologunde, R. Neuroinflammation in Parkinson's disease: Role in neurodegeneration and tissue repair. *Int. J. Neurosci.* **2015**, *125*, 717–725.
24. Hernandez-Baltazar, D.; Zavala-Flores, L.M.; Villanueva-Olivo, A. The 6-hydroxydopamine model and parkinsonian pathophysiology: Novel findings in an older model. *Neurología* **2017**, *32*, 533–539.
25. Masini, D.; Plewnia, C.; Bertho, M.; Scalbert, N.; Caggiano, V.; Fisone, G. A Guide to the Generation of a 6-Hydroxydopamine Mouse Model of Parkinson's Disease for the Study of Non-Motor Symptoms. *Biomedicines* **2021**, *9*, 598.

26. Björklund, A.; Dunnett, S.B. The Amphetamine Induced Rotation Test: A Re-Assessment of Its Use as a Tool to Monitor Motor Impairment and Functional Recovery in Rodent Models of Parkinson's Disease. *J. Parkinsons. Dis.* **2019**, *9*, 17–29.
27. Bensadoun, J.C.; Déglon, N.; Tseng, J.L.; Ridet, J.L.; Zurn, A.D.; Aebischer, P. Lentiviral vectors as a gene delivery system in the mouse midbrain: Cellular and behavioral improvements in a 6-OHDA model of Parkinson's disease using GDNF. *Exp. Neurol.* **2000**, *164*, 15–24.
28. Sossi, V.; de la Fuente-Fernández, R.; Holden, J.E.; Doudet, D.J.; McKenzie, J.; Stoessl, A.J.; Ruth, T.J. Increase in Dopamine Turnover Occurs Early in Parkinson's Disease: Evidence from a New Modeling Approach to PET 18 F-Fluorodopa Data. *J. Cereb. Blood Flow Metab.* **2002**, *22*, 232–239.
29. Sossi, V.; de la Fuente-Fernández, R.; Holden, J.E.; Schulzer, M.; Ruth, T.J.; Stoessl, J. Changes of Dopamine Turnover in the Progression of Parkinson's Disease as Measured by Positron Emission Tomography: Their Relation to Disease-Compensatory Mechanisms. *J. Cereb. Blood Flow Metab.* **2004**, *24*, 869–876.
30. Zigmond, M.J.; Hastings, T.G.; Perez, R.G. Increased dopamine turnover after partial loss of dopaminergic neurons: Compensation or toxicity? *Parkinsonism Relat. Disord.* **2002**, *8*, 389–393.
31. Rabinovic, A..; Lewis, D..; Hastings, T.. Role of oxidative changes in the degeneration of dopamine terminals after injection of neurotoxic levels of dopamine. *Neuroscience* **2000**, *101*, 67–76.
32. Aarsland, D.; Pedersen, K.F.; Ehrt, U.; Bronnick, K.; Gjerstad, M.D.; Larsen, J.P. Neuropsychiatric and cognitive symptoms in Parkinson disease. *Tidsskr. Nor. Laegeforen.* **2008**, *128*, 2072–2076.
33. Sousa, N.; Almeida, O.F.X.; Wotjak, C.T. A hitchhiker's guide to behavioral analysis in laboratory rodents. *Genes, Brain Behav.* **2006**, *5*, 5–24.
34. Schiffmann, S.N. Changes in neural networks by conditional transgenic approach: A key to our comprehension of neuropsychiatric disorders in the basal ganglia system. *Bull. Mem. Acad. R. Med. Belg.* **2009**, *164*, 171–178.
35. Stephen Fink, J.; Smith, G.P. Mesolimbicocortical dopamine terminal fields are necessary for normal locomotor and investigatory exploration in rats. *Brain Res.* **1980**, *199*, 359–384.
36. Jones, G.H.; Robbins, T.W. Differential effects of mesocortical, mesolimbic, and mesostriatal dopamine depletion on spontaneous, conditioned, and drug-induced locomotor activity. *Pharmacol. Biochem. Behav.* **1992**, *43*, 887–895.
37. Levy, R.; Dubois, B. Apathy and the Functional Anatomy of the Prefrontal Cortex–Basal Ganglia Circuits. *Cereb. Cortex* **2006**, *16*, 916–928.
38. Willner, P. Chronic Mild Stress (CMS) Revisited: Consistency and Behavioural-Neurobiological Concordance in the Effects of CMS. *Neuropsychobiology* **2005**, *52*, 90–110.
39. Russo, S.J.; Nestler, E.J. The brain reward circuitry in mood disorders. *Nat. Rev. Neurosci.* **2013**, *14*, 609–625.
40. Tye, K.M.; Mirzabekov, J.J.; Warden, M.R.; Ferenczi, E.A.; Tsai, H.C.; Finkelstein, J.; Kim, S.Y.; Adhikari, A.; Thompson, K.R.; Andalman, A.S.; et al. Dopamine neurons modulate neural encoding and expression of depression-related behaviour. *Nature* **2013**, *493*, 537–541.
41. Alberico, S.L.; Cassell, M.D.; Narayanan, N.S. The vulnerable ventral tegmental area in Parkinson's disease. *Basal Ganglia* 2015, *5*, 51–55.
42. Winter, C.; von Rumohr, A.; Mundt, A.; Petrus, D.; Klein, J.; Lee, T.; Morgenstern, R.; Kupsch, A.; Juckel, G. Lesions of dopaminergic neurons in the substantia nigra pars compacta and in the ventral tegmental area enhance depressive-like behavior in rats. *Behav. Brain Res.* **2007**, *184*, 133–141.
43. McGeer, P.L.; McGeer, E.G. Glial reactions in Parkinson's disease. *Mov. Disord.* **2008**, *23*, 474–483.
44. Su, R.; Zhen, J.; Wang, W.; Zhang, J.; Zheng, Y.; Wang, X. Time-course behavioral features are correlated with Parkinson's disease-associated pathology in a 6-hydroxydopamine hemiparkinsonian rat model. *Mol. Med. Rep.* **2017**, *17*, 3356–3363.
45. Batassini, C.; Broetto, N.; Tortorelli, L.S.; Borsoi, M.; Zanotto, C.; Galland, F.; Souza, T.M.; Leite, M.C.; Gonçalves, C.-A. Striatal Injury with 6-OHDA Transiently Increases Cerebrospinal GFAP and S100B. *Neural Plast.* **2015**, *2015*, 387028.
46. Aponso, P.M.; Faull, R.L.M.; Connor, B. Increased progenitor cell proliferation and astrogenesis in the partial progressive 6-hydroxydopamine model of Parkinson's disease. *Neuroscience* **2008**, *151*, 1142–1153.
47. Morales, I.; Sanchez, A.; Rodriguez-Sabate, C.; Rodriguez, M. The astrocytic response to the dopaminergic denervation of the striatum. *J. Neurochem.* **2016**, *139*, 81–95.
48. Kuter, K.; Olech, Ł.; Głowacka, U. Prolonged Dysfunction of Astrocytes and Activation of Microglia Accelerate Degeneration of Dopaminergic Neurons in the Rat Substantia Nigra and Block Compensation of Early Motor Dysfunction Induced by 6-OHDA. *Mol. Neurobiol.* **2018**, *55*, 3049–3066.
49. Ouchi, Y.; Yoshikawa, E.; Sekine, Y.; Futatsubashi, M.; Kanno, T.; Ogusu, T.; Torizuka, T. Microglial activation and dopamine terminal loss in early Parkinson's disease. *Ann. Neurol.* **2005**, *57*, 168–175.
50. Belloli, S.; Morari, M.; Murtaj, V.; Valtorta, S.; Moresco, R.M.; Gilardi, M.C. Translation Imaging in Parkinson's Disease: Focus on Neuroinflammation. *Front. Aging Neurosci.* **2020**, *12*, 152.
51. Gao, H.-M.; Jiang, J.; Wilson, B.; Zhang, W.; Hong, J.-S.; Liu, B. Microglial activation-mediated delayed and progressive degeneration of rat nigral dopaminergic neurons: Relevance to Parkinson's disease. *J. Neurochem.* **2002**, *81*, 1285–1297.
52. Rodriguez-Pallares, J.; Parga, J.A.; Muñoz, A.; Rey, P.; Guerra, M.J.; Labandeira-Garcia, J.L. Mechanism of 6-hydroxydopamine neurotoxicity: The role of NADPH oxidase and microglial activation in 6-hydroxydopamine-induced degeneration of dopaminergic neurons. *J. Neurochem.* **2007**, *103*, 145–156.

53. Marinova-Mutafchieva, L.; Sadeghian, M.; Broom, L.; Davis, J.B.; Medhurst, A.D.; Dexter, D.T. Relationship between microglial activation and dopaminergic neuronal loss in the substantia nigra: A time course study in a 6-hydroxydopamine model of Parkinson's disease. *J. Neurochem.* **2009**, *110*, 966–975.
54. McGeer, E.G.; Klegeris, A.; McGeer, P.L. Inflammation, the complement system and the diseases of aging. *Neurobiol. Aging* **2005**, *26*, 94–97.
55. Le, W.; Wu, J.; Tang, Y. Protective Microglia and Their Regulation in Parkinson's Disease. *Front. Mol. Neurosci.* **2016**, *9*, 89.
56. Hawkins, P.; Morton, D.B.; Burman, O.; Dennison, N.; Honess, P.; Jennings, M.; Lane, S.; Middleton, V.; Roughan, J.V.; Wells, S.; et al. A guide to defining and implementing protocols for the welfare assessment of laboratory animals: Eleventh report of the BVAAWF/FRAME/RSPCA/UFAW Joint Working Group on Refinement. *Lab. Anim.* **2011**, *45*, 1–13.
57. Silva-Fernandes, A.; Duarte-Silva, S.; Neves-Carvalho, A.; Amorim, M.; Soares-Cunha, C.; Oliveira, P.; Thirstrup, K.; Teixeira-Castro, A.; Maciel, P. Chronic Treatment with 17-DMAG Improves Balance and Coordination in A New Mouse Model of Machado-Joseph Disease. *Neurotherapeutics* **2014**, *11*, 433–449.
58. Rosa, A.I.; Duarte-Silva, S.; Silva-Fernandes, A.; Nunes, M.J.; Carvalho, A.N.; Rodrigues, E.; Gama, M.J.; Rodrigues, C.M.P.; Maciel, P.; Castro-Caldas, M. Tauroursodeoxycholic Acid Improves Motor Symptoms in a Mouse Model of Parkinson's Disease. *Mol. Neurobiol.* **2018**, *55*, 9139–9155.
59. Rogers, D.C.; Fisher, E.M.C.; Brown, S.D.M.; Peters, J.; Hunter, A.J.; Martin, J.E. Behavioral and functional analysis of mouse phenotype: SHIRPA, a proposed protocol for comprehensive phenotype assessment. *Mamm. Genome* **1997**, *8*, 711–713.
60. Lundblad, M.; Andersson, M.; Winkler, C.; Kirik, D.; Wierup, N.; Cenci, M.A. Pharmacological validation of behavioural measures of akinesia and dyskinesia in a rat model of Parkinson's disease. *Eur. J. Neurosci.* **2002**, *15*, 120–132.
61. Grealish, S.; Mattsson, B.; Draxler, P.; Björklund, A. Characterisation of behavioural and neurodegenerative changes induced by intranigral 6-hydroxydopamine lesions in a mouse model of Parkinson's disease. *Eur. J. Neurosci.* **2010**, *31*, 2266–2278.
62. Mateus-Pinheiro, A.; Alves, N.D.; Patrício, P.; Machado-Santos, A.R.; Loureiro-Campos, E.; Silva, J.M.; Sardinha, V.M.; Reis, J.; Schorle, H.; Oliveira, J.F.; et al. AP2γ controls adult hippocampal neurogenesis and modulates cognitive, but not anxiety or depressive-like behavior. *Mol. Psychiatry* **2017**, *22*, 1725–1734.
63. Hagenbuch, N.; Feldon, J.; Yee, B.K. Use of the elevated plus-maze test with opaque or transparent walls in the detection of mouse strain differences and the anxiolytic effects of diazepam. *Behav. Pharmacol.* **2006**, *17*, 31–41.
64. Castagné, V.; Moser, P.; Roux, S.; Porsolt, R.D. Rodent Models of Depression: Forced Swim and Tail Suspension Behavioral Despair Tests in Rats and Mice. *Curr. Protoc. Neurosci.* **2011**, *55*.
65. Yalcin, I.; Belzung, C.; Surget, A. Mouse strain differences in the unpredictable chronic mild stress: A four-antidepressant survey. *Behav. Brain Res.* **2008**, *193*, 140–143.
66. Teixeira, F.G.; Carvalho, M.M.; Panchalingam, K.M.; Rodrigues, A.J.; Mendes-Pinheiro, B.; Anjo, S.; Manadas, B.; Behie, L.A.; Sousa, N.; Salgado, A.J. Impact of the Secretome of Human Mesenchymal Stem Cells on Brain Structure and Animal Behavior in a Rat Model of Parkinson's Disease. *Stem Cells Transl. Med.* **2017**, *6*, 634–646.
67. Young, K.; Morrison, H. Quantifying Microglia Morphology from Photomicrographs of Immunohistochemistry Prepared Tissue Using ImageJ. *J. Vis. Exp.* **2018**, 57648.

SUPPLEMENTARY MATERIAL

Unilateral intrastriatal 6-hydroxydopamine lesion in mice: a closer look into non-motor phenotype and glial response

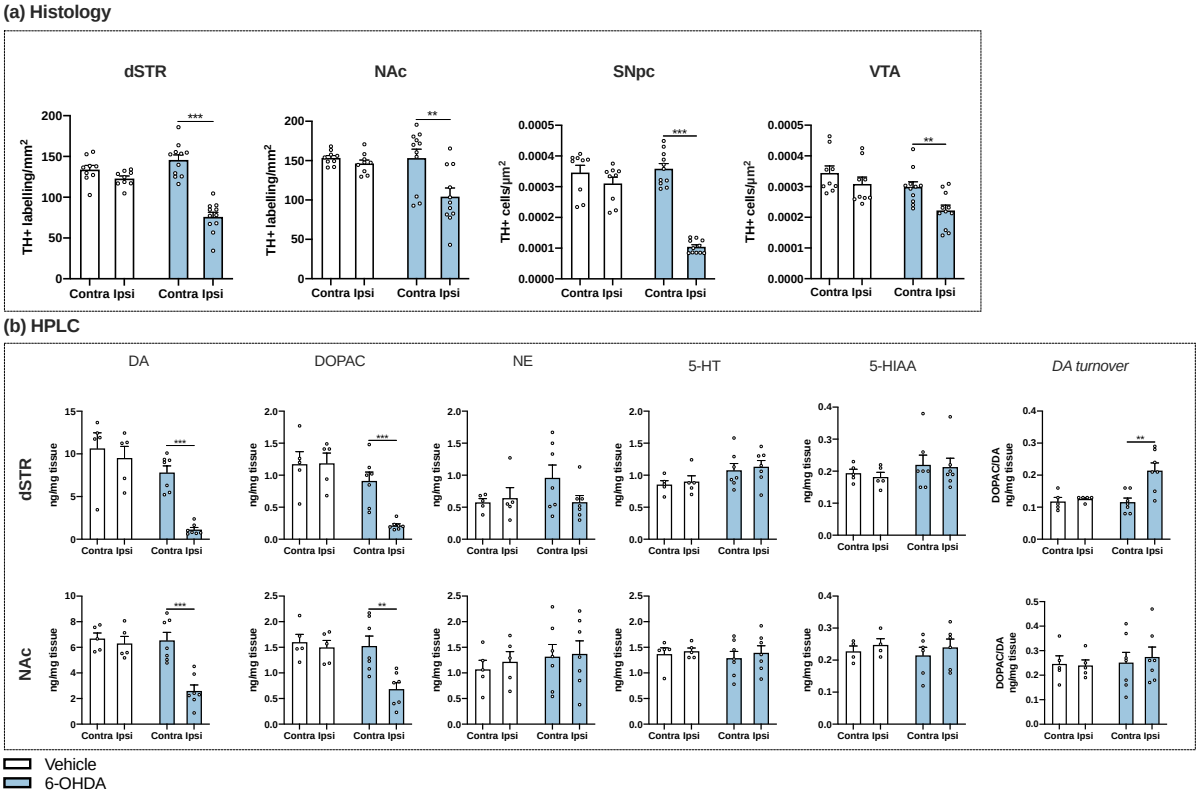
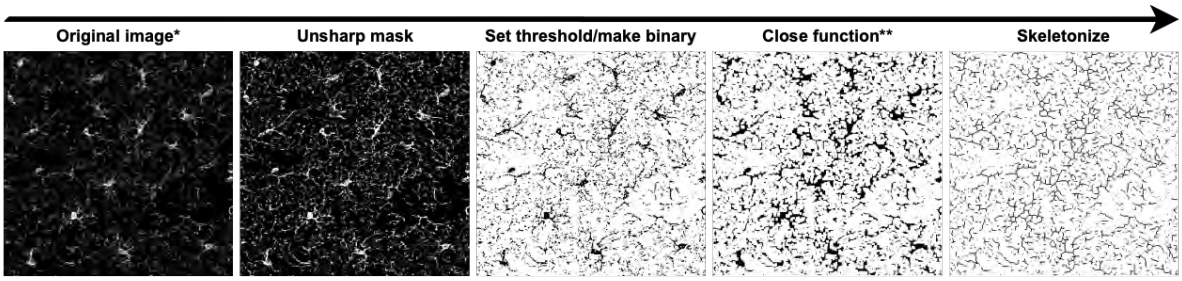


Figure S1. Raw data relative to main Figure 3. Histological characterization **(a)** of intrastriatal 6-OHDA lesions. TH+ labelling was measured in the dorsal striatum and NAc, and TH+ cell counts were performed in the SNpc and VTA. For all regions, significant differences were found between contra- and ipsilateral sides for the 6-OHDA group. Neurochemical analysis **(b)** using HPLC quantification combined with electrochemical detection, showing the dorsal striatum and NAc monoamine profile. Results showed a significant decrease of DA and its metabolite DOPAC for both regions, and an enhancement of DA turnover in the dorsal striatum, when comparing the contra- and ipsilateral sides of the 6-OHDA group. No differences were found for the other monoamines and its derivates (NE, 5-HT, and 5-HIAA) (Student's t test between contra and ipsilateral sides for each group; statistical summary in Table S2; data are presented as mean ± SEM). For histological analysis vehicle n = 9, 6-OHDA n = 11; for HPLC vehicle = 4-5, 6-OHDA n = 6-7. ** $p < 0.01$, *** $p < 0.001$. Abbreviations: dSTR, dorsal striatum; DA, Dopamine; DOPAC, 3,4-Dihydroxyphenylacetic acid; NAc, nucleus accumbens; NE, Norepinephrine; SNpc, substantia nigra pars compacta; TH, tyrosine hydroxylase; VTA, ventral tegmental area; 5-HIAA, 5-Hydroxyindoleacetic acid; 5-HT, serotonin; 6-OHDA, 6-hydroxydopamine.



*Representative section (supposed to be applied to the whole image)

**Joins pixels less than 2 pixels apart

Analyze skeleton function

# Branches	# Junctions	# End-point voxels	# Junction voxels	# Slab voxels	Average Branch Length	# Triple points	# Quadruple points	Maximum Branch Length
1	0	2	0	2	3.045	0	0	3.045
0	0	1	0	0	0.000	0	0	0.000
1	0	2	0	12	12.318	0	0	12.318
0	0	1	0	0	0.000	0	0	0.000
0	0	1	0	0	0.000	0	0	0.000
0	0	1	0	0	0.000	0	0	0.000
3	1	3	3	2	2.076	1	0	2.716
0	0	1	0	0	0.000	0	0	0.000
1	0	2	0	0	1.125	0	0	1.125
0	0	1	0	0	0.000	0	0	0.000
1	0	2	0	8	8.477	0	0	8.477
0	0	1	0	0	0.000	0	0	0.000
1	0	2	0	0	0.795	0	0	0.795
1	0	2	0	5	5.102	0	0	5.102
1	0	2	0	0	0.795	0	0	0.795
1	0	2	0	0	0.795	0	0	0.795
1	0	2	0	5	5.432	0	0	5.432
0	0	1	0	0	0.000	0	0	0.000
1	0	2	0	0	0.795	0	0	0.795
3	1	3	4	5	3.466	1	0	3.841
4	1	4	5	15	5.151	0	1	14.046
0	0	1	0	0	0.000	0	0	0.000
0	0	1	0	0	0.000	0	0	0.000
1	0	2	0	0	0.795	0	0	0.795
0	0	1	0	0	0.000	0	0	0.000

Figure S2. Microglia morphology quantification workflow. Photomicrographs (20x magnification) were analyzed using a semi-automated workflow on FIJI. Microglial branching was assessed with the skeletonize tool after the application of an unsharp mask and the close function. Average branch length ≤ 2 were removed from the analysis (considered as noise). Total branch length (Average branch length x Branches) was normalized by the number of microglial cells (IBA1+ cells) within each image.

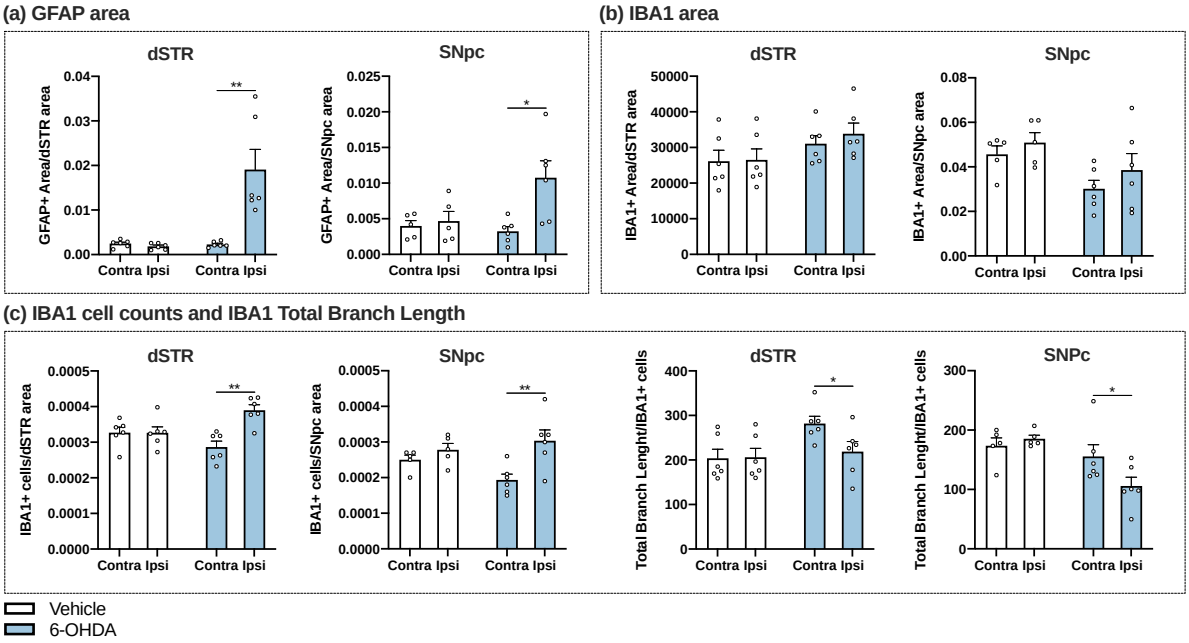


Figure S3. Raw data relative to main Figure 4 and Figure 5. Quantification of area coverage by GFAP+ staining **(a)** showed a significant astrocytic reaction between the contra- and ipsilateral sides for the 6-OHDA group. No differences were found between the contra- and ipsilateral sides of both groups after quantification of area coverage by IBA1+ staining in the dorsal striatum and SNpc **(b)**. A significant increase of IBA1+ cells, as wells as, a significant decrease of IBA1+ total branch length **(c)** in the ipsilateral areas of the 6-OHDA group was observed, indicating the presence of proliferative and activated microglia (Student's t-test; statistical summary in Table S2; data are presented as mean ± SEM). Vehicle n = 4-5, 6-OHDA n = 6-7 (4 slices/animal). * $p < 0.05$, ** $p < 0.01$. Abbreviations: dSTR, dorsal striatum; GFAP, glial fibrillary acidic protein; SNpc, substantia nigra pars compacta; 6-OHDA, 6-hydroxydopamine.

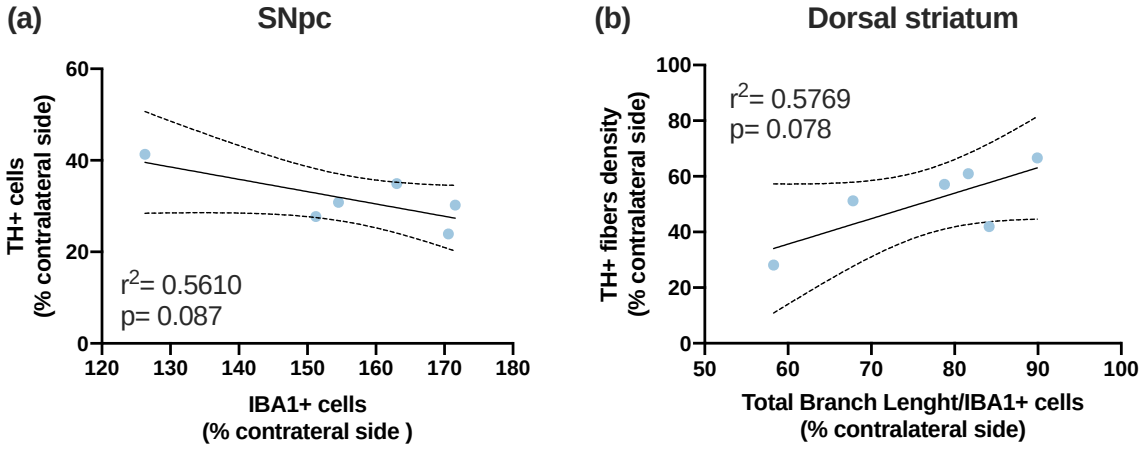


Figure S4. Correlation between dopaminergic loss and microglial cells. Scatter plots representing the correlation between TH+ cells and IBA1+ cells in SNpc **(a)** and TH+ fibers density with microglial branching (total branch length/IBA1+ cells) **(b)** for 6-OHDA-lesioned mice (Pearson correlation; statistical summary in Table S2). 6-OHDA n=6. Abbreviations: SNpc, substantia nigra pars compacta; TH, tyrosine hydroxylase; 6-OHDA, 6-hydroxydopamine.

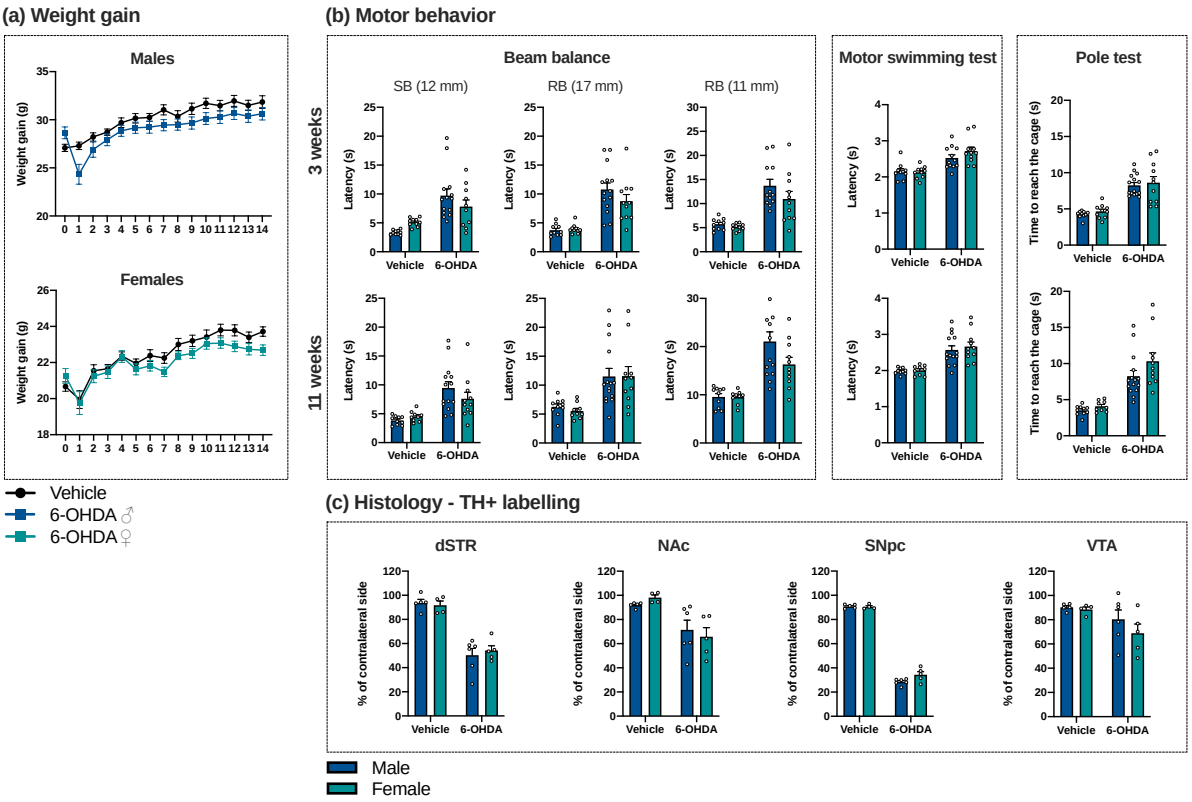


Figure S5. Impact of sex in behavioral and histological outcomes after 6-OHDA intrastriatal lesion. No differences were found in the weight gain for both males **(a)** and females **(b)** after 6-OHDA injections, when compared to the vehicle group, until de the end of the in vivo experiments (14 weeks) (Repeated measures ANOVA; statistical summary in Table S2; data are presented as mean ± SEM). No impact of sex or interaction between sex and group were significative in the motor behavior **(b)** and histological analysis **(c)** (Two-way ANOVA; statistical summary in Table S2; data are presented as mean ± SEM). The only source of variation was the group, i.e. the 6-OHDA lesion (these differences are not represented on the graphs, but are summarized in Table S2). For weight gain and motor behavior: $vehicle_{males} = 10$, $6\text{-}OHDA_{males} = 15$, $vehicle_{females} = 9\text{-}10$, $6\text{-}OHDAfe_{males} = 11$; for histological analysis $vehicle_{males} = 5$, $6\text{-}OHDA_{males} = 6$, $vehicle_{females} = 4$, $6\text{-}OHDAfe_{males} = 5$. Abbreviations: 6-OHDA, 6-hydroxydopamine.

Table S1. Statistical reports of all performed analysis in main Figures

Measure		Statistical report	
		3 weeks	**11 weeks**
Beam balance (Figure 1a) *Latency (s)*	Square beam (12 mm)	$t_{(42)}$=5.03, p<0.001, d=1.58	$t_{(42)}$=4.83, p<0.001, d=1.56
	Round beam (17 mm)	$t_{(43)}$=6.48, p<0.001, d=2.04	$t_{(42)}$=4.44, p<0.001, d=1.43
	Round beam (11 mm)	$t_{(41)}$=6.10, p<0.001, d=1.93	$t_{(42)}$=5.88, p<0.001, d=1.90
Motor swimming test (Figure 1b) *Latency (s)*		$t_{(41)}$=5.51, p<0.001, d=1.71	$t_{(42)}$=6.31, p<0.001, d=2.04
Pole test (Figure 1c) *Time to reach the cage (s)*		$t_{(43)}$=7.92, p<0.001, d=2.54	$t_{(43)}$=6.67, p<0.001, d=2.16
Cylinder test (Figure 1d) *Left paw contacts as % of total*		$t_{(17)}$=4.52, p<0.001, d=2.10	$t_{(15)}$=5.33, p<0.001, d=2.54
Open arena (Figure 1e)	Nr. of squares traveled	U=45, p<0.001	U=73.50, p<0.001
	Gait quality	U=120, p<0.001	U=171, p<0.05
Rotameter test (Figure 1f) *Net rotation*		U=0, p<0.001	
Open field (Figure 2a) *Time in center*		$t_{(43)}$=0.89, p=0.3785	
Elevated-plus maze (Figure 2b) *Time in opened arms*		$t_{(43)}$=1.44, p=0.156	
Forced swim test (Figure 2c) *Immobility time*		$t_{(39)}$=2.30, p<0.05, d=0.75	
Splash-sucrose test (Figure 2d) *Time grooming*		$t_{(41)}$=2.46, p<0.05, d=0.78	
TH+ labelling (Figure 3c/d)	**dSTR**	$t_{(18)}$=9.58, p<0.001, d=4.43	
	NAc	$t_{(18)}$=4.25, p<0.001, d=2.00	
TH+ labelling (Figure 3e/f)	**SNpc**	$t_{(18)}$=33.76, p<0.001, d=15.85	
	VTA	$t_{(18)}$=2.33, p<0.05, d=1.10	
Neurochemical analysis (Figure 3g/h)		**dSTR**	**NAc**
	DA	$t_{(10)}$=6.08, p<0.001, d=3.22	$t_{(10)}$=4.20, p<0.01, d=2.46
	DOPAC	$t_{(10)}$=7.76, p<0.001, d=4.21	$t_{(10)}$=3.25, p<0.01, d=2.00
	NE	$t_{(10)}$=1.63, p=0.135	$t_{(10)}$=0.48, p=0.635
	5-HT	$t_{(10)}$=0.07, p=0.946	$t_{(10)}$=0.19, p=0.856
	5-HIAA	$t_{(10)}$=0.48, p=0.644	$t_{(8)}$=0.53, p=0.609

DA turnover (Figure 3i) dSTR		$t_{(10)}$=2.40, p<0.05, d=1.51
GFAP+ Area (Figure 4c/d)	**dSTR**	$t_{(10)}$=3.36, p<0.01, d=1.94
	SNpc	$t_{(9)}$=3.07, p<0.05, d=1.95
IBA1+ area (Figure 5c/f)	**dSTR**	$t_{(10)}$=0.89, p=0.396
	SNpc	$t_{(9)}$=0.69, p=0.506
IBA1+ cells (Figure 5d/g)	**dSTR**	$t_{(10)}$=3.51, p<0.01, d=2.03
	SNpc	$t_{(9)}$=4.56, p<0.01, d=2.77
IBA1 branch length (Figure 5e/h)	**dSTR**	$t_{(10)}$=4.08, p<0.01, d=2.36
	SNpc	$t_{(9)}$=3.49, p<0.01, d=2.11

Table S2. Statistical reports of all performed analysis in supplementary Figures

Measure		**Statistical report**	
Correlation (Figure S2a) *DA neurons with IBA1+ cells*		r2=0.561, p=0.087	
Correlation (Figure S2b) *DA fibers with Branch Length*		r2=0.577, p=0.078	
Weight gain (Figure S3a)	Males	Time: $F_{(3.7, 86.1)}$=36.41, p<0.001; Group: $F_{(1, 23)}$=2.13, p=0.158 Time x Group: $F_{(14, 322)}$=2.98, p<0.001	
	Females	Time: $F_{(2.7, 48.7)}$=37.52, p<0.001; Group: $F_{(1, 18)}$=1.85, p=0.191 Time x Group: $F_{(14, 252)}$=1.339, p=0.185	
Time Point (Figure S5b)		**3 weeks**	**11 weeks**
Beam balance *Latency (s)*	Square beam (12 mm)	Group: $F_{(1, 40)}$=24.47, p<0.001 Sex: $F_{(1, 40)}$=0.004, p=0.952 Group x Sex: $F_{(1,40)}$=4.07, p=0.051	Group: $F_{(1, 40)}$=22.11, p<0.001 Sex: $F_{(1, 40)}$=0.42, p=0.521 Group x Sex: $F_{(1,40)}$=1.93, p=0.521
	Round beam (17 mm)	Group: $F_{(1, 41)}$=40.68, p<0.001 Sex: $F_{(1, 41)}$=0.96, p=0.333 Group x Sex: $F_{(1,41)}$=1.44, p=0.237	Group: $F_{(1, 41)}$=18.81, p<0.001 Sex: $F_{(1, 41)}$=0.07, p=0.788 Group x Sex: $F_{(1,41)}$=0.09, p=0.772
	Round beam (11 mm)	Group: $F_{(1, 39)}$=37.68, p<0.001 Sex: $F_{(1, 39)}$=2.16, p= 0.150 Group x Sex: $F_{(1,39)}$=0.92, p=0.343	Group: $F_{(1, 40)}$=34.83, p<0.001 Sex: $F_{(1, 40)}$=2.41, p=0.128 Group x Sex: $F_{(1,40)}$=2.28, p=0.139
Motor swimming test *Latency (s)*		Group: $F_{(1, 39)}$=31.49, p<0.001 Sex: $F_{(1, 39)}$=0.94, p=0.340 Group x Sex: $F_{(1,39)}$=1.65, p=0.210	Group: $F_{(1, 40)}$=38.71, p<0.001 Sex: $F_{(1, 40)}$=0.32, p=0.574 Group x Sex: $F_{(1,40)}$=0.12, p=0.734
Pole test		Group: $F_{(1, 42)}$=62.07, p<0.001	Group: $F_{(1, 41)}$=48.77, p<0.001

Time to reach the cage (s)			Sex: $F_{(1, 42)}$=0.57, p=0.456 Group x Sex: $F_{(1,42)}$=0.002, p=0.968	Sex: $F_{(1, 41)}$=2.82, p=0.100 Group x Sex: $F_{(1,41)}$=0.90, p=348
TH+ labelling (Figure S3c)			**dSTR**	Group: $F_{(1, 16)}$=82.04, p<0.001 Sex: $F_{(1, 16)}$=0.04, p=0.847 Group x Sex: $F_{(1,16)}$=0.44, p=0.517
			NAc	Group: $F_{(1, 16)}$=17.54, p<0.001 Sex: $F_{(1, 16)}$=0001, p=0.973 Group x Sex: $F_{(1,16)}$=0.90, p=0.358
TH+ labelling (Figure S3c)			**SNpc**	Group: $F_{(1, 16)}$=1504, p<0.001 Sex: $F_{(1, 16)}$=3.18, p=0.093 Group x Sex: $F_{(1,16)}$=4.25, p=0.060
			VTA	Group: $F_{(1, 16)}$=5.66 p<0.05 Sex: $F_{(1, 16)}$=1.17, p=0.296 Group x Sex: $F_{(1,16)}$=0.60, p=0.448
TH+ labelling (Figure S3a)		**dSTR**	**Vehicle**	$t_{(16)}$=1.77, p=0.0954
			6-OHDA	$t_{(20)}$=8.28, p<0.001
		NAc	**Vehicle**	$t_{(16)}$=1.32, p=0.204
			6-OHDA	$t_{(20)}$=3.12, p<0.01
TH+ cells (Figure S3a)		**SNpc**	**Vehicle**	$t_{(16)}$=1.15, p=0.268
			6-OHDA	$t_{(20)}$=14.39, p<0.001
		VTA	**Vehicle**	$t_{(16)}$=1.12, p=0.279
			6-OHDA	$t_{(20)}$=3.17, p<0.01
Neurochemical analysis (Figure S4b)			**dSTR**	**NAc**
	DA	**Vehicle**	$t_{(8)}$=0.50, p=0.633	$t_{(8)}$=0.54, p=0.601
		6-OHDA	$t_{(12)}$=8.19, p<0.001	$t_{(12)}$=5.11, p<0.001
	DOPAC	**Vehicle**	$t_{(8)}$=0.06, p=0.957	$t_{(8)}$=0.50, p=0.631
		6-OHDA	$t_{(12)}$=4.90, p<0.001	$t_{(12)}$=3.66, p<0.01
	NE	**Vehicle**	$t_{(8)}$=0.38, p=0.715	$t_{(8)}$=0.56, p=0.594
		6-OHDA	$t_{(12)}$=1.68, p=0.119	$t_{(12)}$=0.16, p=0.875
	5-HT	**Vehicle**	$t_{(8)}$=0.42, p=0.685	$t_{(8)}$=0.41, p=0.694
		6-OHDA	$t_{(12)}$=0.39, p=0.704	$t_{(12)}$=0.55, p=0.591
	5-HIAA	**Vehicle**	$t_{(8)}$=0.63, p=0.545	$t_{(6)}$=0.80, p=0.461
		6-OHDA	$t_{(12)}$=0.18, p=0.864	$t_{(12)}$=0.69, p=0.506
	DOPAC/DA	**Vehicle**	$t_{(8)}$=0.61, p=0.557	$t_{(8)}$=0.15, p=0.884
		6-OHDA	$t_{(12)}$=3.66, p<0.01	$t_{(12)}$=0.39, p=0.701
Glial reaction analysis			**dSTR**	**SNpc**

(Figure S5)	**GFAP+ area**	**Vehicle**	$t_{(10)}$=1.41, p=0.189	$t_{(8)}$=0.45, p=0.663
		6-OHDA	$t_{(10)}$=3.71, p<0.01	$t_{(10)}$=3.06, p<0.05
	IBA1+ area	**Vehicle**	$t_{(10)}$=0.09, p=0.933	$t_{(8)}$=0.89, p=0.397
		6-OHDA	$t_{(10)}$=0.75, p=0.469	$t_{(10)}$=1.01, p=0.339
	IBA1+ cells	**Vehicle**	$t_{(10)}$=0.02, p=0.983	$t_{(8)}$=1.26, p=0.243
		6-OHDA	$t_{(10)}$=4.58, p<0.01	$t_{(10)}$=3.17, p<0.01
	IBA1 Total Branch Length	**Vehicle**	$t_{(10)}$=0.08, p=0.936	$t_{(8)}$=0.81, p=0.444
		6-OHDA	$t_{(10)}$=2.26, p<0.05	$t_{(10)}$=2.03, p<0.05

Table S3. Perioperative health assessment and procedures after 6-OHDA injection in mice. Adapted from [1]

Type	Identification	Treatment
General health	Animal's behavior into the home cage: interaction with the environment, cage mates and nest building	-
Dehydration	Reduced skin turgor; recessed eyes and fuzzy fur	Fluid replacement through subcutaneous or intraperitoneal administration of sterile saline (0.9%)
Hypothermia	Body temperature below 36.5°C; animals are cool to the touch	Increase housing room temperature; administration of warm fluids (e.g., warm sterile saline injections)
Aphagia and adipsia	Measurement of food and water consumption; Body weight monitoring	Easy access to palatable food supplementation; hydration complemented with glucose solution
Penile prolapse	Swollen and distended penis	Lubrification; soft bed; local analgesia
Spontaneous turning behavior	Animals spontaneously rotate to the ipsilateral side (unilateral lesion)	Animals adapt to rotational movement

Table S4. Confocal microscopy for glial reaction: acquisition parameters

Region	Antigen	PMT Voltage (V)	Laser Transmissivity (%)	Emission Wavelength (nm)	Detection Wavelength (nm)	Detector Gain	Detector Offset (%)
SNpc Mosaics	DAPI	410	1.01	461	430-470	1.25	8.0
	TH	430	1.80	520	500-540	1.0	10.0
	GFAP	600	6.49	618	570-620	1.0	11.0
	IBA-1	570	4.88	671	650-750	1.0	10.0
Striatum Images	DAPI	410	1.30	461	430-470	1.0	12.0
	TH	460	2.0	520	500-540	1.0	12.0
	GFAP	650	7.0	618	570-620	1.0	14.0
	IBA-1	595	5.0	671	650-750	1.0	13.0

References

1. Masini, D.; Plewnia, C.; Bertho, M.; Scalbert, N.; Caggiano, V.; Fisone, G. A Guide to the Generation of a 6-Hydroxydopamine Mouse Model of Parkinson's Disease for the Study of Non-Motor Symptoms. *Biomedicines* **2021**, *9*, 598, doi:10.3390/biomedicines9060598.

CHAPTER 5

Multiple systemic administration of mesenchymal stem cell secretome showed a higher therapeutical magnitude effect *versus* intracerebral injections in a mouse model of Parkinson's disease

Bárbara Mendes-Pinheiro[1,2], Ana Marote[1,2], Carina Soares-Cunha[1,2], Jorge Cibrão Ribeiro[1,2], Sandra Barata-Antunes[1,2], Jonas Campos[1,2], Sofia C. Serra[1,2], Eduardo Loureiro-Campos[1,2], Sandra I. Anjo[3], Bruno Manadas[3], Sara Duarte-Silva[1,2], Luísa Pinto[1,2], António J. Salgado[1,2#]. (2022). Multiple systemic administration of mesenchymal stem cell secretome showed a higher therapeutical magnitude effect *versus* intracerebral injections in a mouse model of Parkinson's disease.

(manuscript in preparation)

[1]Life and Health Sciences Research Institute (ICVS), School of Medicine, University of Minho, Campus de Gualtar, 4710-057 Braga, Portugal;

[2]ICVS/3B's - PT Government Associate Laboratory, 4805-017 Guimarães, Portugal;

[3]CNC-Center for Neuroscience and Cell Biology, University of Coimbra, 3004-504 Coimbra, Portugal.

#Correspondance: António J. Salgado asalgado@med.uminho.pt

CHAPTER 5 | Multiple systemic administration of mesenchymal stem cell secretome showed a higher therapeutical magnitude effect *versus* intracerebral injections in a mouse model of Parkinson's disease

Abstract

Parkinson's disease (PD) is characterized by severe motor symptoms. Currently, there is no treatment that retards disease progression or reverses damage prior to the time of clinical diagnosis. In the last years, the secretome of mesenchymal stem cells (MSCs) has been suggested as a therapeutical alternative for PD. Relevant data from our group already demonstrated that intracerebral injections of MSC secretome have a beneficial impact on motor improvements and the rescue of dopaminergic loss using a severe 6-hydroxydopamine (6-OHDA) PD animal model. However, the injections of secretome directly into the brain is an invasive method with associated disadvantages from the clinical point of view. In the present study, we compared the efficacy of intracerebral injections (single administration) with repeated systemic administration of bone marrow-derived MSCs (BM-MSCs) secretome in alleviating the phenotype of a 6-OHDA intrastriatal PD mouse model. Overall, the BM-MSC secretome administered from both routes promotes sustained motor behavior alleviation and dopaminergic loss protection, however, multiple systemic administrations showed a higher magnitude therapeutical effect. This study is clinically relevant and makes important contributions to the design of new cell-free clinical approaches for PD based on secretome administration.

1. Introduction

Parkinson's disease (PD) is recognized as a multi-systemic neurodegenerative disorder with motor and non-motor features resulting from a severely perturbed neurotransmitter system. Neuronal loss in the substantia nigra *pars compacta* (SNpc), which causes striatal dopamine (DA) deficiency, and intracellular inclusions containing aggregates of α-synuclein are the neuropathological hallmarks of PD (Bloem et al., 2021; Poewe et al., 2017). Multiple other cell types of the central and peripheral autonomic nervous system are also affected, most likely from the beginning of the disease (Poewe et al., 2017). Motor dysfunctions largely depend on denervation of the nigrostriatal pathway. Therefore, the treatment of PD is anchored on DA pharmacological substitution, in addition to non-dopaminergic approaches to address both motor and non-motor symptoms, as well as deep brain stimulation for those developing levodopa-related motor complications (Zahoor et al., 2018). Although clinical improvements can be achieved, most of the current approaches lead to the development of unsmiling side effects and are only efficient in a subset of affected individuals for a restricted time window (Stoker and Barker, 2020). Moreover, none of them can ameliorate the neuropathological processes leading to progressive cell death.

One of the major challenges in the PD research field is the discovery of disease-modifying therapies that can slow or reverse PD-associated neurodegeneration (Dawson and Dawson, 2019). In line with this, mesenchymal stem cell (MSC)-based approaches have been suggested as promising therapeutical alternatives for neurogenerative disorders due to their inherent characteristics (Han et al., 2019). MSCs are a heterogeneous group of multipotent cells, that are easy to isolate from numerous adult tissues, grow to clinical grades without major ethical issues, are considered non-tumorigenic, and have low immunogenicity (Vizoso et al., 2017). The beneficial effects of MSCs were primarily attributed to their ability to engraft and differentiate into multiple tissue types including dopaminergic neurons. However, recent evidence has revealed that implanted cells do not survive for long periods and that the benefits of MSC therapy are associated with their paracrine activity (Merimi et al., 2021; Vizoso et al., 2017). Indeed, different studies have demonstrated that secretome-derived products from MSCs (e.g., growth factors, cytokines, extracellular vesicles, etc), have neuroregulatory actions on key pathological processes that are associated with basic homeostatic functions, such as cell differentiation and proliferation, angiogenesis and vasculogenesis, inflammation, and oxidative stress (Vizoso et al., 2019). For the past decade, our lab has shown that the intracerebral injections of full bone marrow derived-MSCs (BM-MSCs) secretome was able to protect dopaminergic neurons in lesioned areas and induce

partial motor function recovery in a complete lesion of a 6-hyrdoxydopamine (6-OHDA) rat model of PD (Mendes-Pinheiro et al., 2019; Teixeira et al., 2017; Teixeira et al., 2020). Despite these promising outcomes, brain local infusion approaches are invasive and have disadvantages such as high cost, risk of infection, and a limited delivery brain area (Garcia-Garcia et al., 2005). On the other hand, the use of noninvasive systems for MSC secretome delivery, such as systemic administration, could avoid these problems and may be easily implemented in the clinics, contrary to craniotomy procedures.

In the present study, we compared the efficacy of intracerebral injections (single administration) with multiple systemic administrations of BM-MSC secretome using a unilateral intrastriatal 6-OHDA PD mouse model. Results showed that BM-MSC secretome induced a positive effect in general motor coordination paradigms, as well as the rescue of dopaminergic loss in both approaches, being the effects of systemic administration of higher magnitude. Finally, we characterize the secretome using both non-targeted and targeted proteomic analysis and highlighted possible proteins and mechanisms that could mediate the above-referred actions.

2. Materials and methods

2.1. Human bone marrow-derived MSC culture

Human BM-MSCs (Lonza, Switzerland) were thawed and seeded into T75 cm^2 tissue culture flasks and expanded in Minimum Essential Medium α (α-MEM; ThermoFisher Scientifc, USA) supplemented with 5% human platelet lysate (HPL), 1% Pen-Strep (Gibco, USA), and 1.8 mM heparin (B.Braun, Germany). The medium was renewed every 3 days and upon confluence, cells were dissociated using 0.05% trypsin-EDTA solution (ThermoFisher Scientific). The BM-MSCs used in this work were phenotypically characterized by our laboratory, being positive for the standard MSC markers CD73, CD90, and CD105, and negative for CD45 and HLA-DR. The functional characterization was also evaluated by chondrogenic, osteogenic, and adipogenic differentiation (unpublished data).

2.3. Secretome collection and concentration

The secretome of BM-MSCs was collected under the form of conditioned medium in passage 8 (P8) according to protocols already established in our laboratory, for both intracerebral (IC) and intravenous (IV) injections (Fraga et al., 2013; Teixeira et al., 2016). Briefly, cells were seeded at a density of 5000 cells/cm^2 for the *in vivo* experiments and 12000 cells/cm^2 for proteomic analysis and expanded for 72 h in α-MEM-5% HPL. On the conditioning day, cells were washed with phosphate-buffered saline (PBS)

without Ca^{2+}/Mg^{2+} (Invitrogen, USA) and incubated with Neurobasal A medium (ThermoFisher Scientific) supplemented with 1% kanamycin (Life Technologies, USA). After 24 h, the media containing the factors secreted by BM-MSCs was collected and centrifuged at 1200 rpm for 10 min at 4°C to remove any cell debris. The BM-MSC secretome was 100× concentrated by centrifugation using a 5 kDa cut-off concentrator (Vivaspin, GE Healthcare, UK) and frozen at −80°C until used. Then, total protein quantification of BM-MSC secretome was performed by Bradford assay (based on microassay protocol – Bio-Rad, USA).

2.3. Animals

Ten-weeks old male and female C57/BL6J, weighing 18–28 g at the biggening of the experiment were used according to local regulations on animal care and experimentation (European Union Directive 2010/63/EU), and with consent from the Portuguese national authority for animal research, Direção Geral de Alimentação e Veterinária (ID: DGAV 005,454 23/04/2025, Lisbon, Portugal) and Ethical Subcommittee in Life and Health Sciences (SECVS; ID: SECVS-142/2016, University of Minho, Braga, Portugal). Animals were housed in groups of 5-6 animals, in a temperature and humidity-controlled room, maintained on 12:12 h dark/light cycles, with access to food and water *ad libitum*.

2.4. Lesion surgery and post-operative care

Mice were anesthetized by intraperitoneal injection of ketamine (75 mg/kg) plus medetomidine (1 mg/kg) diluted in 0.9% NaCl, and placed on a stereotaxic apparatus (Stoelting, USA). The lesioned group (n=75) was injected unilaterally with 6 μg/μL of 6-OHDA hydrochloride (H4381, calculated from freebase weight; Sigma, USA; dissolved in of 0.9% NaCl in 0.2 mg/mL ascorbic acid) into the dorsolateral striatum (2 × 1.5 μL) at a rate of 300 nl/min, at the following coordinates (relative to bregma, in mm): (i) AP = +1.0, ML = 2.1, DV = −2.9; (ii) AP = +0.3, ML = −2.3, DV = −2.9. After each injection, the needle was left in place there for 5 min for diffusion and to avoid any backflow. The sham group (n=15) was injected in the same conditions with the neurotoxin vehicle. Anesthesia was reversed using atipamezole (1 mg/mL).

The animals were monitored twice a day for 14 days after surgery, and mice that reached the human endpoints (Hawkins et al., 2011) were euthanized. During the recovery, animals were housed in a warmed room and post-operative care included the administration of nutrients and fluids in addition to post-operative analgesia, as described in detail in Chapter 3.

2.5. Behavioral assessment, secretome treatments and experimental design

Three weeks after 6-OHDA injections, animals were submitted to a first behavioral analysis to assess the motor deficits extent using the beam balance walk test (round beam 11 mm), the motor swimming test, the pole test, some tests of the SHIRPA protocol (open arena: horizontal spontaneous activity and gait quality evaluation; hindlimb tonus; supplementary Figure S2), and the rotameter test using apomorphine. All behavioral tests were performed as previously described in detail in chapter 3. Bodyweight was also registered every week until the end of the experiments (supplementary Figure S1).

After 2 weeks, 6-OHDA-lesioned animals were then randomly divided as follows: 6-OHDA [IC Vehicle] – intracerebral (IC) injections of Neurobasal A medium; 6-OHDA [IC Secretome] – IC injections of BM-MSC CM; 6-OHDA [IV Vehicle] – intravenous (IV) injections of Neurobasal A medium; 6-OHDA [IV Secretome] - IV injections of BM-MSC CM. Regarding IC injections, animals received 2 × 1.5 μL of BM-MSC secretome and the respective vehicle in the dorsal striatum (same coordinates used in lesion surgeries) and 1 μl in SNpc (coordinates related to bregma, in mm: AP = -3.0, ML = 1.2, DV = −4.5). After surgery, all animals were treated with the analgesic buprenorphine at 0.05 mg/kg (Bupaq; Richter Pharma, Austria). The other two groups received IV injections (3 injections in the same week of IC surgeries, and then once a week for 7 weeks) of 100 μL (total amount of protein/IV injection: 31.8 μg) in the tail vein. Motor behavioral analysis was performed 1, 4, and 7 weeks after treatments, and mice were posteriorly sacrificed to proceed with brain tissue analysis (Figure 1).

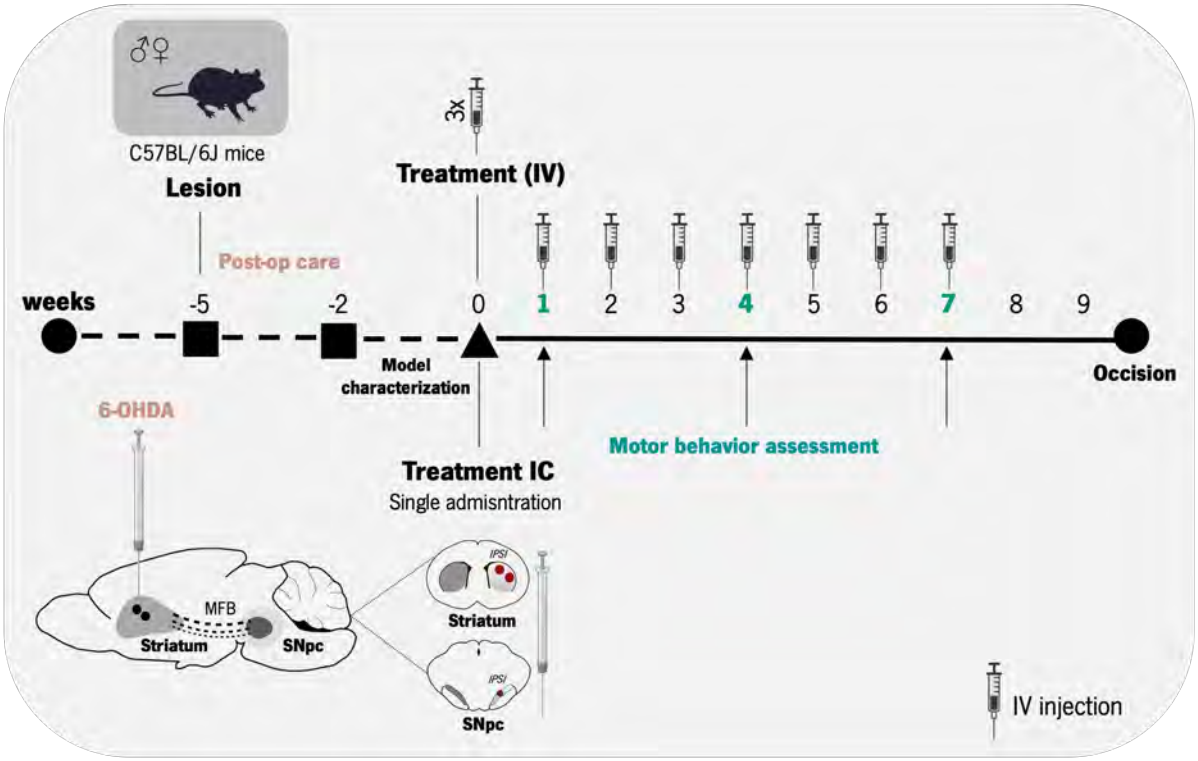


Figure 1. Experimental design. Schematic representation and temporal sequence of performed tasks throughout the in vivo experiment. Animals were injected with 6-OHDA into the dorsolateral striatum (2 injections); Mice were daily monitored during 14 days (post-operative care); 3 weeks after lesion, animals were characterized at motor level to validate the model; At week 5 post-lesion, animals were treated with BM-MSCs secretome using two different routes of administration: IC injections into the striatum and SNpc (2 injections into the striatum, and 1 injection into the SNpc - single administration) and repeated IV injections (3 injections in the first week, and 1 injection per week until the end of the experiment – 10 injections in total). Motor behavioral assessment was performed 1, 4, and 7 weeks after treatments. Animals were sacrificed 12 weeks after lesion surgery and 9 after treatments.

2.6. Histological assessment

To further evaluate the degree of dopaminergic preservation, immunohistochemical staining for tyrosine hydroxylase (TH) was performed. For that, at the end of behavioral analysis, animals were deeply anesthetized with a mixture of ketamine (150 mg/kg) plus medetomidine (0.3 mg/Kg), and a cohort of animals of each group was transcardially perfused with 0.9% saline followed by 4% paraformaldehyde. Brains were collected and transferred to a tube containing 4% PFA in PBS. After 48h of incubation at room temperature (RT), brains were kept in 30% sucrose in PBS containing 0.01% of sodium azide. Afterward, brains were sectioned coronally on a vibratome (VT1000S, Leica, Germany), and four series of coronal sections of striatum and SNpc at a thickness of 40 µm were selected for free-floating

immunohistochemistry. Tyrosine-Hydroxylase (TH) detection was performed using the protocol described previously (Mendes-Pinheiro et al., 2019).

Then, TH+ labelling of dopaminergic fibers was performed in the dorsal striatum (6 slices/animal) and SNpc (4 slices/animal). Digital slides of the striatum were obtained using brightfield illumination (SZX16, Olympus, Japan) and the mean grey value was measured using the ImageJ software (v1.48, National Institute of Health, Stapleton, NY, USA) as previsouly described in detail (Teixeira et al., 2017). Regarding SNpc, TH+ cells were visualized and counted using a brightfield microscope (BX51, Olympus). The boundaries of the SNpc area were drawn, and total TH+ cells were counted in both hemispheres. Data are presented as the percentage (%) of the contralateral side (intact side).

2.7. Untargeted mass spectrometry proteomic analysis

In order to characterize the secretome of BM-MSCs, we performed a non-targeted proteomic analysis based on a combined mass spectrometry (MS) approach as previously described in detail (Mendes-Pinheiro et al., 2018). Only proteins with at least two confidently identified peptides were considered as positive identifications. Peptide's confidence was assessed by a False Discovery Analysis (FDR) and a minimum of 99% confidence (<1% FDR) was used to select the peptides. Three biological replicates of secretome were processed, and proteins that were just identified in a single biological replicate were not considered for analysis.

The final list of proteins (supplementary Table S2) was used for protein-protein interaction network analysis constructed using the online STRING database (https://string-db.org) version 11.5, with a medium confidence level (0.4). Levels 4 and 5 gene ontology analysis was performed through an over-representation analysis using the ConsensusPathDB (Kamburov et al., 2013) for cellular component. Protein complex-based gene sets were determined using the same software, assuming a minimum complex size of 2, minimum overlap with an input list of 2, and *p*-value cutoff of 1%. The most represented protein complexes are shown, based on the *p*-value for the association.

2.9. Protein profile array

To complement the non-targeted proteomic analysis referred to above, some soluble factors present in BM-MSC secretome were identified using a membrane-based antibody array (Human Neuro Discovery Array C1, AAH-NEU-1-2, RayBiotech, USA), following the manufacturer's instructions. For that, after 30 min of blocking, the membrane array was incubated overnight at 4°C with the non-concentrated

conditioned medium containing all the factors secreted by BM-MSCs. On the next day, the binding of secreted factors to the antibodies present in the membrane was detected by incubation with Biotinylated Detection Antibody Cocktail, followed by incubation with Streptavidin Conjugated HRP. Chemiluminescence detection was performed using Sapphire Biomolecular Imager and spot intensity was measured using AzureSpot software (Azure Biosystems, USA).

2.9. Statistical analysis

A confidence interval of 95% was assumed for all statistical tests. The assumption of normality was tested for all continuous variables through evaluation of the frequency distribution histogram, the values of skewness and kurtosis, and through the Shapiro-Wilk test. The assumption of homoscedasticity was tested through Levene's test. Both assumptions were met by all tested continuous variables. All continuous data are shown as the mean as mean ± SEM. For the comparison of means between two groups (rotameter test; discrete data), a Mann-Whitney U test was carried out. For the evaluation of mean differences in samples with one independent and one repeated measures variable, a mixed design ANOVA was carried out, with Tukey's or Dunn's *post-hoc* test for pairwise comparison of the independent variable. Statistical analysis and graphic representation were using the GraphPad Prism ver.8.0c (GraphPad Software; La Jolla, USA). Statistical summary of all conducted analysis is presented in supplementary Table S1.

3. Results

3.1. Effects of BM-MSC secretome on the 6-OHDA intrastriatal PD mouse model

In this work, we addressed the effects of BM-MSC secretome using two different approaches: IC injections into the lesioned areas (i.e., striatum and SNpc) and multiple IV injections administration. To establish an *in vivo* PD model, a total of 18 μg of 6-OHDA were injected at the right dorsolateral striatum, which selectively destroys dopaminergic neurons in the nigrostriatal pathway. In this way, we were able to mimic the dopaminergic degeneration observed in PD on one side, while the other was used as a control of the lesion.

Motor behavior

Three weeks after lesion surgeries, animals were subjected to behavioral characterization at the motor level, including the motor swimming and the pole tests to evaluate motor coordination and strength,

and the beam balance walk test to assess balance and fine motor coordination. The rotameter test was used to evaluate the imbalance in DA release between the denervated and the non-denervated striatum. All animals injected with 6-OHDA presented turning behavior after apomorphine administration, as revealed by the increased number of contralateral rotations of 6-OHDA-injected animals (Figure 2A), thereby confirming the success of the lesions on the ipsilateral side. Moreover, as observed in the first time point of graphs B, C, and D of Figure 2, 6-OHDA lesion caused a significant aggravation of the motor coordination and loss of balance, as measured by the motor swimming, beam balance walk, and pole tests paradigms. After performing the PD model characterization, 6-OHDA-lesioned animals were divided into four treatment groups: two groups received IC injections of Neurobasal A medium (IC Vehicle) or BM-MSC secretome (IC Secretome) in both dorsal striatum and SNpc, and the other two groups received multiple IV injections of Neurobasal A medium (IV Vehicle) or BM-MSC secretome (IV Secretome) as represented in Figure 1. Motor behavioral assessment was performed 1, 4, and 7 weeks after treatments. Results showed that IV Secretome-treated animals present a significantly better performance in the general motor performance paradigms (Figure 2B, C, D) in comparison with non-treated animals (IV Vehicle). Regarding the motor swimming test, this improvement was already visible 1 week after treatment administration and sustained until 7 weeks after treatment (Figure 2B). Although not reaching statistical significance, the treatment with secretome via IC injections also improved the motor phenotype (mostly in the motor swimming and pole tests) of 6-OHDA mice, as it is possible to observe by its large effect size (see supplementary Table S1). Of note, the route of secretome administration proved to be very important for motor function recovery, as the IV injections showed a relevant improvement on motor behavior, as well as a higher effect size over the IC secretome administration. The results of the statistical analyses are presented in supplementary Table S1.

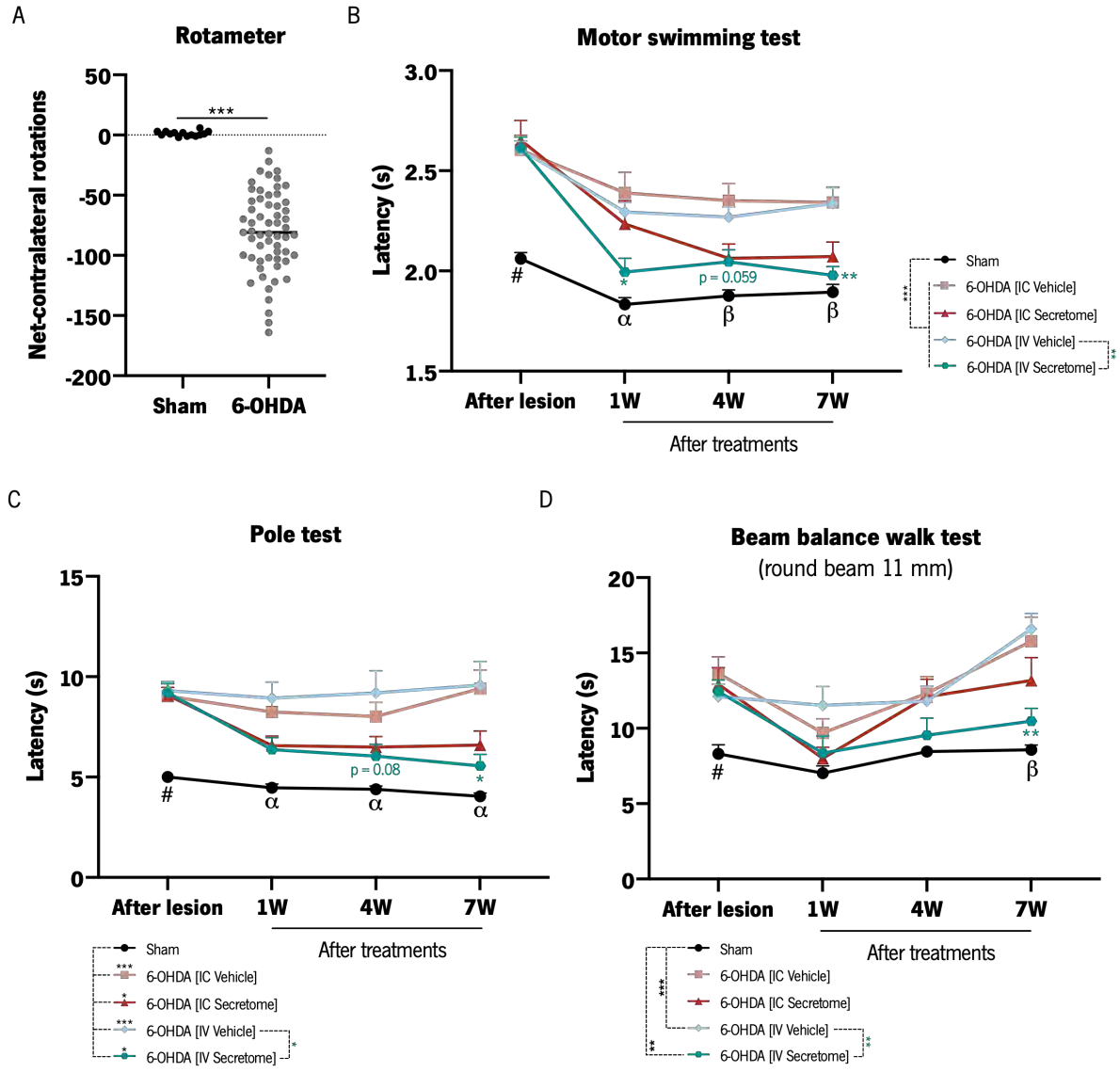


Figure 2. Motor behavior analysis of 6-OHDA-lesioned animals after administration of BM-MSC secretome. **A)** Rotameter test (apomorphine-induced rotations) as a measure of dopaminergic depletion induced by 6-OHDA lesion and compared to Sham animals; Motor performance of mice was evaluated using **B)** motor swimming test, **C)** pole test, and **D)** beam balance walk test to assess the effects of the treatments. n = 13-15 for each group used. Statistical summary in Table S1. Data are presented as mean ± SEM. *p < 0.05, **p < 0.01, ***p < 0.001; #: Sham group statistically different from all groups; α: Sham group statistically different form all groups except from IV Secretome; β: Sham group statistically different form all groups except from IC Secretome and IV Secretome.

Histological analysis

To further analyze the effects of the 6-OHDA injections and the different treatments on the dopaminergic neuronal structure, histological analyses for TH were performed in both lesioned areas – dorsal striatum and SNpc (Figure 3A, C). The 6-OHDA injections caused a significant reduction of TH+

labelling in the dorsal striatum on the side of the lesion when compared to the Sham group (Figure 3B; raw data for Sham group of TH+ labelling/mm^2 – Contralateral side: 154.69 ± 17.01; Ipsilateral side: 141.52 ± 18.27). The same result was also observed after TH+ cell counts in the SNpc (Figure 3D; raw data for Sham group of TH+ cells/mm^2 – Contralateral side: 4.47 ± 0.58; Ipsilateral side: 4.18 ± 0.77).

Both treatments with BM-MSC secretome (i.e., IC and IV injections) were able to significantly minimize the loss of dopaminergic fibers in the dorsal striatum (Figure 3B), which was not verified in the respective lesioned vehicle groups. Nonetheless, the IC Secretome was significantly better in this outcome when compared to the IV Secretome group. On the other hand, in the SNpc, results revealed that IC injection of BM-MSC secretome was able to significantly reduce dopaminergic cell loss in comparison to the non-treated group (Figure 3D). Nonetheless, although no statistical significance was reached between IV Secretome and the respective IV Vehicle, a large effect size was verified, suggesting an effect of this treatment approach in the neuroprotection of dopaminergic neurons in the SNpc. Histological analyses in the lesioned hemisphere were compared and presented as a percentage of the contralateral side, and the results of the statistical analyses are presented in Table S1.

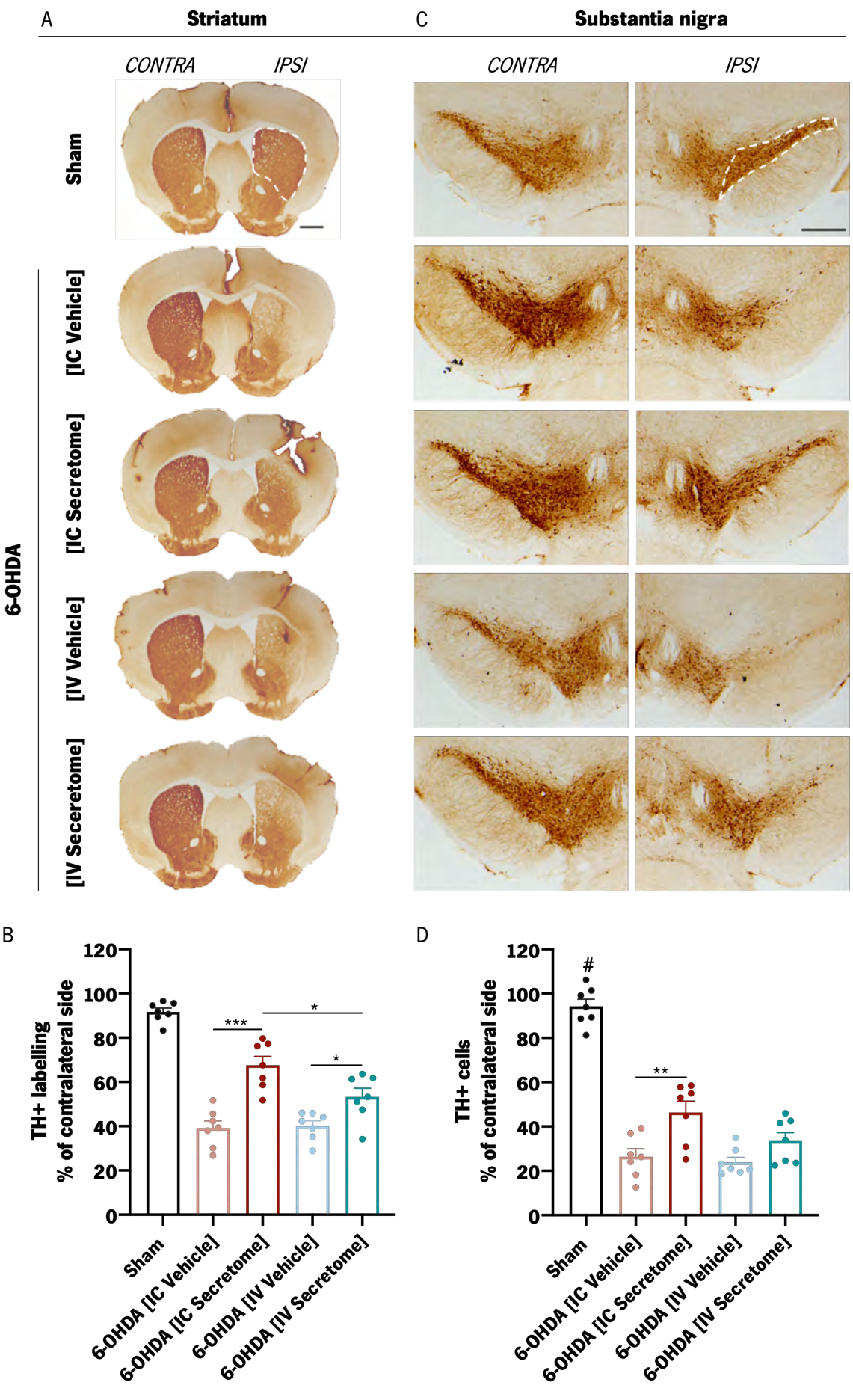

A
Striatum
CONTRA
IPSI
Sham
6-OHDA
[IC Vehicle]
[IC Secretome]
[IV Vehicle]
[IV Secretome]
C
Substantia nigra
CONTRA
IPSI
B
TH+ labelling
% of contralateral side
120
100
80
60
40
20
0
***
*
*
Sham
6-OHDA [IC Vehicle]
6-OHDA [IC Secretome]
6-OHDA [IV Vehicle]
6-OHDA [IV Secretome]
D
TH+ cells
% of contralateral side
120
100
80
60
40
20
0
#
**
Sham
6-OHDA [IC Vehicle]
6-OHDA [IC Secretome]
6-OHDA [IV Vehicle]
6-OHDA [IV Secretome]

Figure 3. Histological analysis of the striatum and SNpc. A) Representative images of the tyrosine hydroxylase (TH) staining on the striatum; **B)** Quantification of TH+ labelling on the dorsal striatum, depicted as a percentage over the non-lesioned side; **C)** Representative images of the TH staining on the ipsilateral and contralateral substantia nigra of the different experimental groups; **D)** Quantification of TH+ cells on the SNpc, depicted as a percentage over the non-lesioned side. n = 7 for each group used. Statistical summary in Table S1. Data are presented as mean ± SEM. *p < 0.05, **p < 0.01, ***p < 0.001. Scale bar = 2 mm.

3.2. BM-MSC secretory profile under hPL supplementation

To identify potential therapeutic molecules in the BM-MSC secretome that could be implicated in the previously described effects, the latter was characterized through a non-biased proteomic analysis based on combined MS approach. We were able to identify 107 proteins (according to the UniProtKB/Swiss-Prot classification) in the BM-MSC secretome common to all replicates (Figure 4A; Table S2). STRING network analysis revealed a strong protein-protein interaction enrichment between identified proteins (p-value = < $1.0e^{-16}$), with an average local clustering coefficient of 0.632. Figure 4B demonstrates the association between these proteins grouped into five clusters, according to their main biological processes/molecular functions. Cluster I have 39 items mainly related to extracellular matrix (ECM) structural constituents, such as different collagen subunits, fibronectin, and proteoglycans with cell-to-cell and cell-to-matrix interactions. This cluster is also enriched in proteins with binding activity mainly with extracellular factors, such as growth factors (e.g., Insulin-like growth factor-binding protein 4, 6, 7, and platelet-derived growth factor), and enzymes (e.g., Metalloproteinase inhibitor 1, and Plasminogen activator inhibitor 1). Another cluster highly enriched in the BM-MSC secretome is cluster III, which contains proteins with catalytic and antioxidant activity, namely Peroxiredoxin-1, Thioredoxin and Glutathione S-transferase P, as well as proteins involved in protein folding (e.g., Peptidyl-prolyl cis-trans isomerase A and B) and molecular chaperones (e.g., members of heat shock protein 70 family). Cluster IV is another small cluster containing proteins involved in the regulation of metabolic processes like negative regulation of gene expression, wherein members from the histone cluster families are found.

A more detailed gene ontology analysis (levels 4 and 5) was then performed using the ConsensusPathDB. Interestingly, the most represented category of cellular component observed was extracellular exosomes (Figure 4C). When it comes to the most represented protein complexes, we identified elements from histones (Figure 4C) as enriched in the secretome which is in accordance with the STRING analysis.

From the identified 107 proteins, some can be highlighted for their therapeutical potential in the PD context such as Thioredoxin, Peroxiredoxin-1, Galactin-1, and Cystatin C. To complement this analysis, we also performed a more targeted analysis of BM-MSC secretome using an antibody array that contains a set of proteins with neuroregulatory effects. From all the proteins analyzed on the array, GCSF, HB-EGF, IL-10, IL-1α, and MIP-1α were not found on BM-MSCs secretome. On the other hand, a panel of growth factors, such as BDNF, β-NGF, GDNF, IGF-1, TGF-β, and VEGF-A, as well as cytokines including IFNγ, IL-1β, IL-6, IL-8, MCP-1, MMP-2 and -3, and TNF-α were present within the secretome.

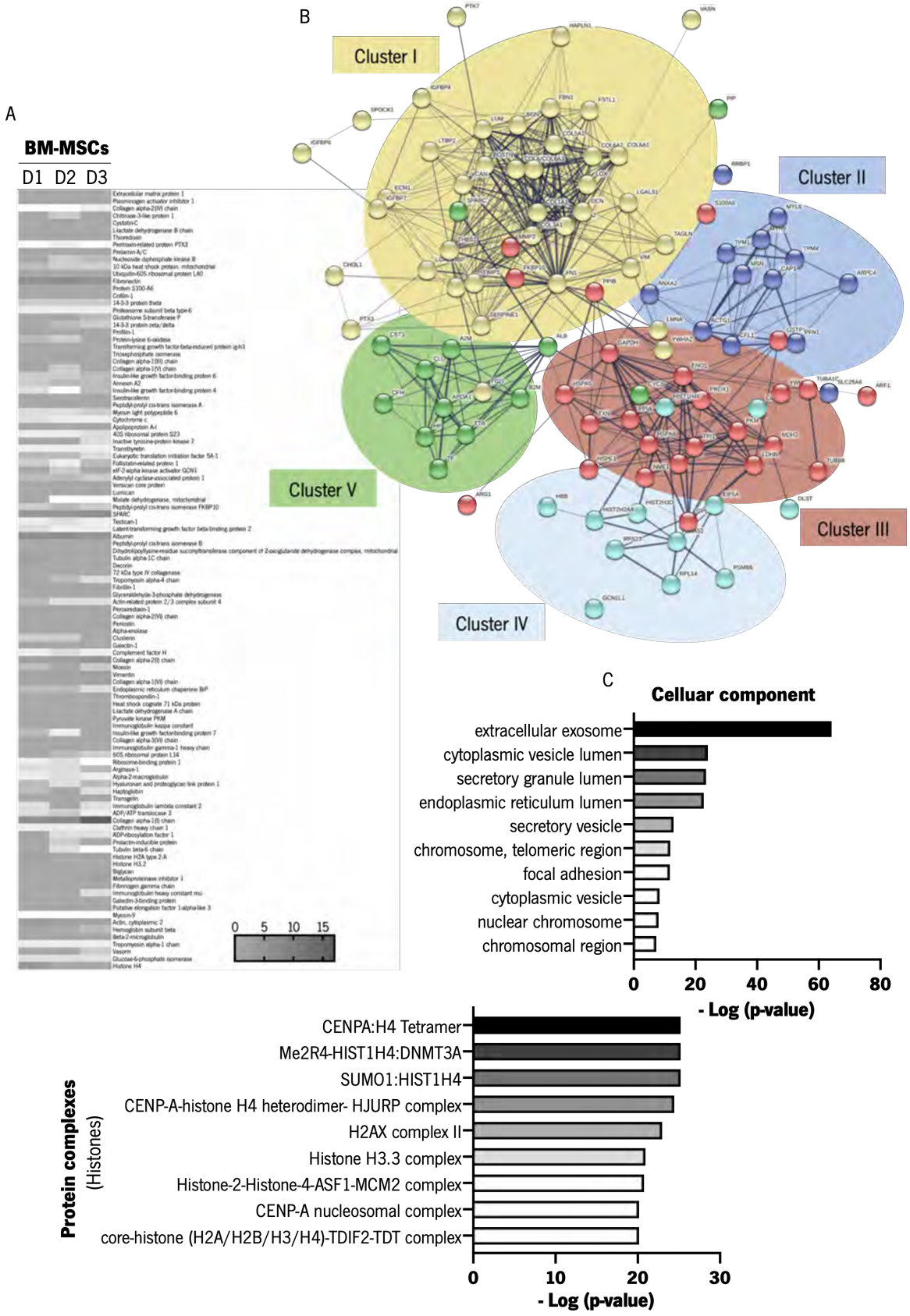


Figure 4. Proteomic analysis of BM-MSC secretome. A) Heatmap representation of all the 107 proteins identified in the BM-MSC secretome from the three independent donors; **B)** Protein-protein interaction network from the STRING

database. Cluster analysis reveal 5 clusters: Cluster I (ECM structural constituent, protein binding, protein-containing complex binding, ECM binding, carbohydrate derivate binding), Cluster II (cytoskeletal protein binding, structural constituent of cytoskeleton), Cluster III (catalytic activity, antioxidant activity, protein binding(, Cluster IV (regulation of metabolic process), and Cluster V (response to stimulus, transport, protein metabolic process); **C)** Categorization of the enrichment of cellular components (left), and elements of the elements of histones (right) using the ConsensusPathDB software (gene ontology levels 4 and 5). Results are shown as the –log of the p-value for the enrichment of each individual category.

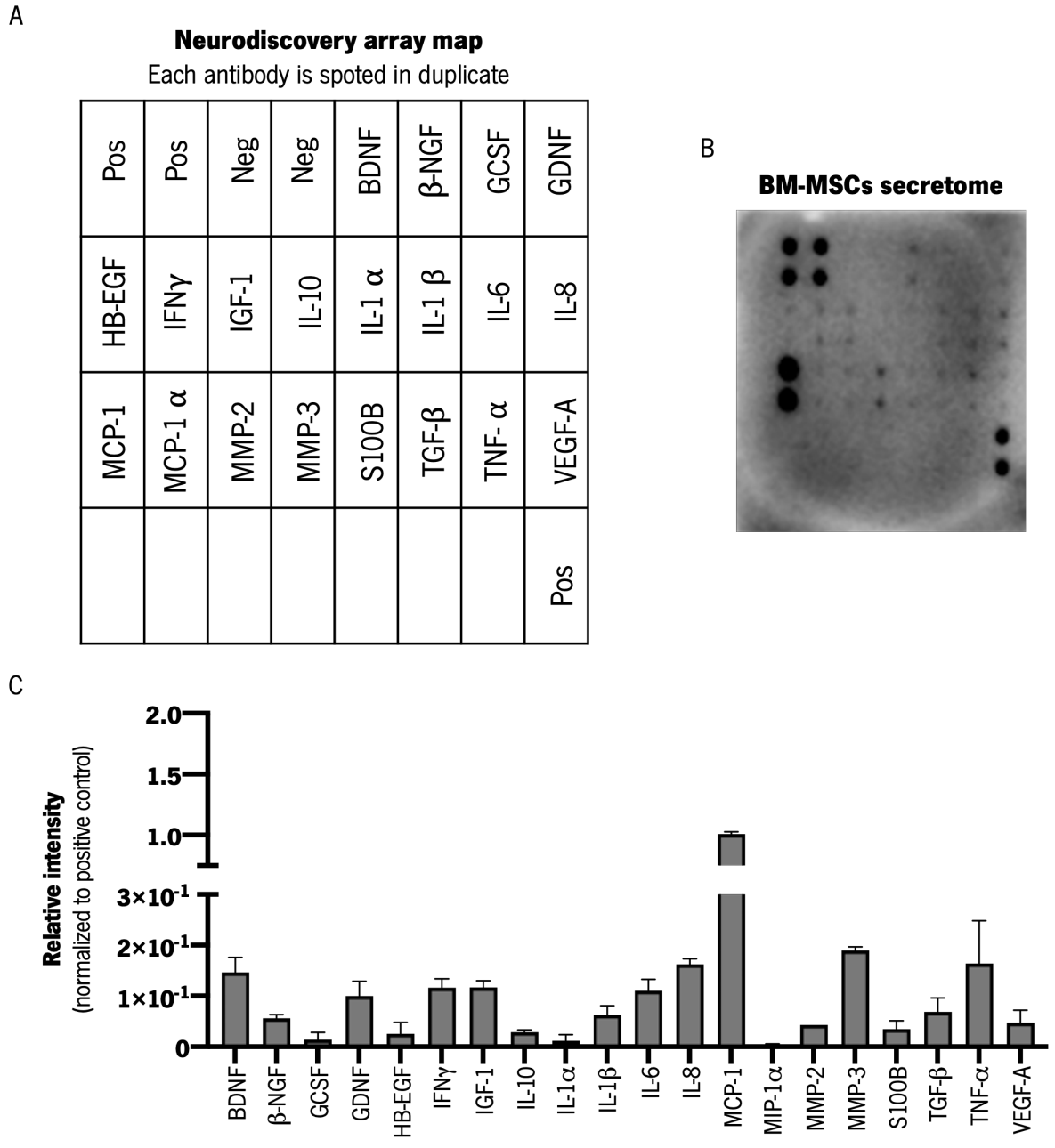


Figure 5. Profile of neuroregulatory proteins present in the secretome of BM-MSCs. A) Human Neurodiscovery membrane array map identifying the position of each antibody on the membrane; **B)** Membrane array depicting the proteins detected on BM-MSCs (pool of 3 donors); **C)** Relative intensity of each protein normalized to the positive control. Data are presented as mean ± SEM of relative intensity for each protein, normalized to positive control intensity.

4. Discussion

PD is clinically characterized by motor disabilities resulting from a preferential dopaminergic degeneration in the nigrostriatal pathway. Current therapies are not being fully effective, and no cure is available for PD (Dawson and Dawson, 2019). In the last years, the therapeutic potential of MSC secretome has been widely reported in preclinical models of PD (Marques et al., 2018). In this work, the main goal was to compare the efficacy of local administration (IC injections in the dorsal striatum and SNpc) with repeated systemic administration (IV injections) in alleviating the phenotype of a 6-OHDA mouse model of PD.

The first objective was to characterize motor behavior impairment in 6-OHDA-lesioned mice. Herein we show that intrastriatal 6-OHDA administration induced significant motor long-term alterations including increased latency in the motor swimming test and beam balance walk test, as well as increased time spent to reach the cage in the pole test (Figure 2). This is in line with our previous results regarding the characterization of the unilateral intrastriatal 6-OHDA lesion in mice (Mendes-Pinheiro et al., 2021; Chapter 3). After treatments, we observed that multiple IV injections administration of BM-MSC secretome showed a higher therapeutic magnitude effect when compared to IC injections, as revealed after significant motor recovery of lesioned mice in general motor paradigms (Figure 2B-D). In line with the results at the motor level, histological analysis disclosed a significant degeneration at the nigrostriatal pathway as a consequence of the 6-OHDA lesion (Figure 3). Significant treatment effects were observed after BM-MSC secretome injections in both administration routes in protecting the TH+ fibers in the dorsal striatum (Figure 3B). However, in theSNpc, a significant increase of TH+ cells were only observed in the IC Secretome group (Figure 3D). Nonetheless, a tendency was observed in the IV Secretome group when compared to the IV Vehicle group with a large effect size. Contrary to the motor behavior results, at the histological level, the IC injections had a higher magnitude effect. This result was not particularly surprising since intracerebral delivery circumvent blood brain barrier (BBB)-associated resistance mechanisms and offers the possibility of reaching higher local substance concentrations in the appropriate target regions. Even though, it was possible to observe a protective effect on the dopaminergic cells of the BM-MSC secretome systemic administration in the lesioned-brain regions, which indicates that probably some secretome molecules are reaching the brain. In other work from our group (unpublished data), a biodistribution study of FITC-labelled BM-MSC secretome indicates that after 5 hours of one IV secretome injection, it was possible to observe fluorescent signal in all peripheric organs measured (spleen, lung, liver, heart, and kidney), but also in the substantia

nigra/ventral tegmental area and amygdala. Nonetheless, this study was done in non-lesioned animals, therefore, it would be interesting to perform the same biodistribution study in 6-OHDA-lesioned mice and using different time-points. Moreover, as previously described (Carvey et al., 2005), 6-OHDA-lesioned animals present compromised BBB integrity, which let us to hypothesized that the factors present in the secretome can more easily penetrate the BBB of lesioned mice. Therefore, we expect to observe the same results or even an increase of the fluorescent signal in the lesioned brains.

More striking were the results related to the motor behavior, were the IV injections led to higher magnitude effects in terms of 6-OHDA-lesioned mice functional improvements. Other studies also assessed the therapeutical effects of MSC secretome using the same route of administration – IV injections into the tail vein. For instance, Nakhaeifard and colleagues assessed the neuroprotective effects of adipose-derived MSC-conditioned medium in unilaterally 6-OHDA-lesioned rats, reporting motor improvements and preservation of dopaminergic neurons in SNpc (Nakhaeifard et al., 2018). Another interesting study using rotenone to induce parkinsonism observed that almost all of the pathological changes (e.g., detection of shrunken dopaminergic cells with small dense nuclei; presence of eosinophilic cytoplasmatic inclusions; disruption and separation of layers and remnant of degenerated organelles inside the axon; among others) in the lesioned rats were ameliorated in both BM-MSCs and conditioned medium-treated groups. However, the conditioned medium showed a superior therapeutic effect establishing nearly the normal histological architecture of the SNpc (Abdelwahab et al., 2021). Although these studies were conducted in rats and using other models besides the 6-OHDA model, similarly to our work, they demonstrated the therapeutic potential of systemic administration of MSCs secretome as a cell-free therapy for PD.

To better dissect the molecular players mediating neuroprotection in the PD model, we fully characterize the BM-MSC secretome using MS proteomic approach (Figure 4). Like our previous characterization of BM-MSC secretome of cells grown in serum-free conditions (Mendes-Pinheiro et al., 2019), in this work using the same population of cells grown in HPL, when we evaluated cellular components at a more detailed level, we observed a very large enrichment of proteins that are part of exosomes. Moreover, this category of proteins was clearly overrepresented when compared with the other top hits (Figure 4C). In fact, MSC secretome includes the entire set of MSC-derived soluble molecules and vesicular components, including exosomes (Marote et al., 2016). MSC-derived exosomes are hypoimmunogenic nanocarriers that contain numerous immunoregulatory components and offer a variety of benefits, including the ability to transverse the BBB and blood capillaries, as well

as being small enough to avoid clearance by the reticuloendothelial system (Baharlooi et al., 2020; D'angelo et al., 2020). Concerning PD, MSC-derived exosomes are shown to be neuroprotective by rescuing dopaminergic neurons from 6-OHDA-induced apoptosis *in vitro* (Chen et al., 2020; Jarmalavičiute et al., 2015). Further, in a PD rat model (6-OHDA lesioned), exosomes crossing the BBB reached the SNpc, improved apomorphine-induced asymmetric rotation, decreased dopaminergic neuronal loss and apoptosis, and upregulated striatal DA levels (Chen et al., 2020). Hence, the beneficial effects of BM-MSCs observed in this work could be mediated by a similar exosome-dependent mechanism. Deeping further into this characterization and similarly to our previous results (Mendes-Pinheiro et al., 2019), we observed again that histones are one of the most represented protein complexes in the BM-MSC secretome. Indeed, histone modifications have been linked with the development, differentiation, and maintenance of DA neurons as demonstrated by different in vitro, in vivo, and PD patient data (Goers et al., 2003; Nicholas et al., 2008; Park et al., 2016; Song et al., 2011, 2010). Altogether, these findings suggest that chromatin remodeling may have an important role in PD pathogenesis, opening the possibility that secretome can somehow modulate these changes. Furthermore, we also found in our proteomic analysis, important proteins known as antioxidant agents, such as Thioredoxin and Peroxiredoxin-1 that have been shown to counteract dopaminergic cell death in different PD models as nicely reviewed by (Pires et al., 2016). Other proteins like Galactin-1 and Cystatin C have also been associated with anti-apoptotic effects in *in vitro* models of PD (Pires et al., 2016). To complement this analysis, a more targeted proteomic analysis of the BM-MSC secretome was performed using a membrane-based antibody array (Figure 5). Among the different growth factors and cytokines detected within the secretome, BDNF and GDNF are well studied neurotrophic factors in the context of PD and known as having an on impact in the enhancement of dopaminergic neuronal survival, improvement of dopaminergic neurotransmission, and motor performance (Allen et al., 2013; Manfredsson et al., 2020; Palasz et al., 2020; Sullivan and Toulouse, 2011). Moreover, the potent and reproducible effects of GDNF in animal models led to the initiation of clinical trials in PD patients, and on the other hand, postmortem studies of PD patients demonstrated that reduced levels of BDNF within the SNpc accompany the disease condition (Baquet et al., 2005). Interestingly, in the same study referred above, Nakhaeifard and colleagues verified that there was a significant decrease in BDNF gene expression in the striatal region of 6-OHDA lesioned rats compared to controls. However, secretome-treated animals showed significant increased levels in the mentioned gene expression compared to the untreated groups (Nakhaeifard et al., 2018). Nonetheless, one point that needs to be clarified is if the encouraging results are due to one or two factors or a combination of different molecules present in the

secretome. Rather than addressing the potential relevance of each detected molecule, we believe it is critical to recognize that the molecules found in the BM-MSC secretome most likely act collectively, activating a variety of signaling pathways implicated in neuroprotection. For instance, defects in the Akt signaling pathway, which is triggered by most of the growth factors and cytokines found on the array, have been associated with dopaminergic neuronal loss in PD, while their activation has been hypothesized to provide neuroprotection of a variety of compounds evaluated in PD animal models (Rai et al., 2019; Timmons et al., 2009).

Noteworthy is the fact that, from our knowledge, this is the first pre-clinical PD model using MSCs that were expanded *in vitro* using hPL as a media supplement. To date, fetal bovine serum (FBS) is the most widely used serum supplement for MSC culture. Although FBS has been used for several clinical studies, it still poses ethical issues over animal welfare, as well as some clinical concerns. FBS has a poorly characterized composition, it can be a source of xenogenic antigens and zoonotic infections, and the lack of standardization of FBS preparations may affect cell culture performance (Becherucci et al., 2018; Hemeda et al., 2014). On the other hand, peripheral blood components such as platelets have a shelf life of 5 days beyond which they are at risk of platelet aggregation and bacterial contamination, making them unfit for transfusion. These expired platelet units are thus classified as biological waste and discarded by blood banks. Platelet granules contain many growth factors, cytokines, and other regulatory chemicals that are released by thrombin activation and clotting. Platelet lysis through freeze-thaw, sonication, or chemical treatment breaks the platelet membrane, allowing these factors to be released more efficiently in vitro (Kandoi et al., 2018). hPL can then be used in direct novel applications in regenerative medicine, such as bone and cartilage regeneration (Zamani et al., 2019), but it can also be used as a supplement for ex vivo cellular expansion. Doucet and colleagues (Doucet et al., 2005) were the first to describe the use of hPL as a clinical alternative to FBS in the expansion of BM-MSCs, stimulating higher proliferation without affecting MSC identity, and since then, its application has been evaluated in other adult sources of MSCs (Astori et al., 2016). hPL offers an animal component-free approach for culturing MSCs that can be produced under good manufacturing practices (GMP) conditions, presents less batch-to-batch variability when compared to FBS, and is cost-effective compared to commercially available serum-free formulations (Becherucci et al., 2018).

Pre-clinical studies are of extreme importance to design rational protocols to be used in the treatment of human patients. Our results are clinically relevant because the possibility of delivering MSC secretome in a non-invasive way is very advantageous from the clinical application point of view. Disadvantages of

intracranial drug/new compound demonstration include the invasive procedure necessary for this delivery, the difficulties associated with the need for long-term administration, and the difficulties associated with the fact that the distribution of an appropriate substance within the brain parenchyma cannot be reliably set to the desired range (Gernert and Feja, 2020).

Given the numerous clinical trials using MSCs, it is very plausible to anticipate the approval of MSC secretome-derived products in the near future. As pertinently raised by Vizoso and colleagues (Vizoso et al., 2017), although the composition of secretome-derived products from MSCs is complex, this should not impede for regulatory approval of a regenerative product, giving the examples of platelet-rich plasma or amniotic fluid, that remain poorly characterized, and are routinely used as a regenerative therapy for multiple applications in wound healing and orthopedics. Nevertheless, regulatory requirements for manufacturing and quality control will be necessary to establish the safety and efficacy profile of BM-MSC secretome.

Author Contributions

Conceptualization, B.M.-P., A.M., S.D.-S., L.P. and A.J.S.; methodology, B.M.-P., A.M., and S.D.-S.; validation, B.M.-P. and A.J.S.; formal analysis, B.M.-P., and S.D.-S.; data curation, B.M.-P.; investigation, B.M.-P., A.M., C.S.-C., J.C.R., S.B.-A., J.C., S.C.S., E.L.-C., S.I.A., and B.M.; resources, A.J.S.; writing-original draft preparation, B.M.-P.; writing—review and editing, B.M.-P., A.M., and A.J.S.; supervision, L.P. and A.J.S.; project administration, A.J.S.; funding acquisition, A.J.S.

Funding

This work was supported by the Foundation for Science and Technology (FCT) through PhD Fellowships attributed to B.M.-P. (SFRH/BD/120124/2016; COVID/BD/151719/2021), J.C.R. (SFRH/BD/145860/2019), S.B.-A. (PD/BDE/135568/2018), J.C. (SFRH/BD/5813/2020), E.L.-C. (SFRH/BD/131278/2017), and CEEC attributed to C.S.-C. (CEECIND/03887/2017), S.D.-S. (CEECIND/00685/2020), and L.P. (CEECIND/02855/2020). ICVS Scientific Microscopy Platform, member of the national infrastructure PPBI-Portuguese Platform of Bioimaging PPBI-POCI-01-0145-FEDER-022122; National funds, through the FCT-project UIDB/50026/2020 and UIDP/50026/2020; the projects NORTE-01-0145-FEDER-000013, NORTE-01-0145-FEDER-000023, and NORTE-01-0145-FEDER-000039, supported by Norte Portugal Regional Operational Programme (NORTE 2020), under the PORTUGAL 2020 Partnership Agreement, through the European Regional Development Fund

(ERDF); Competitiveness Internationalization Operational Programme (POCI), and by National funds, through the FCT, under the scope of the project POCI-01-0145-FEDER-032619. This work was also partially funded by Iniciativa Ibérica de Investigación y Innovación Biomedica and Fundación "a Caixa", under the scope of the "la Caixa" Foundation Health Research 2020 Call (HR20-00249).

Conflicts of interest

The authors declare no conflict of interest.

References

Abdelwahab S, Elsebay SAG, Fouli Gaber M, Abdel-Hafez SMN. 2021. Comparative study between bone marrow mesenchymal stem cell and their conditioned medium in the treatment of rat model of Parkinsonism. *J Cell Physiol* **236**:440–457. doi:10.1002/jcp.29872

Allen SJ, Watson JJ, Shoemark DK, Barua NU, Patel NK. 2013. GDNF, NGF and BDNF as therapeutic options for neurodegeneration. *Pharmacol Ther* **138**:155–175. doi:10.1016/j.pharmthera.2013.01.004

Astori G, Amati E, Bambi F, Bernardi M, Chieregato K, Schäfer R, Sella S, Rodeghiero F. 2016. Platelet lysate as a substitute for animal serum for the ex-vivo expansion of mesenchymal stem/stromal cells: present and future. *Stem Cell Res Ther* **7**:93. doi:10.1186/s13287-016-0352-x

Baharlooi H, Azimi M, Salehi Z, Izad M. 2020. Mesenchymal stem cell-derived exosomes: A promising therapeutic ace card to address autoimmune diseases. *Int J Stem Cells* **13**:13–23. doi:10.15283/ijsc19108

Baquet ZC, Bickford PC, Jones KR. 2005. Brain-derived neurotrophic factor is required for the establishment of the proper number of dopaminergic neurons in the substantia nigra pars compacta. *J Neurosci* **25**:6251–6259. doi:10.1523/JNEUROSCI.4601-04.2005

Becherucci V, Piccini L, Casamassima S, Bisin S, Gori V, Gentile F, Ceccantini R, De Rienzo E, Bindi B, Pavan P, Cunial V, Allegro E, Ermini S, Brugnolo F, Astori G, Bambi F. 2018. Human platelet lysate in mesenchymal stromal cell expansion according to a GMP grade protocol: a cell factory experience. *Stem Cell Res Ther* **9**:124. doi:10.1186/s13287-018-0863-8

Bloem BR, Okun MS, Klein C. 2021. Parkinson's disease. *Lancet* **397**:2284–2303. doi:10.1016/S0140-6736(21)00218-X

Carvey PM, Zhao CH, Hendey B, Lum H, Trachtenberg J, Desai BS, Snyder J, Zhu YG, Ling ZD. 2005. 6-Hydroxydopamine-induced alterations in blood-brain barrier permeability. *Eur J Neurosci*

22:1158–1168. doi:10.1111/j.1460-9568.2005.04281.x

Chen HX, Liang FC, Gu P, Xu BL, Xu HJ, Wang WT, Hou JY, Xie DX, Chai XQ, An SJ. 2020. Exosomes derived from mesenchymal stem cells repair a Parkinson's disease model by inducing autophagy. *Cell Death Dis* **11**:288. doi:10.1038/s41419-020-2473-5

D'angelo M, Cimini A, Castelli V. 2020. Insights into the effects of mesenchymal stem cell-derived secretome in Parkinson's disease. *Int J Mol Sci* **21**:5241. doi:10.3390/ijms21155241

Dawson VL, Dawson TM. 2019. Promising disease-modifying therapies for Parkinson's disease. *Sci Transl Med* **11**:eaba1659. doi:10.1126/scitranslmed.aba1659

Doucet C, Ernou I, Zhang Y, Llense JR, Begot L, Holy X, Lataillade JJ. 2005. Platelet lysates promote mesenchymal stem cell expansion: A safety substitute for animal serum in cell-based therapy applications. *J Cell Physiol* **205**:228–236. doi:10.1002/jcp.20391

Fraga JS, Silva NA, Lourenço AS, Gonçalves V, Neves NM, Reis RL, Rodrigues AJ, Manadas B, Sousa N, Salgado AJ. 2013. Unveiling the effects of the secretome of mesenchymal progenitors from the umbilical cord in different neuronal cell populations. *Biochimie* **95**:2297–2303. doi:10.1016/j.biochi.2013.06.028

Garcia-Garcia E, Andrieux K, Gil S, Couvreur P. 2005. Colloidal carriers and blood-brain barrier (BBB) translocation: A way to deliver drugs to the brain? *Int J Pharm* **298**:274–292. doi:10.1016/j.ijpharm.2005.03.031

Gernert M, Feja M. 2020. Bypassing the blood–brain barrier: Direct intracranial drug delivery in epilepsies. *Pharmaceutics* **12**:1134. doi:10.3390/pharmaceutics12121134

Goers J, Manning-Bog AB, McCormack AL, Millett IS, Doniach S, Di Monte DA, Uversky VN, Fink AL. 2003. Nuclear Localization of α-Synuclein and Its Interaction with Histones. *Biochemistry* **42**:8465–8471. doi:10.1021/bi0341152

Han Yu, Li X, Zhang Y, Han Yuping, Chang F, Ding J. 2019. Mesenchymal Stem Cells for Regenerative Medicine. *Cells* **8**:886. doi:10.3390/cells8080886

Hawkins P, Morton DB, Burman O, Dennison N, Honess P, Jennings M, Lane S, Middleton V, Roughan J V., Wells S, Westwood K. 2011. A guide to defining and implementing protocols for the welfare assessment of laboratory animals: eleventh report of the BVAAWF/FRAME/RSPCA/UFAW Joint Working Group on Refinement. *Lab Anim* **45**:1–13. doi:10.1258/la.2010.010031

Hemeda H, Giebel B, Wagner W. 2014. Evaluation of human platelet lysate versus fetal bovine serum for culture of mesenchymal stromal cells. *Cytotherapy* **16**:170–180. doi:10.1016/j.jcyt.2013.11.004

Jarmalavičiute A, Tunaitis V, Pivoraite U, Venalis A, Pivoriunas A. 2015. Exosomes from dental pulp stem cells rescue human dopaminergic neurons from 6-hydroxy-dopamine-induced apoptosis. *Cytotherapy* **17**:932–939. doi:10.1016/j.jcyt.2014.07.013

Kamburov A, Stelzl U, Lehrach H, Herwig R. 2013. The ConsensusPathDB interaction database: 2013 Update. *Nucleic Acids Res* **41**:793–800. doi:10.1093/nar/gks1055

Kandoi S, L P kumar, Patra B, Vidyasekar P, Sivanesan D, S. V, K. R, Verma RS. 2018. Evaluation of platelet lysate as a substitute for FBS in explant and enzymatic isolation methods of human umbilical cord MSCs. *Sci Rep* **8**:12439. doi:10.1038/s41598-018-30772-4

Manfredsson FP, Polinski NK, Subramanian T, Boulis N, Wakeman DR, Mandel RJ. 2020. The Future of GDNF in Parkinson's Disease. *Front Aging Neurosci* **12**:593572. doi:10.3389/fnagi.2020.593572

Marote A, Teixeira FG, Mendes-Pinheiro B, Salgado AJ. 2016. MSCs-Derived Exosomes: Cell-Secreted Nanovesicles with Regenerative Potential. *Front Pharmacol* **7**:231. doi:10.3389/fphar.2016.00231

Marques CR, Marote A, Mendes-Pinheiro B, Teixeira FG, Salgado AJ. 2018. Cell secretome based approaches in Parkinson's disease regenerative medicine. *Expert Opin Biol Ther* **18**:1235–1245. doi:10.1080/14712598.2018.1546840

Mendes-Pinheiro B, Anjo SI, Manadas B, Da Silva JD, Marote A, Behie LA, Teixeira FG, Salgado AJ. 2019. Bone Marrow Mesenchymal Stem Cells' Secretome Exerts Neuroprotective Effects in a Parkinson's Disease Rat Model. *Front Bioeng Biotechnol* **7**:294. doi:10.3389/fbioe.2019.00294

Mendes-Pinheiro B, Soares-Cunha C, Marote A, Loureiro-Campos E, Campos J, Barata-Antunes S, Monteiro-Fernandes D, Santos D, Duarte-Silva S, Pinto L, José Salgado A. 2021. Unilateral Intrastriatal 6-Hydroxydopamine Lesion in Mice: A Closer Look into Non-Motor Phenotype and Glial Response. *Int J Mol Sci* **22**:11530. doi:10.3390/ijms222111530

Mendes-Pinheiro B, Teixeira FG, Anjo SI, Manadas B, Behie LA, Salgado AJ. 2018. Secretome of Undifferentiated Neural Progenitor Cells Induces Histological and Motor Improvements in a Rat Model of Parkinson's Disease. *Stem Cells Transl Med* **7**:829–838. doi:10.1002/sctm.18-0009

Merimi M, El-Majzoub R, Lagneaux L, Moussa Agha D, Bouhtit F, Meuleman N, Fahmi H, Lewalle P, Fayyad-Kazan M, Najar M. 2021. The Therapeutic Potential of Mesenchymal Stromal Cells for Regenerative Medicine: Current Knowledge and Future Understandings. *Front Cell Dev Biol* **9**:661532. doi:10.3389/fcell.2021.661532

Mi H, Muruganujan A, Thomas PD. 2013. PANTHER in 2013: Modeling the evolution of gene function,

and other gene attributes, in the context of phylogenetic trees. *Nucleic Acids Res* **41**:377–386. doi:10.1093/nar/gks1118

Nakhaeifard M, Kashani MHG, Goudarzi I, Rezaei A. 2018. Conditioned medium protects dopaminergic neurons in Parkinsonian rats. *Cell J* **20**:348–354. doi:10.22074/cellj.2018.5343

Nicholas AP, Lubin FD, Hallett PJ, Vattem P, Ravenscroft P, Bezard E, Zhou S, Fox SH, Brotchie JM, Sweatt JD, Standaert DG. 2008. Striatal histone modifications in models of levodopa-induced dyskinesia. *J Neurochem* **106**:486–494. doi:10.1111/j.1471-4159.2008.05417.x

Palasz E, Wysocka A, Gasiorowska A, Chalimoniuk M, Niewiadomski W, Niewiadomska G. 2020. BDNF as a Promising Therapeutic Agent in Parkinson's Disease. *Int J Mol Sci* **21**:1170. doi:10.3390/ijms21031170

Park G, Tan J, Garcia G, Kang Y, Salvesen G, Zhang Z. 2016. Regulation of histone acetylation by autophagy in Parkinson disease. *J Biol Chem* **291**:3531–3540. doi:10.1074/jbc.M115.675488

Pires AO, Mendes-Pinheiro B, Teixeira FG, Anjo SI, Ribeiro-Samy S, Gomes ED, Serra SC, Silva NA, Manadas B, Sousa N, Salgado AJ. 2016. Unveiling the Differences of Secretome of Human Bone Marrow Mesenchymal Stem Cells, Adipose Tissue-Derived Stem Cells, and Human Umbilical Cord Perivascular Cells: A Proteomic Analysis. *Stem Cells Dev* **25**:1073–1083. doi:10.1089/scd.2016.0048

Poewe W, Seppi K, Tanner CM, Halliday GM, Brundin P, Volkmann J, Schrag A-E, Lang AE. 2017. Parkinson disease. *Nat Rev Dis Prim* **3**:17013. doi:10.1038/nrdp.2017.13

Rai SN, Dilnashin H, Birla H, Singh S Sen, Zahra W, Rathore AS, Singh BK, Singh SP. 2019. The Role of PI3K/Akt and ERK in Neurodegenerative Disorders. *Neurotox Res* **35**:775–795. doi:10.1007/s12640-019-0003-y

Sawilowsky SS. 2009. Very large and huge effect sizes. *J Mod Appl Stat Methods* **8**:597–599. doi:10.22237/jmasm/1257035100

Song C, Kanthasamy A, Anantharam V, Sun F, Kanthasamy AG. 2010. Environmental Neurotoxic Pesticide Increases Histone Acetylation to Promote Apoptosis in Dopaminergic Neuronal Cells: Relevance to Epigenetic Mechanisms of Neurodegeneration. *Mol Pharmacol* **77**:621–632. doi:10.1124/mol.109.062174

Song C, Kanthasamy A, Jin H, Anantharam V, Kanthasamy AG. 2011. Paraquat induces epigenetic changes by promoting histone acetylation in cell culture models of dopaminergic degeneration. *Neurotoxicology* **32**:586–595. doi:10.1016/j.neuro.2011.05.018

Stoker TB, Barker RA. 2020. Recent developments in the treatment of Parkinson's Disease.

F1000Research **9**:F1000. doi:10.12688/f1000research.25634.1

Sullivan AM, Toulouse A. 2011. Neurotrophic factors for the treatment of Parkinson's disease. *Cytokine Growth Factor Rev* **22**:157–165. doi:10.1016/j.cytogfr.2011.05.001

Teixeira FG, Carvalho MM, Panchalingam KM, Rodrigues AJ, Mendes-Pinheiro B, Anjo S, Manadas B, Behie LA, Sousa N, Salgado AJ. 2017. Impact of the Secretome of Human Mesenchymal Stem Cells on Brain Structure and Animal Behavior in a Rat Model of Parkinson's Disease. *Stem Cells Transl Med* **6**:634–646. doi:10.5966/sctm.2016-0071

Teixeira FG, Panchalingam KM, Assunção-Silva R, Serra SC, Mendes-Pinheiro B, Patrício P, Jung S, Anjo SI, Manadas B, Pinto L, Sousa N, Behie LA, Salgado AJ. 2016. Modulation of the Mesenchymal Stem Cell Secretome Using Computer-Controlled Bioreactors: Impact on Neuronal Cell Proliferation, Survival and Differentiation. *Sci Rep* **6**:27791. doi:10.1038/srep27791

Teixeira FG, Vilaça-Faria H, Domingues A V., Campos J, Salgado AJ. 2020. Preclinical Comparison of Stem Cells Secretome and Levodopa Application in a 6-Hydroxydopamine Rat Model of Parkinson's Disease. *Cells* **9**:315. doi:10.3390/cells9020315

Timmons S, Coakley MF, Moloney AM, O' Neill C. 2009. Akt signal transduction dysfunction in Parkinson's disease. *Neurosci Lett* **467**:30–35. doi:10.1016/j.neulet.2009.09.055

Vizoso F, Eiro N, Cid S, Schneider J, Perez-Fernandez R. 2017. Mesenchymal Stem Cell Secretome: Toward Cell-Free Therapeutic Strategies in Regenerative Medicine. *Int J Mol Sci* **18**:1852. doi:10.3390/ijms18091852

Vizoso FJ, Eiro N, Costa L, Esparza P, Landin M, Diaz-Rodriguez P, Schneider J, Perez-Fernandez R. 2019. Mesenchymal stem cells in homeostasis and systemic diseases: Hypothesis, evidences, and therapeutic opportunities. *Int J Mol Sci* **20**:1–23. doi:10.3390/ijms20153738

Zahoor I, Shafi A, Haq E. 2018. Pharmacological Treatment of Parkinson's Disease In: Stoker TB, Greenland JC, editors. Parkinson's Disease: Pathogenesis and Clinical Aspects. Codon Publications. pp. 129–144. doi:10.15586/codonpublications.parkinsonsdisease.2018.ch7

Zamani M, Yaghoubi Y, Movassaghpour A, Shakouri K, Mehdizadeh A, Pishgahi A, Yousefi M. 2019. Novel therapeutic approaches in utilizing platelet lysate in regenerative medicine: Are we ready for clinical use? *J Cell Physiol* **234**:17172–17186. doi:10.1002/jcp.28496

SUPPLEMENTARY MATERIAL

Multiple systemic administration of mesenchymal stem cell secretome showed a higher therapeutical magnitude effect *versus* intracerebral injections in a mouse model of Parkinson's disease

Table S1. Statistical summary

Measure	Statistical Report	*Effect size (weeks after treatments)
Rotameter test *Net-contralateral rotations*	U=0, $p < 0.001$	-
Motor swimming test *Latency (s)*	Time: $F_{(2.67, 176.1)} = 90.72$, $p < 0.001$ Group: $F_{(4, 68)} = 10.91$, $p < 0.001$ Time x Group: $F_{(12, 199)} = 5.12$, $p < 0.001$ **Multiple comparisons** Sham vs 6-OHDA [IC Vehicle]: $p < 0.001$ Sham vs 6-OHDA [IC Secretome]: $p < 0.001$ Sham vs 6-OHDA [IV Vehicle]: $p < 0.001$ Sham vs 6-OHDA [IV Secretome]: $p < 0.001$ 6-OHDA [IC Vehicle] vs 6-OHDA [IC Secretome]: $p = 0.180$ 6-OHDA [IV Vehicle] vs 6-OHDA [IV Secretome]: $p = 0.002$ 6-OHDA [IC Secretome] vs 6-OHDA [IV Secretome]: $p = 0.655$	**1 week** IC Vehicle vs IC Secretome: Cohen's d = 0.37 IV Vehicle vs IV Secretome: Cohen's d = 1.3 **4 weeks** IC Vehicle vs IC Secretome: Cohen's d = 0.97 IV Vehicle vs IV Secretome: Cohen's d = 1.03 **7 weeks** IC Vehicle vs IC Secretome: Cohen's d = 0.96 IV Vehicle vs IV Secretome: Cohen's d = 1.46
Pole test *Time to reach the cage (s)*	Time: $F_{(3, 201)} = 19.57$, $p < 0.001$ Group: $F_{(4, 69)} = 9.92$, $p < 0.001$ Time x Group: $F_{(12, 201)} = 5.03$, $p < 0.001$ **Multiple comparisons** Sham vs 6-OHDA [IC Vehicle]: $p < 0.001$ Sham vs 6-OHDA [IC Secretome]: $p = 0.014$ Sham vs 6-OHDA [IV Vehicle]: $p < 0.001$ Sham vs 6-OHDA [IV Secretome]: $p = 0.047$ 6-OHDA [IC Vehicle] vs 6-OHDA [IC Secretome]: $p = 0.378$ 6-OHDA [IV Vehicle] vs 6-OHDA [IV Secretome]: $p = 0.025$ 6-OHDA [IC Secretome] vs 6-OHDA [IV Secretome]: $p = 0.987$	**1 week** IC Vehicle vs IC Secretome: Cohen's d = 0.71 IV Vehicle vs IV Secretome: Cohen's d = 0.94 **4 weeks** IC Vehicle vs IC Secretome: Cohen's d = 0.64 IV Vehicle vs IV Secretome: Cohen's d = 0.92 **7 weeks** IC Vehicle vs IC Secretome: Cohen's d = 0.90 IV Vehicle vs IV Secretome: Cohen's d = 1.13
Beam balance walk test *Latency (s)*	Time: $F_{(2.53, 159.1)} = 19.70$, $p < 0.001$ Group: $F_{(4, 70)} = 8.90$, $p < 0.001$ Time x Group: $F_{(12, 189)} = 2.25$, $p < 0.05$ **Multiple comparisons** Sham vs 6-OHDA [IC Vehicle]: $p < 0.001$ Sham vs 6-OHDA [IC Secretome]: $p < 0.001$ Sham vs 6-OHDA [IV Vehicle]: $p < 0.001$ Sham vs 6-OHDA [IV Secretome]: $p = 0.0034$ 6-OHDA [IC Vehicle] vs 6-OHDA [IC Secretome]: $p = 0.681$ 6-OHDA [IV Vehicle] vs 6-OHDA [IV Secretome]: $p = 0.008$ 6-OHDA [IC Secretome] vs 6-OHDA [IV Secretome]: $p = 0.441$	**1 week** IC Vehicle vs IC Secretome: Cohen's d = 0.53 IV Vehicle vs IV Secretome: Cohen's d = 0.68 **4 weeks** IC Vehicle vs IC Secretome: Cohen's d = 0.05 IV Vehicle vs IV Secretome: Cohen's d = 0.56 **7 weeks** IC Vehicle vs IC Secretome: Cohen's d = 0.50 IV Vehicle vs IV Secretome: Cohen's d = 1.81
TH+ labelling *Dorsal striatum*	Time: $F_{(4, 30)} = 49.71$, $p < 0.001$ **Multiple comparisons** Sham vs 6-OHDA [IC Vehicle]: $p < 0.001$ Sham vs 6-OHDA [IC Secretome]: $p < 0.001$ Sham vs 6-OHDA [IV Vehicle]: $p < 0.001$ Sham vs 6-OHDA [IV Secretome]: $p < 0.001$ 6-OHDA [IC Vehicle] vs 6-OHDA [IC Secretome]: $p < 0.001$	IC Vehicle vs IC Secretome: Cohen's d = 2.9 IV Vehicle vs IV Secretome: Cohen's d = 1.5

	6-OHDA [IV Vehicle] vs 6-OHDA [IV Secretome]: p = 0.049 6-OHDA [IC Secretome] vs 6-OHDA [IV Secretome]: p = 0.026	
TH+ cells *SNpc*	Time: $F_{(4, 30)}$ = 60.92, p < 0.001 **Multiple comparisons** Sham vs 6-OHDA [IC Vehicle]: p < 0.001 Sham vs 6-OHDA [IC Secretome]: p < 0.001 Sham vs 6-OHDA [IV Vehicle]: p < 0.001 Sham vs 6-OHDA [IV Secretome]: p < 0.001 6-OHDA [IC Vehicle] vs 6-OHDA [IC Secretome]: p = 0.005 6-OHDA [IV Vehicle] vs 6-OHDA [IV Secretome]: p = 0.370 6-OHDA [IC Secretome] vs 6-OHDA [IV Secretome]: p = 0.127	IC Vehicle vs IC Secretome: Cohen's d = 1.7 IV Vehicle vs IV Secretome: Cohen's d = 1.17
Weight gain *Males*	Time: $F_{(3.35, 111.9)}$ = 136.5, p < 0.001 Group: $F_{(4, 34)}$ = 12.18, p < 0.001 Time x Group: $F_{(56, 468)}$ = 3.14, p < 0.001 **Multiple comparisons** Sham vs 6-OHDA [IC Vehicle]: p < 0.001 Sham vs 6-OHDA [IC Secretome]: p < 0.001 Sham vs 6-OHDA [IV Vehicle]: p < 0.001 Sham vs 6-OHDA [IV Secretome]: p < 0.001 6-OHDA [IC Vehicle] vs 6-OHDA [IC Secretome]: p = 0.03 6-OHDA [IV Vehicle] vs 6-OHDA [IV Secretome]: p < 0.001 6-OHDA [IC Secretome] vs 6-OHDA [IV Secretome]: p = 0.998	-
Weight gain *Females*	Time: $F_{(3.67, 113.6)}$ = 121.8, p < 0.001 Group: $F_{(4, 32)}$ = 0.264, p = 0.899 Time x Group: $F_{(56, 434)}$ = 2.32, p < 0.001 **Multiple comparisons** Sham vs 6-OHDA [IC Vehicle]: p = 0.739 Sham vs 6-OHDA [IC Secretome]: p = 0.287 Sham vs 6-OHDA [IV Vehicle]: p = 0.400 Sham vs 6-OHDA [IV Secretome]: p = 0.983 6-OHDA [IC Vehicle] vs 6-OHDA [IC Secretome]: p = 0.927 6-OHDA [IV Vehicle] vs 6-OHDA [IV Secretome]: p = 0.730 6-OHDA [IC Secretome] vs 6-OHDA [IV Secretome]: p = 0.581	-
Horizontal spontaneous activity *Nr of squares traveled (1min)*	**After Lesion:** χ^2= 23.93, p < 0.001 **After treatments** **1 week:** χ^2= 1.92, p = 0.7512 **4 weeks:** χ^2= 8.14, p = 0.087 **7 weeks:** χ^2= 9.12, p = 0.058	-
Gait quality	**After Lesion:** χ^2= 7.91, p = 0.095 **After treatments** **1 week:** χ^2= 6.71, p = 0.152 **4 weeks:** χ^2= 8.36, p = 0.079 **7 weeks:** χ^2= 12.00, p = 0.017	
Hindlimb tonus *Left paw*	**After Lesion:** χ^2= 6.79, p = 0.148 **After treatments** **1 week:** χ^2= 13.00, p = 0.011 **4 weeks:** χ^2= 14.28, p = 0.007 **7 weeks:** χ^2= 13.54, p = 0.0089	

*The definition of small, medium, and large effect size was applied as previously described (Sawilowsky, 2009).

Table S2. List of proteins identified in BM-MSC secretome using untargeted mass spectrometry proteomic analysis

Entry	Entry name	Protein name_UNIRPOT recommended
P24592	IBP6_HUMAN	Insulin-like growth factor-binding protein 6
P02461	CO3A1_HUMAN	Collagen alpha-1(III) chain
P99999	CYC_HUMAN	Cytochrome c
P28072	PSB6_HUMAN	Proteasome subunit beta type-6
P00738	HPT_HUMAN	Haptoglobin
P12109	CO6A1_HUMAN	Collagen alpha-1(VI) chain
P26022	PTX3_HUMAN	Pentraxin-related protein PTX3
P02751	FINC_HUMAN	Fibronectin
P20908	CO5A1_HUMAN	Collagen alpha-1(V) chain
P07195	LDHB_HUMAN	L-lactate dehydrogenase B chain
P13611	CSPG2_HUMAN	Versican core protein
P09486	SPRC_HUMAN	SPARC
P02545	LMNA_HUMAN	Prelamin-A/C
P02787	TRFE_HUMAN	Serotransferrin
Q15582	BGH3_HUMAN	Transforming growth factor-beta-induced protein ig-h3
P07585	PGS2_HUMAN	Decorin
P12110	CO6A2_HUMAN	Collagen alpha-2(VI) chain
P51884	LUM_HUMAN	Lumican
P10909	CLUS_HUMAN	Clusterin
P62987	RL40_HUMAN	Ubiquitin-60S ribosomal protein L40
P28300	LYOX_HUMAN	Protein-lysine 6-oxidase
Q01518	CAP1_HUMAN	Adenylyl cyclase-associated protein 1
P06703	S10A6_HUMAN	Protein S100-A6
P10599	THIO_HUMAN	Thioredoxin
P62937	PPIA_HUMAN	Peptidyl-prolyl cis-trans isomerase A
P01871	IGHM_HUMAN	Immunoglobulin heavy constant mu
P02679	FIBG_HUMAN	Fibrinogen gamma chain
P11021	BIP_HUMAN	Endoplasmic reticulum chaperone BiP
P22392	NDKB_HUMAN	Nucleoside diphosphate kinase B
P61604	CH10_HUMAN	10 kDa heat shock protein, mitochondrial
P0DOX5	IGG1_HUMAN	Immunoglobulin gamma-1 heavy chain
Q96AY3	FKB10_HUMAN	Peptidyl-prolyl cis-trans isomerase FKBP10

Q12841	FSTL1_HUMAN	Follistatin-related protein 1
P27348	1433T_HUMAN	14-3-3 protein theta
Q08380	LG3BP_HUMAN	Galectin-3-binding protein
P07737	PROF1_HUMAN	Profilin-1
P01034	CYTC_HUMAN	Cystatin-C
P08123	CO1A2_HUMAN	Collagen alpha-2(I) chain
P63241	IF5A1_HUMAN	Eukaryotic translation initiation factor 5A-1
P63104	1433Z_HUMAN	14-3-3 protein zeta/delta
Q16610	ECM1_HUMAN	Extracellular matrix protein 1
Q15063	POSTN_HUMAN	Periostin
P09211	GSTP1_HUMAN	Glutathione S-transferase P
P60174	TPIS_HUMAN	Triosephosphate isomerase
Q14767	LTBP2_HUMAN	Latent-transforming growth factor beta-binding protein 2
P60660	MYL6_HUMAN	Myosin light polypeptide 6
P02452	CO1A1_HUMAN	Collagen alpha-1(I) chain
P21810	PGS1_HUMAN	Biglycan
P08572	CO4A2_HUMAN	Collagen alpha-2(IV) chain
P23528	COF1_HUMAN	Cofilin-1
P01033	TIMP1_HUMAN	Metalloproteinase inhibitor 1
Q13308	PTK7_HUMAN	Inactive tyrosine-protein kinase 7
P12111	CO6A3_HUMAN	Collagen alpha-3(VI) chain
P01834	IGKC_HUMAN	Immunoglobulin kappa constant
P61769	B2MG_HUMAN	Beta-2-microglobulin
P06733	ENOA_HUMAN	Alpha-enolase
P22692	IBP4_HUMAN	Insulin-like growth factor-binding protein 4
P08670	VIME_HUMAN	Vimentin
P07996	TSP1_HUMAN	Thrombospondin-1
Q6EMK4	VASN_HUMAN	Vasorin
Q16270	IBP7_HUMAN	Insulin-like growth factor-binding protein 7
P23284	PPIB_HUMAN	Peptidyl-prolyl cis-trans isomerase B
P11142	HSP7C_HUMAN	Heat shock cognate 71 kDa protein
P07355	ANXA2_HUMAN	Annexin A2
P0DOY2	IGLC2_HUMAN	Immunoglobulin lambda constant 2
P08253	MMP2_HUMAN	72 kDa type IV collagenase
P09382	LEG1_HUMAN	Galectin-1
P05121	PAI1_HUMAN	Plasminogen activator inhibitor 1
Q00610	CLH1_HUMAN	Clathrin heavy chain 1

P06744	G6PI_HUMAN	Glucose-6-phosphate isomerase
P36222	CH3L1_HUMAN	Chitinase-3-like protein 1
P50914	RL14_HUMAN	60S ribosomal protein L14
P35579	MYH9_HUMAN	Myosin-9
P04406	G3P_HUMAN	Glyceraldehyde-3-phosphate dehydrogenase
Q06830	PRDX1_HUMAN	Peroxiredoxin-1
P59998	ARPC4_HUMAN	Actin-related protein 2/3 complex subunit 4
P14618	KPYM_HUMAN	Pyruvate kinase PKM
P09493	TPM1_HUMAN	Tropomyosin alpha-1 chain
Q5VTE0	EF1A3_HUMAN	Putative elongation factor 1-alpha-like 3
Q01995	TAGL_HUMAN	Transgelin
P62266	RS23_HUMAN	40S ribosomal protein S23
Q9BQE3	TBA1C_HUMAN	Tubulin alpha-1C chain
P01023	A2MG_HUMAN	Alpha-2-macroglobulin
P05089	ARGI1_HUMAN	Arginase-1
P02647	APOA1_HUMAN	Apolipoprotein A-I
P67936	TPM4_HUMAN	Tropomyosin alpha-4 chain
Q9BUF5	TBB6_HUMAN	Tubulin beta-6 chain
Q92616	GCN1_HUMAN	eIF-2-alpha kinase activator GCN1
P10915	HPLN1_HUMAN	Hyaluronan and proteoglycan link protein 1
Q08629	TICN1_HUMAN	Testican-1
P02766	TTHY_HUMAN	Transthyretin
P00338	LDHA_HUMAN	L-lactate dehydrogenase A chain
Q71DI3	H32_HUMAN	Histone H3.2
P63261	ACTG_HUMAN	Actin, cytoplasmic 2
P62805	H4_HUMAN	Histone H4
Q6FI13	H2A2A_HUMAN	Histone H2A type 2-A
Q9P2E9	RRBP1_HUMAN	Ribosome-binding protein 1
P84077	ARF1_HUMAN	ADP-ribosylation factor 1
P26038	MOES_HUMAN	Moesin
P08603	CFAH_HUMAN	Complement factor H
P68871	HBB_HUMAN	Hemoglobin subunit beta
P40926	MDHM_HUMAN	Malate dehydrogenase, mitochondrial
P35555	FBN1_HUMAN	Fibrillin-1
P36957	ODO2_HUMAN	Dihydrolipoyllysine-residue succinyltransferase component of 2-oxoglutarate dehydrogenase complex, mitochondrial
P12273	PIP_HUMAN	Prolactin-inducible protein
P02768	ALBU_HUMAN	Albumin

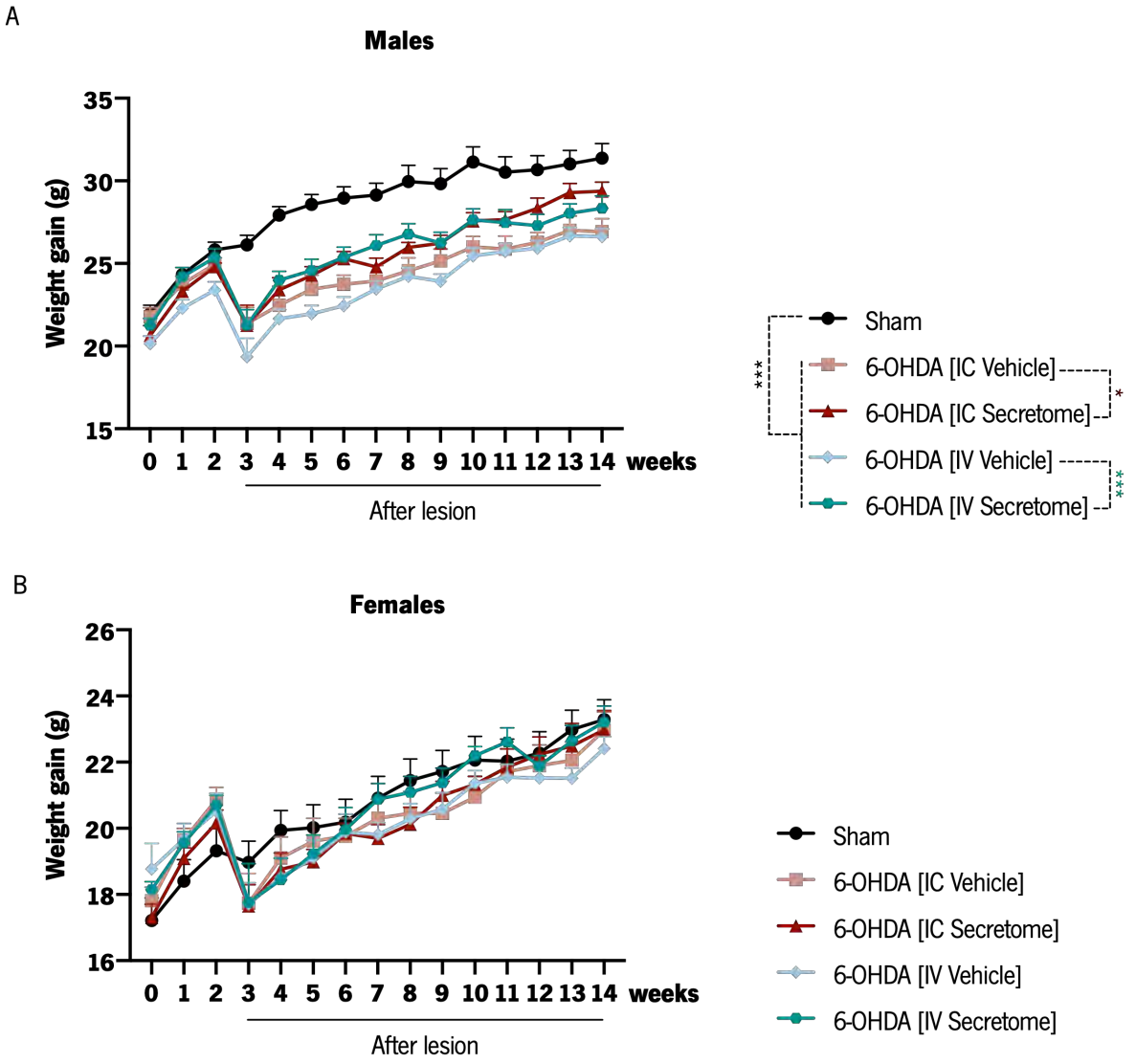


Figure S1. **Weight gain. A)** Significant differences were found in the weight gain in males after lesion (Sham vs 6-OHDA-lesioned animals), and after treatments; **B)** No significant differences were found in the weight gain for females. These results did not interfere with the motor performance of the animals on the different tasks, as observed by using the bodyweight as co-variable or splitting the data by sex (data not shown). $n_{[males]}$ = 6-9/ $n_{[females]}$ = 6-8 for each group used. Statistical summary in Table S1. Data are presented as mean ± SEM. *p < 0.05, ***p < 0.001.

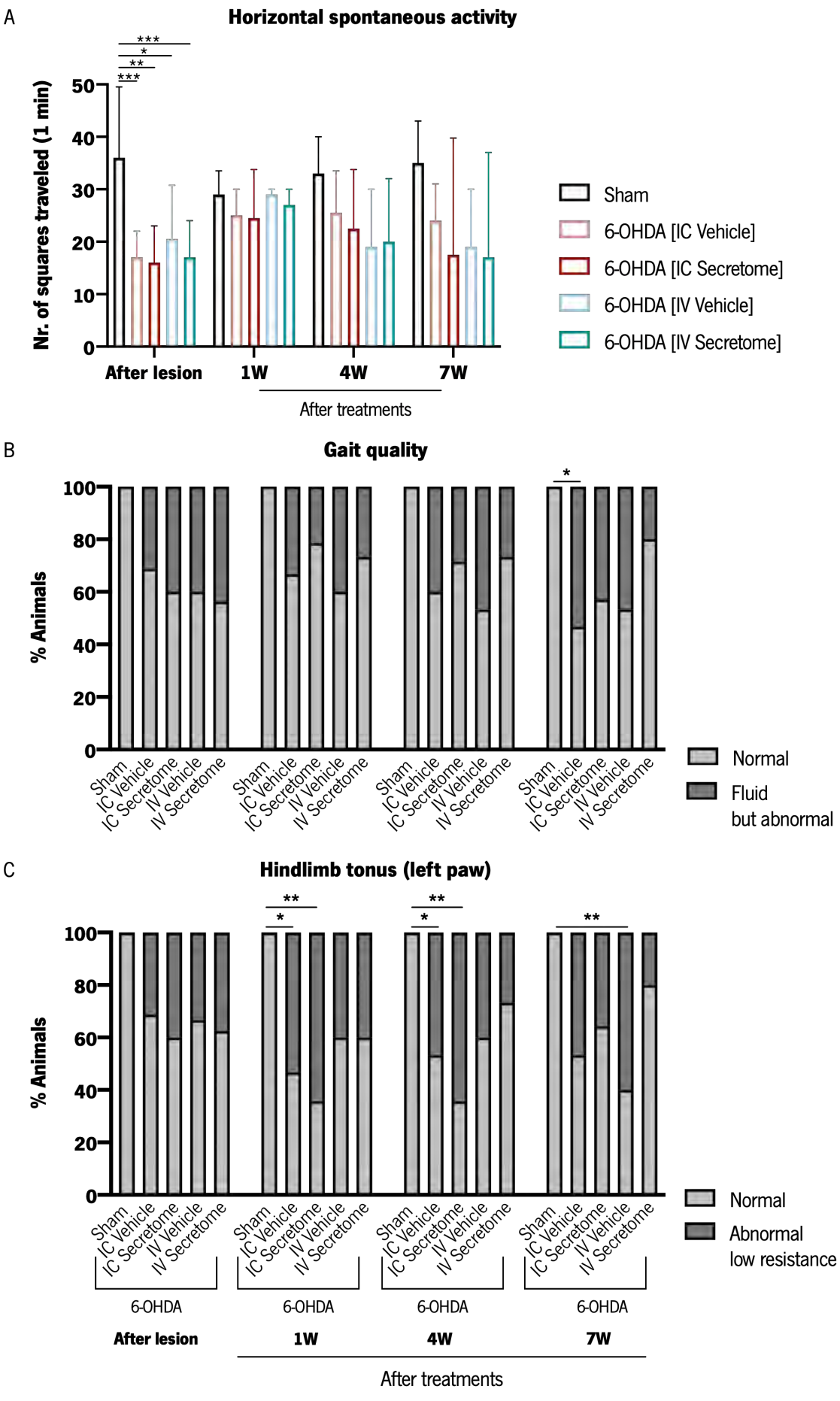

A
Horizontal spontaneous activity
Nr. of squares traveled (1 min)
50
40
30
20
10
0
***
*
**
***
After lesion
1W
4W
7W
After treatments
Sham
6-OHDA [IC Vehicle]
6-OHDA [IC Secretome]
6-OHDA [IV Vehicle]
6-OHDA [IV Secretome]
B
Gait quality
% Animals
100
80
60
40
20
0
*
Sham
IC Vehicle
IC Secretome
IV Vehicle
IV Secretome
Normal
Fluid
but abnormal
C
Hindlimb tonus (left paw)
% Animals
100
80
60
40
20
0
**
*
**
*
**
Sham
IC Vehicle
IC Secretome
IV Vehicle
IV Secretome
6-OHDA
After lesion
1W
4W
7W
After treatments
Normal
Abnormal
low resistance

Figure S2. Phenotypic parameters of the SHIRPA protocol. No major differences were found in the evaluations performed at the open arena regarding **A)** horizontal spontaneous activity and **B)** gait quality, throughout all the in vivo experiment; Some differences were found in the **C)** hindlimb tonus of the left paw (lesioned paw) between Sham group and 6-OHDA-lesioned animals at 1, 4 and 7 weeks after treatment. n = 13-15 for each group used. Statistical summary in Table S1. Data are presented as median ± IQR. *p < 0.05, **p < 0.01, ***p < 0.001.

CHAPTER 6

General discussion and future perspectives

Parkinson's disease (PD) is the second most common neurodegenerative disorder. In recent years, PD has undergone the fastest growth in prevalence and disability among neurological disorders, and it has become one of the leading causes of disability worldwide (Dorsey et al., 2018). PD is characterized by the presence of a typical motor condition comprising bradykinesia, rigidity, rest tremor, and postural instability. However, this disease goes beyond movement markers and causes a broad range of non-motor features including depression, sleep disturbances, and constipation, that take place even before clinical diagnosis (Bloem et al., 2021; Poewe et al., 2017). PD is pathologically defined by the neuronal loss at the substantia nigra *pars compacta* (SNpc), though neurodegeneration does not only affect nigral dopaminergic neurons but also cells in other areas of the neural network (Maiti et al., 2017). Because of its widespread pathology, PD is a very heterogeneous disorder, and no reliable diagnostic test is currently available. Diagnosis is based on the presence of two of the classical motor symptoms above referred, however, a definitive diagnosis requires histopathological assessment, with the identification of α-synuclein-containing Lewy bodies (LBs) (Dickson, 2018). PD is a multifactorial disease, with both genetic and environmental factors playing a role. Although the etiology of PD remains largely unknown, age is the biggest risk factor with the median age of onset being 60 years of age (Bloem et al., 2021). At the molecular and cellular level, damage to vulnerable dopaminergic neurons may arise from cellular disturbances produced by protein misfolding and aggregation, impaired proteostasis, mitochondrial dysfunction, oxidative stress, among others, that probably mutually interact to promote neuronal death (Michel et al., 2016). For more than 50 years, we have had a symptomatic therapy for the classical motor features of PD in the form of levodopa, but its long-term utility is limited by the development of motor fluctuations and dyskinesias in many patients. On the other hand, non-motor symptoms, many of which have a non-dopaminergic nature, can be particularly difficult to treat, demanding a different strategy. More importantly, current therapeutic approaches have no effect on the disease progression, which eventually results in considerable physical and cognitive dysfunction in many individuals (Fang et al., 2020).

Stem cell-based therapies are emerging as a promising option for developing a viable regenerative treatment that could benefit a significant number of patients. Although development has been slow in this sector, several interesting clinical trials have brought stem cell to a point where new approaches in PD can be envisage in the horizon (Stoker and Barker, 2020). Stem cells are immature tissue precursor cells that can self-renew, have the ability to form clonal cell populations, and differentiate into multiple

cell lineages. These unique characteristics make it particularly attractive for restoring function in a variety of tissues. The wide variety of stem cells can be classified into three categories: (i) embryonic stem cells derived from early-stage embryos; (ii) induced pluripotent stem cells (iPSCs); (iii) adult stem cells including hematopoietic stem cells, neural stem cells, and mesenchymal stem cells (MSCs) (Watt and Hogan, 2000). Among stem cell types, MSCs have low immunogenicity, little teratoma risk, minimal ethical issues, and a low likelihood of becoming tumorigenic after transplantation into the human body (Schu et al., 2012). Because of these inherent characteristics, they have been recognized as good candidates in the treatment of a variety of disorders, including PD (Liu and Cheung, 2020). MSCs can be isolated from different adult tissues, including bone marrow, adipose tissue, peripheral blood from adult tissues, Wharton's jelly of the umbilical cord from neonatal tissues, and many others (Pittenger et al., 2019). Although MSCs are found in a variety of tissues, their overall number in the body is small. Because cell therapy techniques often require hundreds of millions of MSCs per treatment, cell growth in vitro for roughly 10 weeks before implantation is required (Sotiropoulou et al., 2006). Furthermore, clinical-grade MSCs often require their transplantation prior to passage 3; however, the cell quantity at this stage is typically insufficient for transplantation (Santos et al., 2011). Moreover, the ideal culture conditions for clinical scale generation of human MSCs are influenced by the patient's age and clinical features (Duggal and Brinchmann, 2011; Sotiropoulou et al., 2006).

MSC therapeutical effects have previously been linked to their ability to engraft and differentiate into different cell types. However, several studies have found that the implantation duration of MSCs is typically too short to have a significant impact, with only 1% of MSCs surviving for more than one week following delivery (Pittenger et al., 2019; Vizoso et al., 2017). In addition to their multipotent differentiation potential, a strong paracrine capacity has been proposed as the principal mechanism that contributes to tissue repair. In fact, MSCs produce a wide range of bioactive substances, which play a crucial role in the control of a variety of physiological processes. As a result, the secretome of MSCs has gotten a lot of attention because of its potential for tissue repair and regeneration.

In this thesis, we used different *in vitro* and *in vivo* PD models to test the secretome of BM-MSCs as a source of therapeutic factors with neuroprotective potential. More specifically, in Chapter 3, we used a guided protocol approach to differentiate human neuroepithelial stem cells (hNESCs) into 3D human midbrain-specific organoids (hMOs). As a proof of concept, we recapitulate toxin-induced dopaminergic neuronal cell death in the midbrain using 6-hydroxydopamine (6-OHDA), and we also generate isogenic hMOs with DJ-1 mutation, modeling in this way different forms of PD. We demonstrated that these

organoids recapitulated key hallmarks of the PD pathology, such as reduced amounts of midbrain dopaminergic neurons and neurite fragmentation. hMOs as a novel *in vitro* model open up new avenues to unravel PD pathophysiology and holds great potential as platforms to test new therapeutic approaches that certainly will complement other model systems. For instance, DJ-1 knockout (KO) mice do not display changes in the integrity of dopaminergic neurons in the SNpc compared to the wild-type littermates (Chandran et al., 2008; Pham et al., 2010). We believe that human-specific phenotype in 3D cultures of midbrain organoids not only adds the observation that the higher dopamine (DA) metabolism observed in human neurons compared to mice contributes to the selective vulnerability of these neurons (Burbulla et al., 2017), but also this system can be extremely useful to study genetic forms of the disease over PD genetic animal models.

Although organoids display attractive features, they still present some limitations. A general problem of all organoid derivation protocols is the lack of vascular cells. Although nutrient and oxygen exchange can be improved when organoids are cultured under dynamic conditions, the core suffers from low oxygen and nutrient levels, resulting in significant cell death (Pham et al., 2018). Therefore, future research to incorporate biomaterials and microfluidic systems could be used to engineer vascular-like networks with perfusion to supply the organoid interior (Qian et al., 2019). Second, microglia are typically missing in organoids. A major feature of neurodegeneration is disruption of the central nervous system homeostasis, during which microglia play diverse roles (Xu et al., 2021). Therefore, it would be essential to incorporate microglia from the same iPSC donor. It is important to highlight that protocols for the generation of iPSC-derived microglia have been developed (Haenseler et al., 2017; Muffat et al., 2016), and very recently they were integrated into the same midbrain organoid system used in this work (Sabate-Soler et al., 2022). Another critical issue is the absence of well-defined neuronal networks between distant brain areas. PD is caused by abnormalities in the basal ganglia, therefore, it is important the creation of organoids encompassing many functional brain areas, and well-defined connectivity. The introduction of fused organoids or assembloid systems is a way to achieve this (Qian et al., 2019). This was already demonstrated by Birey and colleagues (Birey et al., 2017), where they assembled dorsal and ventral organoids to recapitulate saltatory migration of interneurons similar to fetal forebrain. More recently, a 3D system was also developed to create the reciprocal projections between the thalamus and cortex (Xiang et al., 2019). Nonetheless, in this approach the projections develop bidirectionally, contrary to the nigrostriatal projection that is a unidirectional innervation, therefore requiring high-precision microengineering approaches to guide axonal growth pathways from dopaminergic neurons (Hasan and Singh, 2019; Struzyna et al., 2018). Finally, organoids fail to model

the adult human brain. In fact, they resemble the developing human fetal cortex up to the second trimester of development (Paşca et al., 2015; Qian et al., 2016; Yoon et al., 2019). Thus, special attention should be taken into consideration when organoids are used to model age-dependent neurodegenerative diseases like PD. Some strategies could pass by overexpressing progerin in organoids (Miller et al., 2013), or use toxins to increase oxidative stress leading to DNA damage and mitochondrial dysfunction (Grenier et al., 2020). Despite these limitations, which we believe will be overcome in a near future, organoids are complex structures, containing other cell types besides dopaminergic neurons such as astrocytes and oligodendrocytes. Moreover, it was already demonstrated that they present features of neuronal maturation such as myelination, synaptic formation, spontaneous electrophysiological activity, and neural network synchronicity (Kwak et al., 2020; Monzel et al., 2017; Nickels et al., 2020; Yakoub, 2019).

To the best of our knowledge, this is the first time that the BM-MSC secretome effects were explored using this advanced *in vitro* PD models, and we observed that the secretome was capable to protect from the dopaminergic neuronal loss, as well as from induced fragmentation of dopaminergic neurites. Despite these promising results, future ameliorations can be performed on this model, not only to better dissect the mechanisms underlying dopaminergic cell death but also to perform additional molecular and functional readouts to understand which are the mechanisms behind secretome effects. For instance, 6-OHDA is described to selectively destroy dopaminergic neurons via oxidative stress and complex I inhibition (Kulich et al., 2007), and loss of DJ-1 interferes with mitochondrial function and morphology in cellular models (Dolgacheva et al., 2019). Thus, it would be interesting to explore the impact of BM-MSC secretome on mitochondrial dysfunction. Moreover, would also be interesting to do the same experiment if patient-derived hMOs with DJ-1 mutation but also with other associated mutations more frequent in PD such as LRRK2 mutation.

Although 3D cell culture modes like brain organoids are extremely important for biomedical research, offering unprecedented opportunities for understanding the mechanisms underlying PD and to develop new therapies, in the PD field it is undeniable that studies and findings in animal models have played a key role in the development of the treatments that are used today. For example, the development of levodopa resulted from observations in reserpine-treated rats and rabbits; studies in rodent neurotoxin models prompted the development of DA receptor agonists; and the identification of the subthalamic nucleus for deep-brain stimulation therapy was based on functional analysis of basal ganglia circuitry, which was carried out in 1-methyl-4-phenyl-1,2,3,6-tetrahydropyridine (MPTP)-treated monkeys (Duty

and Jenner, 2011). One of the most extensively used approaches for mimicking PD in rodents is the 6-OHDA lesion. Despite being widely used in rats, reproducing a similar injury in mice can be difficult (Heuer et al., 2012; Smith and Heuer, 2011). Furthermore, there is a lack of characterization of the extent of behavioral deficits and of the neuronal loss/neurotransmitter system in unilateral lesion mouse models. In Chapter 4, we aimed to perform an extensive behavioral and histological characterization of a unilateral intrastriatal 6-OHDA mouse model. The results confirm the utility of this model to recapitulate some of the key aspects of PD besides motor deficits and dopaminergic loss in the nigrostriatal pathway, such as non-motor symptoms and glial cell responses. We then used this model to further evaluate the effects of BM-MSC secretome making a direct comparison between intracerebral injections (single administration) with multiple systemic administration. The BM-MSC secretome led to motor function recovery and dopaminergic loss protection, however, multiple systemic administrations showed a higher magnitude therapeutical effect. This result is clinically relevant because the possibility of delivering MSC secretome in a non-invasive way is very advantageous from the clinical application point of view. Important of note is the fact that we observed a stronger impact of secretome effects on the 6-OHDA *in vivo* model when compared to the 6-OHDA *in vitro* model using midbrain organoids. Moreover, the systemic administration on the *in vivo* experiment had a higher impact on the animal's motor recovery over the histological outcomes regarding dopaminergic neurons in the lesioned areas. Thus, we hypothesized that this differential neuroprotective outcome result from an indirect effect of MSCs secretome on dopaminergic neurons.

For instance, the 6-OHDA animal model has been shown to display neuroinflammation (Fricke et al., 2016). Accordingly, in our 6-OHDA PD mouse model characterization we identified a marked astrocytic reaction, and proliferative and reactive microglia in lesioned areas, that persisted even after 14 weeks after lesion surgery. Moreover, MSC secretome has been demonstrated to modulate astrocyte and microglia activity (Baez-Jurado et al., 2019; Campos et al., 2020; Pinho et al., 2022); therefore, it would be important to study if glial cells are important mediators of secretome-induced effects in our model. Moreover, the impact that the systemic injections were having on peripheral organs remains to be answered. Organs such as the liver and spleen are important mediators of systemic metabolic, inflammatory, and immune responses, and therefore, modulation of their functions might also lead to beneficial outcomes in PD.

Current animal models of PD focus on the degeneration of dopaminergic nigrostriatal neurons and the formation of α-synuclein aggregates, but many lack one or the other. In fact, none of the available

animal models perfectly mimic PD neuropathology and cannot replicate the clinical syndrome observed in humans (Konnova and Swanberg, 2018). However, the large diversity of non-human primates, rodent, and non-mammalian models allows targeted studies of different pathological mechanisms of PD. Because a clinical PD diagnosis reflects a heterogeneous group of patients with differences in the onset, progression, symptoms, and neuropathology, the heterogeneity of these models might be viewed as a benefit (Konnova and Swanberg, 2018). Diversifying the animal models can help understand various subtypes of PD and create personalized treatments. Furthermore, considering our promising results regarding DJ-1 genetic model using hMOs and the ones obtained with the 6-OHDA mouse model, it could be interesting in the future the use of a combined PD model. Combined models, in which a neurotoxin is administered to genetically manipulated animals, have recently begun to be used (Kin et al., 2019). These models are based on the fact that some genetic models are more susceptible to neurotoxins. For instance, it was already shown that MPTP and 6-OHDA induced more neuronal loss and increases vulnerability in DJ-1 KO mice, respectively, in comparison with wild-type mice (Kim et al., 2005; Lev et al., 2013). Conducting research with this kind of models enhance PD hallmarks by hitting disease-associated pathways at several levels.

Although the research regarding the impact of stem cell secretome on neurodegenerative disorders is still scarse, several experimental studies already demonstrated the positive effects of the MSC secretome-derived products using different *in vitro* and *in vivo* models of PD (D'angelo et al., 2020). Furthermore, as presented in this thesis and previous studies from our group (Mendes-Pinheiro et al., 2019; Teixeira et al., 2020, 2017; Vilaça-Faria et al., 2021), BM-MSC secretome administration has consistently protected dopaminergic neurons from 6-OHDA-induced cell death accompanied by motor functional recovery, reinforcing their potential role in reducing neurodegeneration in PD patients. Likewise the neuroprotective and neuroregenerative effects, MSC secretome has also been shown to stimulate neurogenesis (Cova et al., 2010; Schwerk et al., 2015a, 2015b), degrade α-synuclein aggregates and inhibition of its transmission (Marques et al., 2021; Oh et al., 2017, 2016), and decrease neuroinflammation (Danielyan et al., 2011; Kim et al., 2009; Suzuki et al., 2015). Thus, the diversity of factors found in MSC secretome may play a role not only on dopaminergic neuronal survival but also on other pathways behind PD pathogenesis, allowing for a multitargeted approach to prevent PD-related neurodegeneration. Nonetheless, the composition and effects of the secretome differ based on MSC anatomical origin, suggesting the need to select the most appropriate MSC source taking into account the secretome application (Assunção-Silva et al., 2018; Pires et al., 2016; Vizoso et al., 2017). This fact allied to other issues such as tissue-derived MSC number, quality, and proliferative capacity

that are dependent on donor's age, raises some problems in terms of standardization and reproducibility of this therapeutical approach. For instance, the generation of MSCs from iPSCs (iMSCs) have been recently put forward as a promising alternative source for obtain large populations of MSC-like cells avoiding some of the issues associated with tissue-derived MSCs. Accessibility (iPSCs are generated form minimal invasive somatic cell sources), and the higher proliferative capacity allowing a superior expansion for the collection of larger amounts of secretome from the same donor, are some of the technical advantages of iMSCs (Hynes et al., 2014; Sabapathy and Kumar, 2016). Moreover, our lab already demonstrated a similar paracrine potential between BM-MSCs and iMSCs in attenuating 6-OHDA induced nigrostriatal degeneration and the resultant motor deficits (Marote et al., in preparation). Although many questions still need to be addressed, iMSCs should be considered as an alternative source of secretome for research and clinical use.

An additional drawback besides the isolation and expansion protocols that varies between laboratories, is the type of media formulation used to culture MSCs. Different medium formulations especially animal-derived supplements (e.g., fetal bovine serum (FBS)) used in MSC manufacturing, may lead to clinical complications and data misinterpretation. Moreover, to use MSCs or their products in the clinics, precise thorough characteristics, large-scale quality, and relatively low-cost production of clinical-grade MSC need to be developed in xeno-free media (Czapla et al., 2019). A good FBS substitute for clinical good manufacturing practice (GMP) production should have a well-defined composition, a reduced degree of contaminants and no risk of xenogeneic compound transmission, cheap production costs, easy availability, and no ethical concerns (Cimino et al., 2017). The majority of these requirements are met by human platelet lysate (hPL) (Burnouf et al., 2016). Results from our group showed that hPL supplementation induced high proliferation from BM-MSCs without affecting their identity (unpublished data). Moreover, in Chapter 5, in which BM-MSCs were expanded *in vitro* using hPL as a supplement, our proteomic analysis revealed a similar secretory profile in comparison with our previous studies using FBS or serum-free media (Assunção-Silva et al., 2018; Mendes-Pinheiro et al., 2019; Pires et al., 2016; Teixeira et al., 2017).

Throughout this work, we also collect secretome from MSCs expanded on the conventional static culture system (i.e., tissue culture flasks). They are cost efficient and easy to operate; however, large quantities of homogeneous high-quality cells are needed for clinical applications, which is not feasible using the traditional methods (McKee and Chaudhry, 2017; Panchalingam et al., 2015). A valid alternative to static cultures is the use of bioreactors, that allow for the reduction of labor and enable

more space-effective production (Panchalingam et al., 2015). Moreover, MSC secretome profile is influenced by the stimuli they receive from the microenvironment. In fact, some studies already demonstrated that the use of bioreactors enhance the neuroregulatory profile of MSC secretome (Hupfeld et al., 2014; Teixeira et al., 2016; Tsai et al., 2020).

Overall, we can state that the work performed and included in this thesis provided interesting approaches regarding the potential use of MSC secretome in PD field. Although more research needs to be done regarding MSC standardization and characterization of secretome composition, it is pretty clear that the use of secretome avoid the problems derived from using MSCs themselves or other types of stem cells, such as i) safety problems derived from transplantation like tumorigenicity, emboli formation, transmissible infections, and the potential entry of cell senescence; ii) can be stored without the use of potentially toxic cryopreservative agents; iii) can be better evaluated in terms of safety and dose; and iv) it is cheaper and practical for clinical use because the secretome could eliminate the time and costs related with expansion and maintenance of clonal cell lines (D'angelo et al., 2020; Fernández-Francos et al., 2021; Marques et al., 2018; Vizoso et al., 2017).

A neuroprotective or disease-modifying therapy that can slow or stop disease progression is the major unmet medical need in the treatment of PD. One of the major obstacles to define a neuroprotective therapy PD include the uncertainty about PD causes and specifically what to target. Moreover, it is increasingly clear that PD is a heterogeneous condition, with clinical subtypes emerging (Marras and Lang, 2013), emphasizing the need for personalized management. Therefore, it would be interesting the determination of the optimal patient group to create a new and useful cell-free therapeutic approach towards a robust clinical outcome for PD patients. For that, unifying efforts between clinical and experimental research are needed to address this complex neurodegenerative disease.

References

Assunção-Silva RC, Mendes-Pinheiro B, Patrício P, Behie LA, Teixeira FG, Pinto L, Salgado AJ. 2018. Exploiting the impact of the secretome of MSCs isolated from different tissue sources on neuronal differentiation and axonal growth. *Biochimie* **155**:83–91. doi:10.1016/j.biochi.2018.07.026

Baez-Jurado E, Hidaldo-Lanussa O, Barrera-Bailón B, Sahebkar A, Md Ashraf G, Echeverria V, Barreto GE. 2019. Secretome of mesenhcymal stem cells and its potential protective effects on brain pathologies. *Mol Neurobiol* **56**:6902-6927. doi: 10.1007/s12035-019-1570-x

Birey F, Andersen J, Makinson CD, Islam S, Wei W, Huber N, Fan HC, Metzler KRC, Panagiotakos G,

Thom N, O'Rourke NA, Steinmetz LM, Bernstein JA, Hallmayer J, Huguenard JR, Pasca SP. 2017. Assembly of functionally integrated human forebrain spheroids. *Nature* **545**:54–59. doi:10.1038/nature22330

Bloem BR, Okun MS, Klein C. 2021. Parkinson's disease. *Lancet* **397**:2284–2303. doi:10.1016/S0140-6736(21)00218-X

Burbulla LF, Song P, Mazzulli JR, Zampese E, Wong YC, Jeon S, Santos DP, Blanz J, Obermaier CD, Strojny C, Savas JN, Kiskinis E, Zhuang X, Krüger R, Surmeier DJ, Krainc D. 2017. Dopamine oxidation mediates mitochondrial and lysosomal dysfunction in Parkinson's disease. *Science* **357**:1255–1261. doi:10.1126/science.aam9080

Burnouf T, Strunk D, Koh MBC, Schallmoser K. 2016. Human platelet lysate: Replacing fetal bovine serum as a gold standard for human cell propagation? *Biomaterials* **76**:371–387. doi:10.1016/j.biomaterials.2015.10.065

Campos J, Guerra-Gomes S, Serra SC, Baltazat G, Oliveira JF, Teixeira FG, Salgado AJ. 2020. Astrocyte signaling impacts the effects of human bone marrow mesenchymal stem cells secretome application into the hippocampus: A proliferation and morphometrical analysis on astrocytic cell populations. *Brain Res* **1732**:146700. doi: 10.1016/j.brainres.2020.146700

Chandran JS, Lin X, Zapata A, Höke A, Shimoji M, Moore SOL, Galloway MP, Laird FM, Wong PC, Price DL, Bailey KR, Crawley JN, Shippenberg T, Cai H. 2008. Progressive behavioral deficits in DJ-1-deficient mice are associated with normal nigrostriatal function. *Neurobiol Dis* **29**:505–514. doi:10.1016/j.nbd.2007.11.011

Cimino M, Gonçalves RM, Barrias CC, Martins MCL. 2017. Xeno-Free Strategies for Safe Human Mesenchymal Stem/Stromal Cell Expansion: Supplements and Coatings. *Stem Cells Int* **2017**:6597815. doi:10.1155/2017/6597815

Cova L, Armentero M-T, Zennaro E, Calzarossa C, Bossolasco P, Busca G, Lambertenghi Deliliers G, Polli E, Nappi G, Silani V, Blandini F. 2010. Multiple neurogenic and neurorescue effects of human mesenchymal stem cell after transplantation in an experimental model of Parkinson's disease. *Brain Res* **1311**:12–27. doi:10.1016/j.brainres.2009.11.041

Czapla J, Matuszczak S, Kulik K, Wiśniewska E, Pilny E, Jarosz-Biej M, Smolarczyk R, Sirek T, Zembala MO, Zembala M, Szala S, Cichoń T. 2019. The effect of culture media on large-scale expansion and characteristic of adipose tissue-derived mesenchymal stromal cells. *Stem Cell Res Ther* **10**:235. doi:10.1186/s13287-019-1331-9

D'angelo M, Cimini A, Castelli V. 2020. Insights into the effects of mesenchymal stem cell-derived

secretome in Parkinson's disease. *Int J Mol Sci* **21**:5241. doi:10.3390/ijms21155241

Danielyan L, Schafer R, von Ameln-Mayerhofer A, Bernhard F, Verleysdonk S, Buadze M, Lourhmati A, Klopfer T, Schaumann F, Schmid B, Koehle C, Proksch B, Weissert R, Reichardt HM, van den Brandt J, Buniatian GH, Schwab M, Gleiter CH, Frey 2nd WH. 2011. Therapeutic efficacy of intranasally delivered mesenchymal stem cells in a rat model of Parkinson disease. *Rejuvenation Res* **14**:3–16. doi:10.1089/rej.2010.1130

Dickson DW. 2018. Neuropathology of Parkinson disease. *Parkinsonism Relat Disord* **46**:S30–S33. doi:10.1016/j.parkreldis.2017.07.033

Dolgacheva LP, Berezhnov A V., Fedotova EI, Zinchenko VP, Abramov AY. 2019. Role of DJ-1 in the mechanism of pathogenesis of Parkinson's disease. *J Bioenerg Biomembr* **51**:175–188. doi:10.1007/s10863-019-09798-4

Dorsey ER, Sherer T, Okun MS, Bloem BR. 2018. The Emerging Evidence of the Parkinson Pandemic. *J Parkinsons Dis* **8**:S3–S8. doi:10.3233/JPD-181474

Duggal S, Brinchmann JE. 2011. Importance of serum source for the in vitro replicative senescence of human bone marrow derived mesenchymal stem cells. *J Cell Physiol* **226**:2908–2915. doi:10.1002/jcp.22637

Duty S, Jenner P. 2011. Animal models of Parkinson's disease: a source of novel treatments and clues to the cause of the disease. *Br J Pharmacol* **164**:1357–1391. doi:10.1111/j.1476-5381.2011.01426.x

Fang C, Lv L, Mao S, Dong H, Liu B. 2020. Cognition Deficits in Parkinson's Disease: Mechanisms and Treatment. *Parkinsons Dis* **2020**:2076942. doi:10.1155/2020/2076942

Fernández-Francos S, Eiro N, Costa LA, Escudero-Cernuda S, Fernández-Sánchez ML, Vizoso FJ. 2021. Mesenchymal Stem Cells as a Cornerstone in a Galaxy of Intercellular Signals: Basis for a New Era of Medicine. *Int J Mol Sci* **22**:3576. doi:10.3390/ijms22073576

Fricke IB, Viel T, Worlitzer MM, Collmann FM, Vrachimis A, Faust A, Wachsmuth L, Faber C, Dollé F, Kuhlmann MT, Schäfers K, Hermann S, Schwamborn JC, Jacobs AH. 2016. 6-hydroxydopamine-induced Parkinson's disease-like degeneration generates acute microgliosis and astrogliosis in the nigrostriatal system but no bioluminescence imaging-detectable alteration in adult neurogenesis. *Eur J Neurosci* **43**:1352–1365. doi:10.1111/ejn.13232

Grenier K, Kao J, Diamandis P. 2020. Three-dimensional modeling of human neurodegeneration: brain organoids coming of age. *Mol Psychiatry* **25**:254–274. doi:10.1038/s41380-019-0500-7

Haenseler W, Sansom SN, Buchrieser J, Newey SE, Moore CS, Nicholls FJ, Chintawar S, Schnell C,

Antel JP, Allen ND, Cader MZ, Wade-Martins R, James WS, Cowley SA. 2017. A Highly Efficient Human Pluripotent Stem Cell Microglia Model Displays a Neuronal-Co-culture-Specific Expression Profile and Inflammatory Response. *Stem Cell Reports* **8**:1727–1742. doi:10.1016/j.stemcr.2017.05.017

Hasan U, Singh SK. 2019. The Astrocyte–Neuron Interface: An Overview on Molecular and Cellular Dynamics Controlling Formation and Maintenance of the Tripartite SynapseMethods in Molecular Biology. pp. 3–18. doi:10.1007/978-1-4939-9068-9_1

Heuer A, Smith GA, Lelos MJ, Lane EL, Dunnett SB. 2012. Unilateral nigrostriatal 6-hydroxydopamine lesions in mice I: Motor impairments identify extent of dopamine depletion at three different lesion sites. *Behav Brain Res* **228**:30–43. doi:10.1016/j.bbr.2011.11.027

Hupfeld J, Gorr IH, Schwald C, Beaucamp N, Wiechmann K, Kuentzer K, Huss R, Rieger B, Neubauer M, Wegmeyer H. 2014. Modulation of mesenchymal stromal cell characteristics by microcarrier culture in bioreactors. *Biotechnol Bioeng* **111**:2290–2302. doi:10.1002/bit.25281

Hynes K, Menicanin D, Mrozik K, Gronthos S, Bartold PM. 2014. Generation of functional mesenchymal stem cells from different induced pluripotent stem cell lines. *Stem Cells Dev* **23**:1084–1096. doi:10.1089/scd.2013.0111

Kim RH, Smith PD, Aleyasin H, Hayley S, Mount MP, Pownall S, Wakeham A, You-Ten AJ, Kalia SK, Horne P, Westaway D, Lozano AM, Anisman H, Park DS, Mak TW. 2005. Hypersensitivity of DJ-1-deficient mice to 1-methyl-4-phenyl-1,2,3,6-tetrahydropyrindine (MPTP) and oxidative stress. *Proc Natl Acad Sci* **102**:5215–5220. doi:10.1073/pnas.0501282102

Kim Y-J, Park H-J, Lee G, Bang OY, Ahn YH, Joe E, Kim HO, Lee PH. 2009. Neuroprotective effects of human mesenchymal stem cells on dopaminergic neurons through anti-inflammatory action. *Glia* **57**:13–23. doi:10.1002/glia.20731

Kin K, Yasuhara T, Kameda M, Date I. 2019. Animal Models for Parkinson's Disease Research: Trends in the 2000s. *Int J Mol Sci* **20**:5402. doi:10.3390/ijms20215402

Konnova EA, Swanberg M. 2018. Animal Models of Parkinson's Disease In: Stoker TB, Greenland JC, editors. Parkinson's Disease: Pathogenesis and Clinical Aspects. Codon Publications. pp. 83–106. doi:10.15586/codonpublications.parkinsonsdisease.2018.ch5

Kulich SM, Horbinski C, Patel M, Chu CT. 2007. 6-Hydroxydopamine induces mitochondrial ERK activation. *Free Radic Biol Med* **43**:372–383. doi:10.1016/j.freeradbiomed.2007.04.028

Kwak TH, Kang JH, Hali S, Kim J, Kim KP, Park C, Lee JH, Ryu HK, Na JE, Jo J, Je HS, Ng HH, Kwon J, Kim NH, Hong KH, Sun W, Chung CH, Rhyu IJ, Han DW. 2020. Generation of homogeneous

midbrain organoids with in vivo-like cellular composition facilitates neurotoxin-based Parkinson's disease modeling. *Stem Cells* **38**:727–740. doi:10.1002/stem.3163

Lev N, Barhum Y, Ben-Zur T, Melamed E, Steiner I, Offen D. 2013. Knocking out DJ-1 attenuates astrocytes neuroprotection against 6-hydroxydopamine toxicity. *J Mol Neurosci* **50**:542–550. doi:10.1007/s12031-013-9984-9

Liu Z, Cheung H-H. 2020. Stem Cell-Based Therapies for Parkinson Disease. *Int J Mol Sci* **21**:8060. doi:10.3390/ijms21218060

Maiti P, Manna J, Dunbar GL. 2017. Current understanding of the molecular mechanisms in Parkinson's disease: Targets for potential treatments. *Transl Neurodegener* **6**:28. doi:10.1186/s40035-017-0099-z

Marote A, Mendes-Pinheiro B, Pinto L, Salgado AJ. Compositions for Therapy or Treatment of Parkinson's Disease, Methods and Uses Thereof. WO/2021/198927, Mar. 30, 2020.

Marques CR, Marote A, Mendes-Pinheiro B, Teixeira FG, Salgado AJ. 2018. Cell secretome based approaches in Parkinson's disease regenerative medicine. *Expert Opin Biol Ther* **18**:1235–1245. doi:10.1080/14712598.2018.1546840

Marques CR, Pereira-Sousa J, Teixeira FG, Sousa RA, Teixeira-Castro A, Salgado AJ. 2021. Mesenchymal stem cell secretome protects against alpha-synuclein-induced neurodegeneration in a Caenorhabditis elegans model of Parkinson's disease. *Cytotherapy* **23**:894–901. doi:10.1016/j.jcyt.2021.04.002

Marras C, Lang A. 2013. Parkinson's disease subtypes: lost in translation? *J Neurol Neurosurg Psychiatry* **84**:409–415. doi:10.1136/jnnp-2012-303455

McKee C, Chaudhry GR. 2017. Advances and challenges in stem cell culture. *Colloids Surfaces B Biointerfaces* **159**:62–77. doi:10.1016/j.colsurfb.2017.07.051

Mendes-Pinheiro B, Anjo SI, Manadas B, Da Silva JD, Marote A, Behie LA, Teixeira FG, Salgado AJ. 2019. Bone Marrow Mesenchymal Stem Cells' Secretome Exerts Neuroprotective Effects in a Parkinson's Disease Rat Model. *Front Bioeng Biotechnol* **7**:294. doi:10.3389/fbioe.2019.00294

Michel PP, Hirsch EC, Hunot S. 2016. Understanding Dopaminergic Cell Death Pathways in Parkinson Disease. *Neuron* **90**:675–691. doi:10.1016/j.neuron.2016.03.038

Miller JD, Ganat YM, Kishinevsky S, Bowman RL, Liu B, Tu EY, Mandal PK, Vera E, Shim J, Kriks S, Taldone T, Fusaki N, Tomishima MJ, Krainc D, Milner TA, Rossi DJ, Studer L. 2013. Human iPSC-Based Modeling of Late-Onset Disease via Progerin-Induced Aging. *Cell Stem Cell* **13**:691–705. doi:10.1016/j.stem.2013.11.006

Monzel AS, Smits LM, Hemmer K, Hachi S, Moreno EL, van Wuellen T, Jarazo J, Walter J, Brüggemann I, Boussaad I, Berger E, Fleming RMT, Bolognin S, Schwamborn JC. 2017. Derivation of Human Midbrain-Specific Organoids from Neuroepithelial Stem Cells. *Stem Cell Reports* **8**:1144–1154. doi:10.1016/j.stemcr.2017.03.010

Muffat J, Li Y, Yuan B, Mitalipova M, Omer A, Corcoran S, Bakiasi G, Tsai L-H, Aubourg P, Ransohoff RM, Jaenisch R. 2016. Efficient derivation of microglia-like cells from human pluripotent stem cells. *Nat Med* **22**:1358–1367. doi:10.1038/nm.4189

Nickels SL, Modamio J, Mendes-Pinheiro B, Monzel AS, Betsou F, Schwamborn JC. 2020. Reproducible generation of human midbrain organoids for in vitro modeling of Parkinson's disease. *Stem Cell Res* **46**:101870. doi:10.1016/j.scr.2020.101870

Oh SH, Kim HN, Park HJ, Shin JY, Bae EJ, Sunwoo MK, Lee SJ, Lee PH. 2016. Mesenchymal Stem Cells Inhibit Transmission of α-Synuclein by Modulating Clathrin-Mediated Endocytosis in a Parkinsonian Model. *Cell Rep* **14**:835–849. doi:10.1016/j.celrep.2015.12.075

Oh SH, Kim HN, Park HJ, Shin JY, Kim DY, Lee PH. 2017. The Cleavage Effect of Mesenchymal Stem Cell and Its Derived Matrix Metalloproteinase-2 on Extracellular α-Synuclein Aggregates in Parkinsonian Models. *Stem Cells Transl Med* **6**:949–961. doi:10.5966/sctm.2016-0111

Panchalingam KM, Jung S, Rosenberg L, Behie LA. 2015. Bioprocessing strategies for the large-scale production of human mesenchymal stem cells: a review. *Stem Cell Res Ther* **6**:225. doi:10.1186/s13287-015-0228-5

Paşca AM, Sloan SA, Clarke LE, Tian Y, Makinson CD, Huber N, Kim CH, Park J-Y, O'Rourke NA, Nguyen KD, Smith SJ, Huguenard JR, Geschwind DH, Barres BA, Paşca SP. 2015. Functional cortical neurons and astrocytes from human pluripotent stem cells in 3D culture. *Nat Methods* **12**:671–678. doi:10.1038/nmeth.3415

Pham MT, Pollock KM, Rose MD, Cary WA, Stewart HR, Zhou P, Nolta JA, Waldau B. 2018. Generation of human vascularized brain organoids. *Neuroreport* **29**:588–593. doi:10.1097/WNR.0000000000001014

Pham TT, Giesert F, Röthig A, Floss T, Kallnik M, Weindl K, Hölter SM, Ahting U, Prokisch H, Becker L, Klopstock T, Hrabé De Angelis M, Beyer K, Görner K, Kahle PJ, Vogt Weisenhorn DM, Wurst W. 2010. DJ-1-deficient mice show less TH-positive neurons in the ventral tegmental area and exhibit non-motoric behavioural impairments. *Genes, Brain Behav* **9**:305–317. doi:10.1111/j.1601-183X.2009.00559.x

Pinho AG, Cibrão JR, Lima R, Gomes ED, Serra SC, Lentilhas-Graça J, Ribeiro C, Lanceros-Mendez S,

Teixeira FG, Monteiro S, Silva NA, Salgado AJ. 2022. Immunomodulatory and regenerative effects of the full and fractioned adipose tissue derived stem cells secretome in spinal cord injury. *Exp Neurol* 113989. doi: 10.1016/j.expneurol.2022.113989.

Pires AO, Mendes-Pinheiro B, Teixeira FG, Anjo SI, Ribeiro-Samy S, Gomes ED, Serra SC, Silva NA, Manadas B, Sousa N, Salgado AJ. 2016. Unveiling the Differences of Secretome of Human Bone Marrow Mesenchymal Stem Cells, Adipose Tissue-Derived Stem Cells, and Human Umbilical Cord Perivascular Cells: A Proteomic Analysis. *Stem Cells Dev* **25**:1073–1083. doi:10.1089/scd.2016.0048

Pittenger MF, Discher DE, Péault BM, Phinney DG, Hare JM, Caplan AI. 2019. Mesenchymal stem cell perspective: cell biology to clinical progress. *npj Regen Med* **4**:22. doi:10.1038/s41536-019-0083-6

Poewe W, Seppi K, Tanner CM, Halliday GM, Brundin P, Volkmann J, Schrag A-E, Lang AE. 2017. Parkinson disease. *Nat Rev Dis Prim* **3**:17013. doi:10.1038/nrdp.2017.13

Qian X, Nguyen HN, Song MM, Hadiono C, Ogden SC, Hammack C, Yao B, Hamersky GR, Jacob F, Zhong C, Yoon K, Jeang W, Lin L, Li Y, Thakor J, Berg DA, Zhang C, Kang E, Chickering M, Nauen D, Ho C-Y, Wen Z, Christian KM, Shi P-Y, Maher BJ, Wu H, Jin P, Tang H, Song H, Ming G. 2016. Brain-Region-Specific Organoids Using Mini-bioreactors for Modeling ZIKV Exposure. *Cell* **165**:1238–1254. doi:10.1016/j.cell.2016.04.032

Qian X, Song H, Ming G. 2019. Brain organoids: advances, applications and challenges. *Development* **146**:dev166074. doi:10.1242/dev.166074

Sabapathy V, Kumar S. 2016. hiPSC-derived iMSCs: NextGen MSCs as an advanced therapeutically active cell resource for regenerative medicine. *J Cell Mol Med* **20**:1571–1588. doi:10.1111/jcmm.12839

Sabate-Soler S, Nickels SL, Saraiva C, Berger E, Dubonyte U, Barmpa K, Lan YJ, Kouno T, Jarazo J, Robertson G, Sharif J, Koseki H, Thome C, Shin JW, Cowley SA, Schwamborn JC. 2022. Microglia integration into human midbrain organoids leads to increased neuronal maturation and functionality. *bioRxiv* 2022.01.21.477192. doi:10.1101/2022.01.21.477192

Santos F Dos, Andrade PZ, Abecasis MM, Gimble JM, Chase LG, Campbell AM, Boucher S, Vemuri MC, Silva CL Da, Cabral JMS. 2011. Toward a clinical-grade expansion of mesenchymal stem cells from human sources: A microcarrier-based culture system under xeno-free conditions. *Tissue Eng - Part C Methods* **17**:1201–1210. doi:10.1089/ten.tec.2011.0255

Schu S, Nosov M, O'Flynn L, Shaw G, Treacy O, Barry F, Murphy M, O'Brien T, Ritter T. 2012.

Immunogenicity of allogeneic mesenchymal stem cells. *J Cell Mol Med* **16**:2094–2103. doi:10.1111/j.1582-4934.2011.01509.x

Schwerk A, Altschüler J, Roch M, Gossen M, Winter C, Berg J, Kurtz A, Akyüz L, Steiner B. 2015a. Adipose-derived human mesenchymal stem cells induce long-term neurogenic and anti-inflammatory effects and improve cognitive but not motor performance in a rat model of Parkinson's disease. *Regen Med* **10**:431–446. doi:10.2217/rme.15.17

Schwerk A, Altschüler J, Roch M, Gossen M, Winter C, Berg J, Kurtz A, Steiner B. 2015b. Human adipose-derived mesenchymal stromal cells increase endogenous neurogenesis in the rat subventricular zone acutely after 6-hydroxydopamine lesioning. *Cytotherapy* **17**:199–214. doi:10.1016/j.jcyt.2014.09.005

Smith GA, Heuer A. 2011. 6-OHDA Toxin Model in Mouse In Walz W, editor. Neuromethods: Volume 61, Animal Models of Movement Disorders. Human Press. pp. 281–297. doi:10.1007/978-1-61779-298-4_14

Sotiropoulou PA, Perez SA, Salagianni M, Baxevanis CN, Papamichail M. 2006. Characterization of the Optimal Culture Conditions for Clinical Scale Production of Human Mesenchymal Stem Cells. *Stem Cells* **24**:462–471. doi:10.1634/stemcells.2004-0331

Stoker TB, Barker RA. 2020. Recent developments in the treatment of Parkinson's Disease. *F1000Research* **9**:1–12. doi:10.12688/f1000research.25634.1

Struzyna LA, Browne KD, Brodnik ZD, Burrell JC, Harris JP, Chen HI, Wolf JA, Panzer K V, Lim J, Duda JE, España RA, Cullen DK. 2018. Tissue engineered nigrostriatal pathway for treatment of Parkinson's disease. *J Tissue Eng Regen Med* **12**:1702–1716. doi:10.1002/term.2698

Suzuki S, Kawamata J, Iwahara N, Matsumura A, Hisahara S, Matsushita T, Sasaki M, Honmou O, Shimohama S. 2015. Intravenous mesenchymal stem cell administration exhibits therapeutic effects against 6-hydroxydopamine-induced dopaminergic neurodegeneration and glial activation in rats. *Neurosci Lett* **584**:276–281. doi:10.1016/j.neulet.2014.10.039

Teixeira FG, Carvalho MM, Panchalingam KM, Rodrigues AJ, Mendes-Pinheiro B, Anjo S, Manadas B, Behie LA, Sousa N, Salgado AJ. 2017. Impact of the Secretome of Human Mesenchymal Stem Cells on Brain Structure and Animal Behavior in a Rat Model of Parkinson's Disease. *Stem Cells Transl Med* **6**:634–646. doi:10.5966/sctm.2016-0071

Teixeira FG, Panchalingam KM, Assunção-Silva R, Serra SC, Mendes-Pinheiro B, Patrício P, Jung S, Anjo SI, Manadas B, Pinto L, Sousa N, Behie LA, Salgado AJ. 2016. Modulation of the Mesenchymal Stem Cell Secretome Using Computer-Controlled Bioreactors: Impact on Neuronal

Cell Proliferation, Survival and Differentiation. *Sci Rep* **6**:27791. doi:10.1038/srep27791

Teixeira FG, Vilaça-Faria H, Domingues A V., Campos J, Salgado AJ. 2020. Preclinical Comparison of Stem Cells Secretome and Levodopa Application in a 6-Hydroxydopamine Rat Model of Parkinson's Disease. *Cells* **9**:315. doi:10.3390/cells9020315

Tsai A-C, Jeske R, Chen X, Yuan X, Li Y. 2020. Influence of Microenvironment on Mesenchymal Stem Cell Therapeutic Potency: From Planar Culture to Microcarriers. *Front Bioeng Biotechnol* **8**:640. doi:10.3389/fbioe.2020.00640

Vilaça-Faria H, Marote A, Lages I, Ribeiro C, Mendes-Pinheiro B, Domingues AV, Campos J, Lanceros-Mendez S, Salgado AJ, Teixeira FG. 2021. Fractionating stem cells secretome for Parkinson's disease modeling: Is it the whole better than the sum of its parts? *Biochimie* **189**:87–98. doi:10.1016/j.biochi.2021.06.008

Vizoso F, Eiro N, Cid S, Schneider J, Perez-Fernandez R. 2017. Mesenchymal Stem Cell Secretome: Toward Cell-Free Therapeutic Strategies in Regenerative Medicine. *Int J Mol Sci* **18**:1852. doi:10.3390/ijms18091852

Watt FM, Hogan and BLM. 2000. Out of Eden: Stem Cells and Their Niches. *Science* **287**:1427–1430. doi:10.1126/science.287.5457.1427

Xiang Y, Tanaka Y, Cakir B, Patterson B, Kim K, Sun P, Kang Y, Zhong M, Liu X, Patra P, Lee S, Weissman SM, Park I. 2019. hESC-Derived Thalamic Organoids Form Reciprocal Projections When Fused with Cortical Organoids. *Cell Stem Cell* **24**:487-497.e7. doi:10.1016/j.stem.2018.12.015

Xu Y, Jin MZ, Yang ZY, Jin WL. 2021. Microglia in neurodegenerative diseases. *Neural Regen Res* **16**:270–280. doi:10.4103/1673-5374.290881

Yakoub A. 2019. Cerebral organoids exhibit mature neurons and astrocytes and recapitulate electrophysiological activity of the human brain. *Neural Regen Res* **14**:757. doi:10.4103/1673-5374.249283

Yoon S-J, Elahi LS, Paşca AM, Marton RM, Gordon A, Revah O, Miura Y, Walczak EM, Holdgate GM, Fan HC, Huguenard JR, Geschwind DH, Paşca SP. 2019. Reliability of human cortical organoid generation. *Nat Methods* **16**:75–78. doi:10.1038/s41592-018-0255-0